APPLICATION OF MOLECULAR METHODS TO UNDERSTAND MICROBIAL PROCESSES, INCLUDING CARBON AND NITROGEN CYCLING AND CONTAMINANT BIODEGRADATION

By

Zheng Li

A DISSERTATION

Submitted to
Michigan State University
in partial fulfillment of the requirements
for the degree of

Environmental Engineering – Doctor of Philosophy

2024

ABSTRACT

Microorganisms play important roles in complex and dynamic environments such as agricultural soils and contaminated site sediments. Molecular methods have greatly advanced the understanding of microbial processes, such as nitrogen cycling, carbon cycling and contaminant biodegradation, by providing insights into the structure, function and dynamics of microbial communities.

The first project evaluated the impact of four agricultural management practices (no tillage, conventional tillage, reduced input, biologically based) on the abundance and diversity of microbial communities regulating nitrogen cycling using shotgun sequencing. The relative abundance values, diversity and richness indices, taxonomic classification and genes associated with nitrogen metabolism were examined. The microbial communities involved in nitrogen metabolism are sensitive to varying soil conditions, which in turn, likely has important implications for N_2O emissions.

The second project examined the impact of plant diversity, soil pore size, and incubation time on soil microbial communities in responses to new carbon inputs (glucose). Soil cores from three plant systems (no plants, monoculture switchgrass, and high diversity prairie) were incubated with labeled and unlabeled glucose. The phylotypes responsible for the carbon uptake from glucose were identified using stable isotope probing (SIP). The microbial communities were influenced by plan diversity but not by pore size or incubation time. The differentiated carbon assimilators may be linked to different carbon assimilation strategies (r- vs. K-strategists) depending on pore size.

The third and fourth projects focused on the biodegradation of the common groundwater contaminant, 1,4-dioxane. A major challenge in addressing 1,4-dioxane contamination concerns

chemical characteristics that result in migration and persistence. Given the limitations associated with traditional remediation methods, interest has turned to bioremediation to address 1,4-dioxane contamination. The third project examined the impact of yeast extract and basal salts medium (BSM) on 1,4-dioxane biodegradation rates and the microorganisms involved in carbon uptake from 1,4-dioxane. For this, laboratory sample microcoms and abiotic controls were inoculated with three soils and amended with media (water or BSM and yeast) and 2 mg/L 1,4-dioxane. SIP was then utilized to identify the active phylotypes involved in the 1,4-dioxane biodegradation. The amendment of BSM and yeast enhanced the 1,4-dioxane degradation in all three soil types. *Gemmatimonas*, unclassified *Solirubacteraceae* and *Solirubrobacter* were associated with carbon uptake from 1,4-dioxane and may represent novel degraders. *Solirubrobacter* and *Pseudonocardia* were associated with propane monooxygenases genes which potentially function in 1,4-dioxane biodegradation.

The fourth project further explored the impact of yeast extract on 1,4-dioxane degradation at low concentrations (< 500 μg/L) using sediment from three impacted sites and four agricultural soils. 1,4-Dioxane biodegradation trends differed between inocula sources and treatments. For two of the impacted sites, no 1,4-dioxane biodegradation was observed for any treatment, indicating a lack of 1,4-dioxane degraders. In contrast, 1,4-dioxane degradation occurred in all treatments in microcosms inoculated with the agricultural soil or the other impacted site sediments. Bioaugmentation with agricultural soils initiated 1,4-dioxane biodegradation in the sediments with no intrinsic degradation capacities. Overall, yeast extract enhances 1,4-dioxane biodegradation in specific sediments. Bioaugmenting site sediments with agricultural soils may represent a promising approach for the remediation of 1,4-dioxane contaminated sites.

To my husband and my parents,
for loving me and having my back as always.

ACKNOWLEDGEMENTS

Firstly, I would like to express my deepest gratitude to my Ph.D. advisor, Dr. Cupples, for her unwavering support, understanding, encouragement and guidance. Throughout these four years, I encountered many challenges, including the disruptions caused by the COVID-19 pandemic and difficulties in my research. I would not have moved forward and overcome these obstacles without her support. Thanks to the rest of my Ph.D. committee members, Dr. Syed Hashsham, Dr. Irene Xagoraraki, and Dr. Dawn Dechand, for their valuable research advice.

I would like to thank the past and current members in our lab. Thanks to Dr. Hongyu Dang for his support and guidance during the early months of Ph.D. journey. Thanks to Zohre Eshghdoostkhatami and Mohsen Faghihinezhad for their insightful discussions and inspiration.

I would like to thank Lori Larner and Bailey Weber for placing research supplies orders. Thanks to Yanlyang Pan for technical support. Also, thanks to the support and other administrative staff in the Department of Civil and Environmental Engineering.

I would like to thank support of the Research Technology and Support Facility (RTSF) at Michigan State University. Thanks to Dr. Casey Johnny, James O'Keefe, and Dr. Anthony Schilmiller at the Mass Spectrometry Laboratory at the RTSF (MSU) for 1,4-dioxane analytical method support. Thanks to the genomics facility for their support in DNA sequencing.

I would like to thank all my friends. Your presence has made my life so much better. Special thanks to Ze Zhang, Jiaxin Zhang, Yiyi Chu, Yiqi Wang, Chi Zhan, Tianxudong Tang, Zefang Qi, Her Jiang, Yichen Tao, Nafeisha Maimaiti, Siquan Sun and Bo Nan. I am deeply grateful for your companionship, support, thoughts, and the happiness you have brought to me.

Finally, I would like to express my heartfelt thanks to my families throughout this journey. To my husband, thank you for coming into my life and filling it with so many colors

and warmth. Thank you for being a good listener, offering thoughtful advice and for telling me I don't have to be perfect. Thank you for being kind, patient, gentle and respectful. Thank you for on my side no matter whatever I want to do, wherever I want to go, and whoever I want to be. Thank you for choosing me as your wife, for building a home together, and for showing me that I deserve all the love and support in the world. Your heart, encouragement, support, and love mean everything to me.

To my parents, thank you for your unconditional love and support. I would never be more grateful for what you have done for me. I also want to extend my thanks to my parents-in-law for incredible support in the past few months.

A special thanks to Piggy, the ragdoll cat that I raised for half a year. Without you, I would not have made it through the toughest times in 2020.

TABLE OF CONTENTS

LIST OF ABBREVIATIONS

BSM —— Basal Salts Medium

CsCl —— Cesium Chloride

DIAMOND —— Double Index Alignment of Next-generation Sequencing Data

HPCC —— High Performance Computing Cluster

KEGG —— Kyoto Encyclopedia of Genes and Genomes

KO —— KEGG Orthologs

MG-RAST —— Meta Genome Rapid Annotation using Subsystem Technology

N_2O —— Nitrous Oxide

NO_2^- —— Nitrite

NO_3^- —— Nitrate

OTU —— Operational Taxonomic Units

PCA —— Principal Component Analysis

PCoA —— Principal Coordinate Analysis

PERMANOVA —— Permutational Multivariate Analysis of Variance

RI —— Refractive Index

RTSF —— Research Technology Support Facility

SDIMO —— Soluble Di-iron Monooxygenase

SIP —— Stable Isotope Probing

SPME —— Solid Phase Micro Extraction

STAMP —— Statistical Analysis of Taxonomic and Functional Profiles

TCA cycle —— Citrate Cycle

USEPA —— US Environmental Protection Agency

CHAPTER 1: INTRODUCTION

1.1 Nitrogen cycling

The emissions of greenhouse gas due to human activities have changed the global climate significantly over the years. Nitrous oxide (N_2O) is a greenhouse gas that contributes to ozone layer depletion and has ~300 times greater global warming potential than CO_2 (Richardson et al., 2009). Many researchers have studied the impacts of various agriculture management practices on N_2O emissions. Nitrogen-based fertilizers are extensively utilized across the world to improve agricultural production and meet the consuming demand of the enlarged human population. The increasing use of nitrogen fertilizer in agricultural practice has accordingly increased the N_2O production (Davidson, 2009). No till has gained much attention due to the potential to reduce soil erosion (Halvorson, Mosier et al. 2006) and improve the soil quality and crop productivity (Hungria, Franchini et al. 2009). Although the production of N_2O involves complex biological pathways, denitrification is a dominant process (Zumft 1997). N_2O emission rates are greatly influenced by the abundance and diversity of the genes related to the production and consumption of N_2O.

1.2 Carbon turnover in the soils

Bioenergy crops reduce the dependence of fossil fuels, mitigate the emission of atmospheric CO_2 and enhance soil carbon sequestration. Switchgrass (Panicum virgatum L.) is a particularly promising perennial bioenergy feedstock in the USA (Sanderson, Adler et al. 2006). Switchgrass can increase carbon sequestration in the long-term (after 10 years) (Ma, Wood et al. 2000) and promote carbon accumulation compared to annual systems due to the more root-derived carbon inputs (Adkins, Jastrow et al. 2016). However, there are also reports suggesting that switchgrass is slow to accumulate the soil organic carbon (Chimento, Almagro et al. 2016,

Sprunger and Robertson 2018). Carbon stored in soils is driven by the balance of root litter production, root exudates and the microbial decomposition of these compounds (Jastrow, Amonette et al. 2007). Fine roots are important for carbon accumulation in soils and diverse biofuel cropping systems are likely to hold more fine roots than monoculture systems (Sprunger, Oates et al. 2017). Plant diversity influences carbon inputs in soils and further the resident microbial populations and activities (Carney and Matson 2006, Zhang, Wang et al. 2010, Lamb, Kennedy et al. 2011, Ravenek, Bessler et al. 2014, Lange, Eisenhauer et al. 2015). Soil pore structure also plays an important role in shaping the microbial community in soils (Chenu, Hassink et al. 2001, Carson Jennifer, Gonzalez-Quiñones et al. 2010, Sleutel, Bouckaert et al. 2012, Kravchenko, Negassa et al. 2014, Negassa, Guber et al. 2015, Kravchenko and Guber 2017, Kravchenko, Guber et al. 2021, Xia, Zheng et al. 2022).

1.3 1,4-Dioxane degradation

1,4-Dioxane is classified as a probable human carcinogen (Derosa, Wilbur et al. 1996) and is widespread in aquifers around the world. 1,4-Dioxane was used as a solvent and stabilizer for the chlorinated solvents, particularly 1,1,1-trichloroethane (USEPA 2013). The US Environmental Protection Agency (USEPA) set health advisory levels of 1,4-dioxane between 0.35 and 35 μg/l, corresponding to a lifetime cancer risk of 1 in a million and 1 in 10,000. Tradition remediation methods are challenging due to low Henry's law constant (4.80×106 atm-m^3/mol at 25 °C), low Kow (Log Kow: 0.27) and low Koc (Log Koc: 1.23) (USEPA 2013). Given the limitations associated with traditional remediation methods, interest has turned to bioremediation to address 1,4-dioxane contamination.

Both metabolic (Parales, Adamus et al. 1994, Kelley, Aitchison et al. 2001, Mahendra and Alvarez-Cohen 2005, Kim, Jeon et al. 2009, Huang, Shen et al. 2014) and co-metabolism

processes (Vainberg, McClay et al. 2006, House and Hyman 2010) have been reported for 1,4-dioxane biodegradation.. In metabolic processes, degraders utilize 1,4-dioxane as a carbon and energy source for growth. Parales et al. (1994) first isolated *Actinomycete* CB1190 from a 1,4-dioxane-contaminated sludge sample. This *Actinomycete* CB1190 strain used 1,4-dioxane as a growth substrate and was further characterized as *Pseudonocardia dioxanivorans* sp. nov CB1190 (Mahendra and Alvarez-Cohen 2005). Isolates that could metabolize 1,4-dioxane also include *Mycobacterium* sp. PH-06 (Kim, Jeon et al. 2009), *Acinetobacter baumannii* DD1 (Huang, Shen et al. 2014), *Afipia broomeae* D1(Isaka, Udagawa et al. 2016) and *Rhodococcus ruber* 219 (Simmer, Richards et al. 2021). Numerous strains also grow on different substrates and degrade 1,4-dioxane co-metabolically (Vainberg, McClay et al. 2006, House and Hyman 2010, Sun, Ko et al. 2011). For example, *Pseudonocardia* sp. strain ENV478 can degrade 1,4-dioxane when growing on tetrahydrofuran, sucrose, lactate, yeast extract, 2-propanol and propane (Vainberg, McClay et al. 2006). *Flavobacterium* co-metabolically degrades 1,4-dioxane following tetrahydrofuran degradation (Sun, Ko et al. 2011).

1.4 Dissertation outline and objectives

The dissertation work is described below in the following chapters.

Chapter 2: This project examined shotgun sequencing data from agricultural soils under four different management practices. The overall objective was to investigate the impact of four agricultural management on the abundance and diversity of microbial communities regulating nitrogen cycling (primarily denitrification).

Chapter 3: The objectives of this work were to investigate the effects of 1) cropping system (no plants, switchgrass, high diversity prairie), 2) soil pore size and 3) incubation time (24 hr and 30 days) on the microbial communities involved in the utilization of a newly added

carbon (glucose). The impacts of those factors on the overall composition and diversity of the soil microbial communities were also investigated.

Chapter 4: The objectives were to 1) examine the impact of yeast extract and BSM on 1,4-dioxane degradation rates in microcosms amended with different inocula (agricultural soil, wetland sediment and impacted site sediments), 2) identify the phylotypes involved in carbon uptake from 1,4-dioxane using stable isotope probing (SIP), and 3) determine the functional genes putatively associated with 1,4-dioxane biodegradation.

Chapter 5: The objectives of this study are to 1) examine the impact of varying concentrations of yeast extract on biodegradation kinetics of 1,4-dioxane at low concentrations in mixed microbial communities; 2) investigate the phylotypes deriving a growth benefit from the 1,4-dioxane of low concentration of 1,4-dioxane and 3) examine the impact of bioaugmentation with agricultural soil microorganisms on 1,4-dioxane removal rates in site sediments.

Chapter 6: The conclusions of this dissertation are outlined in this chapter along with directions for future work.

REFERENCES

Adkins, J., Jastrow, J. D., Morris, G. P., Six, J., & de Graaff, M.-A. (2016). Effects of switchgrass cultivars and intraspecific differences in root structure on soil carbon inputs and accumulation. *Geoderma*, *262*, 147-154. https://doi.org/https://doi.org/10.1016/j.geoderma.2015.08.019

Carney, K. M., & Matson, P. A. (2006). The influence of tropical plant diversity and composition on soil microbial communities. *Microbial Ecology*, *52*(2), 226-238.

Carson Jennifer, K., Gonzalez-Quiñones, V., Murphy Daniel, V., Hinz, C., Shaw Jeremy, A., & Gleeson Deirdre, B. (2010). Low Pore Connectivity Increases Bacterial Diversity in Soil. *Applied and Environmental Microbiology*, *76*(12), 3936-3942. https://doi.org/10.1128/AEM.03085-09

Chenu, C., Hassink, J., & Bloem, J. (2001). Short-term changes in the spatial distribution of microorganisms in soil aggregates as affected by glucose addition. *Biology and Fertility of Soils*, *34*(5), 349-356. https://doi.org/10.1007/s003740100419

Chimento, C., Almagro, M., & Amaducci, S. (2016). Carbon sequestration potential in perennial bioenergy crops: the importance of organic matter inputs and its physical protection. *Gcb Bioenergy*, *8*(1), 111-121.

Derosa, C. T., Wilbur, S., Holler, J., Richter, P., & Stevens, Y.-W. (1996). Health Evaluation of 1,4-Dioxane. *Toxicology and Industrial Health*, *12*(1), 1-43. https://doi.org/10.1177/074823379601200101

Halvorson, A. D., Mosier, A. R., Reule, C. A., & Bausch, W. C. (2006). Nitrogen and tillage effects on irrigated continuous corn yields. *Agronomy Journal*, *98*(1), 63-71. https://doi.org/10.2134/agronj2005.0174

House, A. J., & Hyman, M. R. (2010). Effects of gasoline components on MTBE and TBA cometabolism by Mycobacterium austroafricanum JOB5. *Biodegradation*, *21*, 525-541.

Huang, H., Shen, D., Li, N., Shan, D., Shentu, J., & Zhou, Y. (2014). Biodegradation of 1, 4-dioxane by a novel strain and its biodegradation pathway. *Water, Air, & Soil Pollution*, *225*, 1-11.

Hungria, M., Franchini, J. C., Brandao, O., Kaschuk, G., & Souza, R. A. (2009). Soil microbial activity and crop sustainability in a long-term experiment with three soil-tillage and two crop-rotation systems [Article]. *Applied Soil Ecology*, *42*(3), 288-296. https://doi.org/10.1016/j.apsoil.2009.05.005

Isaka, K., Udagawa, M., Sei, K., & Ike, M. (2016). Pilot test of biological removal of 1,4-dioxane from a chemical factory wastewater by gel carrier entrapping Afipia sp. strain D1. *J Hazard Mater*, *304*, 251-258. https://doi.org/10.1016/j.jhazmat.2015.10.066

Jastrow, J. D., Amonette, J. E., & Bailey, V. L. (2007). Mechanisms controlling soil carbon turnover and their potential application for enhancing carbon sequestration. *Climatic Change*, *80*(1), 5-23.

Kelley, S. L., Aitchison, E. W., Deshpande, M., Schnoor, J. L., & Alvarez, P. J. (2001). Biodegradation of 1, 4-dioxane in planted and unplanted soil: effect of bioaugmentation with Amycolata sp. CB1190. *Water Research*, *35*(16), 3791-3800.

Kim, Y.-M., Jeon, J.-R., Murugesan, K., Kim, E.-J., & Chang, Y.-S. (2009). Biodegradation of 1, 4-dioxane and transformation of related cyclic compounds by a newly isolated Mycobacterium sp. PH-06. *Biodegradation*, *20*(4), 511-519.

Kravchenko, A., Guber, A., Gunina, A., Dippold, M., & Kuzyakov, Y. (2021). Pore-scale view of microbial turnover: Combining 14C imaging, μCT and zymography after adding soluble carbon to soil pores of specific sizes. *European Journal of Soil Science*, *72*(2), 593-607.

Kravchenko, A. N., & Guber, A. K. (2017). Soil pores and their contributions to soil carbon processes. *Geoderma*, *287*, 31-39. https://doi.org/https://doi.org/10.1016/j.geoderma.2016.06.027

Kravchenko, A. N., Negassa, W. C., Guber, A. K., Hildebrandt, B., Marsh, T. L., & Rivers, M. L. (2014). Intra-aggregate pore structure influences phylogenetic composition of bacterial community in macroaggregates. *Soil Science Society of America Journal*, *78*(6), 1924-1939.

Lamb, E. G., Kennedy, N., & Siciliano, S. D. (2011). Effects of plant species richness and evenness on soil microbial community diversity and function. *Plant and Soil*, *338*(1), 483-495. https://doi.org/10.1007/s11104-010-0560-6

Lange, M., Eisenhauer, N., Sierra, C. A., Bessler, H., Engels, C., Griffiths, R. I., Mellado-Vázquez, P. G., Malik, A. A., Roy, J., Scheu, S., Steinbeiss, S., Thomson, B. C., Trumbore, S. E., & Gleixner, G. (2015). Plant diversity increases soil microbial activity and soil carbon storage. *Nature Communications*, *6*(1), 6707. https://doi.org/10.1038/ncomms7707

Ma, Z., Wood, C., & Bransby, D. I. (2000). Soil management impacts on soil carbon sequestration by switchgrass. *Biomass and bioenergy*, *18*(6), 469-477.

Mahendra, S., & Alvarez-Cohen, L. (2005). Pseudonocardia dioxanivorans sp. nov., a novel actinomycete that grows on 1, 4-dioxane. *International Journal of Systematic and Evolutionary Microbiology*, *55*(2), 593-598.

Negassa, W. C., Guber, A. K., Kravchenko, A. N., Marsh, T. L., Hildebrandt, B., & Rivers, M. L. (2015). Properties of Soil Pore Space Regulate Pathways of Plant Residue Decomposition and Community Structure of Associated Bacteria. *PLOS ONE*, *10*(4), e0123999. https://doi.org/10.1371/journal.pone.0123999

Parales, R., Adamus, J., White, N., & May, H. (1994). Degradation of 1, 4-dioxane by an actinomycete in pure culture. *Applied and Environmental Microbiology*, *60*(12), 4527-4530.

Ravenek, J. M., Bessler, H., Engels, C., Scherer-Lorenzen, M., Gessler, A., Gockele, A., De Luca, E., Temperton, V. M., Ebeling, A., Roscher, C., Schmid, B., Weisser, W. W., Wirth, C., de Kroon, H., Weigelt, A., & Mommer, L. (2014). Long-term study of root biomass in a biodiversity experiment reveals shifts in diversity effects over time. *Oikos*, *123*(12), 1528-1536. https://doi.org/10.1111/oik.01502

Sanderson, M. A., Adler, P. R., Boateng, A. A., Casler, M. D., & Sarath, G. (2006). Switchgrass as a biofuels feedstock in the USA. *Canadian Journal of Plant Science*, *86*(Special Issue), 1315-1325.

Simmer, R. A., Richards, P. M., Ewald, J. M., Schwarz, C., da Silva, M. L. B., Mathieu, J., Alvarez, P. J. J., & Schnoor, J. L. (2021). Rapid Metabolism of 1,4-Dioxane to below Health Advisory Levels by Thiamine-Amended Rhodococcus ruber Strain 219. *Environmental Science & Technology Letters*, *8*(11), 975-980. https://doi.org/10.1021/acs.estlett.1c00714

Sleutel, S., Bouckaert, L., Buchan, D., Van Loo, D., Cornelis, W. M., & Sanga, H. G. (2012). Manipulation of the soil pore and microbial community structure in soil mesocosm incubation studies. *Soil Biology and Biochemistry*, *45*, 40-48. https://doi.org/https://doi.org/10.1016/j.soilbio.2011.09.016

Sprunger, C. D., Oates, L. G., Jackson, R. D., & Robertson, G. P. (2017). Plant community composition influences fine root production and biomass allocation in perennial bioenergy cropping systems of the upper Midwest, USA. *Biomass and bioenergy*, *105*, 248-258. https://doi.org/https://doi.org/10.1016/j.biombioe.2017.07.007

Sprunger, C. D., & Robertson, G. P. (2018). Early accumulation of active fraction soil carbon in newly established cellulosic biofuel systems. *Geoderma*, *318*, 42-51.

Sun, B., Ko, K., & Ramsay, J. A. (2011). Biodegradation of 1, 4-dioxane by a Flavobacterium. *Biodegradation*, *22*, 651-659.

USEPA. (2013). *Integrated Risk Information System (IRIS) on 1,4-Dioxane*

Vainberg, S., McClay, K., Masuda, H., Root, D., Condee, C., Zylstra, G. J., & Steffan, R. J. (2006). Biodegradation of ether pollutants by Pseudonocardia sp. strain ENV478. *Applied and Environmental Microbiology*, *72*(8), 5218-5224.

Xia, Q., Zheng, N., Heitman, J. L., & Shi, W. (2022). Soil pore size distribution shaped not only compositions but also networks of the soil microbial community. *Applied Soil Ecology*, *170*, 104273. https://doi.org/https://doi.org/10.1016/j.apsoil.2021.104273

Zhang, C.-B., Wang, J., Liu, W.-L., Zhu, S.-X., Ge, H.-L., Chang, S. X., Chang, J., & Ge, Y. (2010). Effects of plant diversity on microbial biomass and community metabolic profiles

in a full-scale constructed wetland. *Ecological Engineering*, *36*(1), 62-68. https://doi.org/https://doi.org/10.1016/j.ecoleng.2009.09.010

Zumft, W. G. (1997). Cell biology and molecular basis of denitrification. *Microbiology and Molecular Biology Reviews*, *61*(4), 533-+. https://doi.org/10.1128/.61.4.533-616.1997

CHAPTER 2: DIVERSITY OF NITROGEN CYCLING GENES AT A MIDWEST LONG TERM ECOLOGICAL RESEARCH SITE

This chapter is a modified version of a published work in Applied Microbiology and Biotechnology: Li, Z. and A. M. Cupples (2021). "Diversity of nitrogen cycling genes at a Midwest long-term ecological research site with different management practices." Applied Microbiology and Biotechnology 105(10): 4309-4327.

2.1 Abstract

Nitrogen fertilizer results in the release of nitrous oxide (N_2O), a concern because N_2O is an ozone-depleting substance and a greenhouse gas. Although the reduction of N_2O to nitrogen gas can control emissions, the factors impacting the enzymes involved have not been fully explored. The current study investigated the abundance and diversity of genes involved in nitrogen cycling (primarily denitrification) under four agricultural management practices (no tillage [NT], conventional tillage [CT], reduced input, biologically based). The work involved examining soil shotgun sequencing data for nine genes (*napA, narG, nirK, nirS, norB, nosZ, nirA, nirB, nifH*). For each gene, relative abundance values, diversity and richness indices and taxonomic classification were determined. Additionally, the genes associated with nitrogen metabolism (defined by the KEGG hierarchy) were examined. The data generated were statistically compared between the four management practices. The relative abundance of four genes (*nifH*, *nirK nirS* and *norB*) were significantly lower in the NT treatment compared to one or more of the other soils. The abundance values of *napA*, *narG*, *nifH*, *nirA* and *nirB* were not significantly different between NT and CT. The relative abundance of *nirS* was significantly higher in the CT treatment compared to the others. Diversity and richness values were higher for

four of the nine genes (*napA, narG, nirA, nirB*). Based on *nirS/nirK* ratios, CT represents the highest N_2O consumption potential in four soils. In conclusion, the microbial communities involved in nitrogen metabolism were sensitive to different agricultural practices, which in turn, likely has implications for N_2O emissions.

2.2 Introduction

An understanding of the terrestrial nitrogen cycle is important both for optimizing agricultural productivity as well as for minimizing environmental impacts, such as water pollution or global warming. Nitrous oxide (N_2O) is a predominant ozone-depleting substance and an important and potent greenhouse gas with a global warming potential over 100 years of ~298 and 11.9 times that of CO_2 and CH_4, respectively (Ravishankara, Daniel et al. 2009, Domeignoz-Horta, Philippot et al. 2018). The majority (almost 70%) of the total global N_2O atmospheric loading can be accounted for by terrestrial ecosystems, and at least 45% of this has been attributed to microbial cycling of nitrogen in agricultural systems (Rudy, Harris et al. 2008, Syakila and Kroeze 2011). The increasing use of nitrogen fertilizer in agricultural practice has accordingly increased N_2O production (Davidson, 2009). The nitrogen cycle involves two key microbial processes for the emission of N_2O from soils. During nitrification, bacteria produce N_2O during the first step, when ammonia is oxidized to nitrite via hydroxylamine (Prosser and Nicol 2012). Denitrification is another key microbial process for the release of N_2O, involving the respiratory reduction of nitrate (NO_3^-) to nitrite (NO_2^-) and their subsequent reduction to gaseous forms (NO, N_2O, N_2). Although the microbial reduction of N_2O to nitrogen gas is vital for controlling emissions from terrestrial ecosystems, the determinants for a soil to act as a source or a sink remain uncertain (Butterbach-Bahl, Baggs et al. 2013).

A number of enzymes are associated with denitrification, including those encoded by nitrate reductases (*napA*/*narG*), nitrite reductases (*nirk*/*nirS*); nitric oxide reductase (*norB*) and nitrous oxide reductase (*nosZ*) (Philippot, Hallin et al. 2007). Many researchers have suggested that the abundance and diversity of such genes can impact N_2O emission rates. For instance, researchers found corrections between the relative abundance of *nosZ* and the potential N_2O production (Domeignoz-Horta, Putz et al. 2016). In another study, low N_2O emission rates were explained by soils properties (up to 59%), whereas high rates were explained by the abundance and diversity of the microbial communities (up to 68%) (Domeignoz-Horta, Philippot et al. 2018). The same study found that the diversity of *nosZ* was important to explain the variation in N_2O emissions (Domeignoz-Horta, Philippot et al. 2018). Others found that *nirK* gene copy numbers correlated with potential denitrification, but *nirS* gene copy numbers did not (Attard, Recous et al. 2011). Further, researchers have provided evidence of higher *nirS*/*nirK* ratios and higher N_2O consumption (Jones, Spor et al. 2014).

Agricultural practices are also known to influence denitrification trends. Although the impact of no tillage (NT) on N_2O emissions has been widely investigated, the results have been varied. Some studies reported minimal differences of N_2O emissions between NT and conventional tillage (CT) soil (Kaharabata, Drury et al. 2003, Lee, Six et al. 2006, Melero, Perez-de-Mora et al. 2011). For example, the potential denitrification rates and the ratios of N_2O/N_2 were similar in NT and CT after harvesting in a rainfed crop rotation system in Spain (Melero, Perez-de-Mora et al. 2011). Others found that NT stimulates denitrification (Calderon, Jackson et al. 2001, Baudoin, Philippot et al. 2009, Wang and Zou 2020). The denitrification enzyme activity and denitrification gene abundances (*nirK* and *nosZ*) were enhanced in NT in a soybean/rice crop system in Madagascar (Baudoin, Philippot et al. 2009). Similar results for the

increase of denitrification gene abundance in NT was also observed under sub-zero temperatures (Tatti, Goyer et al. 2015). The general trend that NT favored the denitrification rates, the abundance of denitrifying genes and N_2O emission was demonstrated at a global scale (Wang and Zou 2020).

Research has also addressed the differential consequences of tillage management on the microbial community structure and diversity. CT has a positive influence on the bacterial richness and diversity in clay soil in central Italy (Pastorelli, Vignozzi et al. 2013). However, some studies found opposite results. Minimal tillage enriched the microbial population and diversity relative to CT in a recent global meta-analysis (Li, Zhang et al. 2020). The bacteria diversity (represented by all the alpha-diversity indices) was higher in the NT soils compared to CT soils in a winter wheat cropping system in northern China (Dong, Liu et al. 2017). They also found that *Actinobacteria*, *Alphaproteobacteria*, *Gammaproteobacteria* and *Betaproteobacteria* were more abundant at class level in NT whereas CT had more sequences belong to *Acidobacteria*. In an experiment conducted in the agricultural fields in Indiana (USA), more DNA sequences related to the nitrogen metabolism were observed in the NT soils compared to CT soils, indicating the higher potential of nitrogen cycling (Smith, Blair et al. 2016).

Although researchers have previously studied the impacts of various agricultural management practices on denitrification and N_2O emission, the information on the taxonomic distributions and functional sequences related to nitrogen metabolism under different managements in the field-crop ecosystems is still limited, especially in the U.S Midwest. The objective of this research was to investigate the impact of four agricultural management on the abundance and diversity of microbial communities regulating nitrogen cycling (primarily denitrification). The work focused on the agricultural sites at the Long Term Ecological Research

(LTER) Site at Kellogg Biological Station (KBS), in southwest Michigan, southwest of the campus of Michigan State University (MSU). This LTER has field-crop ecosystems typical of the U.S. Midwest. The work is unique because it examines the key functional genes for nitrogen cycling over four long-term systems and detects a wider range of sequences through high throughput shotgun sequencing.

2.3 Methods

2.3.1 Sample Collection, DNA Extraction and Shotgun Sequencing

The DNA examined in the current work was generated from a previous study by our group (Thelusmond, Strathmann et al. 2019), involving an examination of the genes associated with xenobiotic biodegradation. Our previous work did not investigate the genes involved in nitrogen cycling. Briefly, four soils were collected from 5 sampling stations in 6 replicate plots for Treatments 1, 2, 3 and 4 within the Michigan State University Main Cropping System Experiment at Kellogg Biological Station Long-Term Ecological Research (KBS LTER) (42°24'N, 85°23'W). The agricultural management practices for each Treatment are illustrated in Table 1 and for additional information see https://lter.kbs.msu.edu/research/site-description-and-maps/. The physical and chemical characteristics of the soils were previously determined (A & L Great Lakes Laboratories, Inc., Fort Wayne, IN) with all being classified as loam soils. DNA extraction was completed using the DNA extraction kit (DNeasy PowerLyzer PowerSoil Kit, Mo Bio, USA) according to the manual protocol. Shotgun sequencing was performed with the Illumina HiSeq 4000 (2 × 150 bp) platform at the Research Technology Support Facility (RTSF) at Michigan State University (MSU), as previously described (Thelusmond, Strathmann et al. 2019).

2.3.2 Processing, DIAMOND Alignment, Diversity Analysis and Enrichments in Each Soil

Low quality sequences and Illumina adapters were removed from the HiSeq fastq.gz files using Trimmomatic with the Paired End Mode settings (Bolger, Lohse et al. 2014) (Version 0.36). Protein sequences for each of the nine genes were collected from the FunGene website (http://fungene.cme.msu.edu/) using a filter minimum HMM coverage of 70% (Cole, Wang et al. 2011, Fish, Chai et al. 2013). Following this, the FunGene Pipeline Dereplicator tool was used to dereplicate these sequences (Cole, Wang et al. 2011, Fish, Chai et al. 2013). Table A2.1 provides a summary of the sequences obtained at each step.

The dereplicated sequences were then aligned against the trimmomatic files using DIAMOND (double index alignment of next-generation sequencing data) (Version 2.0.1) (Buchfink, Xie et al. 2015). Only reads that exhibited an identity of ≥ 60 % and an alignment length ≥ 49 amino acids to the reference sequences were retained. For each, relative abundance values were calculated using the number of aligned reads divided by the total number of sequences for each sample. The relative abundance values were then normalized by (divided by) the number of dereplicated reference sequences for each gene. Diversity indices (Chao 1, Chao2, Inverse Simpson and Shannon values) were determined (using the number of aligned reads for each gene) using EstimateS (Version 8.2.0) (Colwell 2006). The accession numbers of sequences statistically enriched in each soil (as described below) were determined. The R package Taxonomizr (Sherrill-Mix 2009) was used with R (Version 3.5.1) (R_Core_Team 2018) in RStudio (Version 0.9.24) (RStudio_Team 2020) to determine the taxonomic classification of each sequence. The data were illustrated with bar charts in Excel (Version 2010).

2.3.3 Phylogenetic Trees

The 50 most abundant sequences for each gene, averaged across all samples, were

determined in Excel. The list of accession number for each were uploaded to COBALT: constraint-based alignment tool for multiple protein sequences (https://www.ncbi.nlm.nih.gov/tools/cobalt/cobalt.cgi) (Papadopoulos and Agarwala 2007). The downloaded alignments (fasta plus gaps) from COBALT were then submitted for MAFFT (multiple alignment using fast Fourier transform) alignment using an online server (https://mafft.cbrc.jp/alignment/server/) (Katoh, Rozewicki et al. 2019) (Version 7). Trees, also obtained from the same website, by the Neighbor-Joining method were exported in Newick format. The downloaded tree files were uploaded to the Interactive Tree of Life (https://itol.embl.de) (Letunic and Bork 2019) (Version 5.5.1). Sequences were colored depending on their classification and relative abundance values were added using the Datasets function called simple bar chart.

2.3.4 MG-RAST Analysis

Shotgun sequences were also analyzed by MG-RAST (Meta Genome Rapid Annotation using Subsystem Technology, Version 4.0.2) (Meyer, Paarmann et al. 2008). The processing pipeline includes removing artificial replicate sequences by dereplication and removing low quality sequencing by using SolexaQA (Cox, Peterson et al. 2010). The taxonomic analysis included RefSeq (Pruitt, Tatusova et al. 2005) database and the KEGG (Kanehisa 2002) database. The sequences are available publicly on the MG-RAST and the summary of the MG-RAST data is presented in Table A2.2.

2.3.5 Statistical Analysis

RStudio was used to perform a number of statistical tests, as follows (Version 0.9.24) (Team 2020). One-way ANOVA or Kruskal-Wallis tests were performed using the “aov” or “kruskal.test” functions as implemented in R package “car” (Fox, Weisberg et al. 2020) to

determine if there were statistically significant differences between 1) relative abundance of functional genes obtained by DIAMOND and 2) richness and diversity values (Chao 1, Chao2, Inverse Simpson and Shannon values). First, Levene's test was carried out to assess the homogeneity of variance of the data using the "leveneTest" function in the R package "car" (Fox, Weisberg et al. 2020). The Shapiro-Wilk test was conducted to evaluate the normality of the data using the "shapiro_test" function in the R package 'rstatix' (Kassambara 2020). When the *p* values from both of the Levene's and the Shapiro-Wilk tests were more than 0.05, the differences between the means were determined by one-way ANOVA. When the *p* values from the one-way ANOVA were less than 0.05, multiple pairwise comparison between the means were performed using Tukey's Honest Significant Difference test using the "TukeyHSD" function in the "stats" R package. When the *p* values from the Shapiro-Wilk test were less than 0.05, the non-parametric alternative to a one-way ANOVA, the test Kruskal-Wallis (function "kruskal.test" in the "stats" package), was used. When *p* values were less than 0.05 for the Kruskal-Wallis text, Dunn's test, using the "dunnTest" function in the R package "FSA", (Ogle , Wheeler et al. 2020)) was utilized to determine differences between means. Spearman's Rank Correlation test was carried out to explore the strength of correlation between the relative abundance of different genes using the "cor.test" function (with method = "spearman") in the R package "stats".

Principle component analysis (PCA) was performed within Microsoft Excel using XLSTAT (Addinsoft 2020) (Version 2020.3.1) to visualize the effect of the addition of pharmaceuticals on the gene relative abundance in different managed soils. STAMP (Statistical Analysis of Taxonomic and Functional Profiles, Version 2.1.3) (Parks, Tyson et al. 2014) was used to statistically analyze the MG-RAST data. Specifically, extended error bars were generated

to illustrate significant differences (Welch's two-sided *t*-test, two group analysis option, $p < 0.05$) in the gene relative abundance for the genes associated with nitrogen metabolism (as defined by the KEGG hierarchy). The data (generated in MG-RAST, six metagenomes for each soil) were analyzed using STAMP with the two group analysis option (each soil compared to the other three soils) and Welch's two sided t-test ($p<0.05$).

2.3.6 Analysis of Assembled Sequences

Shotgun sequences processed by Trimmomatic were assembled with Megahit (Li, Luo et al. 2016) (Version 1.2.4) with the pair end plus single end option (minimum and maximum kmer size were 27 and 127 with a kmer size step of 10). TaxIds for the FunGene *nifH* database (as described above, except no dereplication occurred) were obtained with the R package taxonomizr (Sherrill-Mix 2009), RStudio (Team 2020) (Version 0.9.24) and R (Team 2018) (Version 3.5.1). The analysis targeted *nifH* because no significant differences were found between soils in the analysis described above (before assembly). Following the deletion of duplicate values, the taxids obtained were used to analyze the assembled reads using the NCBI nucleotide database (nt) with the taxids option in BLASTN (Altschul, Gish et al. 1990) (Version 2.10.0-Linux_x86_64). BLASTN command lines also included the following options: identity ≥ 60 %, evalue ≤ 1×10^{-5}. The txt files generated from BLASTN were imported into Megan (Huson, Beier et al. 2016) (community edition Version 6.19.7). In Megan, the option "Compare" was used to combine all twenty-four data sets and then the combined dataset (at species level) was exported (using the STAMP export option) for analysis in STAMP. Additionally, the assembled contigs were aligned against the entire nt database using BLASTN without the taxids option (identity ≥ 60 %, evalue ≤ 1×10^{-5}). The output files were first imported and then in Megan, following this, the file was exported into STAMP to compare the communities between

soils.

2.4 Results

2.4.1 Abundance and Diversity of Functional Genes

The relative abundance of genes associated with nitrogen fixation, denitrification or dissimilatory nitrate reduction in all four management systems are presented (Figure 2.1A), with the lowest abundance for *nifH* and highest for *nirK*. Two sets of genes were observed to have the approximately same level of abundance in the soils: the nitrate reductase genes *napA* and *narG*; and the nitrite reductase genes *nirA* and *nirB*. The distribution of the relative abundance of *nirK*, *norB* and *nosZ* were not as tightly grouped compared to the other genes, suggesting a greater spread in abundance of these genes across the metagenomes. Principle component analysis of the functional genes (Figure 2.1B) indicated the nitrite reductase gene *nirK* was positively correlated with the nitrite reductase gene *nirS*, nitric oxide reductase gene *norB* and nitrous oxide reductase gene *nosZ*. Further, the nitrate reductase gene *napA* was positively correlated with the nitrite reductase gene *nirA*. In contrast, the nitrite reductase gene *nirB* did not appear to correlate with any other gene. The addition of pharmaceuticals impacted the functional genes in two treatments (conventional tillage and reduced input soils).

The average relative abundance of the twelve genes across the four management systems is displayed in Figure 2.2. Four genes (*nifH*, *nirK nirS* and *norB*) were significantly lower in the NT treatment compared to one or more of the other treatments. The average relative abundance of *nirS* was significantly higher in the CT treatment compared to the other treatments. It was also interesting to note that the average relative abundance of *nosZ* was approximately 50% lower in the NT soil compared to the other soils, although the difference was not statistically confirmed. The results of the statistical analysis tests (Levene's test, Shapiro-Wilk, One-way ANOVA,

Tukey's Honest Significant Difference, Kruskal-Wallis, Dunn's test) on these data sets are summarized (Tables A2.3-A2.5).

Table 2.1 Summary of the KBS agricultural management approaches for the four soils examined.

Conventional	This system is practiced by most farmers in this region. Tilled corn–soybean–winter wheat (c–s–w) rotation; standard chemical inputs, chisel-plowed, no cover crops, no manure or compost
No-till	No-till c–s–w rotation; standard chemical inputs, permanent no-till, no cover crops, no manure or compost
Reduced Input	Biologically based c–s–w rotation managed to reduce synthetic chemical inputs; chisel-plowed, winter cover crop of red clover or annual rye, no manure or compost
Biologically Based	Biologically based c–s–w rotation managed without synthetic chemical inputs; chisel-plowed, mechanical weed control, winter cover crop of red clover or annual rye, no manure or compost; USDA-certified organic

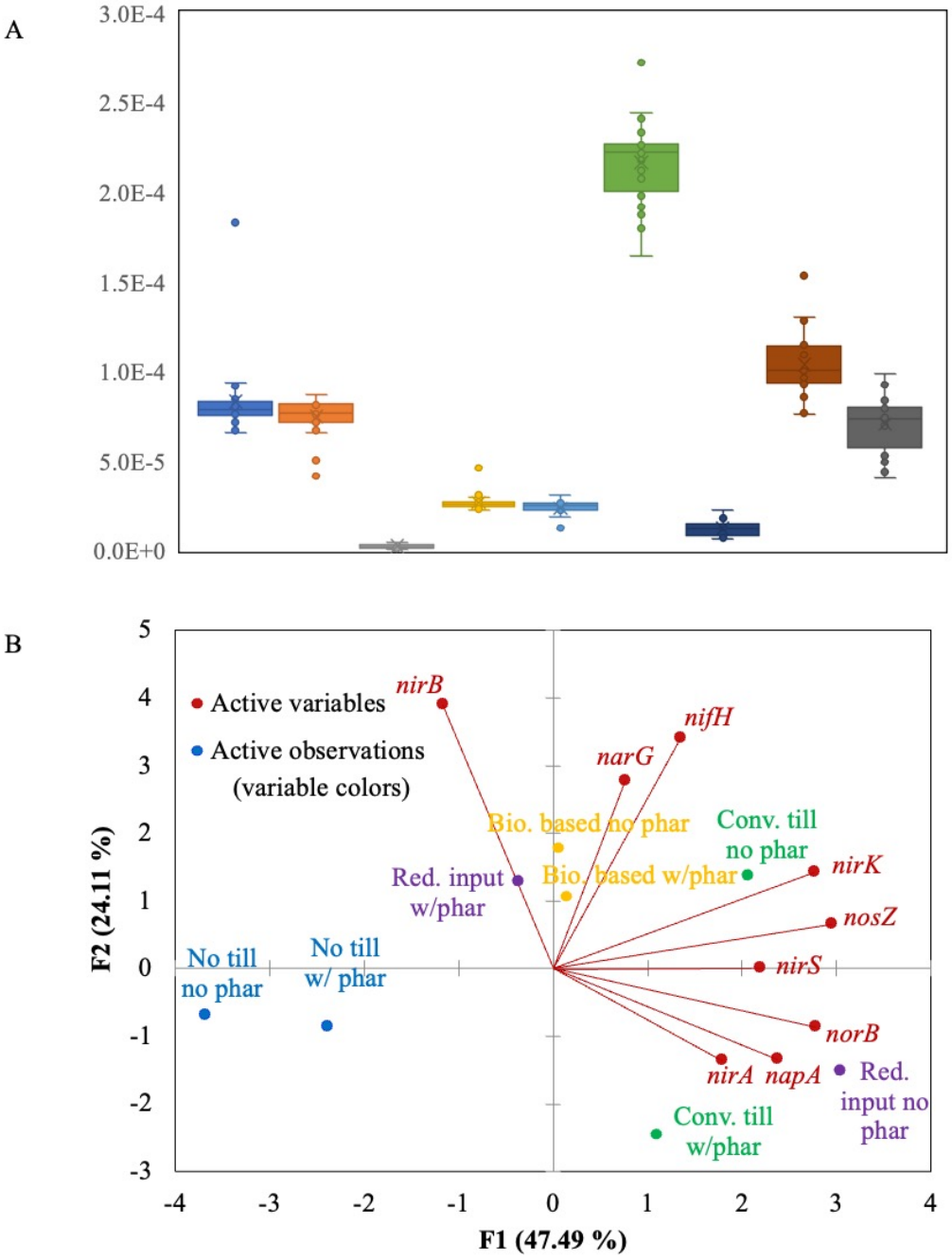

Figure 2.1 Box and whisker plot of relative abundance of genes (A) and Principal Component Analysis of the genes across the four management practices (with or without pharmaceuticals added) (B).

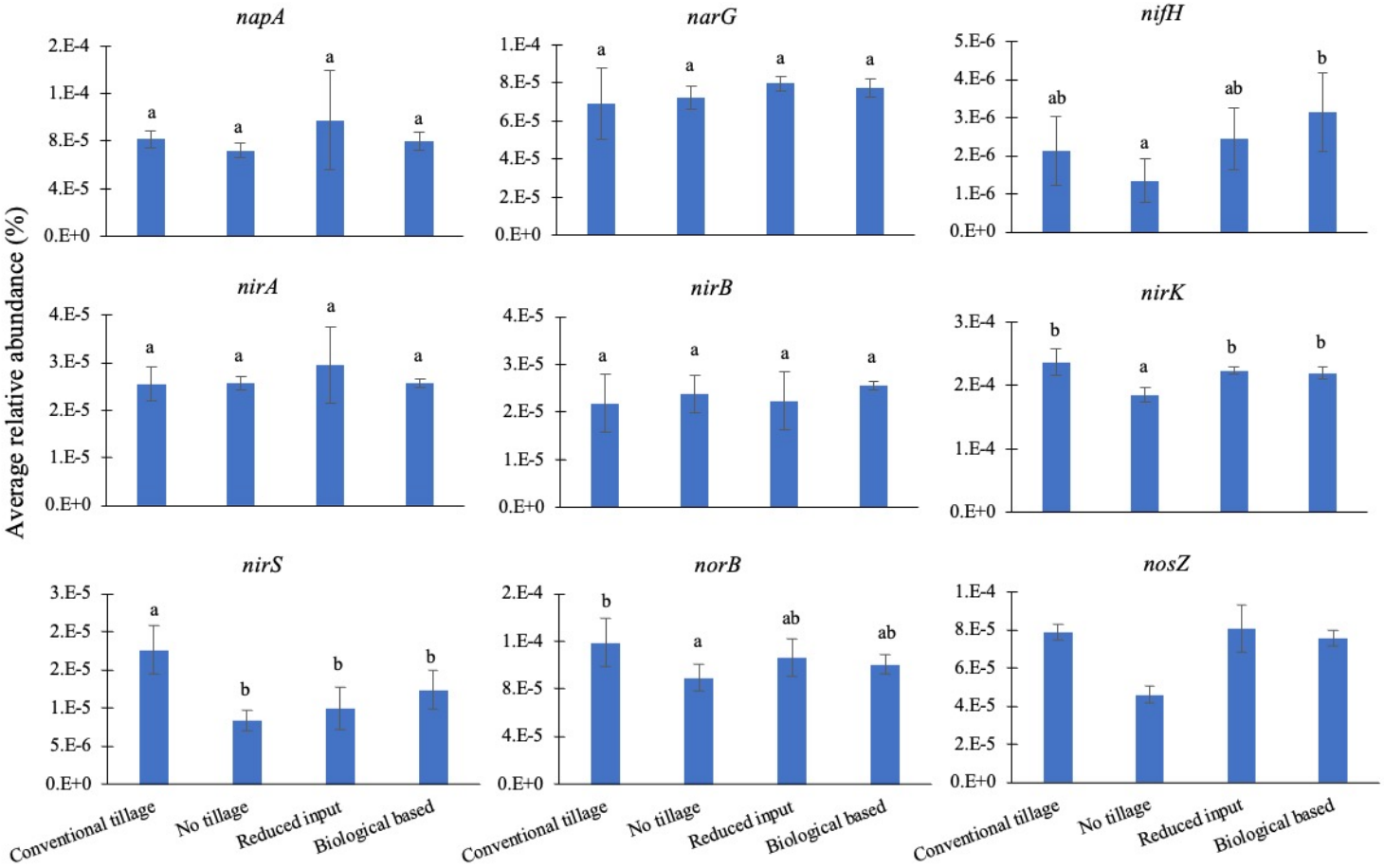

Figure 2.2 Average relative abundance values (%, as determined by DIAMOND) for each soil (n=6) with standard deviations illustrated with the bars. Values that are statistically significantly different (ANOVA or Kruskal-Wallis test, p<0.05) are shown with different letters. Letters are missing for *nosZ* because the statistical assumptions were not met for either test (unequal variance). Note, all y-axis have different scales.

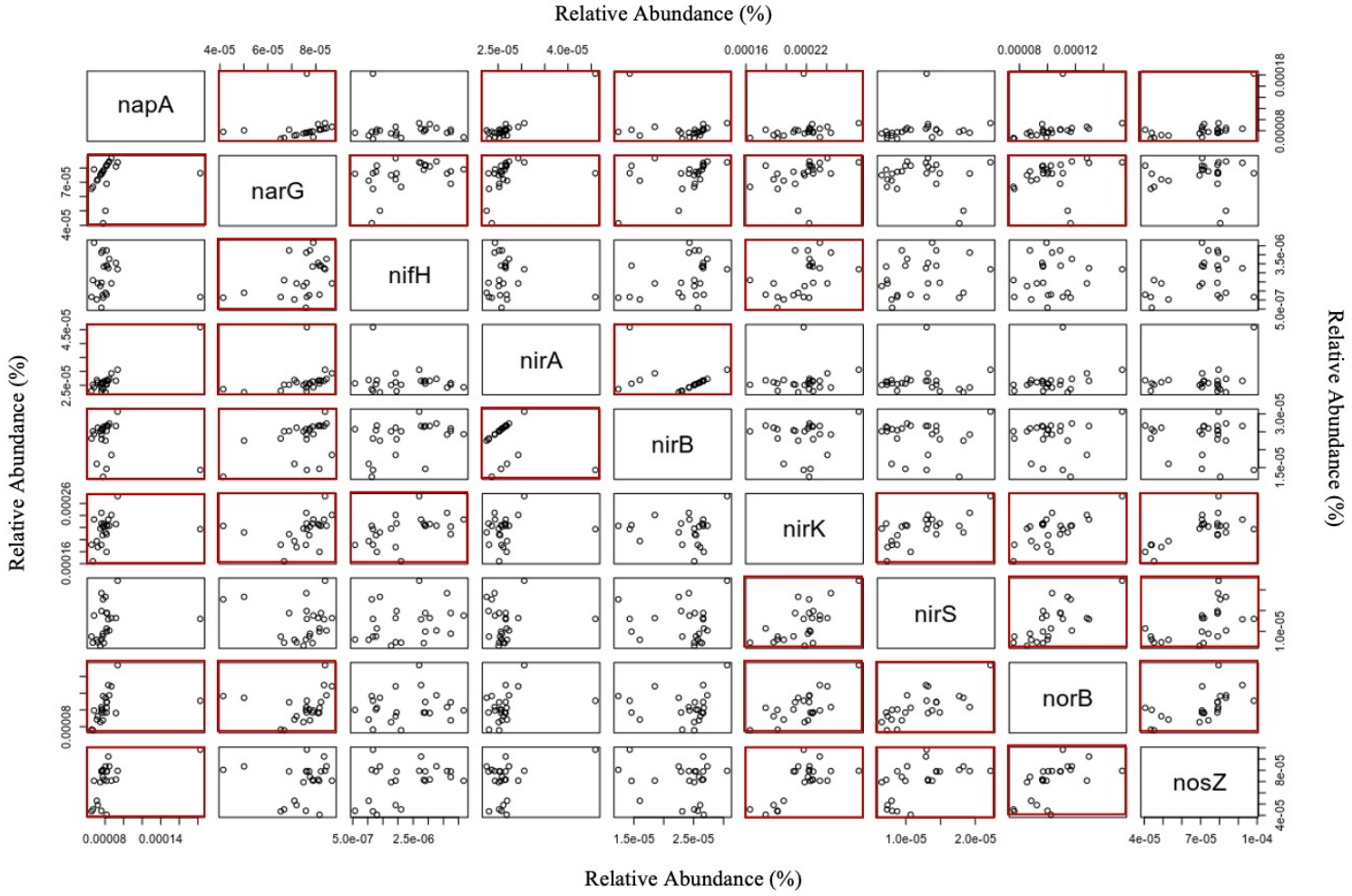

Figure 2.3 Scatterplots comparing relative abundance values of all genes across all samples. Correlations that were statistically significant (Spearman's rank test, $p<0.05$) are boxed in red.

Figure 2.3 illustrates correlations between gene relative abundance percentages across all samples with all statistically significant positive correlations (Spearman's rank test) being boxed in red. The abundance *napA* significantly correlated with six genes (*narG, nirA, nirB, nirK, norB, nosZ*), as did the abundance of *narG* (*napA, nifH, nirA, nirB, nirK, norB)*. In contrast, *nifH* correlated with two genes (*narG* and *nirK*). The abundance of both *nirA* and *nirB* correlated with *napA, narG* and to each other. Additionally, *nirK*, *nirS*, *norB*, *nosZ* all correlated positively to each other. The *p*-values and Spearman's correlation coefficients for the Spearman's rank tests are shown in Tables A2.6& A2.7.

The values of richness estimators (Chao 1 and Chao 2) and diversity indexes (Shannon and Inverse Simpson) determined by EstimateS are summarized (Figure 2.4). The results of the statistical analysis (Levene's test, Shapiro-Wilk, One-way ANOVA, Tukey's Honest Significant Difference, Kruskal-Wallis, Dunn's test) on this data set are also summarized (Tables A2.8-2.17). Overall, higher Chao 1 and Chao2 values (~8000-9000) were found for four genes (*napA, narG, nirA, nirB*), whereas lower values (~500-1500) were estimated for the five other genes (*nifH, nirK, nirS, norB, nosZ*). For Chao 2 no significant differences were found between the four treatments for all genes. The only significant difference for Chao 1 between treatments was for *nirS, nirK* and *nifH*. Chao1 values were higher in both the CT treatment and the biological based treatment compared to the NT treatment for *nirS*. For *nirK*, Choa 1 was lower for the CT treatment compared to the reduced input treatment. For *nifH*, the Choa 1 value in the reduced input treatment was lower than the biological based treatment.

The average values for Shannon and Inverse Simpson were higher (~1000-2000 and ~7.2-8.1) for four genes (*napA, narG, nirA, nirB*) compared to the rest (~100-400 and ~5.4-6.4). For the Inverse Simpson values, at least one significant difference between treatments was noted

for six genes (*napA, nirA, nirB, nirK, nirS, norB*), with the most notable number of differences between treatments being for *nirK, nirS* and *norB*. For *nirK* and *norB*, Inverse Simpson values were significantly higher in the NT treatment compared to the other treatments. For *nirA* and *nirB*, Inverse Simpson values were significantly higher in the reduced input treatment compared to the CT and NT treatments. For the Shannon Index values, at least one significant difference was found between at least two treatments for all genes except *nifH* and *nirB*. For *napA*, Shannon Index (and Inverse Simpson) values were significantly higher in the reduced input treatment compared to the CT and NT treatments. For *nosZ*, Shannon values were significantly lower in CT treatment compared to the other treatments. It was also interesting to note that the Shannon values of *nirA* were higher in the reduced input treatment than in the conventional and no tillage treatments.

The abundance of the genes associated with the nitrogen metabolism (as defined in the KEGG hierarchy) were investigated to determine if there were significant differences between management systems. For this, each dataset was compared individually with the other three datasets (Figure 2.5). Only one gene (*norF*; nitric-oxide reductase NorF protein) was more abundant in the CT soil compared to the other three (Figure 2.5A). In contrast, six genes were more abundant in the NT soil compared to the other three soils (*nirA*; ferredoxin-nitrite reductase, *cynT*, *can*; carbonic anhydrase, nitronate monooxygenase, nitrate reductase (NADH), *nrfD*; protein NrfD and *hao*; hydroxylamine oxidase) (Figure 2.5B). Three genes (*nirB*; nitrite reductase (NAD(P)H) large subunit, *nosZ*; nitrous-oxide reductase, and *nirD*; nitrite reductase (NAD(P)H) small subunit (Figure 2.5C)) and one gene (nitronate monooxygenase) were dominant in the reduced input soil and biological based soil, respectively (Figure 2.5D).

2.4.2 Phylotypes Associated with Nitrogen Metabolism

The phylotypes (at the class level) associated with the nitrogen metabolism genes have been summarized (Figures 2.6 and 2.7). The CT soil was dominated by *Betaproteobacteria* for *napA*, *narG*, *nirA*, *nirB*, *nirK*, *nirS* and *norB* and by *Cytophagia* for *nosZ*. Further, in many cases (*napA*, *narG*, *nirA*, *nirB*, *nirK, norB*) *Betaproteobacteria* were more abundant in the CT soil compared to the other three soils. For several genes (*napA*, *narG*, *nirK*, *nosZ*), *Alphaproteobacteria* were more abundant in the NT soil compared to the other soils. While for *nirA* and *nirB*, *Alphaproteobacteria* were more abundant in the biological based soil compared to the other three soils. For the genes *napA*, *narG*, *nirK* and *norB*, *Actinobacteria* were more abundant in the NT soil compared to the other three soils. For *nirA* and *nirB*, *Actinobacteria* was approximately at the same level in biological based soil compared to the NT soil while somewhat lower in the conventional tillage and reduced input soils. Additional trends included the dominance of the *Gammaproteobacteria* for two of the four soils for *norB* as well as the dominance of unclassified sequences and *Flavobacteriia* across various soils for *nosZ.*

As no significant differences were noted for *nifH* for the above analysis, differences were investigated for this gene within the assembled contigs. Significant differences at the genera level associated with *nifH* gene between the CT and the other three soils are shown (Figure A2.1). The genus *Frankia* was significantly more abundant in the NT, reduced input and biological based soils compared to the CT soils. Several genera were enriched for this gene in the CT soil compared to the NT soil (e.g. *Rubrivivax, Leptothrix, Cupriavidus*). Also, two (*Paraburkholderia* and *Burkholderia*) were more enriched in the CT compared to the reduced input soils (Figure A2.1B). Four genera were more highly enriched in the comparison between the CT and the biological based soil for this gene (Figure A2.1C).

2.4.3 Comparison of Microbial Communities

When the entire microbial community from the assembled contigs was compared between treatments significant differences were found and are illustrated at the genus level (Figure A2.2). No enriched genera were found in the NT soil compared to the CT soil. Four genera (*Nocardioides*, *Mycobacterium*, *Nakamurella* and *Microvirga*) were enriched in both the reduced input and biological based compared to the CT soil. The other more abundant genera identified in the reduced input compared to the CT soil were *Pseudonocardia* and *Archangium*. The other enriched genera identified in the biological based compared to the CT soil included *Candidatus Nitrosotalea*, *Nitrospira*, *Bradyrhizobium, Actinoplanes, Nonomuraea, Skermanella, Sulfuritortus, Pigmentiphaga and Variibacter.*

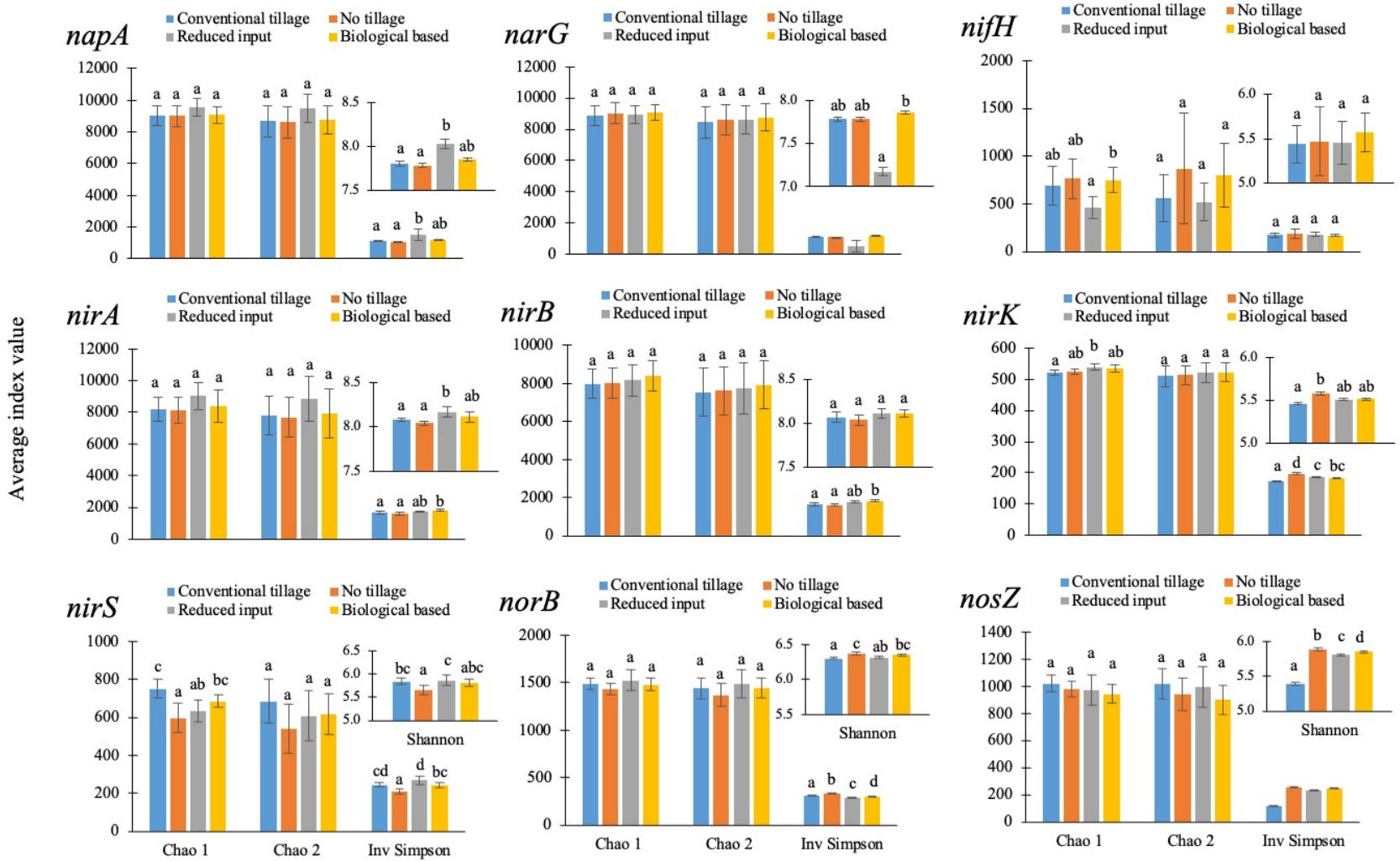

Figure 2.4 Average index diversity values and richness estimators for each soil (as determined by EstimateS, n=6) with standard deviations. Values that are statistically significantly different (ANOVA or Kruskal-Wallis test, p<0.05) are shown with different letters. In some cases, letters are missing because the statistical assumptions were not met for either test. Note, the scale on the y-axis differs between graphs.

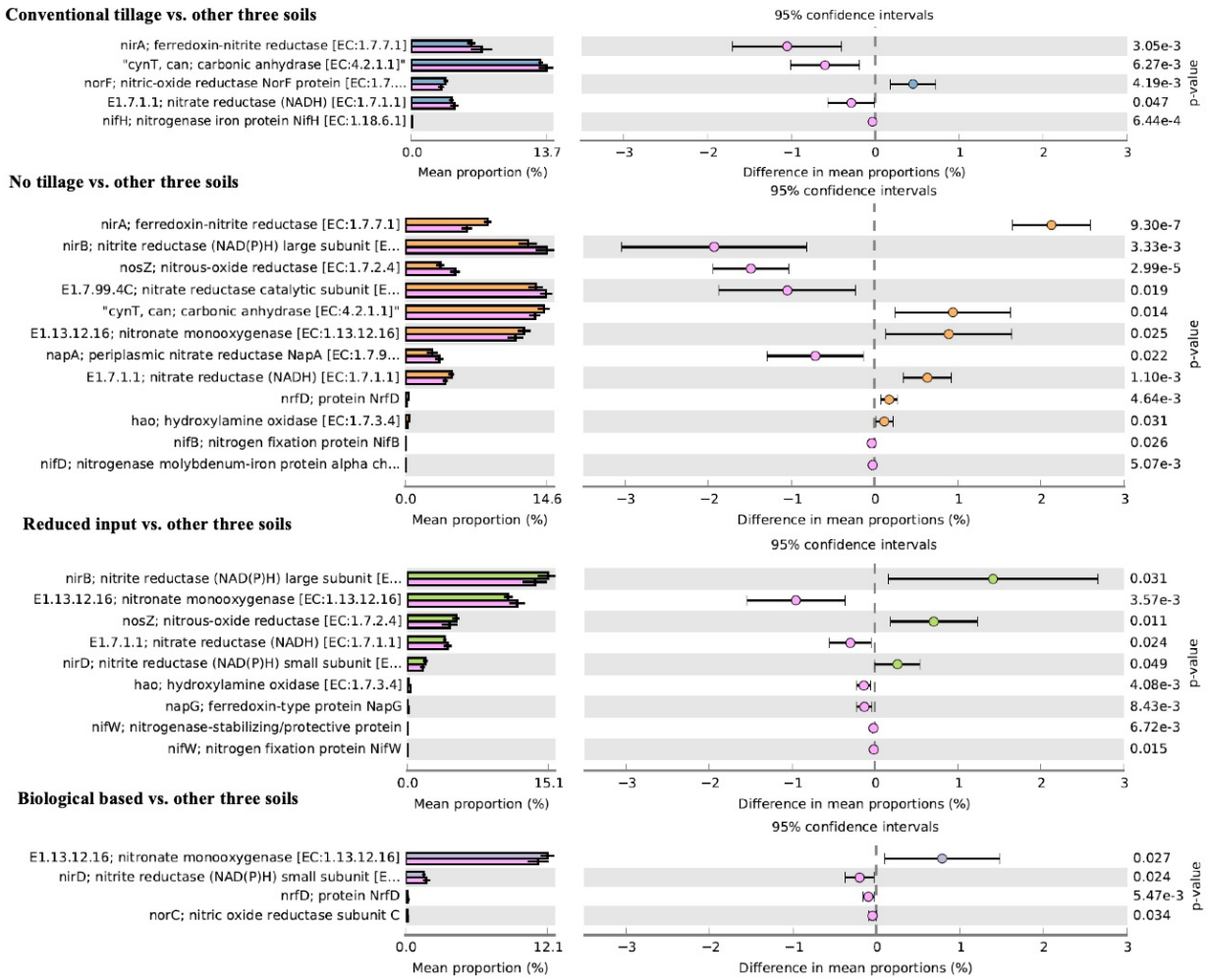

Figure 2.5 Extended error bars illustrating the differences between each treatment compared to the other three treatments for the genes associated with nitrogen metabolism (as defined by the KEGG hierarchy). The data (generated in MG-RAST, six metagenomes for each soil) were analyzed using STAMP with the two-group analysis option (each soil compared to the other three soils) and Welch's two sided t-test (p<0.05).

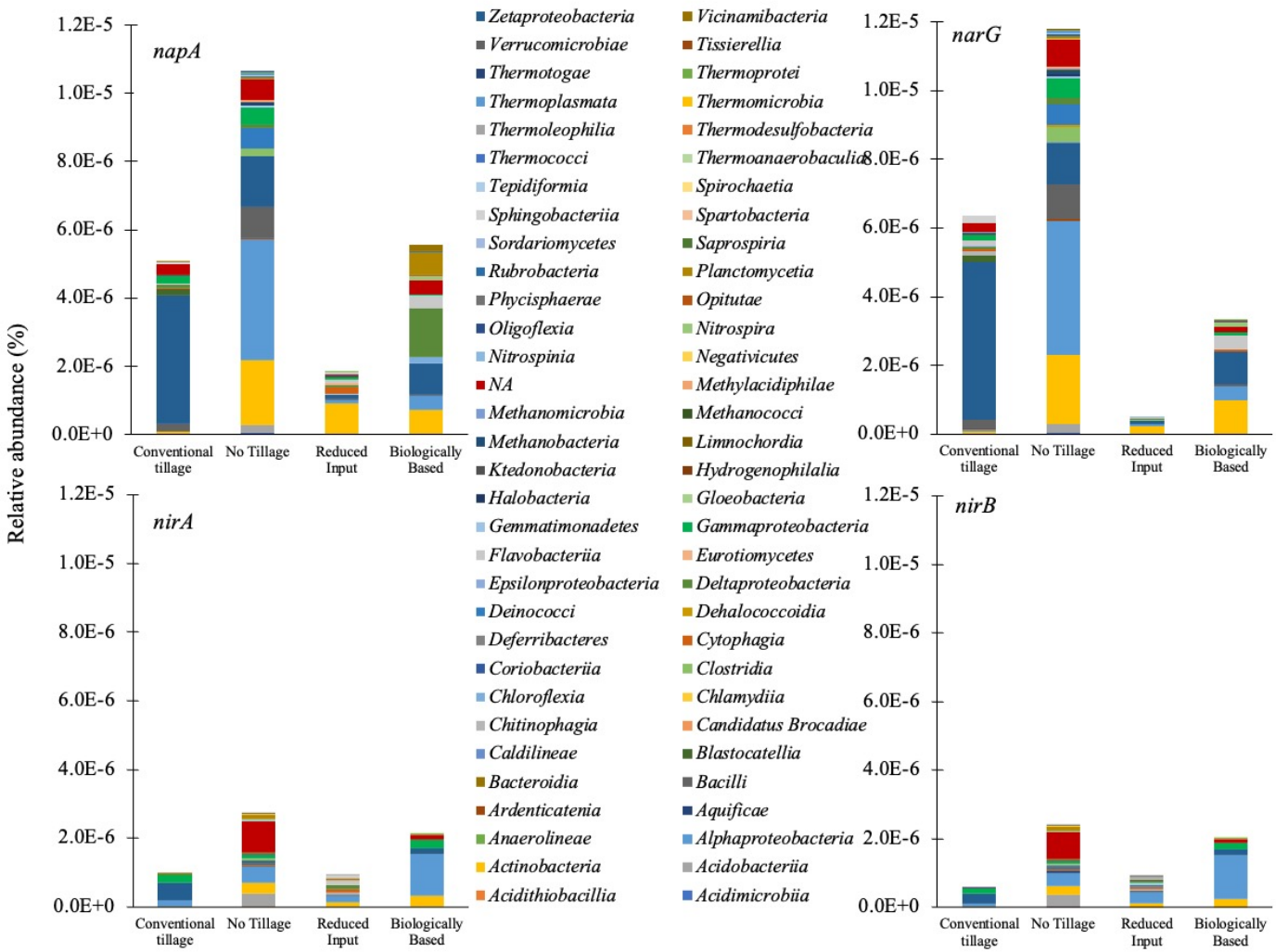

Figure 2.6 Phylotypes enriched in each soil associated with the genes *napA, narG, nirA* and *nirB* at the level of class. All y-axis have the same scale.

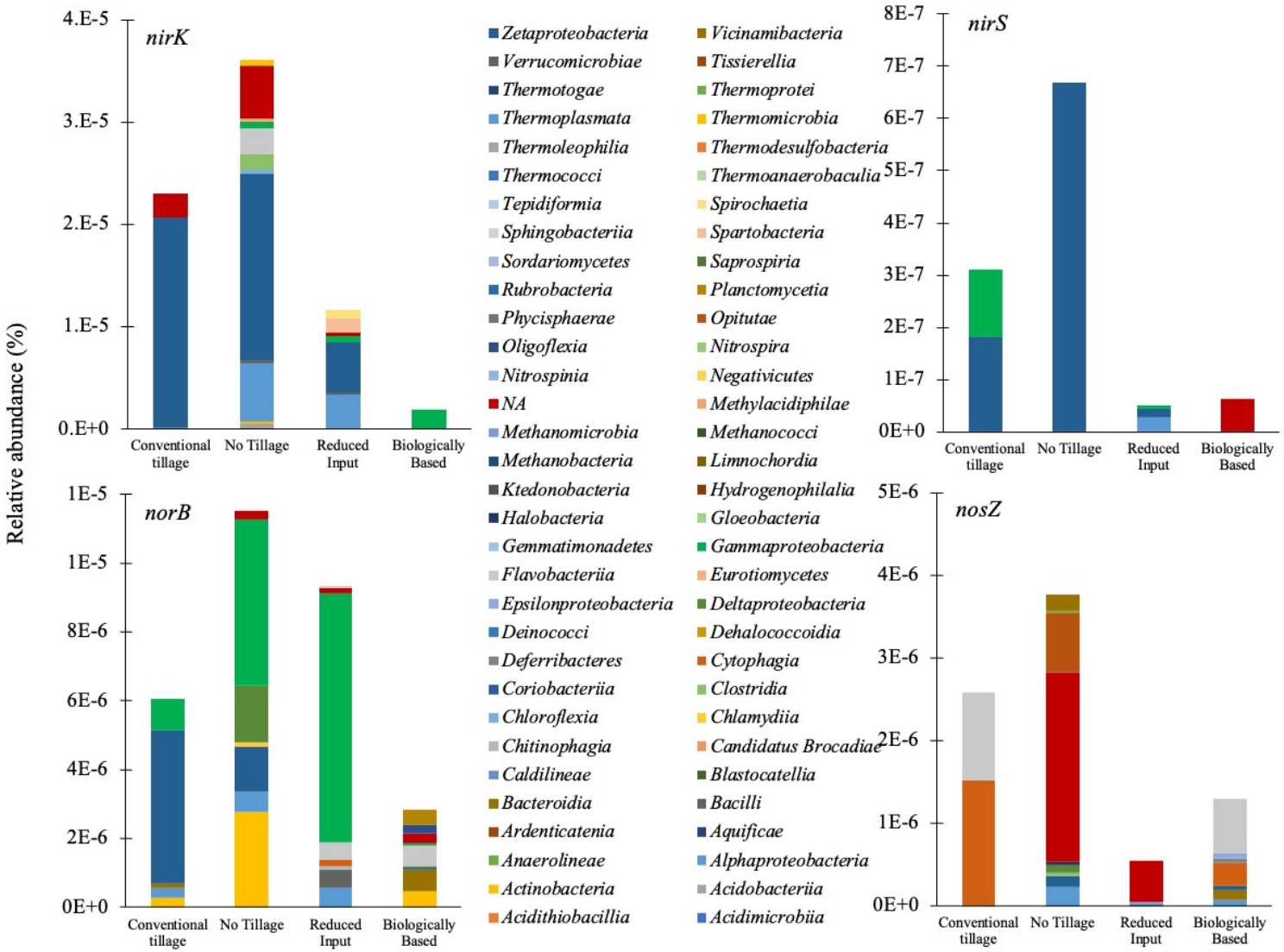

Figure 2.7 Phylotypes enriched in each soil associated with the genes *nirK, nirS, norB* and *nosZ* at the level of class. Note, the y-axis scales on each are different. There was minimal enrichment for any soil for *nifH*, therefore no graph was generated.

(1) *napA*

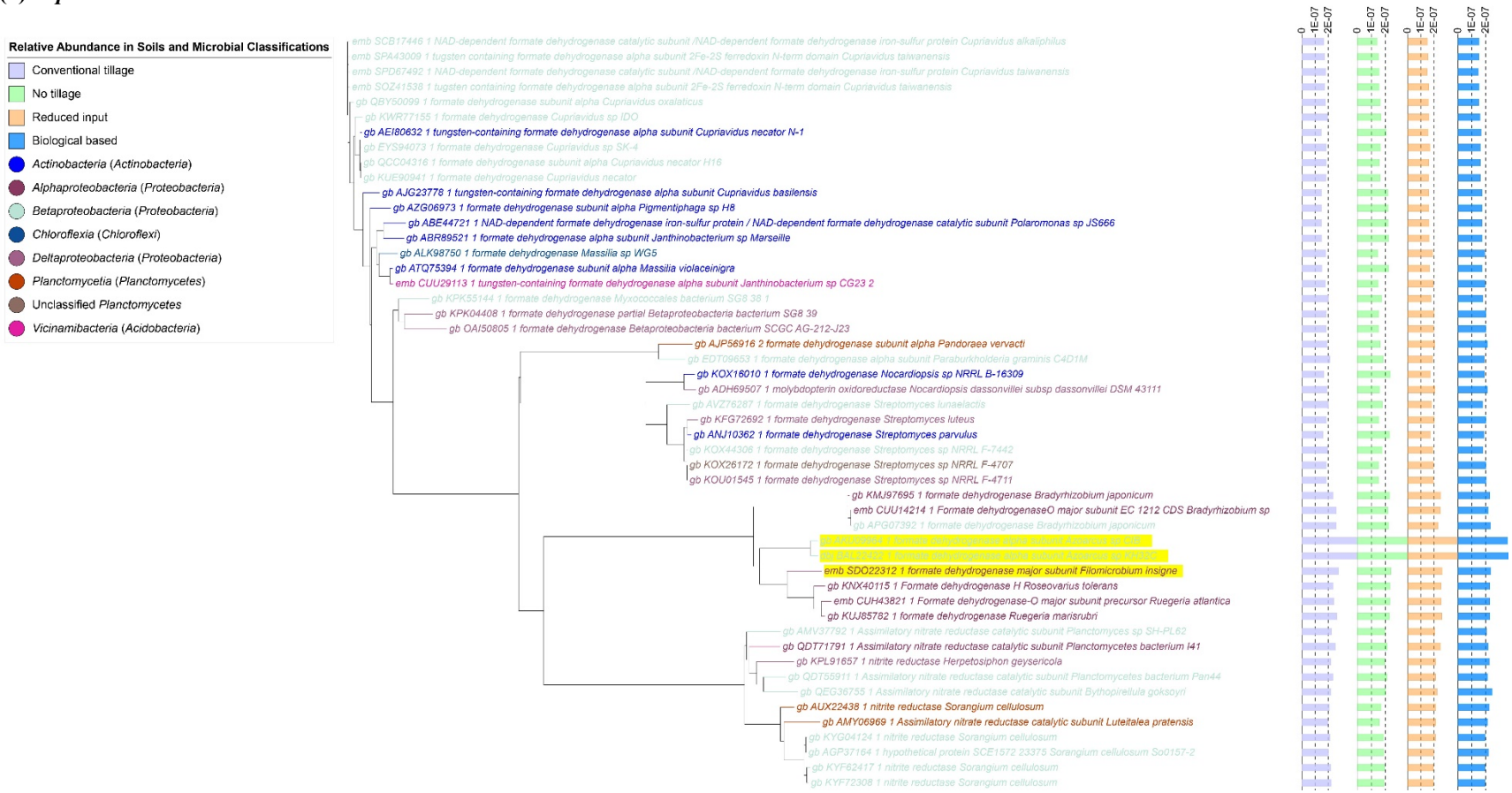

Figure 2.8 Neighbour-Joining phylogenetic trees of fifty most abundant sequences in each soil associated with the genes *napA*, *narG*, *nifH*, *nirA*, *nirB*, *nirK, nirS, norB* and *nosZ*. Note, the bar charts illustrate the relative abundance (%) of the sequences in each soil. The three most abundant sequences are highlighted in yellow.

Figure 2.8 (cont'd)

(2) *narG*

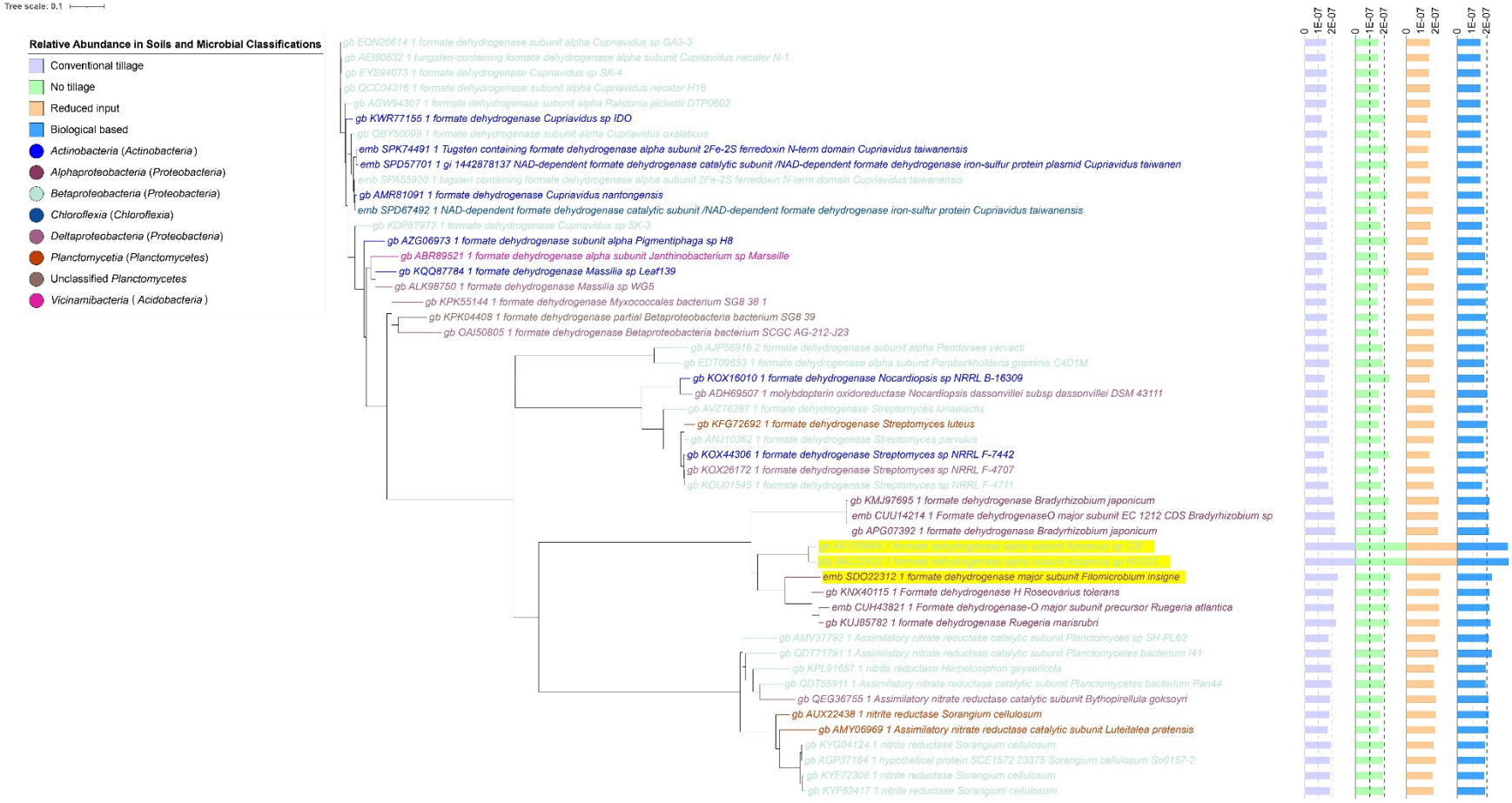

Figure 2.8 (cont'd)

(3) *nifH*

Figure 2.8 (cont'd)

(4) *nirA*

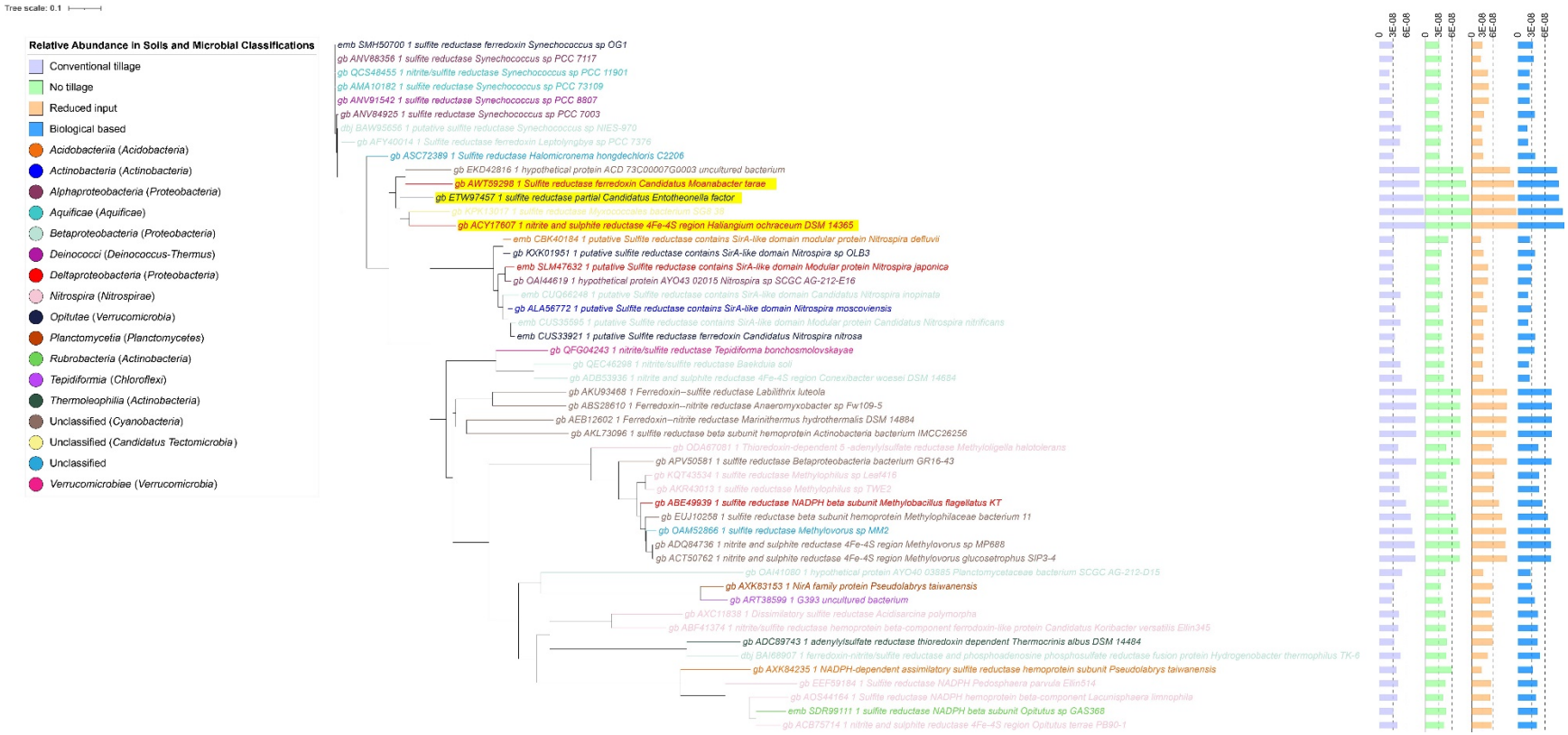

Figure 2.8 (cont'd)

(5) *nirB*

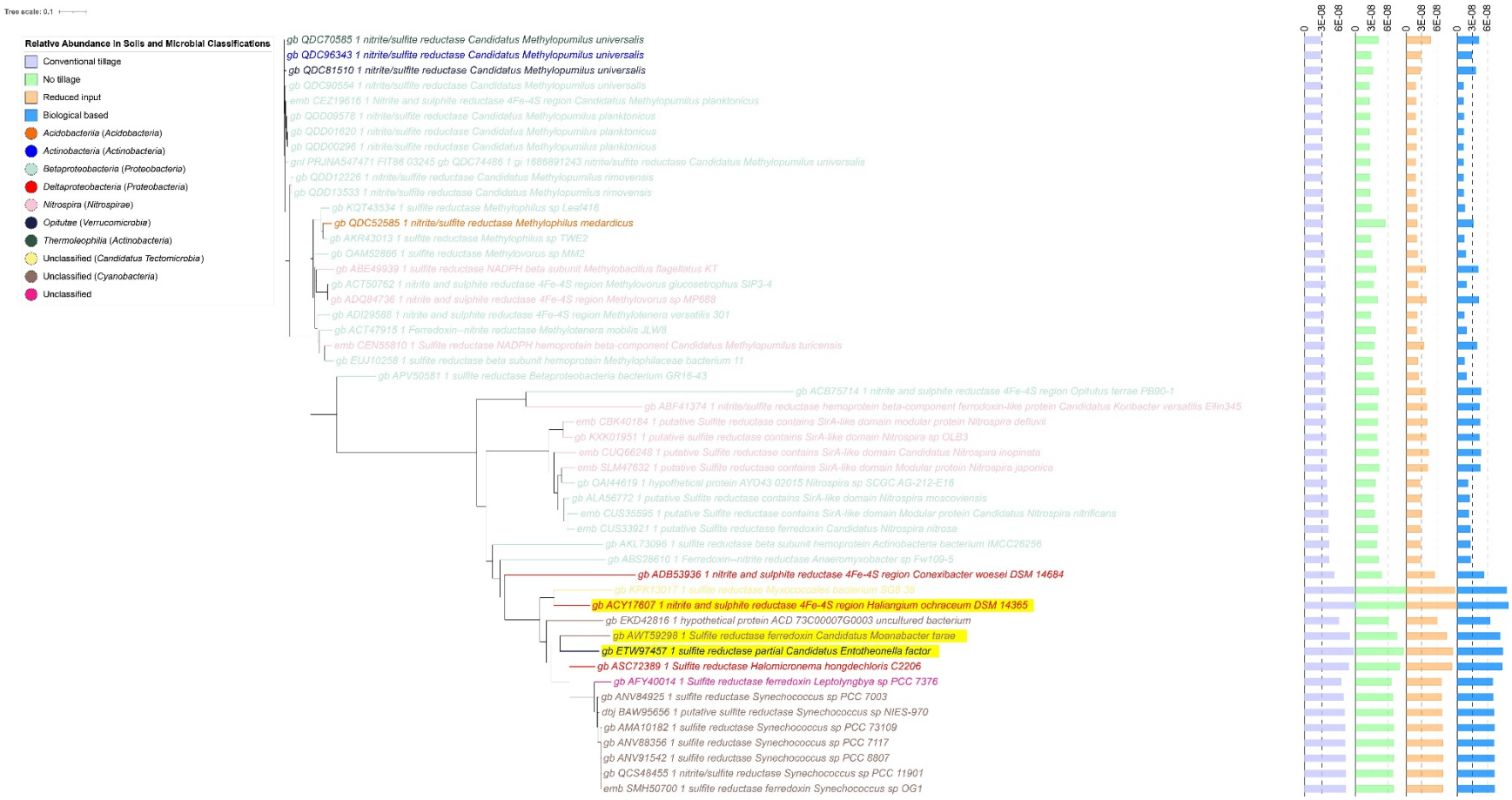

Figure 2.8 (cont'd)

(6) *nirK*

Figure 2.8 (cont'd)

(7) *nirS*

2.4.4 Phylogeny of Most Abundant Sequences

The phylogenetic relationships of the representative sequences (fifty most abundant sequences, before contigs were assembled) for the genes related to nitrogen metabolism in the four soils are shown (Figure 2.8). The three most abundant sequences for *napA* and *narG* were the same sequences and classified as *Betaproteobacteria* and *Alphaproteobacteria*. Similarly, the three most abundant sequences for *nirA* and *nirB* were the same and belonged to *Deltaproteobacteria*, *Opitutae* and the unclassified. The three most abundant sequences for *norB* belonged to *Alphaproteobacteria* and were phylogenetically close to each other. For *nirK* and *nirS*, both the majority of the fifty most abundant sequences and the three most abundant sequences belonged to *Betaproteobacteria*. Moreover, the predominant representative sequences belonged to *Betaproteobacteria* for *nirB*, *nirK* and *nirS* and belonged to *Alphaproteobacteria*, and *Flavobacteriia* for *nifH* and *nosZ*, respectively.

2.5 Discussion

The influence of different agricultural management practices on nitrogen metabolism is important for understanding N_2O emissions from agricultural soils. Here, the taxonomic and functional profiles of the soil microbial communities associated with nitrogen metabolism, primarily denitrification, were characterized in Mid-West agricultural soils under four different management practices. From the nine nitrogen metabolism genes examined in the soil metagenomes, the most abundant was *nirK*. Denitrifying microorganisms contain either a Cu-nitrite reductase or a cytochrome cd_1 nitrite reductase, encoded by *nirK* and *nirS* respectively (Zumft 1997). In the current study, *nirK* was approximately 17.9 times more abundant than *nirS* when all of the soil metagenomes were considered together. Further, consistent with other researchers, *nirK* and *nirS* gene abundance were significantly correlated (Enwall, Throback et al.

2010). Others have also reported higher levels of *nirK* compared to *nirS* in soil metagenomes, for example, *nirK* was up to 3.8 times more abundant than *nirS* in 35 from 37 soils (Jones, Spor et al. 2014). Additionally, *nirK* was more abundant compared to *nirS* during agricultural waste composting (Zhang, Zeng et al. 2015). In another study, *nirK* copy numbers were approximately two orders of magnitude higher than *nirS*, regardless of tillage treatment (Kim, Riggins et al. 2021). These two genes are considered to be mutually exclusive, representing two ecologically distinct denitrifying communities (Enwall, Throback et al. 2010, Jones and Hallin 2010). To date, no microorganism has been reported to contain both types of reductases. It has been suggested that higher *nirS/nirK* ratios may indicate higher N_2O consumption trends (Jones, Spor et al. 2014). Based on this, in the current study, CT represents the highest N_2O consumption potential in four soils examined. Specifically, the average *nirS/nirK* ratios were 0.074, 0.045, 0.045 and 0.056 for CT, NT, reduced input and biological based, respectively. Concerning other genes impacting N_2O depletion and formation, here, *nosZ* was less abundant compared to *norB* and (*nirK*+*nirS*). Others have also reported that *nir* gene abundance can exceed that of *nosZ* by up to one order of magnitude (Hallin, Jones et al. 2009, Garcia-Lledo, Vilar-Sanz et al. 2011, Philippot, Andert et al. 2011). This may be explained by the absence of *nosZ* in nearly one-third of genomes which contained *nir* and *nor* genes (Jones, Stres et al. 2008) and because *nosZ* has been found on plasmids (Zumft 1997).

When considering the different management practices, the abundance of *napA*, *narG*, *nifH*, *nirA* and *nirB* was not significantly different between NT and CT. The same trend was reported for *nifH* and *narG* by others (Liu, Carvalhais et al. 2016). In contrast, we found that *nirK, nirS* and *norB* were statistically significantly lower in the NT compared to the CT treatment. Others have reported an increase in the abundance of denitrifying genes in response to

NT (Baudoin, Philippot et al. 2009, Wang and Zou 2020) or minimal tillage (Kaurin, Mihelic et al. 2018). However, in an experiment across arable soils, the abundance of *nirS*- and *nirK*-denitrifiers were not significantly different between agricultural practices (Domeignoz-Horta, Philippot et al. 2018). Similarly, in another study, the abundance of *nirK* and *nirS* did not differ between NT and CT (Puerta, Six et al. 2019). The authors speculated that NT could have promoted denitrification in the form of higher activity but not the abundance of denitrifying genes. NT was reported to greatly increase the RNA/DNA ratios for *nirS* and *nosZ* denitrifiers (Tatti, Goyer et al. 2015). They hypothesized that anoxic conditions (e.g., water content) contributed more to the *nirS* and *nosZ* transcription under NT compared to CT (Tatti, Goyer et al. 2015). NT tends to reduce the oxygen level below the surface (Pastorelli, Vignozzi et al. 2013) and increase the water-filled pore space because of greater soil moisture and bulk density (Wang and Zou 2020). These two factors may contribute to the potential enhanced anaerobic denitrification in NT soil. No correlation was found between denitrification enzyme activity and the abundances of *nirK*- and *nirS*- denitrifiers (Yin, Fan et al. 2014). More information is needed to determine the real impact of lower *nirK, nirS* and *norB* gene abundances in NT in the current system.

The microbial community richness (Chao1 and Chao2) and diversity (Shannon index and Inverse of Simpson) indices were generally higher for the genes associated with nitrate reduction (*napA* and *narG)* and dissimilatory nitrite reduction (*nirA* and *nirB*) compared to the other genes. For *nirK*, *norB* and *nosZ* for at least one and up to three richness and diversity indexes were significantly greater in NT soil compared to CT soil, indicating a potential higher species richness and diversity in the current NT soil for these genes. In other research, higher alpha diversity of soil bacterial community was found in NT treatment compared to tilled treatment

(Dong, Liu et al. 2017, Liu, Li et al. 2020). Similarly, the richness and diversity of bacteria (characterized by phospholipid fatty acids analysis) were greater in NT over CT soil (Zhang, Li et al. 2015). This may be due to crop residues under the soil surface in NT soils being utilized as food sources (Zhang, Li et al. 2015). Another possible reason is that NT soil contains larger soil aggregates which could provide more organic matter for the microorganisms, therefore enhancing the bacterial diversity (Peixoto, Coutinho et al. 2006). It was demonstrated that denitrification activity was greatly influenced by denitrifier diversity but not the abundance. Using a dilution approach to manipulate the soil microbial community, researchers found that a decrease in the potential denitrification activity could be a result of denitrifier diversity loss and not the lower denitrifier biomass (Philippot, Spor et al. 2013). These trends could suggest that the NT examined in the current study may have a higher denitrification potential due to higher *norB* and *nosZ* diversity, although more research is needed to confirm this hypothesis. It is interesting to note that Chao 1, Shannon and Inverse of Simpson were significantly higher in CT soil compared to NT soils for *nirS*. Inversely, for *nirK*, Shannon and Inverse of Simpson were significantly higher in NT soil over CT soil. A previous study reported that diversity indices targeting *nirS* were more sensitive to environmental factors compared to *nirK* (e.g., ammonium content, total organic carbon and total N) (Li, Li et al. 2017). It was also found that *nirS*-denitrifiers rely more on the full anaerobic conditions than *nirK*-denitrifiers (Yuan, Liu et al. 2012). The greater diversity of *nirK* in NT in the current study could indicate oxygen levels and other environmental conditions in NT soil may be more favorable for *nirK*-denitrifiers than *nirS*-denitrifiers.

Several trends were noted concerning the taxonomy of the microorganisms associated with the functional genes studied. For example, the most abundant sequences classified within

the *Proteobacteria* (primarily *Betaproteobacteria*) for *nirK* and *nirS*. Further, NT illustrated equal or more abundant levels of *Betaproteobacteria* (phylum *Proteobacteria*) compared to CT soil for a number of the genes examined (*nirK*, *nirS, norB and nosZ*). In other systems, *Betaproteobacteria* often dominates microbial populations due to high growth rates under available carbon substrates (Jenkins, Rushton et al. 2010). For *nifH*, *Frankia* (phylum *Actinobacteria*) was enriched in NT reduced input and biologically based soils compared to the CT soil. *Frankia* is a typical nitrogen-fixed organism both in free-living and symbiotic conditions (Sellstedt and Richau 2013).

Two phyla, *Actinobacteria* and *Acidobacteria,* were notably less enriched or absent in CT for several genes (*napA*, *narG, nirA*, *nirB* and *nirK)* compared to the other three soils. Relating these results to previous research, others have examined soil microbial communities under different management systems. For example, one-time tillage increased the abundance of *Actinobacteria* and *Acidobacteria* in an acidic Solonetz with a 19-year NT management in Australia (Liu, Carvalhais et al. 2016). In another study, the abundance of *Acidobacteria* was higher in CT over NT, with the pH of 7.4 and 7.5, respectively (Dong, Liu et al. 2017). *Acidobacteria* are acidophilic and could be favored by slightly to moderately acidic growth conditions (Sait, Davis et al. 2006). Moreover, *Acidobacteria* exhibit the functional ability of the degradation of plant-derived organic matter (Naumoff and Dedysh 2012) and thus play an important role in the decomposition of organic matter (Rampelotto, Ferreira et al. 2013).

For *nosZ*, the most abundant sequences belonged to the *Bacteroidetes* (with the dominant class of *Flavobacteria*). Others have reported *Bacteroidetes* display copiotrophic characteristics and are favored by increased nutrient availability (McHugh and Schwartz 2015). We found *Flavobacteria* was absent in NT soil but dominated in CT soil for *nosZ*. Consistent with these

results, microbial community studies have reported more *Bacteroidetes* in CT compared to NT soil (Yin, Mueth et al. 2017). *Bacteroidetes* were also more dominant in one soil compared to the same soil under non-disturbed grass systems (Acosta-Martinez, Dowd et al. 2008). However, others have reported that *Bacteroidetes* were more abundant under NT compared to CT in winter wheat cropping system (Dong, Liu et al. 2017) and non-disturbed grass system in comparison with agricultural rotation system (Zhang, Wu et al. 2014). Besides, NT increased the abundance of *Flavobacteria* compared to the tilled treatment under semi-arid conditions (Liu, Li et al. 2020). Notably, the above studies did not examine the taxonomy of the microorganisms linked with *nosZ* and so it is difficult to conclude if our results are typical of NT compared to CT soils.

In conclusion, the agricultural management practices investigated here impacted gene abundance as well as the taxonomy of microorganisms associated with the nitrogen metabolism. From the nine genes examined, *nirK* was the most abundant and *nifH* was the least abundant. The *nirS/nirK* ratios were highest for the CT system, which may indicate a greater potential for N_2O consumption. Three genes (*nirK, nirS* and *norB*) were statistically significantly lower in the NT compared to the CT treatment. The microbial community richness and diversity indices were generally higher for the genes associated with nitrate reduction (*napA* and *narG)* and dissimilatory nitrite reduction (*nirA* and *nirB*) compared to the other genes. For *nirK*, *norB* and *nosZ* a number of the richness and diversity indexes were significantly greater in NT soil compared to CT soil, indicating a potentially a higher denitrification potential. A number of trends were noted for the taxonomy of the functional genes across agricultural systems. The genus *Frankia* was significantly more abundant in the NT, reduced input and biological based soils compared to the CT soils. The CT soil was dominated by *Betaproteobacteria* for seven genes and by *Cytophagia* for *nosZ*. Also, for six of these genes, *Betaproteobacteria* were more

abundant in the CT soil compared to the other three soils. *Alphaproteobacteria* were more abundant in the NT soil compared to the other soils for several genes. While for *nirA* and *nirB*, *Alphaproteobacteria* were more abundant in the biological based soil compared to the other three soils. For *napA*, *narG*, *nirK* and *norB*, *Actinobacteria* were more abundant in the NT soil compared to the other three soils. Overall, these results suggest microbial communities involved in nitrogen metabolism are sensitive to varying soil conditions, which in turn, likely has important implications for N_2O emissions.

Acknowledgements

This work was, in part, supported by USDA (Agriculture and Food Research Initiative, Number 2014-67024) and KBS LTER (Kellogg Biological Station Long-Term Ecological Research). Thanks to Stacey VanderWulp from MSU for providing the soil samples from KBS LTER.

REFERENCES

Acosta-Martinez V, Dowd S, Sun Y, Allen V (2008) Tag-encoded pyrosequencing analysis of bacterial diversity in a single soil type as affected by management and land use. Soil Biology & Biochemistry 40(11):2762-2770 doi:10.1016/j.soilbio.2008.07.022

Addinsoft (2020) XLSTAT statistical and data analysis solution., 2020.3.1 edn, New York, USA, p https://www.xlstat.com

Altschul SF, Gish W, Miller W, Myers EW, Lipman DJ (1990) Basic local alignment search tool. J Mol Biol 215(3):403-10 doi:10.1016/S0022-2836(05)80360-2

Attard E, Recous S, Chabbi A, De Berranger C, Guillaumaud N, Labreuche J, Philippot L, Schmid B, Le Roux X (2011) Soil environmental conditions rather than denitrifier abundance and diversity drive potential denitrification after changes in land uses. Global Change Biology 17(5):1975-1989 doi:10.1111/j.1365-2486.2010.02340.x

Baudoin E, Philippot L, Cheneby D, Chapuis-Lardy L, Fromin N, Bru D, Rabary B, Brauman A (2009) Direct seeding mulch-based cropping increases both the activity and the abundance of denitrifier communities in a tropical soil. Soil Biology & Biochemistry 41(8):1703-1709 doi:10.1016/j.soilbio.2009.05.015

Bolger AM, Lohse M, Usadel B (2014) Trimmomatic: a flexible trimmer for Illumina sequence data. Bioinformatics 30(15):2114-20 doi:10.1093/bioinformatics/btu170

Buchfink B, Xie C, Huson DH (2015) Fast and sensitive protein alignment using DIAMOND. Nature Methods 12(1):59-60 doi:10.1038/nmeth.3176

Butterbach-Bahl K, Baggs EM, Dannenmann M, Kiese R, Zechmeister-Boltenstern S (2013) Nitrous oxide emissions from soils: how well do we understand the processes and their controls? Philosophical Transactions of the Royal Society B-Biological Sciences 368(1621) doi:10.1098/rstb.2013.0122

Calderon FJ, Jackson LE, Scow KM, Rolston DE (2001) Short-term dynamics of nitrogen, microbial activity, and phospholipid fatty acids after tillage. Soil Science Society of America Journal 65(1):118-126 doi:10.2136/sssaj2001.651118x

Cole JR, Wang Q, Chai B, Tiedje JM (2011) The Ribosomal Database Project: Sequences and Software for High-Throughput rRNA Analysis. Nucleic Acids Research 42:D633–D642 doi:10.1002/9781118010518.ch36

Colwell RK (2006) EstimateS : statistical estimation of species richness and shared species from simples, version 8.0. http://purloclcorg/estimates

Cox MP, Peterson DA, Biggs PJ (2010) SolexaQA: At-a-glance quality assessment of Illumina second-generation sequencing data. Bmc Bioinformatics 11:6 doi:10.1186/1471-2105-11-485

Domeignoz-Horta LA, Philippot L, Peyrard C, Bru D, Breuil MC, Bizouard F, Justes E, Mary B, Leonard J, Spor A (2018) Peaks of in situ N2O emissions are influenced by N2O-producing and reducing microbial communities across arable soils. Global Change Biology 24(1):360-370 doi:10.1111/gcb.13853

Domeignoz-Horta LA, Putz M, Spor A, Bru D, Breuil MC, Hallin S, Philippot L (2016) Non-denitrifying nitrous oxide-reducing bacteria - An effective N2O sink in soil. Soil Biology & Biochemistry 103:376-379 doi:10.1016/j.soilbio.2016.09.010

Dong W, Liu E, Yan C, Tian J, Zhang H, Zhang Y (2017) Impact of no tillage vs. conventional tillage on the soil bacterial community structure in a winter wheat cropping succession in northern China. European Journal of Soil Biology 80:35-42 doi:10.1016/j.ejsobi.2017.03.001

Enwall K, Throback IN, Stenberg M, Soderstrom M, Hallin S (2010) Soil resources influence spatial patterns of denitrifying communities at scales compatible with land management. Applied and Environmental Microbiology 76(7):2243-2250 doi:10.1128/Aem.02197-09

Fish JA, Chai BL, Wang Q, Sun YN, Brown CT, Tiedje JM, Cole JR (2013) FunGene: the functional gene pipeline and repository. Frontiers in Microbiology 4:14 doi:10.3389/fmicb.2013.00291

Fox J, Weisberg S, Price B, Adler D, Bates D, Baud-Bovy G, Bolker B, Ellison S, Firth D, Friendly M, Gorjanc G, Graves S, Heiberger R, Krivitsky P, Laboissiere R, Maechler M, Monette G, Murdoch D, Nilsson H, Ogle D, Ripley B, Venables W, Walker S, Winsemius D, Zeileis A, R-Core (2020) Package'car': Companion Applied Regression. 3.0-8 edn

Garcia-Lledo A, Vilar-Sanz A, Trias R, Hallin S, Baneras L (2011) Genetic potential for N2O emissions from the sediment of a free water surface constructed wetland. Water Research 45(17):5621-5632 doi:10.1016/j.watres.2011.08.025

Hallin S, Jones CM, Schloter M, Philippot L (2009) Relationship between N-cycling communities and ecosystem functioning in a 50-year-old fertilization experiment. Isme Journal 3(5):597-605 doi:10.1038/ismej.2008.128

Huson DH, Beier S, Flade I, Gorska A, El-Hadidi M, Mitra S, Ruscheweyh HJ, Tappu R (2016) MEGAN Community Edition - Interactive Exploration and Analysis of Large-Scale Microbiome Sequencing Data. PLoS Comput Biol 12(6):e1004957 doi:10.1371/journal.pcbi.1004957

Jenkins SN, Rushton SP, Lanyon CV, Whiteley AS, Waite IS, Brookes PC, Kemmitt S, Evershed RP, O'Donnell AG (2010) Taxon-specific responses of soil bacteria to the addition of low level C inputs. Soil Biology & Biochemistry 42(9):1624-1631 doi:10.1016/j.soilbio.2010.06.002

Jones CM, Hallin S (2010) Ecological and evolutionary factors underlying global and local assembly of denitrifier communities. Isme Journal 4(5):633-641 doi:10.1038/ismej.2009.152

Jones CM, Spor A, Brennan FP, Breuil MC, Bru D, Lemanceau P, Griffiths B, Hallin S, Philippot L (2014) Recently identified microbial guild mediates soil N2O sink capacity. Nature Climate Change 4(9):801-805 doi:10.1038/nclimate2301

Jones CM, Stres B, Rosenquist M, Hallin S (2008) Phylogenetic analysis of nitrite, nitric oxide, and nitrous oxide respiratory enzymes reveal a complex evolutionary history for denitrification. Molecular Biology and Evolution 25(9):1955-1966 doi:10.1093/molbev/msn146

Kaharabata SK, Drury CF, Priesack E, Desjardins RL, McKenney DJ, Tan CS, Reynolds D (2003) Comparing measured and Expert-N predicted N2O emissions from conventional till and no till corn treatments. Nutrient Cycling in Agroecosystems 66(2):107-118 doi:10.1023/a:1023978830307

Kanehisa M (2002) The KEGG database. In Silico Simulation of Biological Processes 247:91-103

Kassambara A (2020) rstatix: Pipe-Friendly Framework for Basic Statistical Tests. 0.6.0 edn

Katoh K, Rozewicki J, Yamada KD (2019) MAFFT online service: multiple sequence alignment, interactive sequence choice and visualization. Brief Bioinform 20(4):1160-1166 doi:10.1093/bib/bbx108

Kaurin A, Mihelic R, Kastelec D, Grcman H, Bru D, Philippot L, Suhadolc M (2018) Resilience of bacteria, archaea, fungi and N-cycling microbial guilds under plough and conservation tillage, to agricultural drought. Soil Biology & Biochemistry 120:233-245 doi:10.1016/j.soilbio.2018.02.007

Kim N, Riggins CW, Rodriguez-Zas S, Zabaloy MC, Villamil MB (2021) Long-term residue removal under tillage decreases amoA-nitrifiers and stimulates nirS-denitrifier groups in the soil. Applied Soil Ecology 157 doi:10.1016/j.apsoil.2020.103730

Lee J, Six J, King AP, Van Kessel C, Rolston DE (2006) Tillage and field scale controls on greenhouse gas emissions. Journal of Environmental Quality 35(3):714-725 doi:10.2134/jeq2005.0337

Letunic I, Bork P (2019) Interactive Tree Of Life (iTOL) v4: recent updates and new developments. Nucleic Acids Res 47(W1):W256-W259 doi:10.1093/nar/gkz239

Li D, Luo R, Liu CM, Leung CM, Ting HF, Sadakane K, Yamashita H, Lam TW (2016) MEGAHIT v1.0: A fast and scalable metagenome assembler driven by advanced methodologies and community practices. Methods 102:3-11 doi:10.1016/j.ymeth.2016.02.020

Li F, Li M, Shi W, Li H, Sun Z, Gao Z (2017) Distinct distribution patterns of proteobacterial nirK- and nirS-type denitrifiers in the Yellow River estuary, China. Canadian Journal of Microbiology 63(8):708-718 doi:10.1139/cjm-2017-0053

Li Y, Zhang Q, Cai Y, Yang Q, Chang SX (2020) Minimum tillage and residue retention increase soil microbial population size and diversity: Implications for conservation tillage. Science of the Total Environment 716 doi:10.1016/j.scitotenv.2020.137164

Liu C, Li LL, Xie JH, Coulter JA, Zhang RZ, Luo ZZ, Cai LQ, Wang LL, Gopalakrishnan S (2020) Soil Bacterial Diversity and Potential Functions Are Regulated by Long-Term Conservation Tillage and Straw Mulching. Microorganisms 8(6) doi:10.3390/microorganisms8060836

Liu H, Carvalhais LC, Crawford M, Dang YP, Dennis PG, Schenk PM (2016) Strategic tillage increased the relative abundance of Acidobacteria but did not impact on overall soil microbial properties of a 19-year no-till Solonetz. Biology and Fertility of Soils 52(7):1021-1035 doi:10.1007/s00374-016-1138-0

McHugh TA, Schwartz E (2015) Changes in plant community composition and reduced precipitation have limited effects on the structure of soil bacterial and fungal communities present in a semiarid grassland. Plant and Soil 388(1-2):175-186 doi:10.1007/s11104-014-2269-4

Melero S, Perez-de-Mora A, Manuel Murillo J, Buegger F, Kleinedam K, Kublik S, Vanderlinden K, Moreno F, Schloter M (2011) Denitrification in a vertisol under long-term tillage and no-tillage management in dryland agricultural systems: Key genes and potential rates. Applied Soil Ecology 47(3):221-225 doi:10.1016/j.apsoil.2010.12.003

Meyer F, Paarmann D, D'Souza M, Olson R, Glass EM, Kubal M, Paczian T, Rodriguez A, Stevens R, Wilke A, Wilkening J, Edwards RA (2008) The metagenomics RAST server - a public resource for the automatic phylogenetic and functional analysis of metagenomes. Bmc Bioinformatics 9:8 doi:10.1186/1471-2105-9-386

Naumoff DG, Dedysh SN (2012) Lateral gene transfer between the Bacteroidetes and Acidobacteria: The case of alpha-L-rhamnosidases. Febs Letters 586(21):3843-3851 doi:10.1016/j.febslet.2012.09.005

Ogle D, Wheeler P, Dinno A (2020) FSA: Simple Fisheries Stock Assessment Methods. 0.8.30 edn

Papadopoulos JS, Agarwala R (2007) COBALT: constraint-based alignment tool for multiple protein sequences. Bioinformatics 23(9):1073-9 doi:10.1093/bioinformatics/btm076

Parks DH, Tyson GW, Hugenholtz P, Beiko RG (2014) STAMP: statistical analysis of taxonomic and functional profiles. Bioinformatics 30(21):3123-3124 doi:10.1093/bioinformatics/btu494

Pastorelli R, Vignozzi N, Landi S, Piccolo R, Orsini R, Seddaiu G, Roggero PP, Pagliai M (2013) Consequences on macroporosity and bacterial diversity of adopting a no-tillage farming system in a clayish soil of Central Italy. Soil Biology & Biochemistry 66:78-93 doi:10.1016/j.soilbio.2013.06.015

Peixoto RS, Coutinho HLC, Madari B, Machado PLOA, Rumjanek NG, Van Elsas JD, Seldin L, Rosado AS (2006) Soil aggregation and bacterial community structure as affected by tillage and cover cropping in the Brazilian Cerrados. Soil & Tillage Research 90(1-2):16-28 doi:10.1016/j.still.2005.08.001

Philippot L, Andert J, Jones CM, Bru D, Hallin S (2011) Importance of denitrifiers lacking the genes encoding the nitrous oxide reductase for N2O emissions from soil. Global Change Biology 17(3):1497-1504 doi:10.1111/j.1365-2486.2010.02334.x

Philippot L, Hallin S, Schloter M (2007) Ecology of denitrifying prokaryotes in agricultural soil. In: Sparks DL (ed) Advances in Agronomy, Vol 96. Advances in Agronomy, vol 96. Elsevier Academic Press Inc, San Diego, pp 249-305

Philippot L, Spor A, Henault C, Bru D, Bizouard F, Jones CM, Sarr A, Maron P-A (2013) Loss in microbial diversity affects nitrogen cycling in soil. Isme Journal 7(8):1609-1619 doi:10.1038/ismej.2013.34

Prosser JI, Nicol GW (2012) Archaeal and bacterial ammonia-oxidisers in soil: the quest for niche specialisation and differentiation. Trends in Microbiology 20(11):523-531 doi:10.1016/j.tim.2012.08.001

Pruitt KD, Tatusova T, Maglott DR (2005) NCBI Reference Sequence (RefSeq): a curated non-redundant sequence database of genomes, transcripts and proteins. Nucleic Acids Research 33:D501-D504 doi:10.1093/nar/gki025

Puerta VL, Six J, Wittwer R, van der Heijden M, Pereira EIP (2019) Comparable bacterial-mediated nitrogen supply and losses under organic reduced tillage and conventional intensive tillage. European Journal of Soil Biology 95 doi:10.1016/j.ejsobi.2019.103121

R_Core_Team (2018) R: A language and environment for statistical computing. vol URL https://www.R-project.org/, Vienna, Austria.

Rampelotto PH, Ferreira AdS, Muller Barboza AD, Wurdig Roesch LF (2013) Changes in Diversity, Abundance, and Structure of Soil Bacterial Communities in Brazilian Savanna Under Different Land Use Systems. Microbial Ecology 66(3):593-607 doi:10.1007/s00248-013-0235-y

Ravishankara AR, Daniel JS, Portmann RW (2009) Nitrous Oxide (N2O): The dominant ozone-depleting substance emitted in the 21st Century. Science 326(5949):123-125 doi:10.1126/science.1176985

RStudio_Team (2020) RStudio: Integrated Development for R. RStudio, PBC. Boston, MA pURL http://www.rstudio.com/

Rudy AP, Harris CK, Thomas BJ, Worosz MR, Kaplan SC, O'Donnell EC (2008) The political ecology of Southwest Michigan Agriculture, 1837-200. In: Redman CL, Foster DR (eds) Agrarian landscapes in transition. Oxford University Press, New York

Sait M, Davis KER, Janssen PH (2006) Effect of pH on isolation and distribution of members of subdivision 1 of the phylum Acidobacteria occurring in soil. Applied and Environmental Microbiology 72(3):1852-1857 doi:10.1128/aem.72.3.1852-1857.2006

Sellstedt A, Richau KH (2013) Aspects of nitrogen-fixing Actinobacteria, in particular free-living and symbiotic Frankia. FEMS Microbiology Letters 342(2):179-186 doi:10.1111/1574-6968.12116

Sherrill-Mix S (2009) taxonomizr: Functions to Work with NCBI Accessions and Taxonomy., R package 0.5.3 edn

Sherrill-Mix S (2019) taxonomizr: Functions to Work with NCBI Accessions and Taxonomy. . R package version 0.5.3. edn

Smith CR, Blair PL, Boyd C, Cody B, Hazel A, Hedrick A, Kathuria H, Khurana P, Kramer B, Muterspaw K, Peck C, Sells E, Skinner J, Tegeler C, Wolfe Z (2016) Microbial community responses to soil tillage and crop rotation in a corn/soybean agroecosystem. Ecology and Evolution 6(22):8075-8084 doi:10.1002/ece3.2553

Syakila A, Kroeze C (2011) The global nitrous oxide budget revisited. Greenhouse Gas Measurement Management 1:17-26

Tatti E, Goyer C, Burton DL, Wertz S, Zebarth BJ, Chantigny M, Filion M (2015) Tillage Management and Seasonal Effects on Denitrifier Community Abundance, Gene Expression and Structure over Winter. Microbial Ecology 70(3):795-808 doi:10.1007/s00248-015-0591-x

Team R (2020) RStudio: Integrated Development for R. RStudio, PBC. Boston, MA

Team RC (2018) R: A language and environment for statistical computing. R Foundation for Statistical Computing, Vienna, Austria.

Thelusmond JR, Strathmann TJ, Cupples AM (2019) Carbamazepine, triclocarban and triclosan biodegradation and the phylotypes and functional genes associated with xenobiotic degradation in four agricultural soils. Science of the Total Environment 657:1138-1149 doi:10.1016/j.scitotenv.2018.12.145

Wang J, Zou J (2020) No-till increases soil denitrification via its positive effects on the activity and abundance of the denitrifying community. Soil Biology & Biochemistry 142 doi:10.1016/j.soilbio.2020.107706

Yin C, Fan F, Song A, Li Z, Yu W, Liang Y (2014) Different denitrification potential of aquic brown soil in Northeast China under inorganic and organic fertilization accompanied by

distinct changes of nirS- and nirK-denitrifying bacterial community. European Journal of Soil Biology 65:47-56 doi:10.1016/j.ejsobi.2014.09.003

Yin CT, Mueth N, Hulbert S, Schlatter D, Paulitz TC, Schroeder K, Prescott A, Dhingra A (2017) Bacterial Communities on Wheat Grown Under Long-Term Conventional Tillage and No-Till in the Pacific Northwest of the United States. Phytobiomes Journal 1(2):83-90 doi:10.1094/pbiomes-09-16-0008-r

Yuan Q, Liu P, Lu Y (2012) Differential responses of nirK- and nirS-carrying bacteria to denitrifying conditions in the anoxic rice field soil. Environmental Microbiology Reports 4(1):113-122 doi:10.1111/j.1758-2229.2011.00311.x

Zhang L, Zeng G, Zhang J, Chen Y, Yu M, Lu L, Li H, Zhu Y, Yuan Y, Huang A, He L (2015a) Response of denitrifying genes coding for nitrite (nirK or nirS) and nitrous oxide (nosZ) reductases to different physico-chemical parameters during agricultural waste composting. Applied Microbiology and Biotechnology 99(9):4059-4070 doi:10.1007/s00253-014-6293-3

Zhang S, Li Q, Lü Y, Sun X, Jia S, Zhang X, Liang W (2015b) Conservation tillage positively influences the microflora and microfauna in the black soil of Northeast China. Soil and Tillage Research 149:46 - 52 doi:https://doi.org/10.1016/j.still.2015.01.001

Zhang W, Wu XK, Liu GX, Dong ZB, Zhang GS, Chen T, Dyson PJ (2014) Tag-encoded pyrosequencing analysis of bacterial diversity within different alpine grassland ecosystems of the Qinghai-Tibet Plateau, China. Environmental Earth Sciences 72(3):779-786 doi:10.1007/s12665-013-3001-z

Zumft WG (1997) Cell biology and molecular basis of denitrification. Microbiology and Molecular Biology Reviews 61(4):533-+ doi:10.1128/.61.4.533-616.1997

APPENDIX

Table A2.1 DIAMOND sequence data summary.

	On Fungene	Minimum HMM Coverage 70%	Dereplicated
napA	74937	40226	11395
narG	50753	49174	11395
nosZ	5304	3787	1266
norB	13238	7054	1778
nifH	19514	3474	1562
nirK	7988	3367	556
nirS	25330	3020	993
nirA	54085	51514	12955
nirB	90760	45767	12955

Table A2.2 MG-RAST sequence data summary.

Soil type	MG-RAST ID	Post QC: bp Count	Post QC: Sequences Count	Post QC: Mean Sequence Length bp
Conventional tillage	mgm4887245.3	1,049,991,462 bp	4,562,115	230 ± 37 bp
Conventional tillage	mgm4889385.3	865,087,512 bp	3,773,767	229 ± 38 bp
Conventional tillage	mgm4887247.3	873,760,585 bp	3,805,693	230 ± 38 bp
Conventional tillage	mgm4887261.3	1,042,733,021 bp	4,497,130	232 ± 37 bp
Conventional tillage	mgm4887259.3	1,186,811,683 bp	5,171,096	230 ± 37 bp
Conventional tillage	mgm4887263.3	1,049,806,246 bp	4,606,628	228 ± 38 bp
No tillage	mgm4887248.3	978,574,572 bp	4,289,260	228 ± 38 bp
No tillage	mgm4887249.3	1,021,883,457 bp	4,491,203	228 ± 38 bp
No tillage	mgm4887251.3	893,615,124 bp	3,901,326	229 ± 38 bp
No tillage	mgm4887262.3	1,052,482,005 bp	4,556,161	231 ± 37 bp
No tillage	mgm4887265.3	1,171,824,030 bp	5,106,093	229 ± 37 bp
No tillage	mgm4887264.3	1,151,447,486 bp	5,131,392	224 ± 39 bp
Reduced input	mgm4887252.3	1,020,227,225 bp	4,473,295	228 ± 38 bp
Reduced input	mgm4887253.3	1,156,421,815 bp	5,084,544	227 ± 38 bp
Reduced input	mgm4887254.3	845,604,740 bp	3,689,278	229 ± 38 bp
Reduced input	mgm4887267.3	904,740,521 bp	3,896,151	232 ± 37 bp
Reduced input	mgm4887266.3	1,216,560,266 bp	5,320,030	229 ± 38 bp
Reduced input	mgm4887268.3	923,078,351 bp	4,016,875	230 ± 37 bp
Biological based	mgm4887255.3	1,070,768,940 bp	4,666,479	229 ± 38 bp
Biological based	mgm4887256.3	1,048,398,089 bp	4,589,220	228 ± 38 bp
Biological based	mgm4887258.3	1,095,942,092 bp	4,834,482	227 ± 38 bp
Biological based	mgm4887270.3	1,410,382,064 bp	6,169,872	229 ± 38 bp
Biological based	mgm4887289.3	1,149,249,456 bp	5,008,186	229 ± 37 bp
Biological based	mgm4887290.3	1,303,754,397 bp	5,670,793	230 ± 37 bp

Table A2.3 P-values for statistical tests with the relative abundance of genes associated with nitrogen metabolism copies. "N/A" indicates the test was not appropriate and p-values in bold indicate a significant difference ($p \leq 0.05$).

Test	**Shapiro-Wilk test**				**Levene's test**	**One-way ANOVA**	**Kruskal-Wallis test**
Null Hypothesis	**The sample distribution is normal**				**$\sigma_1=\sigma_2$**	**$\mu_1=\mu_2$**	**$Median_1=Median_2$**
Soil groups	**Conventional tillage**	**No tillage**	**Reduced input**	**Biological based**			
napA	1.57E-01	7.77E-01	**2.50E-04**	7.69E-01	5.35E-01	N/A	6.02E-02
narG	1.59E-01	7.66E-01	6.31E-01	1.71E-01	9.14E-02	2.74E-01	N/A
nifH	6.03E-01	7.31E-01	2.20E-01	2.44E-01	8.27E-01	**1.26E-02**	N/A
nirA	7.19E-02	2.20E-01	**3.40E-04**	5.73E-01	5.45E-01	N/A	4.81E-01
nirB	8.65E-01	**2.11E-02**	1.34E-02	5.69E-01	3.49E-01	N/A	4.09E-01
nirK	7.12E-01	3.27E-01	6.55E-01	5.24E-01	1.33E-01	**1.61E-05**	N/A
nirS	9.31E-01	1.16E-01	3.44E-01	4.63E-02	4.37E-01	**2.22E-05**	N/A
norB	5.97E-01	3.68E-01	8.43E-01	5.68E-01	3.81E-01	**1.85E-02**	N/A
nosZ	N/A	N/A	N/A	N/A	5.81E-03	N/A	N/A

Table A2.4 P-values for Tukey HSD test with the relative abundance of genes associated with nitrogen metabolism copies. "N/A" indicates the test was not appropriate and p-values in bold indicate a significant difference ($p \leq 0.05$).

Test	**Tukey's HSD test**								
Null Hypothesis	**$\mu_1 = \mu_2$**								
Genes	***napA***	***narG***	***nifH***	***nirA***	***nirB***	***nirK***	***nirS***	***norB***	***nosZ***
Conventional tillage - No tillage	N/A	N/A	4.14E-01	N/A	N/A	**1.14E-05**	**2.07E-05**	**1.16E-02**	N/A
Conventional tillage - Reduced input	N/A	N/A	9.03E-01	N/A	N/A	3.84E-01	**2.33E-04**	4.65E-01	N/A
Conventional tillage - Biological based	N/A	N/A	1.89E-01	N/A	N/A	1.79E-01	**9.27E-03**	1.65E-01	N/A
No tillage - Reduced input	N/A	N/A	1.42E-01	N/A	N/A	**4.10E-04**	6.94E-01	2.22E-01	N/A
No tillage- Biological based	N/A	N/A	**7.59E-03**	N/A	N/A	**1.26E-03**	5.82E-02	5.68E-01	N/A
Reduced input - Biological based	N/A	N/A	5.06E-01	N/A	N/A	9.60E-01	3.88E-01	9.00E-01	N/A

Table A2.5 P-values for Dunn's test with the relative abundance of genes associated with nitrogen metabolism copies. "N/A" indicates the test was not appropriate and p-values in bold indicate a significant difference ($p \leq 0.05$).

Test	**Dunn's test**								
Null Hypothesis	**$\mu_1 = \mu_2$**								
Genes	***napA***	***narG***	***nifH***	***nirA***	***nirB***	***nirK***	***nirS***	***norB***	***nosZ***
Conventional tillage - No tillage	N/A	N/A	N/A	N/A	N/A	N/A	N/A	N/A	N/A
Conventional tillage - Reduced input	N/A	N/A	N/A	N/A	N/A	N/A	N/A	N/A	N/A
Conventional tillage - Biological based	N/A	N/A	N/A	N/A	N/A	N/A	N/A	N/A	N/A
No tillage - Reduced input	N/A	N/A	N/A	N/A	N/A	N/A	N/A	N/A	N/A
No tillage - Biological based	N/A	N/A	N/A	N/A	N/A	N/A	N/A	N/A	N/A
Reduced input - Biological based	N/A	N/A	N/A	N/A	N/A	N/A	N/A	N/A	N/A

Table A2.6 Summary of the p values from Spearman's rank correlation tests with gene relative abundance data. Values in bold indicate a significant difference ($p \leq 0.05$).

Genes	***napA***	***narG***	***nifH***	***nirA***	***nirB***	***nirK***	***nirS***	***norB***	***nosZ***
napA		**1.66E-07**	4.74E-01	**< 2.2e-16**	**1.43E-08**	**2.30E-06**	8.67E-02	**1.28E-08**	**4.26E-06**
narG	**1.66E-07**		**4.11E-02**	**2.74E-04**	**8.32E-03**	**3.30E-03**	4.70E-01	**3.12E-02**	3.63E-01
nifH	4.74E-01	**4.11E-02**		9.83E-01	7.64E-02	**7.37E-03**	2.02E-01	8.42E-01	2.86E-01
nirA	**< 2.2e-16**	**2.74E-04**	9.83E-01		**4.60E-02**	5.80E-01	6.15E-01	1.08E-01	5.87E-01
nirB	**1.43E-08**	**8.32E-03**	7.64E-02	**4.60E-02**		8.05E-01	6.89E-01	5.47E-01	9.87E-01
nirK	**2.30E-06**	**3.30E-03**	**7.37E-03**	5.80E-01	8.05E-01		**4.84E-03**	**1.98E-02**	**1.26E-02**
nirS	8.67E-02	4.70E-01	2.02E-01	6.15E-01	6.89E-01	**4.84E-03**		**2.12E-04**	**1.76E-03**
norB	**1.28E-08**	**3.12E-02**	8.42E-01	1.08E-01	5.47E-01	**1.98E-02**	**2.12E-04**		**7.65E-05**
nosZ	**4.26E-06**	3.63E-01	2.86E-01	5.87E-01	9.87E-01	**1.26E-02**	**1.76E-03**	**7.65E-05**	

Table A2.7 Summary of Spearman's correlation coefficient (rho) for Spearman's rank correlation test with gene relative abundance data. Rho values in bold indicate a statistically significant correlation ($p \leq 0.05$), as shown above.

Genes	***napA***	***narG***	***nifH***	***nirA***	***nirB***	***nirK***	***nirS***	***norB***	***nosZ***
napA		**8.48E-01**	1.54E-01	**9.81E-01**	**8.80E-01**	**8.03E-01**	3.57E-01	**8.81E-01**	**7.91E-01**
narG	**8.48E-01**		**4.20E-01**	**6.78E-01**	5.26E-01	**5.75E-01**	1.55E-01	**4.41E-01**	1.94E-01
nifH	1.54E-01	**4.20E-01**		-4.57E-03	3.69E-01	**5.33E-01**	2.70E-01	4.29E-02	2.27E-01
nirA	**9.81E-01**	**6.78E-01**	-4.57E-03		**4.11E-01**	1.19E-01	-1.08E-01	3.37E-01	1.17E-01
nirB	**8.80E-01**	5.26E-01	3.69E-01	**4.11E-01**		5.31E-02	-8.62E-02	1.29E-01	3.48E-03
nirK	**8.03E-01**	**5.75E-01**	**5.33E-01**	1.19E-01	5.31E-02		**5.55E-01**	**4.72E-01**	**5.01E-01**
nirS	3.57E-01	1.55E-01	2.70E-01	-1.08E-01	-8.62E-02	**5.55E-01**		**6.87E-01**	**6.04E-01**
norB	**8.81E-01**	**4.41E-01**	4.29E-02	3.37E-01	1.29E-01	**4.72E-01**	**6.87E-01**		**7.19E-01**
nosZ	**7.91E-01**	1.94E-01	2.27E-01	1.17E-01	3.48E-03	**5.01E-01**	**6.04E-01**	**7.19E-01**	

Table A2.8 P-values for statistical tests with the richness index chao 1 of genes associated with nitrogen metabolism copies. "N/A" indicates the test was not appropriate and p-values in bold indicate a significant difference ($p \leq 0.05$).

Test	**Shapiro-Wilk test**				**Levene's test**	**One-way ANOVA**	**Kruskal-Wallis test**
Null Hypothesis	**The sample distribution is normal**				**$\sigma_1=\sigma_2$**	**$\mu_1=\mu_2$**	**$Median_1=Median_2$**
Soil groups	**Conventional tillage**	**No tillage**	**Reduced input**	**Biological based**			
napA	4.89E-01	6.42E-01	2.90E-01	2.63E-01	9.37E-01	3.56E-01	N/A
narG	4.66E-01	5.43E-01	2.78E-01	2.82E-01	9.42E-01	9.37E-01	N/A
nifH	9.76E-01	**3.87E-03**	6.53E-01	9.76E-01	7.80E-01	N/A	**1.80E-02**
nirA	5.72E-01	4.34E-01	4.55E-01	5.53E-01	9.60E-01	2.65E-01	N/A
nirB	4.85E-01	4.86E-01	3.71E-01	5.47E-01	9.99E-01	7.99E-01	N/A
nirK	2.50E-01	**3.67E-02**	7.66E-02	**1.05E-03**	9.88E-01	N/A	**1.68E-02**
nirS	8.12E-01	1.16E-01	3.55E-01	8.13E-01	6.72E-01	**8.52E-04**	N/A
norB	9.10E-01	**2.92E-03**	9.44E-01	5.08E-01	2.25E-01	N/A	2.35E-01
nosZ	7.47E-01	4.99E-01	8.99E-01	4.85E-01	5.12E-01	5.86E-01	N/A

Table A2.9 P-values for Tukey's HSD test with the richness index chao 1 of counts of genes associated with nitrogen metabolism copies. "N/A" indicates the test was not appropriate and p-values in bold indicate a significant difference ($p \leq 0.05$).

Test	**Tukey's HSD test**								
Null Hypothesis	**$\mu_1 = \mu_2$**								
Genes	***napA***	***narG***	***nifH***	***nirA***	***nirB***	***nirK***	***nirS***	***norB***	***nosZ***
Conventional tillage - No tillage	N/A	N/A	N/A	N/A	N/A	N/A	**7.37E-04**	N/A	N/A
Conventional tillage - Reduced input	N/A	N/A	N/A	N/A	N/A	N/A	**8.59E-03**	N/A	N/A
Conventional tillage - Biological based	N/A	N/A	N/A	N/A	N/A	N/A	2.11E-01	N/A	N/A
No tillage - Reduced input	N/A	N/A	N/A	N/A	N/A	N/A	7.05E-01	N/A	N/A
No tillage- Biological based	N/A	N/A	N/A	N/A	N/A	N/A	**6.50E-02**	N/A	N/A
Reduced input - Biological based	N/A	N/A	N/A	N/A	N/A	N/A	4.07E-01	N/A	N/A

Table A2.10 P-values for Dunn's test with the richness index chao 1 of counts of genes associated with nitrogen metabolism copies. "N/A" indicates the test was not appropriate and p-values in bold indicate a significant difference ($p \leq 0.05$).

Test	**Dunn's test**								
Null Hypothesis	$\mu_1 = \mu_2$								
Genes	***napA***	***narG***	***nifH***	***nirA***	***nirB***	***nirK***	***nirS***	***norB***	***nosZ***
Conventional tillage - No tillage	N/A	N/A	1.00E+00	N/A	N/A	1.00E+00	N/A	N/A	N/A
Conventional tillage - Reduced input	N/A	N/A	1.33E-01	N/A	N/A	**2.91E-02**	N/A	N/A	N/A
Conventional tillage - Biological based	N/A	N/A	1.00E+00	N/A	N/A	2.03E-01	N/A	N/A	N/A
No tillage - Reduced input	N/A	N/A	5.39E-02	N/A	N/A	1.65E-01	N/A	N/A	N/A
No tillage - Biological based	N/A	N/A	1.00E+00	N/A	N/A	7.85E-01	N/A	N/A	N/A
Reduced input - Biological based	N/A	N/A	**3.30E-02**	N/A	N/A	1.00E+00	N/A	N/A	N/A

Table A2.11 P-values for statistical tests with the richness index chao 2 of counts of genes associated with nitrogen metabolism copies. "N/A" indicates the test was not appropriate and p-values in bold indicate a significant difference ($p \leq 0.05$).

Test	**Shapiro-Wilk test**				**Levene's test**	**One-way ANOVA**	**Kruskal-Wallis test**
Null Hypothesis	**The sample distribution is normal**				**$\sigma_1=\sigma_2$**	**$\mu_1=\mu_2$**	**$Median_1=Median_2$**
Soil groups	**Conventional tillage**	**No tillage**	**Reduced input**	**Biological based**			
napA	3.27E-01	4.60E-01	4.26E-01	2.38E-01	9.19E-01	4.17E-01	N/A
narG	2.88E-01	4.18E-01	2.19E-01	2.26E-01	9.91E-01	9.51E-01	N/A
nifH	7.54E-01	2.38E-01	1.62E-01	2.98E-01	5.93E-01	3.00E-01	**N/A**
nirA	3.24E-01	2.55E-01	4.23E-01	3.80E-01	9.32E-01	4.55E-01	N/A
nirB	2.55E-01	2.75E-01	2.57E-01	3.74E-01	9.98E-01	9.55E-01	N/A
nirK	5.32E-02	**7.63E-03**	**8.64E-03**	**6.93E-03**	9.95E-01	N/A	**2.18E-01**
nirS	3.70E-01	2.47E-01	2.80E-01	4.17E-01	9.87E-01	2.57E-01	N/A
norB	3.29E-01	6.27E-02	7.21E-01	1.90E-01	8.45E-01	4.62E-01	N/A
nosZ	2.30E-01	6.70E-01	7.22E-01	5.40E-01	6.34E-01	6.51E-01	N/A

Table A2.12 P-values for statistical tests with the Simpson diversity of the counts of genes associated with nitrogen metabolism copies. "N/A" indicates the test was not appropriate and p-values in bold indicate a significant difference ($p \leq 0.05$).

Test	**Shapiro-Wilk test**				**Levene's test**	**One-way ANOVA**	**Kruskal-Wallis test**
Null Hypothesis	**The sample distribution is normal**				**$\sigma_1=\sigma_2$**	**$\mu_1=\mu_2$**	**$Median_1=Median_2$**
Soil groups	**Conventional tillage**	**No tillage**	**Reduced input**	**Biological based**			
napA	4.73E-01	**6.37E-03**	**5.07E-03**	**6.37E-03**	3.63E-01	N/A	**6.96E-05**
narG	N/A	N/A	N/A	N/A	**4.44E-05**	N/A	N/A
nifH	1.27E-01	2.66E-01	2.08E-01	1.60E-01	2.00E-01	6.52E-01	N/A
nirA	9.00E-02	1.25E-01	1.70E-01	**2.87E-02**	6.90E-01	N/A	**8.84E-04**
nirB	1.49E-01	2.33E-01	9.44E-02	**2.87E-02**	6.16E-01	N/A	**5.77E-04**
nirK	6.00E-02	9.95E-02	1.81E-01	2.05E-01	4.85E-01	**<2e-16**	N/A
nirS	2.26E-01	7.08E-02	1.79E-01	1.15E-01	6.44E-01	**1.57E-05**	N/A
norB	2.15E-01	7.04E-02	1.06E-01	8.94E-02	3.11E-01	**8.76E-15**	N/A
nosZ	N/A	N/A	N/A	N/A	**1.33E-04**	N/A	N/A

Table A2.13 P-values for Tukey's HSD test with the Simpson diversity of genes associated with nitrogen metabolism copies. "N/A" indicates the test was not appropriate and p-values in bold indicate a significant difference ($p \leq 0.05$).

Test	**Tukey's HSD test**								
Null Hypothesis	**$\mu_1 = \mu_2$**								
Genes	***napA***	***narG***	***nifH***	***nirA***	***nirB***	***nirK***	***nirS***	***norB***	***nosZ***
Conventional tillage - No tillage	N/A	N/A	N/A	N/A	N/A	**0.00E+00**	**2.73E-03**	**0.00E+00**	N/A
Conventional tillage - Reduced input	N/A	N/A	N/A	N/A	N/A	**0.00E+00**	5.67E-02	**5.00E-07**	N/A
Conventional tillage - Biological based	N/A	N/A	N/A	N/A	N/A	**0.00E+00**	9.98E-01	**2.62E-02**	N/A
No tillage - Reduced input	N/A	N/A	N/A	N/A	N/A	**0.00E+00**	**6.40E-06**	**0.00E+00**	N/A
No tillage- Biological based	N/A	N/A	N/A	N/A	N/A	**0.00E+00**	**4.18E-03**	**0.00E+00**	N/A
Reduced input - Biological based	N/A	N/A	N/A	N/A	N/A	3.45E-01	**3.86E-02**	**3.18E-04**	N/A

Table A2.14 P-values for Dunn's test with the Simpson diversity of genes associated with nitrogen metabolism copies. "N/A" indicates the test was not appropriate and p-values in bold indicate a significant difference ($p \leq 0.05$).

Test	**Dunn's test**								
Null Hypothesis	**$\mu_1 = \mu_2$**								
Genes	***napA***	***narG***	***nifH***	***nirA***	***nirB***	***nirK***	***nirS***	***norB***	***nosZ***
Conventional tillage - No tillage	**8.35E-01**	N/A	N/A	1.00E+00	1.00E+00	N/A	N/A	N/A	N/A
Conventional tillage - Reduced input	**1.86E-02**	N/A	N/A	1.00E+00	4.31E-01	N/A	N/A	N/A	N/A
Conventional tillage - Biological based	**5.49E-05**	N/A	N/A	1.81E-01	1.12E-01	N/A	N/A	N/A	N/A
No tillage - Reduced input	**8.35E-01**	N/A	N/A	**2.87E-02**	**9.14E-03**	N/A	N/A	N/A	N/A
No tillage - Biological based	**1.86E-02**	N/A	N/A	**6.14E-04**	**1.18E-03**	N/A	N/A	N/A	N/A
Reduced input - Biological based	**8.35E-01**	N/A	N/A	5.15E-01	1.00E+00	N/A	N/A	N/A	N/A

Table A2.15 P-values for statistical tests with the Shannon diversity of genes associated with nitrogen metabolism copies. "N/A" indicates the test was not appropriate and p-values in bold indicate a significant difference ($p \leq 0.05$).

Test	**Shapiro-Wilk test**				**Levene's test**	**One-way ANOVA**	**Kruskal-Wallis test**
Null Hypothesis	**The sample distribution is normal**				**$\sigma_1=\sigma_2$**	**$\mu_1=\mu_2$**	**$Median_1=Median_2$**
Soil groups	**Conventional tillage**	**No tillage**	**Reduced input**	**Biological based**			
napA	**3.28E-02**	**3.17E-02**	2.50E-01	**3.28E-02**	2.09E-01	N/A	**2.03E-04**
narG	**2.47E-02**	**1.55E-02**	9.26E-01	6.07E-01	1.38E-01	N/A	**1.90E-04**
nifH	2.08E-01	2.63E-01	3.25E-01	3.08E-01	6.31E-01	8.35E-01	N/A
nirA	9.44E-02	6.95E-02	2.21E-01	1.31E-01	9.65E-01	**3.55E-03**	N/A
nirB	5.13E-02	5.13E-02	6.92E-02	2.07E-01	9.59E-01	5.85E-02	N/A
nirK	7.78E-02	5.51E-02	**3.29E-02**	9.11E-02	9.24E-01	N/A	**1.77E-04**
nirS	1.88E-01	1.35E-01	1.73E-01	1.52E-01	8.03E-01	**2.76E-03**	N/A
norB	1.61E-01	**1.55E-02**	7.96E-02	**1.01E-02**	9.52E-01	N/A	**1.44E-03**
nosZ	7.63E-01	5.08E-02	1.61E-01	7.03E-02	8.11E-01	**<2E-16**	N/A

Table A2.16 P-values for Tukey's HSD test with the Shannon diversity of genes associated with nitrogen metabolism copies. "N/A" indicates the test was not appropriate and p-values in bold indicate a significant difference ($p \leq 0.05$).

Test	**Tukey's HSD test**								
Null Hypothesis	$\mu_1 = \mu_2$								
Genes	***napA***	***narG***	***nifH***	***nirA***	***nirB***	***nirK***	***nirS***	***norB***	***nosZ***
Conventional tillage - No tillage	N/A	N/A	N/A	N/A	N/A	**0.00E+00**	**2.73E-03**	**0.00E+00**	N/A
Conventional tillage - Reduced input	N/A	N/A	N/A	N/A	N/A	**0.00E+00**	5.67E-02	**5.00E-07**	N/A
Conventional tillage - Biological based	N/A	N/A	N/A	N/A	N/A	**0.00E+00**	9.98E-01	**2.62E-02**	N/A
No tillage - Reduced input	N/A	N/A	N/A	N/A	N/A	**0.00E+00**	**6.40E-06**	**0.00E+00**	N/A
No tillage- Biological based	N/A	N/A	N/A	N/A	N/A	**0.00E+00**	**4.18E-03**	**0.00E+00**	N/A
Reduced input - Biological based	N/A	N/A	N/A	N/A	N/A	3.45E-01	**3.86E-02**	**3.18E-04**	N/A

Table A2.17 P-values for Dunn's test with the Shannon diversity of genes associated with nitrogen metabolism copies. "N/A" indicates the test was not appropriate and p-values in bold indicate a significant difference ($p \leq 0.05$).

Test	**Dunn's test**								
Null Hypothesis	$\mu_1 = \mu_2$								
Genes	***napA***	***narG***	***nifH***	***nirA***	***nirB***	***nirK***	***nirS***	***norB***	***nosZ***
Conventional tillage - No tillage	1.00E+00	1.00E+00	N/A	N/A	N/A	**4.88E-05**	N/A	**0.00E+00**	N/A
Conventional tillage - Reduced input	**1.37E-02**	1.75E-01	N/A	N/A	N/A	1.63E-01	N/A	**5.00E-07**	N/A
Conventional tillage - Biological based	**1.77E-04**	1.42E-01	N/A	N/A	N/A	1.46E-01	N/A	**2.62E-02**	N/A
No tillage - Reduced input	9.11E-01	1.42E-01	N/A	N/A	N/A	1.46E-01	N/A	**0.00E+00**	N/A
No tillage - Biological based	6.29E-02	1.75E-01	N/A	N/A	N/A	1.63E-01	N/A	**0.00E+00**	N/A
Reduced input - Biological based	6.35E-01	**5.27E-05**	N/A	N/A	N/A	1.00E+00	N/A	**3.18E-04**	N/A

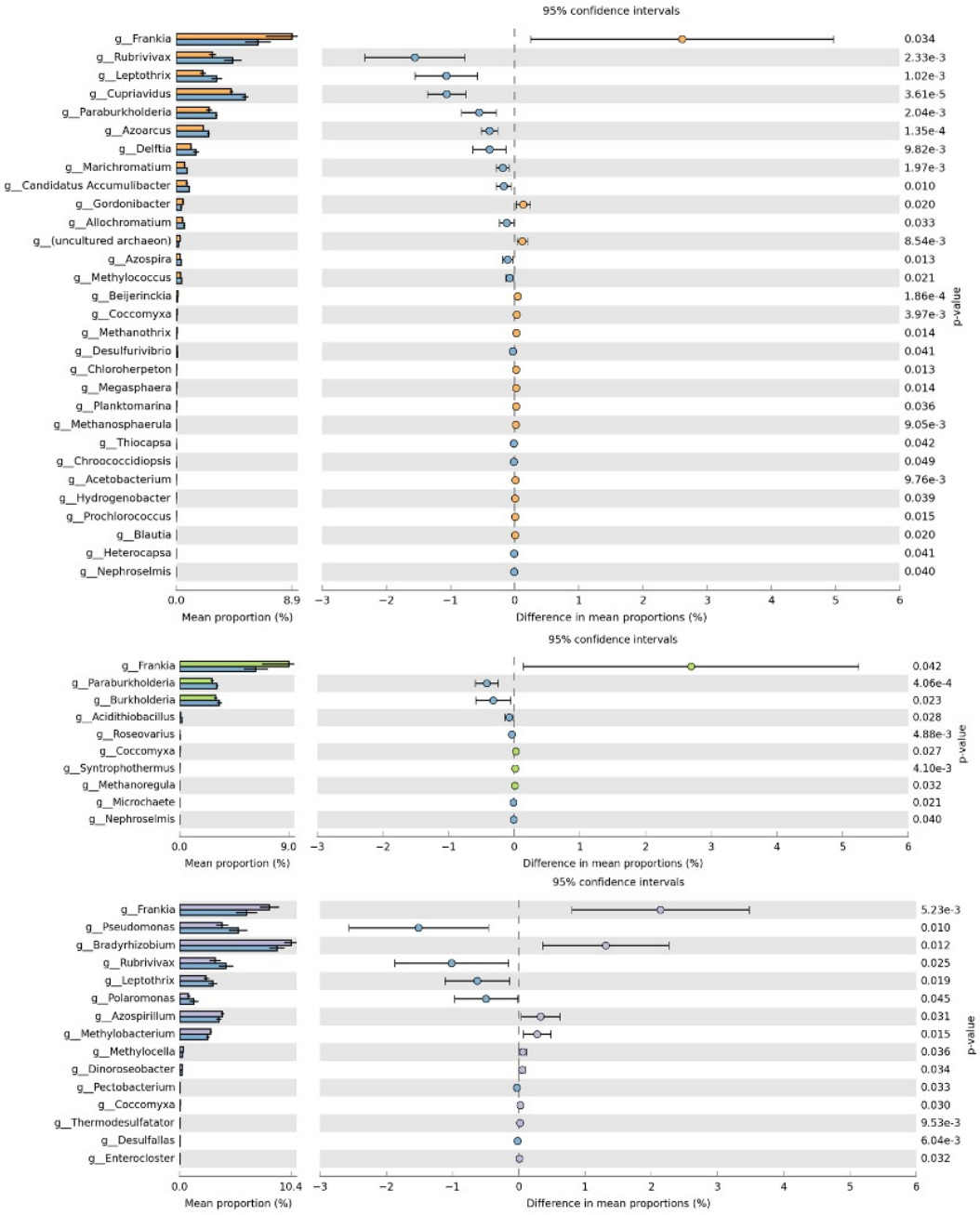

Figure A2.1 Genera with *nifH* genes significantly different between conventional tillage soil (in blue) and the other soils from the assembled contigs. Those enriched in no tillage soil compared to conventional tillage soil are shown in yellow (A), those enriched in reduced input soil compared to conventional tillage soil are shown in green (B) and those enriched in biologically based soil compared to conventional tillage soil are shown in purple (C). The data (generated in Megan, six metagenomes for each soil) were analyzed using STAMP with the two group analysis option (each soil compared to conventional tillage soil) and Welch's two sided t-test (p<0.05).

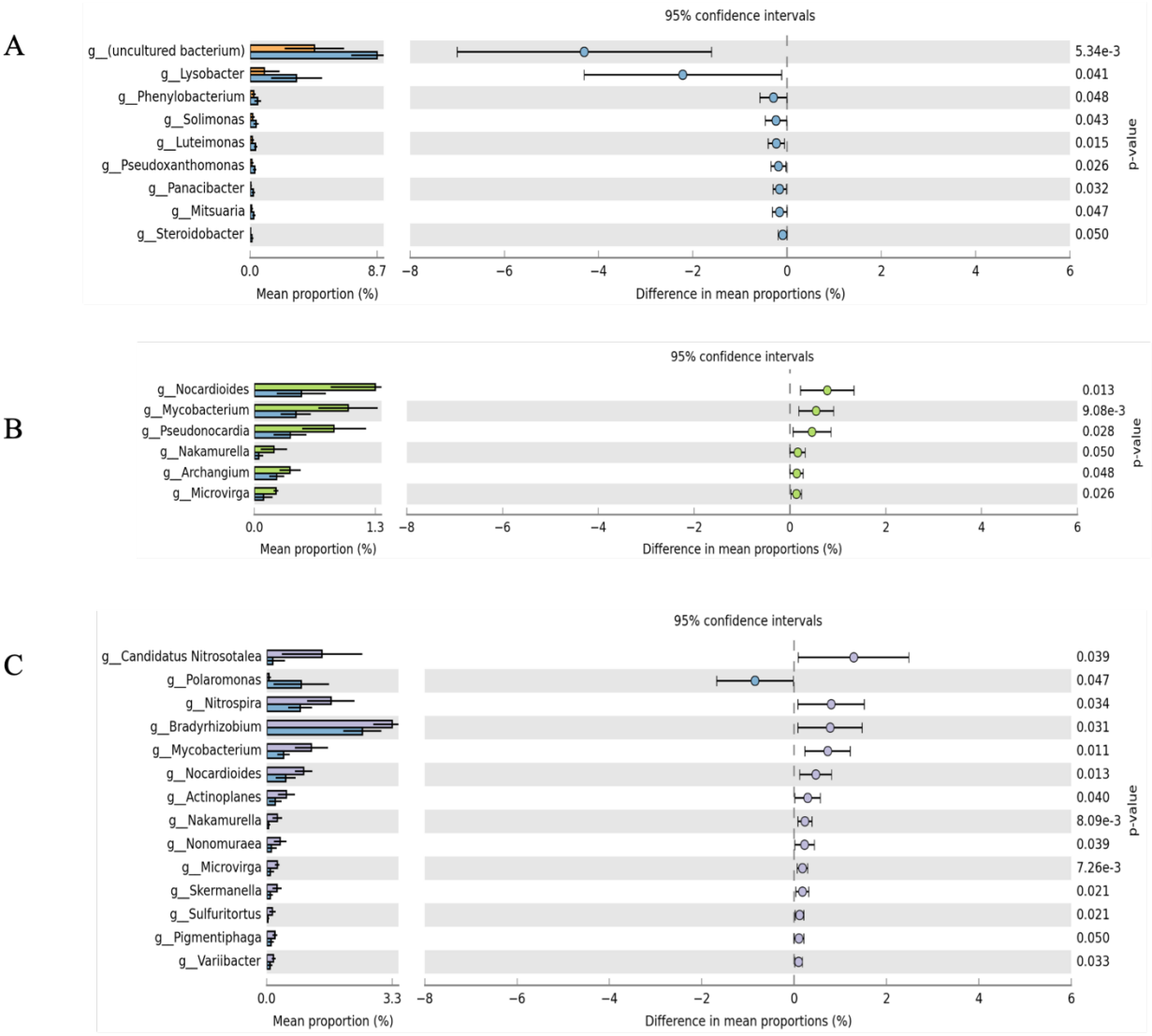

Figure A2.2 Genera significantly different between conventional tillage (in blue) and the other three soils from the assembled contigs. Those enriched in soil 1 compared to no tillage soil are shown in blue (no genera were enriched in no tillage soil compared to conventional tillage soil) (A), those enriched in reduced input soil compared to conventional tillage soil are shown in green (B) and those enriched in biologically based soil compared to conventional tillage soil are shown in purple (C). The data (generated in Megan, six metagenomes for each soil) were analyzed using STAMP with the two group analysis option (each soil compared to conventional tillage soil) and Welch's two sided t-test (p<0.05).

CHAPTER 3: SOIL MICROORGANISMS INVOLVED IN GLUCOSE ASSIMILATION IN SMALL AND LARGE PORE MICRO-HABITATS

This chapter is a modified version of a published work in Nature Communications: Li, Z., A. N. Kravchenko, A. Cupples, A. K. Guber, Y. Kuzyakov, G. Philip Robertson and E. Blagodatskaya (2024). "Composition and metabolism of microbial communities in soil pores." Nature Communications 15(1): 3578.

3.1 Abstract

High plant diversity is known to increase carbon inputs to soils, impact soil microbial community composition and promote soil microbial activity. Large pores are likely to hold more roots residues, provide more efficient oxygen supply, and have more dissolved nutrients and carbon carried by water fluxes. Soil pore structure also impacts the activities of soil microbial communities. The objectives of this study were to investigate the effects of 1) plant systems, representing a 9-year gradient of plant diversity (no plants, monoculture switchgrass (*Panicum virgatum* L.), and high diversity prairie), 2) soil pore size (small (4-10 μm Ø) and large (30-150 μm Ø)), and 3) incubation time (24 hr (short-term) and 30 days (long-term)) on the microbial communities involved in the utilization of a newly added carbon (glucose). This is the first work to explore the influence of soil micro-habitat, as presented by pores of different sizes ranges, on the microbial communities' responses to new carbon inputs. The intact soil cores (5 cm Ø) from the three systems were supplied with either 50 μM C g^{-1} soil of ^{13}C labeled glucose, unlabeled glucose, or no glucose. Glucose was added to small or large pores based on matrix potential approach. After 24 hr or 30 day incubations stable isotope probing (SIP) was used to identify the phylotypes actively responsible for glucose assimilation in the small and large pore micro-

habitats. Both extracted DNA and the fractions separated by SIP were subject to 16S rRNA gene sequencing. PICRUSt2 was used to predict the microbial functions of the sequencing data from KEGG orthologs. The overall microbial communities were affected by multiple years of contrasting vegetation, but not by pore sizes or incubation times. *Pseudomonas* (*Proteobacteria*) played an important role in carbon uptake from glucose in all short-term incubations and in the long-term incubations within large pores. In the long-term incubations of both switchgrass and prairie systems' soils, the community compositions of carbon consumers acting within the small and large pore micro-habitats differed and could be linked to disparate carbon assimilation strategies (*r*- vs. *K*-strategists) and to disparate carbon acquisition ecological strategies (plant polymer decomposers, microbial necromass decomposers, predators, and passive consumers). The predicted enriched functional genes indicated the dominance of glucokinase in the soil of the prairie, but not switchgrass system, suggesting a competitive advantage for consuming glucose.

3.2 Introduction

Bioenergy crops are important for decreasing the impacts of climate change as they reduce our dependence on fossil fuels, mitigate the emission of atmospheric CO_2 and enhance soil carbon sequestration (Follett 2001, West and Post 2002, McLauchlan, Hobbie et al. 2006, Ogle, Swan et al. 2012, Post, Izaurralde et al. 2012, IPCC 2014, Sprunger and Robertson 2018). Much interest has been directed towards switchgrass (*Panicum virgatum* L.) as a perennial bioenergy feedstock (Sanderson, Adler et al. 2006). Switchgrass can increase carbon sequestration in the long-term (after 10 years) (Ma, Wood et al. 2000) and promote carbon accumulation compared to annual systems due to more root-derived carbon inputs (Adkins, Jastrow et al. 2016). However, there are also reports suggesting switchgrass is slow to accumulate soil organic carbon (Chimento, Almagro et al. 2016, Sprunger and Robertson 2018).

Carbon stored in soils is driven by the balance of root litter production, root exudates and the microbial decomposition of these compounds (Jastrow, Amonette et al. 2007). Important knowledge gaps involve the comparison of switchgrass to other crops concerning the impact of soil architecture (soil pores) on soil carbon uptake and the identification of the active microbial communities involved.

Plant diversity is known to impact carbon inputs to soils, soil microbial community composition and soil microbial activity (Carney and Matson 2006, Zhang, Wang et al. 2010, Lamb, Kennedy et al. 2011, Ravenek, Bessler et al. 2014, Lange, Eisenhauer et al. 2015). For example, total root biomass and root residue concentrations increased with increased plant species richness (Ravenek, Bessler et al. 2014). Such higher root biomass due to more diverse plants can then result in carbon accrual in soils (Fornara and Tilman 2008). These plant-derived carbon inputs provide more carbon substrates for microbial populations (Eisenhauer, Bessler et al. 2010). Plant diversity can also promote soil microbial activity (Zak, Holmes et al. 2003, Eisenhauer, Bessler et al. 2010, Lange, Eisenhauer et al. 2015). Further, microclimatic conditions, such as increased soil moisture, have been identified as important mechanisms for how plant diversity impacts soil microbial biomass (Lange, Habekost et al. 2014).

Soil pore structure has also impacted the activities of soil microbial communities (Chenu, Hassink et al. 2001, Carson Jennifer, Gonzalez-Quiñones et al. 2010, Sleutel, Bouckaert et al. 2012, Kravchenko, Negassa et al. 2014, Negassa, Guber et al. 2015, Kravchenko and Guber 2017, Kravchenko, Guber et al. 2021, Xia, Zheng et al. 2022). Large pores are likely to hold more roots residues (diameters of the finest roots are between 30 and 40 μm) (Kuchenbuch and Jungk 1982). Oxygen supply, dissolved nutrients and carbon carried by water fluxes are also more sufficient in large pores (Or, Smets et al. 2007, Kravchenko, Guber et al. 2021). In

comparison to monocultures, diverse plant communities have been linked to the development of 30–150 μm pores, which have been associated with higher enzyme activities, and consequently soil carbon storage capacity (Kravchenko, Guber et al. 2019). Further, large pores promoted the prevalence of *r*-strategists, ^{14}C-CO_2 release and dissolved organic ^{14}C while small pores held more ^{14}C microbial biomass (Kravchenko, Guber et al. 2021). In addition, there were stronger associations between β-glucosidase activity and glucose-derived carbon when glucose was added to the large pores (Kravchenko, Guber et al. 2021). Fine roots are important for the carbon accumulation in soils and diverse biofuel cropping systems are likely to hold more fine roots than monoculture systems (Sprunger, Oates et al. 2017). In fact, plant-stimulated soil pore formation was previously reported to be a major determinant of whether new carbon inputs are stored or lost (Kravchenko, Guber et al. 2019).

Researchers have found soil microbial communities differ depending on soil pore size (Kravchenko, Negassa et al. 2014, Negassa, Guber et al. 2015, Xia, Rufty et al. 2020, Xia, Zheng et al. 2022). For example, *Betaproteobacteria*, *Bacteroidetes*, and *Eurotiales* (order of fungi) were more abundant in the large pores of row crop soils (> 30 μm), whereas *Alphaproteobacteria*, *Sordariomycetes* (class of fungi), and *Chaetothyriales* (order of fungi) were more abundant in the small pores of row crop soils (< 30 μm) (Xia, Zheng et al. 2022). Others have also found *Betaproteobacteria* to be more abundant in large pores (Xia, Rufty et al. 2020). In a study involving the addition of plant residues to different soil pore sizes, the communities in the samples with large pores (> 30 μm) contained more cellulose decomposers, including *Bacteroidetes, Proteobacteria, Actinobacteria* and *Firmicutes*, while oligotrophic *Acidobacteria* were more abundant on the plant residue from the samples with small pores (Negassa, Guber et al. 2015). In research with two contrasting agricultural

systems, *Actinobacteria*, *Proteobacteria*, and *Firmicutes* were positively correlated with the presence of large pores (> 110 μm) (Kravchenko, Negassa et al. 2014). Although previous research has discovered differences in microbial communities between pores of different sizes, limited efforts have been made to identify which phylotypes are actively responsible for carbon assimilation in those pores.

To address this the unknowns in this research area, the current study applied stable isotope probing (SIP) to determine which microorganisms were responsible for the assimilation of a labile carbon source (glucose) in different sized soil pores in three soils; bare soil and soil under either switchgrass or high diversity prairie crops. Although SIP has been widely used to identify microbial populations involved in carbon metabolism, e.g. glucose (Padmanabhan, Padmanabhan et al. 2003, Lemanski and Scheu 2014, Zhang, Ding et al. 2015, Kong, Zhu et al. 2018), root exudate (Rangel‐Castro, Killham et al. 2005, Haichar, Heulin et al. 2016) and cellulose assimilation (el Zahar Haichar, Achouak et al. 2007, Eichorst Stephanie and Kuske Cheryl 2012, Štursová, Žifčáková et al. 2012), this is the first study to explore the influence of soil pore sizes and plant diversity on the microbial communities responsible for carbon uptake.

The rationale behind this work is that root systems of diverse plant communities are likely more effective than monocultures in creating optimal micro-environments and pore structures for microbial functioning. The creation of such optimal micro-environments leads to a greater spread of active microbial communities throughout the soil, and hence, to a greater volume of the soil matrix where root-derived and microbially-processed carbon inputs can be entombed and, subsequently, protected. The objectives of this work were to investigate the effects of 1) cropping system (no plants, switchgrass, high diversity prairie), 2) soil pore size and 3) incubation time (24 hr and 30 days) on the microbial communities involved in the utilization

of a newly added carbon (glucose). Also, the impacts of those factors on the overall composition and diversity of the soil microbial communities were also investigated.

3.3 Methods

3.3.1 Soils and Incubations

Soils were collected from replicate treatment blocks of the Cellulosic Biofuel Diversity Experiment at the W.K. Kellogg Biological Station Long-Term Ecological Research (KBS LTER), located between Kalamazoo and Battle Creek, Michigan. A map of the experimental design of the KBS LTER can be found at https://lter.kbs.msu.edu/maps/images/current-cellulosic-biofuel-map.pdf. Soil cores were collected from four blocks of CE1 (hereafter called bare soil), three blocks of CE7 (hereafter called switchgrass) and three blocks of CE12 (hereafter called high diversity prairie). Soil cores were incubated with 50 μM C g^{-1} soil of ^{13}C labeled glucose, unlabeled glucose or no glucose at 20-25 °C for 24 hours or 30 days. Additional details on the blocks and incubation times investigated for each treatment have been summarized (Table 3.1).

Table 3.1 Treatment summary of the samples and replicate blocks analyzed.

24 hours only	24 hours and 30 days	24 hours and 30 days	Block	Pore size	Glucose added
Bare soil	Switchgrass	High Diversity	1	Small pore	13C
Bare soil	Switchgrass	High Diversity	1	Small pore	12C
Bare soil	Switchgrass	High Diversity	1	N/A	No glucose
Bare soil	Switchgrass	High Diversity	1	Large pore	13C
Bare soil	Switchgrass	High Diversity	1	Large pore	12C
Bare soil	Switchgrass	High Diversity	2	Small pore	13C
Bare soil	Switchgrass	High Diversity	2	Small pore	12C
Bare soil	Switchgrass	High Diversity	2	N/A	No glucose
Bare soil	Switchgrass	High Diversity	2	Large pore	13C
Bare soil	Switchgrass	High Diversity	2	Large pore	12C
Bare soil	N/A	N/A	3	Small pore	13C
Bare soil	N/A	N/A	3	Small pore	12C
Bare soil	N/A	N/A	3	N/A	No glucose
Bare soil	N/A	N/A	3	Large pore	13C
Bare soil	N/A	N/A	3	Large pore	12C
Bare soil	Switchgrass	High Diversity	4	Small pore	13C
Bare soil	Switchgrass	High Diversity	4	Small pore	12C
Bare soil	Switchgrass	High Diversity	4	N/A	No glucose
Bare soil	Switchgrass	High Diversity	4	Large pore	13C
Bare soil	Switchgrass	High Diversity	4	Large pore	12C

3.3.2 DNA Extraction, Ultracentrifugation and Fractioning

DNA was extracted using the DNeasy PowerSoil kit or the DNeasy PowerSoil Pro kit (Qiagen, USA) following the manufacturer's protocols. For this, approximately 1 g of each soil was used for DNA extraction. Carnation instant nonfat dry milk (40 mg, Nestlé, Rosslyn, VA) was added at the beginning of the extraction process to improve the DNA yield (Yuko Takada-Hoshino and Naoyuki 2004). DNA concentrations from each extraction were determined using the Qubit fluorometer (Thermo Fisher, USA) with the ds DNA HS Assay kit. For ultracentrifugation, approximately 10 µg of each DNA extract was mixed with Tris-EDTA buffer (10 mM Tris, 1mM EDTA, pH 8) and cesium chloride (CsCl) solution (1.62 M) and loaded into Quick-Seal Round-Top Polypropylene tubes (13×51 mm, 5 ml; Beckman Coulter, USA). Refractive index (RI) values of each solution were determined using AR200 digital refractometer (Leica Microsystems Inc., Buffalo Grove, IL) and the RI was adjusted to between (1.4069 - 1.4071) by adding small volumes of TE buffer or CsCl solution. The sealed tubes were ultracentrifuged at 178,000 ×*g* (20 °C) for 46 h in a StepSaver 70 V6 vertical titanium rotor (8 by 5.1 mL capacity) within a Sorvall WX 80 Ultra Series centrifuge (Thermo Scientific, Waltham, MA). Following ultracentrifugation, each tube was placed onto a fraction collection system (Beckman Coulter) to generate ~26 fractions (200 µL). The RI of each fraction was determined, and, from this, buoyant density values were calculated. CsCl in the fractions was removed using linear polyacrylamide (Thermo-Scientific, USA) and a polyethylene glycol solution (1.6M NaCl, 30% PEG solution; Thermo-Scientific, USA). The DNA concentration in each fraction was determined using the ds DNA HS Assay kit to identify the four heaviest fractions with the minimum amount of DNA for high throughput sequencing. For each of the labelled and unlabeled glucose amended samples, sixteen tubes were ultracentrifuged: four replicate blocks

(B1, B2, B3, B4) for the bare soil 24 hour incubation; three replicate blocks (B1, B2, B4) for both the switchgrass 24 hour incubation and the high diversity prairie 24 hour incubations; and three replicate blocks (B1, B2, B4) for both the switchgrass 30 day incubation and the high diversity prairie 30 day incubations. As both small pores and large pore incubations were also examined, in total, sixty-four tubes were ultracentrifuged (2 glucose forms [^{12}C and ^{13}C] X 16 treatments/blocks X 2 pore sizes).

3.3.3 Miseq Illumina Sequencing and Mothur Analysis

Total genomic DNA extracts (before ultracentrifugation) and ultracentrifugation fractions were submitted to the Research Technology Support Facility (RTSF) at MSU for 16S rRNA gene amplicon sequencing. For each of the sixty-four ultracentrifugation runs (as described above), three heavy fractions (buoyant density 1.73-1.75 g/ml) and one light fraction (~1.70 g/ml) were submitted in triplicate for sequencing. This involved amplification of the V4 region of the 16S rRNA gene using dual indexed Illumina compatible primers 515f/806r, as previously described (Kozich, Westcott et al. 2013). PCR products were batch normalized using Invitrogen SequalPrep DNA Normalization plates and the products recovered from the plates pooled. The pool was cleaned up and concentrated using AmpureXP magnetic beads; it was QC'd and quantified using a combination of Qubit dsDNA HS, Agilent 4200 TapeStation HS DNA1000 and Kapa Illumina Library Quantification qPCR assays. The pool was loaded onto an Illumina MiSeq v2 standard flow cell and sequencing was performed in a 2 × 250 bp paired end format using a MiSeq v2 500 cycle reagent cartridge. Custom sequencing and index primers were added to appropriate wells of the reagent cartridge. Base calling was performed by Illumina Real Time Analysis (RTA) v1.18.54 and output of RTA was demultiplexed and converted to FastQ format with Illumina Bcl2fastq v2.19.1. The amplicon sequencing data in the fastq format was analyzed

by Mothur (Schloss, Westcott et al. 2009) using the Mothur MiSeq SOP (accessed August 2021) (Kozich, Westcott et al. 2013). Briefly, the Mothur analysis involved trimming the raw sequences and quality control. The SILVA bacteria database (Release 138) for the V4 region (Pruesse, Quast et al. 2007) was used for the alignment. Chimeras, mitochondrial and chloroplast lineage sequences were removed, then the sequences were classified into operational taxonomic units (OTUs) at 0.03 cutoff. The OTUs were then grouped into taxonomic levels and the downstream analysis was conducted in R (version 4.0.2) (R_Core_Team 2020) with RStudio (version 1.5042) (RStudio_Team 2020). The sequencing data of the total DNA and SIP fractions were submitted to NCBI under Bioproject PRJNA801760 (accession numbers SAMN25378717 to SAMN25378796) and Bioproject PRJNA802612 (accession numbers SAMN25563888 to SAMN25564655), respectively. Sequencing data from the total DNA extracts and the ultracentrifugation fractions were analyzed separately, as described below.

3.3.4 Total DNA Community Analysis

For the analysis of the total DNA samples, two Mothur files (shared file and taxonomy file) along with an independently created metafile were used as the input for packages phyloseq (McMurdie and Holmes 2013) (version 1.34.0), file2meco (version 0.1.0) (Liu, Cui et al. 2021) and microeco (version 0.5.1) (Liu, Cui et al. 2021). This resulted in the creation of 1) a phylum level bar chart, 2) a Venn diagram of OTU abundance and 3) two box plots at the genus and order level. The packages phyloseq (McMurdie and Holmes 2013) (version 1.34.0), microbiome (Lahti and Shetty 2012-2019) (version 1.12.0) and ampvis2 (version 2.7.11) (Andersen, Kirkegaard et al. 2018) were used to 1) generate heatmaps of the most abundant genera, 2) perform alpha diversity analysis (Chao1, ACE, Shannon's values, Simpson, Inverse Simpson, and Fisher indices) and 3) create barplots for the most abundant classes. The “adonis” function in

the package vegan (version 2.5.7) (Oksanen, Blanchet et al. 2020) was used to test differences between microbial communities in different soil treatments with Permutational Multivariate Analysis of Variance (PERMANOVA). The "pairwise.adonis" function in package pairwiseAdonis (version 0.4) (Martinez 2017) was used for the comparison of significant PERMANOVA results ($p<0.05$). The "simper" function in the package vegan (version 2.5.7) (Oksanen, Blanchet et al. 2020) was used for dissimilarity analyses for the significant comparison results ($p<0.05$). The abundance and the classification of top twenty OTUs contributing to the difference between treatments and the connection between the OTUs and different samples was determined using the circlize package (version 0.4.13) (Gu, Gu et al. 2014).

3.3.5 Identification of Enriched Phylotypes

Sequencing datasets were compared between the heavy and light fractions of the ^{13}C glucose amended samples and fractions of similar buoyant density from the ^{12}C glucose amended samples to determine which phylotypes were responsible for label uptake. For this, data generated from the packages phyloseq (McMurdie and Holmes 2013) (version 1.34.0), and microbiome (Lahti and Shetty 2012-2019) (version 1.12.0) were analyzed using the packages dplyr (version 1.0.7) (Wickham, François et al. 2021), tidyr (version 1.1.4) (Wickham 2021), ggpubr (version 0.4.0) (Kassambara 2020)and rstatix (version 0.7.0) (Kassambara 2021). Specifically, those enriched in the heavy fractions of the ^{13}C glucose amended samples (compared to the same fractions in the ^{12}C glucose amended samples) were determined using the Wilcoxon test (function wilcox_test) in RStudio (one sided, $p < 0.05$). From those significantly enriched, the six most abundant were selected for the creation of boxplots using ggplot2 (version 3.3.5) (Wickham 2016). The analysis also included the comparison of phylotypes in the light

fractions of the ^{13}C glucose amended fractions compared to the light fractions of the ^{12}C glucose amended samples. Those enriched in the light fractions of the ^{13}C glucose amended samples were removed from the above analysis.

3.3.6 Function Prediction by PICRUSt2

PICRUSt2 (Douglas, Maffei et al. 2020) was used to predict the microbial functions of the sequencing data from the Kyoto Encyclopedia of Genes and Genomes (KEGG) orthologs (KO) (Kanehisa, Sato et al. 2016). Biom and fasta files generated by Mothur were used for this analysis. The PICRUSt2 analysis included sequence placement with EPA-NG (Barbera, Kozlov et al. 2019) and gappa (Czech, Barbera et al. 2020), hidden state prediction with castor R package (Louca and Doebeli 2017) and pathway abundance inference with MinPath (Ye and Doak 2009).

The KO functions associated with carbohydrate metabolism and energy metabolism were examined, including citrate cycle (TCA cycle) [PATHko00020], glycolysis gluconeogenesis [PATHko00010], methane metabolism [PATHko00680] and nitrogen metabolism [PATHko00910]. The metagenome output files were analyzed with ggplot2 (version 3.3.5) (Wickham 2016) and ggpubr (version 0.4.0) (Kassambara 2020) in RStudio (version 1.5042) (RStudio_Team 2020). The relative abundance of genes associated with carbohydrate metabolism and energy metabolism were also determined for each treatment. The enriched genes in the samples amended with ^{13}C glucose were determined using a similar approach as described above for the enriched phylotypes (Wilcoxon test, $p < 0.05$). The eight most abundant genes associated with the carbohydrate metabolism and energy metabolism were displayed in barplots. The most abundant phylotypes associated with methane metabolism and nitrogen metabolism for the total DNA samples were determined in RStudio (version 1.5042) (RStudio_Team 2020). The

connections between the phylotypes and genes associated methane metabolism and nitrogen metabolism for the total DNA sequences for each treatment were created with the circlize package (version 0.4.13) (Gu, Gu et al. 2014). Genera with the most abundant relative abundance for each set of functional genes were selected for building the chord diagrams for the methane/ammonia monooxygenase genes (taxon_rel_function_abun > 0.008), nitrate and nitrite reductase genes (taxon_rel_function_abun > 0.1) and nitric and nitrous oxide reductase genes (taxon_rel_function_abun > 0.2).

3.4 Results

3.4.1 Microbial Community Analysis

The microbial community structure was compared between the three treatments/soils (bare soil, switchgrass, high diversity prairie) and between the two pore sizes (large and small). The basic soil characteristics of the three soils are presented in Table A3.1. Principal Coordinate Analysis (PCoA) indicated a separation between the bare soil community and the two other treatments (Figure 3.1A). Both the switchgrass and high diversity prairie treatments clustered together (Figure 3.1A). Richness (Chao1, ACE) and diversity (Shannon, Simpson, Inverse of Simpson and Fisher) indices were determined and compared between treatments and pore sizes (Figure A3.1 and Tables A3.2 and A3.3). For the 24 hr incubations, there were significant differences (ANOVA, $p < 0.05$) between the three treatments for all except for Fisher (Table A3.3). Further analysis (24 hr incubations, t-test, two-tailed) revealed the values were higher for the high diversity prairie compared to the bare soil treatment for Chao1 ($p < 0.018$), ACE ($p < 0.015$), Shannon ($p < 0.017$), Simpson ($p < 0.034$) and Inverse Simpson ($p < 0.022$). The values were also higher for the switchgrass compared to the bare soil (24 hr incubations, t-test, two-tailed) for Shannon ($p < 0.038$), Simpson ($p < 0.031$) and Inverse Simpson ($p < 0.022$). In

contrast to this, there were no significant differences ($p > 0.05$) for any richness or diversity value between the switchgrass and high diversity prairie treatments for either incubation time. The impacts of pore size on the richness and diversity values were limited (evaluated with t-tests, two-tailed). Specifically, there were no significant differences ($p > 0.05$) between any richness or diversity value between the large pores and the small pores for the bare soil or the switchgrass treatments (Table A3.2). However, for the high diversity treatment, values for Shannon ($p < 0.044$), Simpson ($p < 0.027$), and Inverse Simpson ($p < 0.03$) were higher for the small pores compared to the large pores (when both incubation times were considered) (Table A3.2).

The most abundant phyla were determined for the three treatments (Figure 3.2A). Compared to bare soil, the relative abundance of *Latescibacteria*, *Gemmatimonadetes*, *Planctomycetes, Proteobacteria* and *Verrucomicrobia* appeared greater in the high diversity prairie and switchgrass treatments. In contrast, in many cases, the relative abundance of *Firmicutes, Chloroflexi, Bacteroidetes* and *Actinobacteria* appeared greater in bare soil than the other two treatments. As shown in the Venn diagram (Figure 3.2B), the proportion of shared operational taxonomic units (OTU) between the bare soil and high diversity prairie (4.7 %) was higher than the corresponding proportion of shared OTUs between the bare soil and switchgrass (3.9 %) and between the switchgrass and high diversity prairie (1.7 %). The proportions of unique OTUs in the bare soil, switchgrass, and high diversity prairie were 4.7, 0.7, and 0.7 %, respectively.

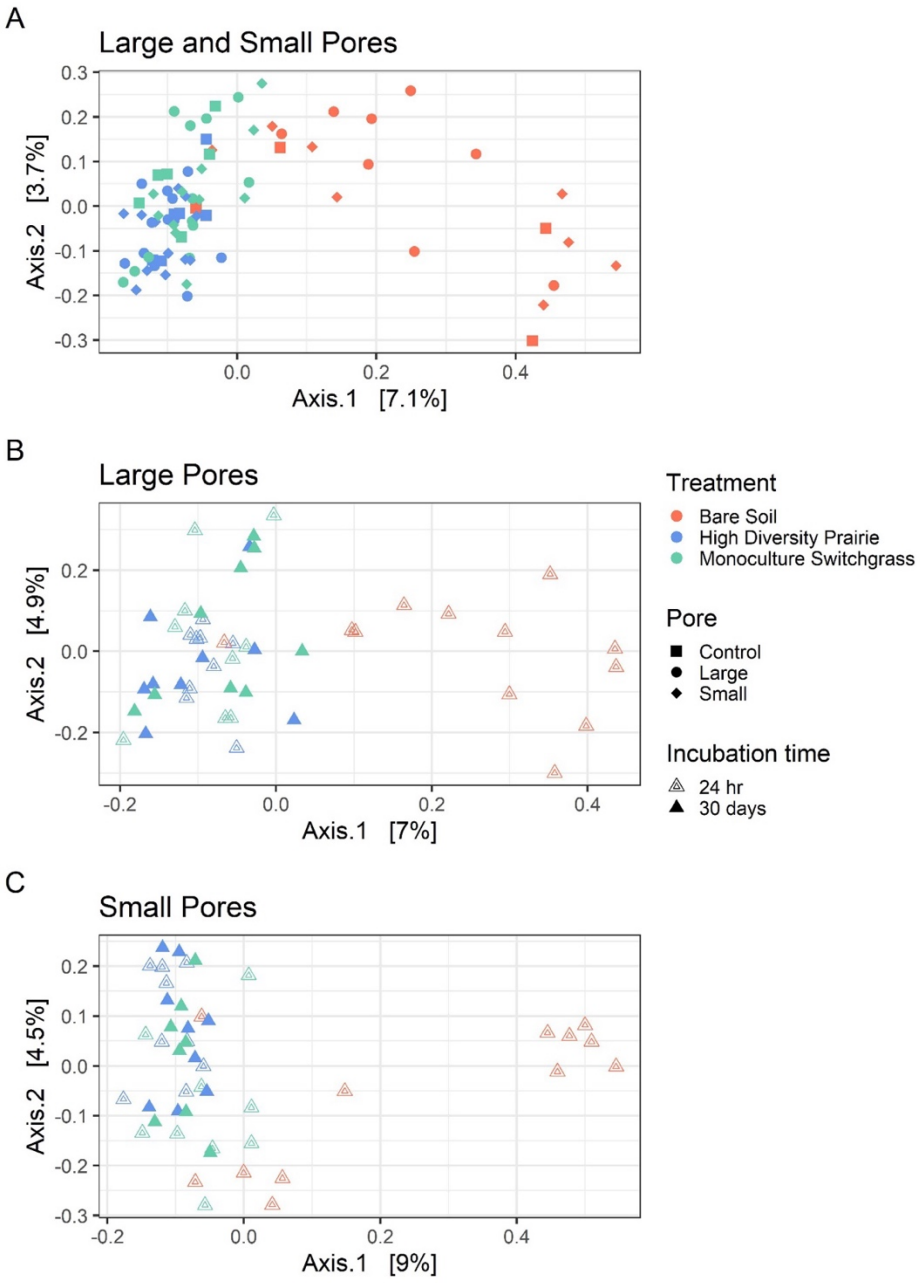

Figure 3.1 Principal Coordinate Analysis (PCoA) plots for both small and large pores (A), large pores only (B) and small pores only (C) for the three treatments and two incubation times.

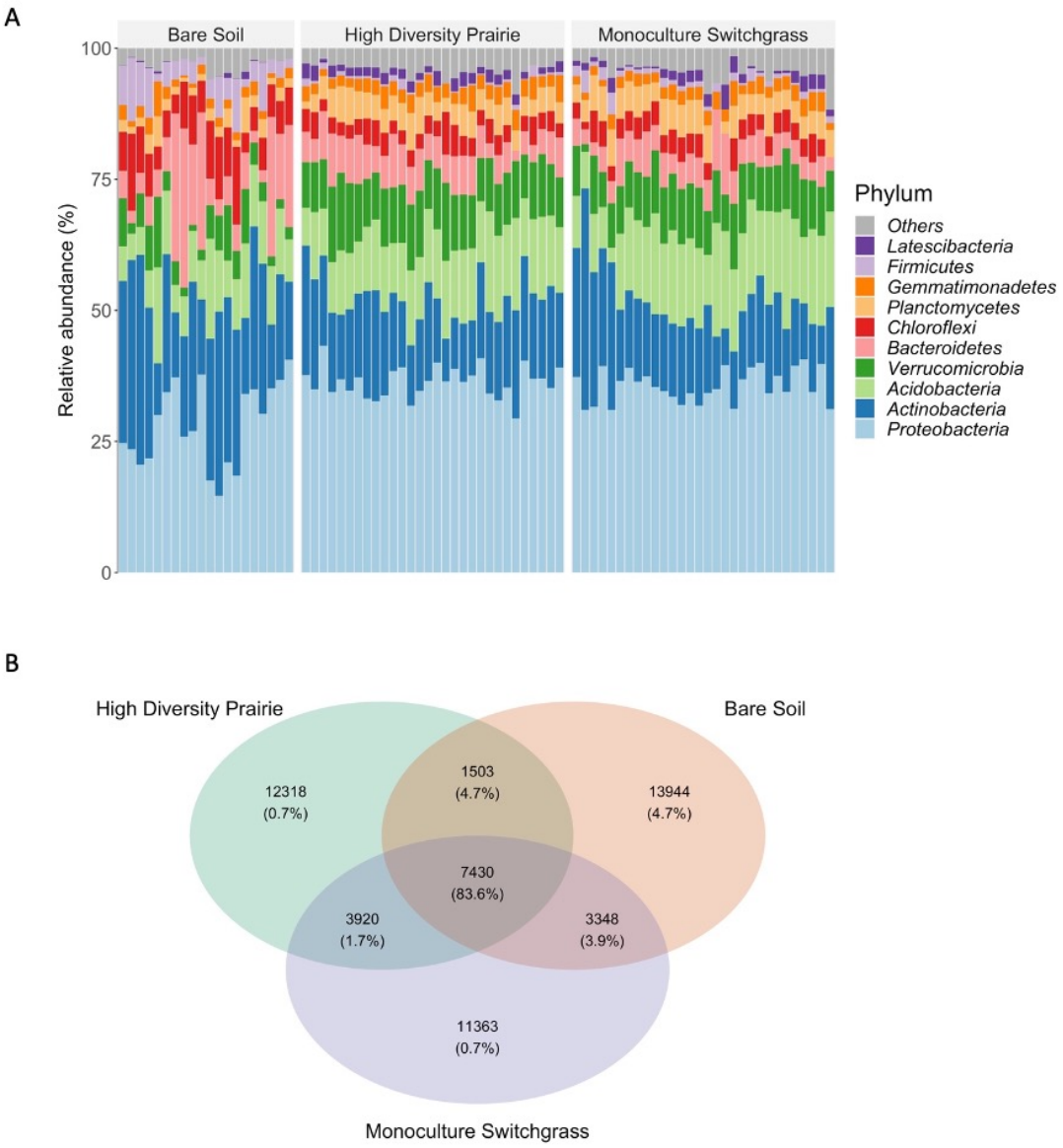

Figure 3.2 A bar chart illustrating relative abundance of the most abundant phyla for each treatment (A) and a Venn diagram showing the number of OTUs and percentage of the total OTUs for each treatment (B). In the Venn diagram, the integers are the OTU number and the percentages are the sequence number/total sequence number.

Of the most abundant genera (Figure 3.3A), two (*Acidothermus* and *Chujaibacter*) illustrated higher relative abundance values in the bare soil compared to the high diversity prairie and switchgrass treatments. For many of the other abundant genera, relative abundance values in the bare soil were lower compared to the other treatments (Figure 3.3A). The most abundant genera were also determined for each treatment, pore size and incubation time (Figure A3.2). The two most abundant genera (*Subgroup 6 ge* and *Candidatus Udaeobacter*) for the high diversity prairie and switchgrass treatments were the same for both the large pores (Figure S2A) and small pores (Figure A3.2B) for both incubation times. Whereas the most abundant genera in the bare soils were *Acidothermus* and *uncultured ge* in the large pore samples and *Chitinophagaceae_unclassified*, *Acidothermus*, and *Chujaibacter* in the small pore samples (Figure A3.2). At the order level, *Gaiellales*, *Frankiales*, *Acidobacteriales*, *Xanthomonadales*, *Bacillales* and *Ktedonobacterales* were less abundant in the switchgrass and high diversity prairie treatments than in the bare soil samples (Figure 3.3). The relative abundance values of other orders were similar between the switchgrass and high diversity prairie treatments (Figure 3.3B).

The differences in the microbial communities at the OTU level between treatments were further investigated using PERMANOVA (Tables A3.5& A3.6). The differences were not significant for soil pore sizes in the bare soil, switchgrass and high diversity prairie treatments and were also not significant for the incubation time in switchgrass and high diversity prairie ($p > 0.05$). However, the bacterial communities were significantly different between the three treatments incubated for 24 hr and also between the two treatments (switchgrass and high diversity prairie) incubated for 30 days ($p < 0.05$). These trends are consistent with the chaos clusters between soil pore sizes or incubation time as well as the obvious differentiation between

soil treatments in PCoA plots (Figure 3.1).

A similarity percentage analysis (simper) revealed the bacteria contributing to 50% dissimilarity at the phylum and class levels between treatments. The two dominant phyla contributing to the 50% difference were *Proteobacteria* and *Actinobacteria* between bare soil and high diversity prairie incubated for 24 hr (Table A3.6), between bare soil and switchgrass incubated for 24 hr (Table A3.7), as well as between switchgrass and high diversity prairie incubated for 24 hr (Table A3.8). While *Proteobacteria* and *Acidobacteria* were the key contributing phyla for the differences between the switchgrass and high diversity prairie incubated for 30 days (Table A3.7). The top 20 OTUs contributing to the differences of communities between treatments are also shown (Figure A3.3). Most of the contributing OTUs were more abundant in bare soil compared to the switchgrass and high diversity prairie incubated for 24 hr. Some OTUs from *Actinobacteria* with low abundance illustrated high contributions between the switchgrass and high diversity prairie incubated for 24 hr and 30 days. At the class level, each treatment, pore size and incubation time illustrated a range of different classes (Figure A3.4).

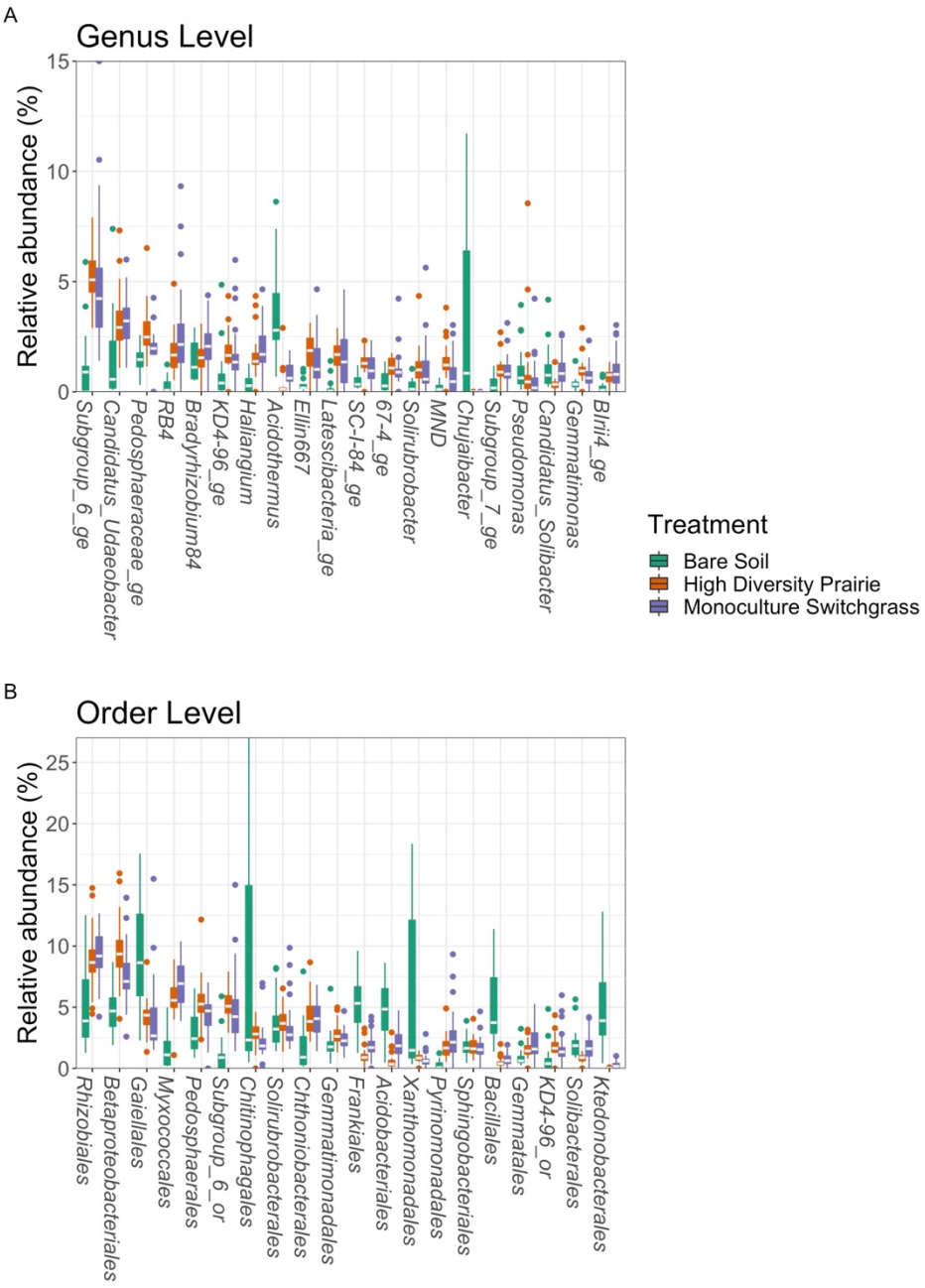

Figure 3.3 Box and whisker plots illustrating the relative abundance of the most abundant genera (A) and orders (B) in the three treatments.

3.4.2 Enriched Phylotypes for 13C Uptake from Glucose

The phylotypes significantly enriched (Wilcoxon test, $p < 0.05$) in the ^{13}C labelled glucose amended heavy fractions compared to unlabeled glucose amended heavy fractions were determined for the bare soil, switchgrass and high diversity prairie treatments for both pore sizes and incubation times (Figure 3.4). For the bare soil treatment (incubated for 24 hr) *Pseudomonas* and *Planococcus* were the dominant phylotypes incorporating the label in the large pores soils (Figure 3.4A). The trend was similar for the equivalent treatment for small pores soils (Figure 3.4F). Additional phylotypes incorporating the label in both the large and small pores of the bare soil treatment included *Micrococcaceae* and *Burkholderia* (Figure 3.4A & F). For the switchgrass treatment (24 hr incubation), *Burkholderia, Pseudomonas* and *Duganella* were involved in label uptake in the heavy fractions of both the large and small pores (Figure 3.4B & G). For the same treatment, label uptake was also attributed to *Burkholderiaceae, Cupriavidus* and *Azoarcus* (Figure 3.4B) in the large pores and *Clostridium, Geobacter*, and *Pseudarthrobacter* in the small pores (Figure 3.4G). For the high diversity prairie treatment (24 hr incubation), *Pseudomonas, Clostridium, Pseudarthrobacter* and *Burkholderiaceae* were the dominant phylotypes for label uptake in both large and small pores (Figure 3.4C & H). For the same treatment, *Allorhizobiume* and *Dechlorosoma* were associated with label uptake in the large and small pores, respectively (Figure 3.4C & H).

Overall, the phylotypes enriched after 30 days were different from those enriched after 24 hr, although a number of similar phylotypes were also observed. Similar to the switchgrass 24 hr incubation, *Burkholderia* and *Pseudomonas* were also associated with label uptake for the large pores after 30 days (Figure 3.4D). However, for the small pores, in contrast to the shorter incubation, *Burkholderia* and *Pseudomonas* were not associated with label uptake (Figure 3.4I).

Instead, *Spirochaeta, Dechlorosoma, Nakamurella, Geobacter* and *Burkholderiaceae* were dominant phylotypes associated with label uptake in small pores soils after 30 days (Figure 3.4I). Two phylotypes were different between the shorter and the longer switchgrass incubations for the large pores (*Duganella* and *Azoarcus* were replaced by *Nakamurella* and *Mycobacterium*) (Figure 3.4B and D). Whereas five phylotypes were different between the shorter and the longer switchgrass incubations for the small pores (*Geobacter* was the only similar phylotype) (Figure 3.4G & D). For the high diversity prairie treatment incubated for 30 days, *Pseudomonas* only exhibited label uptake for the large pores (Figure 4E). For the large pores, in contrast to the earlier incubation for this treatment (Figure 4C), four phylotypes were different (*Nakamurella, Spirochata, Mycobacterium* and *Bradyhizobium*) (Figure 4E). For the small pores high diversity prairie, five phylotypes were different (*Nakamurella*, *Cellulomonus*, *Candidatus, Solirubrobacter, Mycobacterium*) between the shorter and longer incubation times (*Burkholderiaceae* was the only similar phylotype) (Figure 4H & J).

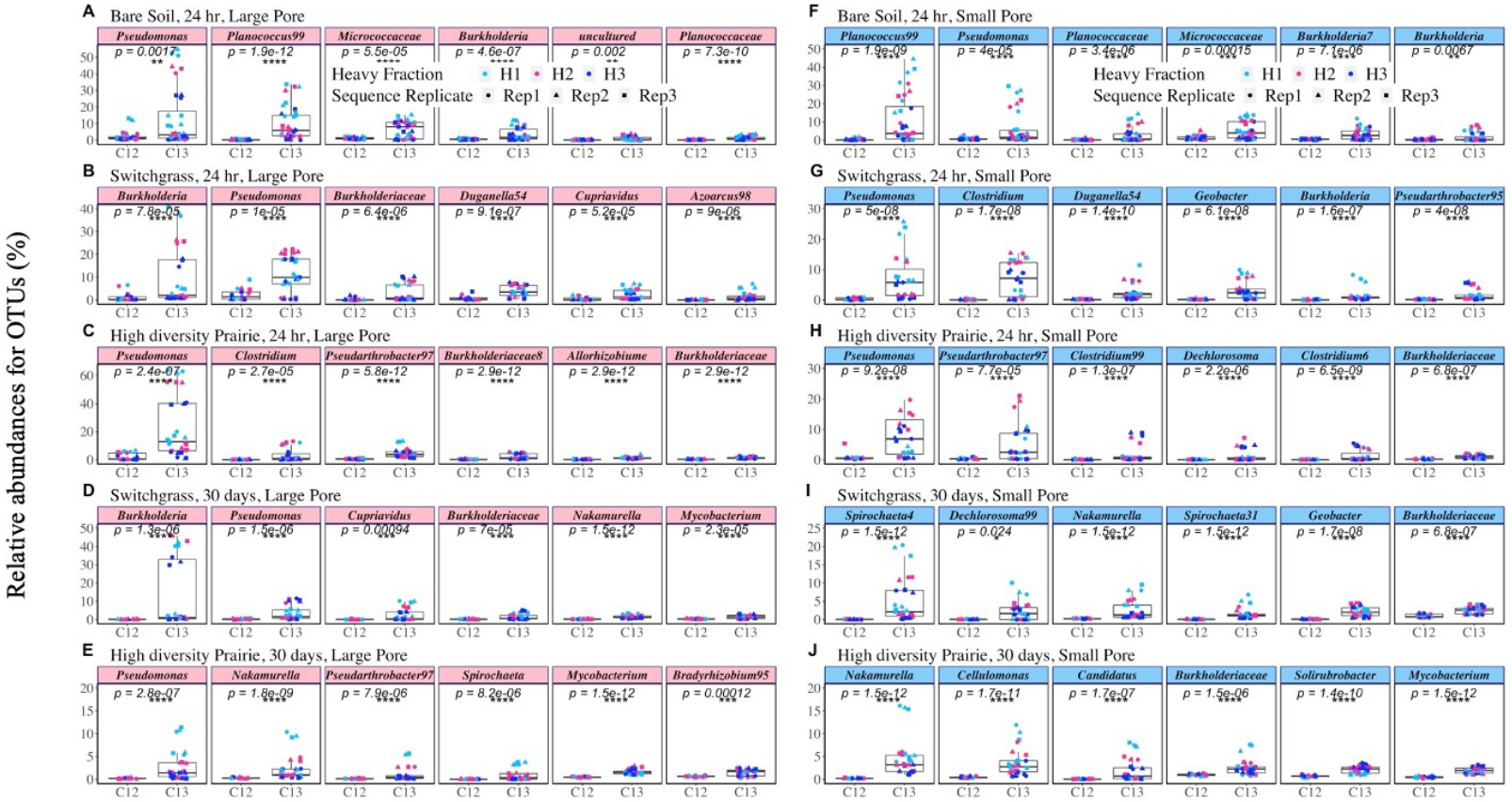

Figure 3.4 Phylotypes statistically significantly enriched (Wilcoxon test, one sided, $p < 0.05$) in the bare soil, switchgrass and high diversity prairie incubated for 24 hr or 30 days for the large pore (A-E) and the small pore (F-J) samples. Wilcoxon test one-sided p values of 0.0001, 0.001, 0.01, and 0.05 are represented by ****, ***, **, *. The six most abundant are shown for each treatment (A-J).

3.4.3 Functional Genes Predicted and Connections with Phylotypes

The KO functions associated with carbohydrate metabolism and energy metabolism (including citrate cycle, glycolysis gluconeogenesis, methane metabolism and nitrogen metabolism) were investigated in the bare soil, switchgrass and high diversity prairie treatments. The most abundant genes significantly enriched in the ^{13}C-glucose amended soils compared to the unlabeled glucose amended soils are shown (Figures A3.5-A3.9). The gene descriptions associated with each pathway are provided (Tables A3.10-A3.13). All genes significantly enriched for each pathway in the soil treatments are also summarized (Tables A3.14-A3.17). Differences were observed in the most enriched predicted genes between large and small pores soils for switchgrass and high diversity prairie incubated for 30 days (Figures 3.5 & Figures A3.10-A3.12). Notable trends included the enrichment of *glk* (glucokinase [EC:2.7.1.2], responsible for the conversion of glucose into glucose-6 phosphate, first step of glycolysis) in both the large and small pores high diversity prairie, but not in the switchgrass treatments (Figure 3.5). Additionally, the small pores soils were more dominated by genes associated with the later steps in the glycolysis/ gluconeogenesis pathways compared to the large pores soils for both switchgrass and high diversity prairie incubated for 30 days (Figure 3.5). Specifically, genes responsible for the conversion from pyruvate to acetyl-CoA were enriched in the small pores soils (incubated for 30 days) for the switchgrass and high diversity prairie treatments compared to large pores soils (Figure 3.5).

The phylotypes predicted to be associated with a subset of genes are shown with chord diagrams (Figures 3.6, 3.7 & Figure A3.13). The phylotypes associated with methane/ammonia monooxygenase are shown for all three treatments and eight, ten and thirteen phylotypes were associated with all three subunits (*pmoA-amoA*, *pmoB-amoB* and *pmoC-amoC*) in the bare soil,

switchgrass and high diversity prairie treatments (Figure A3.13). Unclassified *Beijerinckiaceae*, *Bauldia*, unclassified *Betaproteobacteriales* and *A21b_ge* were associated the methane/ ammonia monooxygenase genes in all the three soils. The dominant phylotypes included *Nitrosospira* and *Bauldia* for bare soils, *Methylovirgula* and unclassified *Nitrosomonadaceae* for switchgrass and unclassified *Nitrosomonadaceae* and unclassified *Beijerinckiaceae* for high diversity prairie.

As shown in Figure 6, no phylotype was associated with all the nitrate reductase genes (*napA* and *napB*) and nitrite reductase genes (*nirK* and *nirS*). One, four and five phylotypes contained *napA*, *napB* and *nirK* for the bare soil, switchgrass and high diversity prairie treatments, respectively. All four phylotypes containing *napA*, *napB* and *nirK* in switchgrass were included in high diversity prairie treatment (Figure 3.6B and C). Unclassified *Xanothobacteraceae* was the dominant phylotype containing *napA*, *napB* and *nirK* in all three treatments. Zero, two and one phylotypes contained *napA*, *napB* and *nirS* for the bare soil, switchgrass and high diversity prairie treatments, respectively (Figure 3.6). Phylotypes containing *napA*, *napB* and *nirS* were *Pseudomonas* and unclassified *Betaproteobacteriales* in the switchgrass treatment and *A21b_ge* in high diversity prairie treatment (Figure 3.6B and C). For the phylotypes associated with nitric oxide reductase and nitrous oxide reductase genes, two, six and two contained all three (*norB*, *norC* and *nosZ*) in the bare soil, switchgrass and high diversity prairie treatments, respectively (Figure 3.7). Unclassified *Xanthobacteraceae* contained all three genes (*norB*, *norC* and *nosZ*) for all the three treatments (Figure 3.7). Dominant phylotypes associated with nitric oxide reductase and nitrous oxide reductase genes included *Sediminibacterium* and *Halomonas* for the switchgrass treatment. The relative abundance of the phylotypes associated with the key functional genes in the 24 hr incubated and 30 day incubated soils are also shown (Figures A3.14-A3.17). Unclassified *Xanthobacteraceae* was more

abundant in the 24 hr incubated switchgrass treatment and high diversity prairie treatment than in the 30 day incubated soils (Figures A3.15 &A3.16).

A. High Diversity Prairie, Large Pores

B. High Diversity Prairie, Small Pores

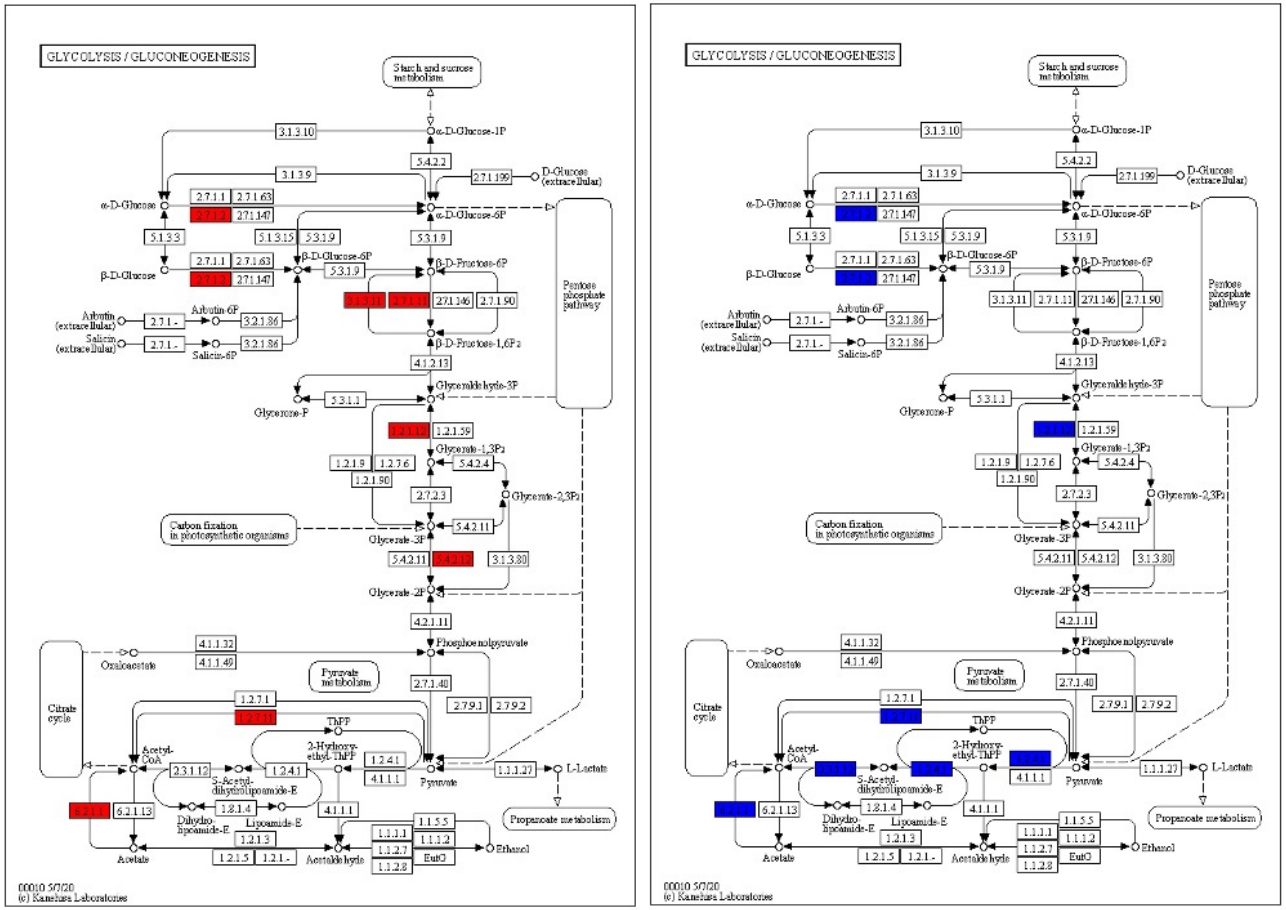

Figure 3.5 Genes enriched in glycolysis/gluconeogenesis pathway in the high diversity prairie soil (A, B) and in the switchgrass soil (C, D) after 30 days of incubation.

Figure 3.5 (cont'd)

C. Switchgrass, Large Pores

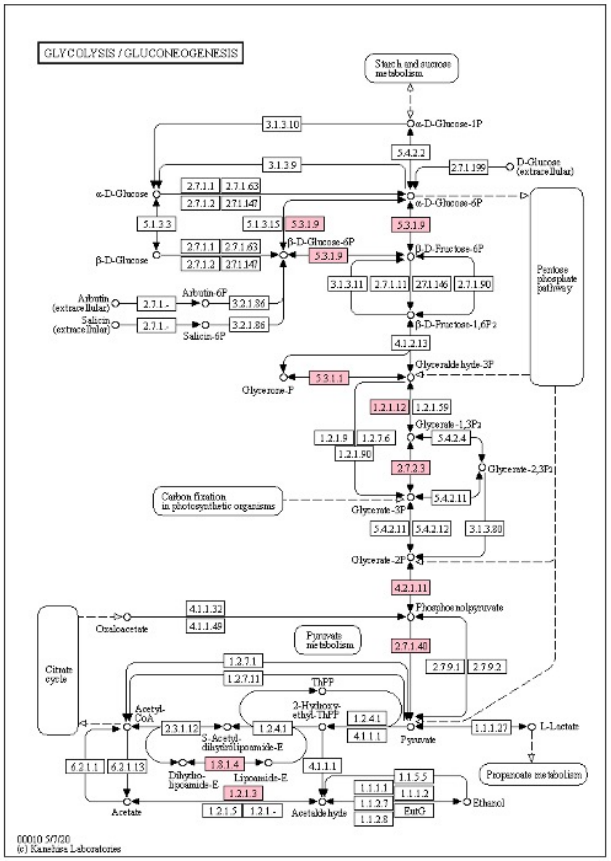

D. Switchgrass, Small Pores

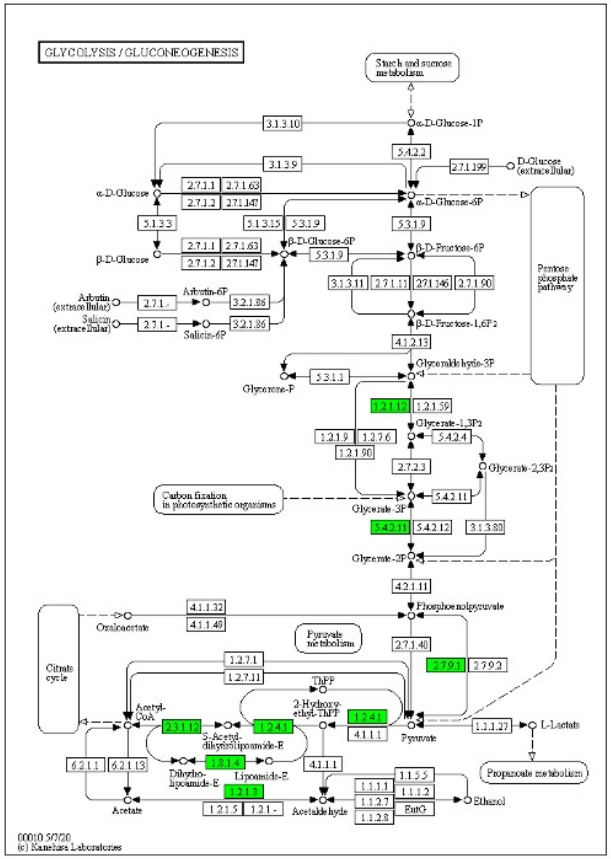

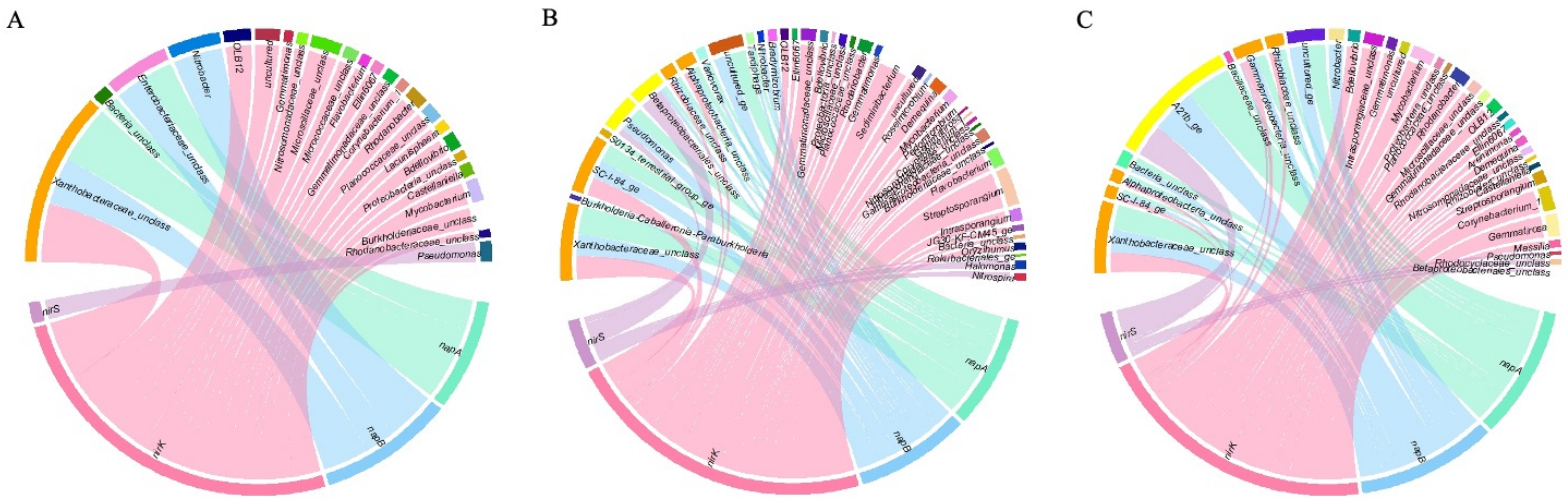

Figure 3.6 Phylotypes associated with nitrate reductase genes (*napA* and *napB*) and nitrite reductase genes (*nirK* and *nirS*) in bare soil (A), switchgrass soil (B) and high diversity prairie soil (C) (both 24 hours and 30 days). To limit the number of phylotypes on each figure, the relative abundance threshold was set to > 0.1. One, four and five phylotypes (in orange) contained *napA*, *napB* and *nirK* for the bare soil (A), switchgrass (B) and high diversity prairie (C) samples, respectively. Zero, two and one phylotypes (in yellow) contained *napA*, *napB* and *nirS* for the bare soil (A), switchgrass (B) and high diversity prairie (C) samples, respectively.

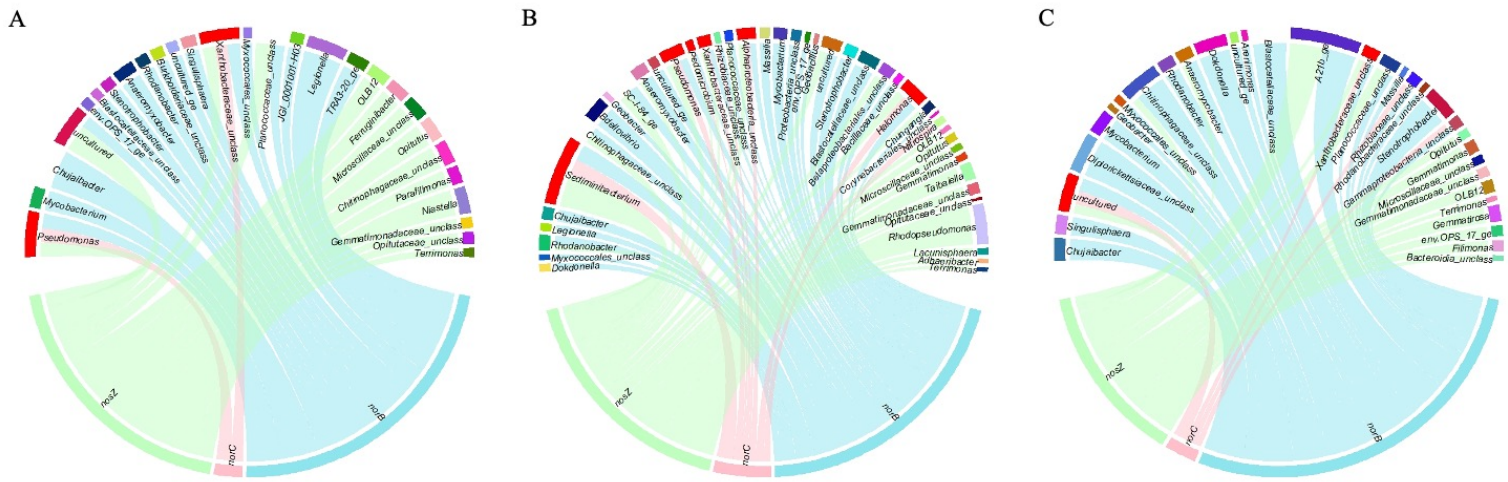

Figure 3.7 Phylotypes associated with nitric oxide reductase genes (*norB* and *norC*) and nitrous oxide reductase gene (*nosZ*) in the bare soil (A), switchgrass soil (B) and high diversity prairie soil (C) (both 24 hours and 30 days). To limit the number of phylotypes on each figure, the relative abundance threshold was set to > 0.2. Two, six and two phylotypes (in red) contained all three genes for the bare soil (A), switchgrass (B) and high diversity prairie (C) samples, respectively.

3.5 Discussion

The impacts of soil pore size and treatment (bare soil, switchgrass, high diversity prairie) on the microbial communities involved in the utilization of a newly added carbon source (glucose) were assessed. The temporal fate of the added carbon was also explored by incubating the switchgrass and high diversity prairie soils over two time periods. SIP and high throughput 16S rRNA gene amplicon sequencing were combined to characterize the microbial communities active in carbon uptake. The overall microbial communities were not significantly different between soil pores sizes or incubation times but varied significantly between treatments. In contrast, the active microorganisms capable of utilizing the newly added carbon source (identified via SIP) differed between soil pores sizes, treatments and incubation times. The enriched functional genes associated with carbohydrate metabolism and energy metabolism, as predicted by PICRUSt2 (Douglas, Maffei et al. 2020), also differed depending on the soil pore size and soil treatment.

Soil organic matter levels varied between the three soils (greatest in high plant diversity, followed by the switchgrass, then the bare soil). Consistent with this, others have reported high diversity plants exhibited increased root carbon inputs and root biomass concentration (Fornara and Tilman 2008, Ravenek, Bessler et al. 2014). Further, higher soil organic carbon content was observed in more diverse systems (Kravchenko, Guber et al. 2019). High plant diversity also increased the rhizosphere carbon inputs into soil microbial communities (Lange, Eisenhauer et al. 2015).

The overall microbial communities were significantly different between the three treatments and differences were also observed for the microbial richness and diversity indices. Specifically, these values were significantly lower in bare soil compared to high diversity prairie

or switchgrass treatments. Correlations between plant diversity and microbial activity or diversity have also been reported by others. For example, biomass, carbon use efficiency, microbial respiration and respiratory response to nutrients changed with increasing plant species richness (Eisenhauer, Bessler et al. 2010). The researchers concluded the quality of litter and rhizodeposits were key factors impacting the soil microbial community (Eisenhauer, Bessler et al. 2010). In the current study, considering the overall microbial community, all three treatments were dominated by *Proteobacteria* and *Actinobacteria*. Both phyla also accounted for the majority of the community differences between treatments. Both *Proteobacteria* and *Actinobacteria* have been closely linked to the metabolism of labile organic substrates (Goldfarb, Karaoz et al. 2011) and were also enriched in other glucose amended soils (Wang, Zhang et al. 2021).

There was no significant impact of pore size on the microbial diversity or richness values for the bare soil or switchgrass treatments. However, for the high diversity treatment, the small pores illustrated significantly higher diversity values (Shannon, Simpson, Inverse Simpson) compared to the large pores for the overall microbial community. Previous studies have also documented the impact of pore size and/or pore connectivity on soil microbial communities. It has been suggested that soils with a higher proportion of large pores are more likely to have disconnected water films, leading to a decline in microbial activity and microbial competitive interactions, thus potentially contributing to increased bacterial diversity (Carson, Gonzalez-Quinones et al. 2010, Chau , Bagtzoglou et al. 2011, Xia, Zheng et al. 2022). Bacterial species richness in acidic forest soils significantly increased with soil coarseness (quantified as % sand) (Chau , Bagtzoglou et al. 2011). The authors suggested the increase in species richness is due to the increased number of isolated water films in soils with larger pores. However, no significant

relationship was noted between the Shannon index and soil coarseness (% sand). A more recent study on the impact of macropores (>30 μm) and micropores (<30 μm) on soil microbial communities under row crop production reported no significant difference for Shannon diversity values between macropores and micropores for the total microbial community (Xia, Zheng et al. 2022). The range of previous and current results concerning the impact of pore size on microbial diversity and richness may be due to variations in methodologies, soil types, treatments and/or water availability.

SIP enabled the identification of microorganisms assimilating carbon from the amended glucose. A notable trend involved the dominance of *Pseudomonas* (*Proteobacteria*) in carbon uptake in all short-term incubations and in the large pore, longer incubations (switchgrass and high diversity prairie). Similarly, in field soil SIP biodegradation assays, others also identified *Pseudomonas* as being important for glucose metabolism (Padmanabhan, Padmanabhan et al. 2003). In another study, *Pseudomonas* was the most abundant genus utilizing added ^{13}C -glucose in rhizosphere soils after 3, 7 and 15 days (Zhou, Qin et al. 2021). It has been suggested that *Pseudomonas* species grow faster on labile substrates and are less able to compete for more recalcitrant substrates, thus have a putative role as a copiotroph (Bittman, Forge et al. 2005, Adamczyk, Perez-Mon et al. 2020). Fast-growing (*r*-strategists) copiotrophic microbes usually respond to labile carbon substrates quickly, whereas slow-growing (*K*-strategists) oligotrophic microbes grow on more recalcitrant carbon compounds (e.g., lignin) (Fierer, Bradford et al. 2007, Adamczyk, Perez-Mon et al. 2020).

In the short-term SIP incubations, dominant carbon assimilators varied between treatments. *Pseudarthrobacter* (*Actinobacteria*) was identified as an active assimilator of carbon in the high diversity prairie treatment, short-term incubation, in both of the large and small pores

soils. In other research, strains of *Pseudarthrobacter* (from permafrost soils) were found to be among the fastest growing microorganisms, suggesting they are likely copiotrophic (Adamczyk, Perez-Mon et al. 2020). *Pseudarthrobacter* has also been associated with plant growth promoting activities (Abadi, Sepehri et al. 2020, Tapia-García, Hernández-Trejo et al. 2020, Ham, Yoon et al. 2021) and the degradation of organic contaminants, such as 2,4,6-trinitrotoluene and phthalic acid esters (Chen, Chen et al. 2021, Lamba, Anand et al. 2021). *Duganella* (*Proteobacteria*) was an active assimilator of carbon in the switchgrass treatment, short-term incubation, in both of the large and small pores soils. *Duganella* was previously linked to the promotion of plant growth (Verma, Yadav et al. 2014) and the suppression of plant pathogens (Haack, Poehlein et al. 2016). *Pseudomonas* and *Planococcus* (*Firmicutes*) were the dominant active assimilators of carbon in the bare soil treatment, short-term incubation, in both of the large and small pores soils. Consistent with this, others have considered *Firmicutes* to be copiotrophic (Verastegui, Cheng et al. 2014, Pepe-Ranney, Campbell et al. 2016). *Planococcus* has been associated with the biodegradation of aromatic hydrocarbons as well as the production of biosurfactants, which can make carbon compounds more accessible (Waghmode, Suryavanshi et al. 2020).

Other key variables investigated with SIP in the current study involved soil pore size and incubation time. Although the overall microbial communities did not differ significantly based on OTU level between large and small pores sizes for each soil treatment ($p > 0.05$), the microorganisms actively responsible for carbon uptake (identified with SIP) differed between large and small pores sizes. For the shorter incubations, the numbers of unique phylotypes involved in carbon assimilation between large and small pores were zero, three and one for the bare soil, switchgrass and high diversity prairie treatments, respectively. However, for the longer incubations, the majority of the enriched phylotypes were different between the small and large

pore soils. In the large pores of the switchgrass and high diversity prairie treatments, approximately half of the enriched phylotypes were the same between incubation times. Although for the small pores of the same treatments, the phylotypes involved in carbon assimilation were largely different between incubation times, suggesting the active communities were more impacted by time in the small pores compared to the large pores.

For the shorter incubation of the switchgrass treatment, except for *Pseudomonas*, *Burkholderia* was dominant in the large pores while *Clostridium* (*Firmicutes*) was dominant in the small pores. Similarly, others have identified *Pseudomonas* and *Burkholderia* as responders to amendments of ^{14}C-glucose in soils (Jenkins, Rushton et al. 2010). This is consistent with their putative roles as *r*-strategists (Bittman, Forge et al. 2005). *Clostridium* has been associated with the biodegradation of complex carbohydrates (e.g., glucose, cellulose) (Warnick, Methé et al. 2002, Abd-Alla, Zohri et al. 2015, Figueiredo, Lopes et al. 2020). In flooded paddy soils, *Clostridium* communities illustrated a higher abundance with the addition of glucose (Li, Qu et al. 2017). In the shorter incubation of the high diversity treatment, the dominant phylotype for carbon assimilation was *Pseudomonas* in the large pores, while both *Pseudomonas* and *Pseudarthrobacter* were dominant in the small pores. However, for the longer incubation, *Pseudomonas* was only dominant in the large pores, suggesting the longer incubation time impacted the active microbial populations. The results are consistent with the theory of the dominance of *r*-strategists in large pores compared to small pores (Kravchenko, Guber et al. 2021).

Many previous studies have documented the impact of soil pore scale on microbial community structures (Ruamps, Nunan et al. 2013, Kravchenko, Negassa et al. 2014, Negassa, Guber et al. 2015, Kravchenko and Guber 2017, Xia, Zheng et al. 2022). Large pore soils are

likely to hold more plant roots due to the typical diameter of roots (30 μm) (Kuchenbuch and Jungk 1982), have better air diffusion, greater O_2 availability (Or, Smets et al. 2007), have more dissolved carbon and nutrients carried by the water fluxes (Kravchenko, Guber et al. 2021) as well as higher enzyme activity (Kravchenko, Guber et al. 2019). One conceptual model is that in large pores, *r*-strategists process labile carbon, enhance CO_2 emission and increase concentrations of dissolved organic carbon (Kravchenko, Guber et al. 2021). The necromass of r-strategists is then linked to the stimulation of *K*-strategists, which respond by enhanced extracellular enzyme production and microbial biomass growth (Kravchenko, Guber et al. 2021). In contrast, in the small pores, *K*-strategists dominate, as they are adapted to low carbon inputs (Kravchenko, Guber et al. 2021).

A key finding concerning the predicted enriched functional genes was the dominance of glucokinase (first step of glycolysis) in both the large and small pores of high diversity prairie treatment, but not in the switchgrass treatment. The trend suggests microorganisms in the high diversity prairie soil have a competitive advantage for consuming glucose. Another key finding concerns the dominance of genes associated with the later steps in the glycolysis/ gluconeogenesis pathways in the small pores compared to the large pores soils for both switchgrass and high diversity prairie. This is consistent with the theory that small pores favor *K*-strategists that are more likely to consume degradation products.

Dominant phylotypes predicted to be associated with the methane/ammonia monooxygenase genes (*pmoA-amoA*, *pmoB-amoB* and *pmoC-amoC*) included *Nitrosospira* and *Bauldia* for the bare soils, *Methylovirgula* and unclassified *Nitrosomonadaceae* for the switchgrass treatment and unclassified *Nitrosomonadaceae* and unclassified *Beijerinckiaceae* for high diversity prairie. Unclassified *Beijerinckiaceae* and *Nitrospira* were also predicted to be

associated with *pmoA/amoA* in other research (Cupples and Thelusmond 2022). *Beijerinckiaceae* is a family known to contain methanotrophs (Knief 2015). *Nitrosomonadaceae* are lithoautotrophic ammonia oxidizers (Prosser, Head et al. 2014). *Nitrospira* is a commonly reported ammonia oxidizing bacteria (Norton 2011).

More phylotypes contained *napA*, *napB* and *nirK* compared to those containing *napA*, *napB* and *nirS.* This is consistent with previous reports of the greater occurrence of *nirK* compared to *nirS* (Zhang, Zeng et al. 2015, Kim, Riggins et al. 2021, Li and Cupples 2021). For example, *nirK* was up to 3.8 times more abundant than *nirS* in 35 from 37 soils (Jones, Spor et al. 2014). The two genes are thought to be mutually exclusive, indicative of two ecologically distinct denitrifying communities (Enwall, Throback et al. 2010, Jones and Hallin 2010). Fewer phylotypes contained all three (of either group) in the bare soil compared to the switchgrass or high diversity prairie treatment, suggesting greater functional diversity in the latter two treatments. The switchgrass treatment contained the highest number of phylotypes containing nitric oxide reductase and nitrous oxide reductase genes (*norB*, *norC* and *nosZ*). Unclassified *Xanthobacteraceae* contained all three genes (*norB*, *norC* and *nosZ*) for all the three treatments. Interestingly, the same phylotype was the dominant phylotype containing *napA*, *napB* and *nirK* in all three treatments. Members of this family grow as aerobic chemoheterotrophs, but facultative chemolithoautotrophy (with hydrogen and/or reduced sulfur compounds) has also been reported (Oren 2014). The current study indicates an important role for an unclassified *Xanthobacteraceae* phylotype in denitrification for all three treatments.

3.6 Conclusions

The overall microbial communities as well as the active microorganisms capable of carbon uptake from glucose were determined in three soils (bare soil, switchgrass and high

diversity prairie treatments) for two pore sizes. The overall microbial communities were significantly different between the three treatments, but not between pore sizes or incubation times. *Proteobacteria* and *Actinobacteria* accounted for the majority of the community differences between the three treatments. Lower microbial diversity values were observed in the bare soil compared to switchgrass and high prairie diversity soils. Although no significant differences were noted in microbial diversity and richness values between the small and large pore sizes of the bare soil and the switchgrass treatments, the small pores of the high diversity prairie treatment exhibited higher microbial diversity values compared to the large pores.

SIP enabled the identification of the microorganisms assimilating carbon from the amended glucose. The active phylotypes responsible for carbon uptake varied between treatments, soil pore sizes and incubation times. *Pseudomonas* (*Proteobacteria*) played an important role in carbon uptake from glucose in all short-term incubations and in the large pore long-term incubations. A key finding included the identification of different carbon assimilators in the longer incubations between the small and large pore sizes for both the switchgrass and the high diversity prairie treatments. Such trends may be linked to different carbon assimilation strategies (*r*- vs. *K*-strategists) depending on pore size. The predicted enriched functional genes indicated the dominance of glucokinase in the high diversity prairie, but not in the switchgrass treatments, suggesting a competitive advantage for consuming glucose. The genes associated with the later steps in the glycolysis/gluconeogenesis pathways were dominant in the small pores compared to the large pores for both switchgrass and high diversity prairie, consistent with the theory that small pores favor *K*-strategists. To my knowledge, this is the first study to examine carbon assimilation from glucose as a function of pore architecture in these agricultural systems.

Acknowledgement

This research funded by USDA (grant number 2019-67019-29361). Support for this research was also provided by the Great Lakes Bioenergy Research Center, U.S. Department of Energy, Office of Science, Office of Biological and Environmental Research (Award DE-SC0018409), by the National Science Foundation Long-term Ecological Research Program (DEB 1832042) at the Kellogg Biological Station, and by MSU AgBioResearch. I would like to thank Maxwell Oerther and Thi Thuy Linh Nguyen for assistance with soil processing.

REFERENCES

Abadi, V. A. J. M., Sepehri, M., Rahmani, H. A., Zarei, M., Ronaghi, A., Taghavi, S. M., & Shamshiripour, M. (2020). Role of dominant phyllosphere bacteria with plant growth–promoting characteristics on growth and nutrition of Maize (*Zea mays L.*). *Journal of Soil Science and Plant Nutrition*, *20*, 2348-2363.

Abd-Alla, M. H., Zohri, A.-N. A., El-Enany, A.-W. E., & Ali, S. M. (2015). Acetone–butanol–ethanol production from substandard and surplus dates by Egyptian native Clostridium strains. *Anaerobe*, *32*, 77-86.

Adamczyk, M., Perez-Mon, C., Gunz, S., & Frey, B. (2020). Strong shifts in microbial community structure are associated with increased litter input rather than temperature in High Arctic soils. *Soil Biology and Biochemistry*, *151*, 108054. https://doi.org/https://doi.org/10.1016/j.soilbio.2020.108054

Adkins, J., Jastrow, J. D., Morris, G. P., Six, J., & de Graaff, M.-A. (2016). Effects of switchgrass cultivars and intraspecific differences in root structure on soil carbon inputs and accumulation. *Geoderma*, *262*, 147-154. https://doi.org/https://doi.org/10.1016/j.geoderma.2015.08.019

Andersen, K. S., Kirkegaard, R. H., Karst, S. M., & Albertsen, M. (2018). ampvis2: an R package to analyse and visualise 16S rRNA amplicon data. *bioRxiv*, 299537. https://doi.org/10.1101/299537

Barbera, P., Kozlov, A. M., Czech, L., Morel, B., Darriba, D., Flouri, T., & Stamatakis, A. (2019). EPA-ng: Massively Parallel Evolutionary Placement of Genetic Sequences. *Systematic Biology*, *68*(2), 365-369. https://doi.org/10.1093/sysbio/syy054

Bittman, S., Forge, T. A., & Kowalenko, C. G. (2005). Responses of the bacterial and fungal biomass in a grassland soil to multi-year applications of dairy manure slurry and fertilizer. *Soil Biology and Biochemistry*, *37*(4), 613-623. https://doi.org/https://doi.org/10.1016/j.soilbio.2004.07.038

Carney, K. M., & Matson, P. A. (2006). The influence of tropical plant diversity and composition on soil microbial communities. *Microbial Ecology*, *52*(2), 226-238.

Carson Jennifer, K., Gonzalez-Quiñones, V., Murphy Daniel, V., Hinz, C., Shaw Jeremy, A., & Gleeson Deirdre, B. (2010). Low Pore Connectivity Increases Bacterial Diversity in Soil. *Applied and Environmental Microbiology*, *76*(12), 3936-3942. https://doi.org/10.1128/AEM.03085-09

Carson, J. K., Gonzalez-Quinones, V., Murphy, D. V., Hinz, C., Shaw, J. A., & Gleeson, D. B. (2010). Low pore connectivity increases bacterial diversity in soil. *Appl Environ Microbiol*, *76*(12), 3936-3942. https://doi.org/10.1128/AEM.03085-09

Chau , J. F., Bagtzoglou, A. C., & Willig, M. R. (2011). The effect of soil texture on richness and diversity of bacterial communities. *Environmental Forensics*, *12*, 333-341.

Chen, F. Y., Chen, Y. C., Chen, C., Feng, L., Dong, Y. Q., Chen, J., Lan, J. R., & Hou, H. B. (2021). High-efficiency degradation of phthalic acid esters (PAEs) by Pseudarthrobacter defluvii E5: Performance, degradative pathway, and key genes. *Science of the Total Environment*, *794*, 148719.

Chenu, C., Hassink, J., & Bloem, J. (2001). Short-term changes in the spatial distribution of microorganisms in soil aggregates as affected by glucose addition. *Biology and Fertility of Soils*, *34*(5), 349-356. https://doi.org/10.1007/s003740100419

Chimento, C., Almagro, M., & Amaducci, S. (2016). Carbon sequestration potential in perennial bioenergy crops: the importance of organic matter inputs and its physical protection. *Gcb Bioenergy*, *8*(1), 111-121.

Cupples, A. M., & Thelusmond, J.-R. (2022). Predicting the occurrence of monooxygenases and their associated phylotypes in soil microcosms. *Journal of Microbiological Methods*, *193*, 106401.

Czech, L., Barbera, P., & Stamatakis, A. (2020). Genesis and Gappa: processing, analyzing and visualizing phylogenetic (placement) data. *Bioinformatics*, *36*(10), 3263-3265. https://doi.org/10.1093/bioinformatics/btaa070

Douglas, G. M., Maffei, V. J., Zaneveld, J. R., Yurgel, S. N., Brown, J. R., Taylor, C. M., Huttenhower, C., & Langille, M. G. I. (2020). PICRUSt2 for prediction of metagenome functions [Letter]. *Nature Biotechnology*, *38*(6), 685-688. https://doi.org/10.1038/s41587-020-0548-6

Eichorst Stephanie, A., & Kuske Cheryl, R. (2012). Identification of Cellulose-Responsive Bacterial and Fungal Communities in Geographically and Edaphically Different Soils by Using Stable Isotope Probing. *Applied and Environmental Microbiology*, *78*(7), 2316-2327. https://doi.org/10.1128/AEM.07313-11

Eisenhauer, N., Bessler, H., Engels, C., Gleixner, G., Habekost, M., Milcu, A., Partsch, S., Sabais, A. C. W., Scherber, C., Steinbeiss, S., Weigelt, A., Weisser, W. W., & Scheu, S. (2010). Plant diversity effects on soil microorganisms support the singular hypothesis. *Ecology*, *91*(2), 485-496. https://doi.org/10.1890/08-2338.1

el Zahar Haichar, F., Achouak, W., Christen, R., Heulin, T., Marol, C., Marais, M.-F., Mougel, C., Ranjard, L., Balesdent, J., & Berge, O. (2007). Identification of cellulolytic bacteria in soil by stable isotope probing. *Environmental Microbiology*, *9*(3), 625-634. http://ezproxy.msu.edu/login?url=https://search.ebscohost.com/login.aspx?direct=true&AuthType=ip,uid,cookie&db=edsovi&AN=edsovi.00125945.200703000.00007&site=eds-live

Enwall, K., Throback, I. N., Stenberg, M., Soderstrom, M., & Hallin, S. (2010). Soil resources influence spatial patterns of denitrifying communities at scales compatible with land management [Appl. Env. Micro.]. *Applied and Environmental Microbiology*, *76*(7), 2243-2250. https://doi.org/10.1128/Aem.02197-09

Fierer, N., Bradford, M. A., & Jackson, R. B. (2007). Toward an ecological classification of soil bacteria. *Ecology*, *88*(6), 1354-1364.

Figueiredo, G. G. O., Lopes, V. R., Romano, T., & Camara, M. C. (2020). Chapter 22 - Clostridium. In N. Amaresan, M. Senthil Kumar, K. Annapurna, K. Kumar, & A. Sankaranarayanan (Eds.), *Beneficial Microbes in Agro-Ecology* (pp. 477-491). Academic Press. https://doi.org/https://doi.org/10.1016/B978-0-12-823414-3.00022-8

Follett, R. F. (2001). Soil management concepts and carbon sequestration in cropland soils. *Soil and Tillage Research*, *61*, 77-92.

Fornara, D. A., & Tilman, D. (2008). Plant functional composition influences rates of soil carbon and nitrogen accumulation. *Journal of Ecology*, *96*(2), 314-322. https://doi.org/10.1111/j.1365-2745.2007.01345.x

Goldfarb, K., Karaoz, U., Hanson, C., Santee, C., Bradford, M., Treseder, K., Wallenstein, M., & Brodie, E. (2011). Differential Growth Responses of Soil Bacterial Taxa to Carbon Substrates of Varying Chemical Recalcitrance [Original Research]. *Frontiers in Microbiology*, *2*(94). https://doi.org/10.3389/fmicb.2011.00094

Gu, Z., Gu, L., Eils, R., Schlesner, M., & Brors, B. (2014). circlize implements and enhances circular visualization in R. *Bioinformatics*, *30*(19), 2811-2812. https://doi.org/10.1093/bioinformatics/btu393

Haack, F. S., Poehlein, A., Kröger, C., Voigt, C. A., Piepenbring, M., Bode, H. B., Daniel, R., Schäfer, W., & Streit, W. R. (2016). Molecular Keys to the Janthinobacterium and Duganella spp. Interaction with the Plant Pathogen Fusarium graminearum [Original Research]. *Frontiers in Microbiology*, *7*(1668). https://doi.org/10.3389/fmicb.2016.01668

Haichar, F. e. Z., Heulin, T., Guyonnet, J. P., & Achouak, W. (2016). Stable isotope probing of carbon flow in the plant holobiont. *Current Opinion in Biotechnology*, *41*, 9-13. https://doi.org/https://doi.org/10.1016/j.copbio.2016.02.023

Ham, S., Yoon, H., Park, J. M., & Park, Y. G. (2021). Optimization of fermentation medium for indole acetic acid production by *Pseudarthrobacter* sp. NIBRBAC000502770. *Applied Biochemistry and Biotechnology*, *193*, 2567-2579.

IPCC. (2014). *Climate Change 2014: Synthesis Report. Contribution of Working Groups I, II and III to the Fifth Assessment Report of the Intergovernmental Panel on Climate Change*.

Jastrow, J. D., Amonette, J. E., & Bailey, V. L. (2007). Mechanisms controlling soil carbon turnover and their potential application for enhancing carbon sequestration. *Climatic Change*, *80*(1), 5-23.

Jenkins, S. N., Rushton, S. P., Lanyon, C. V., Whiteley, A. S., Waite, I. S., Brookes, P. C., Kemmitt, S., Evershed, R. P., & O'Donnell, A. G. (2010). Taxon-specific responses of

soil bacteria to the addition of low level C inputs. *Soil Biology & Biochemistry*, *42*(9), 1624-1631. https://doi.org/10.1016/j.soilbio.2010.06.002

Jones, C. M., & Hallin, S. (2010). Ecological and evolutionary factors underlying global and local assembly of denitrifier communities. *Isme Journal*, *4*(5), 633-641. https://doi.org/10.1038/ismej.2009.152

Jones, C. M., Spor, A., Brennan, F. P., Breuil, M. C., Bru, D., Lemanceau, P., Griffiths, B., Hallin, S., & Philippot, L. (2014). Recently identified microbial guild mediates soil N2O sink capacity. *Nature Climate Change*, *4*(9), 801-805. https://doi.org/10.1038/nclimate2301

Kanehisa, M., Sato, Y., Kawashima, M., Furumichi, M., & Tanabe, M. (2016). KEGG as a reference resource for gene and protein annotation. *Nucleic Acids Research*, *44*(D1), D457-D462. https://doi.org/10.1093/nar/gkv1070

Kassambara, A. (2020). *ggpubr: 'ggplot2' Based Publication Ready Plots*. In (Version 0.4.0) https://CRAN.R-project.org/package=ggpubr

Kassambara, A. (2021). *rstatix: Pipe-Friendly Framework for Basic Statistical Tests*. In (Version 0.7.0) https://CRAN.R-project.org/package=rstatix

Kim, N., Riggins, C. W., Rodriguez-Zas, S., Zabaloy, M. C., & Villamil, M. B. (2021). Long-term residue removal under tillage decreases *amoA*-nitrifiers and stimulates *nirS*-denitrifier groups in the soil. *Applied Soil Ecology*, *157*. https://doi.org/10.1016/j.apsoil.2020.103730

Knief, C. (2015). Diversity and habitat preferences of cultivated and uncultivated aerobic methanotrophic bacteria evaluated based on *pmoA* as molecular marker. *Frontiers in Microbiology*, *6*, 1346.

Kong, Y., Zhu, C., Ruan, Y., Luo, G., Wang, M., Ling, N., Shen, Q., & Guo, S. (2018). Are the microbial communities involved in glucose assimilation in paddy soils treated with different fertilization regimes for three years similar? *Journal of Soils and Sediments*, *18*(7), 2476-2490. https://doi.org/10.1007/s11368-018-1961-z

Kozich, J. J., Westcott, S. L., Baxter, N. T., Highlander, S. K., & Schloss, P. D. (2013). Development of a Dual-Index Sequencing Strategy and Curation Pipeline for Analyzing Amplicon Sequence Data on the MiSeq Illumina Sequencing Platform [Article]. *Applied and Environmental Microbiology*, *79*(17), 5112-5120. https://doi.org/10.1128/aem.01043-13

Kravchenko, A., Guber, A., Gunina, A., Dippold, M., & Kuzyakov, Y. (2021a). Pore-scale view of microbial turnover: Combining 14C imaging, μCT and zymography after adding soluble carbon to soil pores of specific sizes. *European Journal of Soil Science*, *72*(2), 593-607,.

Kravchenko, A., Guber, A., Gunina, A., Dippold, M., & Kuzyakov, Y. (2021b). Pore-scale view of microbial turnover: Combining 14C imaging, μCT and zymography after adding soluble carbon to soil pores of specific sizes. *European Journal of Soil Science*, *72*(2), 593-607.

Kravchenko, A. N., & Guber, A. K. (2017). Soil pores and their contributions to soil carbon processes. *Geoderma*, *287*, 31-39. https://doi.org/https://doi.org/10.1016/j.geoderma.2016.06.027

Kravchenko, A. N., Guber, A. K., Razavi, B. S., Koestel, J., Quigley, M. Y., Robertson, G. P., & Kuzyakov, Y. (2019). Microbial spatial footprint as a driver of soil carbon stabilization. *Nature Communications*, *10*(1), 3121. https://doi.org/10.1038/s41467-019-11057-4

Kravchenko, A. N., Negassa, W. C., Guber, A. K., Hildebrandt, B., Marsh, T. L., & Rivers, M. L. (2014). Intra-aggregate pore structure influences phylogenetic composition of bacterial community in macroaggregates. *Soil Science Society of America Journal*, *78*(6), 1924-1939.

Kuchenbuch, R., & Jungk, A. (1982). A method for determining concentration profiles at the soil-root interface by thin slicing rhizospheric soil. *Plant and Soil*, *68*(3), 391-394.

Lahti, L., & Shetty, S. (2012-2019). *microbiome R package*. In http://microbiome.github.io

Lamb, E. G., Kennedy, N., & Siciliano, S. D. (2011). Effects of plant species richness and evenness on soil microbial community diversity and function. *Plant and Soil*, *338*(1), 483-495. https://doi.org/10.1007/s11104-010-0560-6

Lamba, J., Anand, S., Dutta, J., Chatterjee, S., Nagar, S., Celin, S. M., & Rai, P. K. (2021). Study on aerobic degradation of 2,4,6-trinitrotoluene (TNT) using pseudarthrobacter chlorophenolicuscollected from the contaminated site. *Environ. Monit. Assess.* , *193*, 80.

Lange, M., Eisenhauer, N., Sierra, C. A., Bessler, H., Engels, C., Griffiths, R. I., Mellado-Vázquez, P. G., Malik, A. A., Roy, J., Scheu, S., Steinbeiss, S., Thomson, B. C., Trumbore, S. E., & Gleixner, G. (2015). Plant diversity increases soil microbial activity and soil carbon storage. *Nature Communications*, *6*(1), 6707. https://doi.org/10.1038/ncomms7707

Lange, M., Habekost, M., Eisenhauer, N., Roscher, C., Bessler, H., Engels, C., Oelmann, Y., Scheu, S., Wilcke, W., Schulze, E. D., & Gleixner, G. (2014). Biotic and Abiotic Properties Mediating Plant Diversity Effects on Soil Microbial Communities in an Experimental Grassland. *Plos One*, *9*(5), Article e96182. https://doi.org/10.1371/journal.pone.0096182

Lemanski, K., & Scheu, S. (2014). Incorporation of 13C labelled glucose into soil microorganisms of grassland: Effects of fertilizer addition and plant functional group composition [Article]. *Soil biology & biochemistry*, *69*, 38-45. http://ezproxy.msu.edu/login?url=https://search.ebscohost.com/login.aspx?direct=true&AuthType=ip,uid,cookie&db=edscal&AN=edscal.28214333&site=eds-live

Li, L.-n., Qu, Z., Wang, B.-l., & Qu, D. (2017). Dynamics of the abundance and structure of metabolically active Clostridium community in response to glucose additions in flooded paddy soils: closely correlated with hydrogen production and Fe(III) reduction. *Journal of Soils and Sediments*, *17*(6), 1727-1740. https://doi.org/10.1007/s11368-016-1637-5

Li, Z., & Cupples, A. M. (2021). Diversity of nitrogen cycling genes at a Midwest Long Term Ecological Research site with different management practices. *Applied Microbiology and Biotechnology*, *108*, 4309-4327.

Liu, C., Cui, Y., Li, X., & Yao, M. (2021). microeco: an R package for data mining in microbial community ecology. *FEMS Microbiology Ecology*, *97*(2). https://doi.org/10.1093/femsec/fiaa255

Louca, S., & Doebeli, M. (2017). Efficient comparative phylogenetics on large trees. *Bioinformatics*, *34*(6), 1053-1055. https://doi.org/10.1093/bioinformatics/btx701

Ma, Z., Wood, C., & Bransby, D. I. (2000). Soil management impacts on soil carbon sequestration by switchgrass. *Biomass and bioenergy*, *18*(6), 469-477.

Martinez, A. P. (2017). pairwiseAdonis: Pairwise Multilevel Comparison using Adonis. R package version 0.4.

McLauchlan, K. K., Hobbie, S. E., & Post, W. M. (2006). Conversion from agriculture to grassland builds soil organic matter on decadal timescales. *Ecological Applications*, *16*(1), 143-153. http://www.jstor.org.proxy1.cl.msu.edu/stable/40061787

McMurdie, P. J., & Holmes, S. (2013). phyloseq: An R Package for Reproducible Interactive Analysis and Graphics of Microbiome Census Data. *PLOS ONE*, *8*(4), e61217. https://doi.org/10.1371/journal.pone.0061217

Negassa, W. C., Guber, A. K., Kravchenko, A. N., Marsh, T. L., Hildebrandt, B., & Rivers, M. L. (2015). Properties of Soil Pore Space Regulate Pathways of Plant Residue Decomposition and Community Structure of Associated Bacteria. *Plos One*, *10*(4), e0123999. https://doi.org/10.1371/journal.pone.0123999

Norton, J. M. (2011). Diversity and environmental distribution of ammonia-oxidizing bacteria. In B. B. Ward, D. J. Arp, & M. G. Klotz (Eds.), *Nitrification* (pp. 39-55). Amer Soc Micro.

Ogle, S. M., Swan, A., & Paustian, K. (2012). No-till management impacts on crop productivity, carbon input and soil carbon sequestration. *Agriculture, Ecosystems and Environment*, *149*, 37-49.

Oksanen, J., Blanchet, F. G., Friendly, M., Kindt, R., Legendre, P., McGlin, D., Minchin, R. P., O'Hara, R. B., Simpson, G. L., Peter, S., Stevens, M. H. H., Szoecs, E., & Wagner, H. (2020). *vegan: Community Ecology Package*. In https://CRAN.R-project.org/package=vegan

Or, D., Smets, B. F., Wraith, J. M., Dechesne, A., & Friedman, S. P. (2007). Physical constraints affecting bacterial habitats and activity in unsaturated porous media – a review. *Advances in Water Resources*, *30*(6), 1505-1527. https://doi.org/https://doi.org/10.1016/j.advwatres.2006.05.025

Oren, A. (2014). The Family Xanthobacteraceae. In E. Rosenberg, E. F. DeLong, S. Lory, E. Stackebrandt, & F. Thompson (Eds.), *The Prokaryotes: Alphaproteobacteria and Betaproteobacteria* (pp. 709-726). Springer Berlin Heidelberg. https://doi.org/10.1007/978-3-642-30197-1_258

Padmanabhan, P., Padmanabhan, S., DeRito, C., Gray, A., Gannon, D., Snape, J. R., Tsai, C. S., Park, W., Jeon, C., & Madsen, E. L. (2003). Respiration of 13C-Labeled Substrates Added to Soil in the Field and Subsequent 16S rRNA Gene Analysis of 13C-Labeled Soil DNA. *Applied and Environmental Microbiology*, *69*(3), 1614-1622. https://doi.org/10.1128/AEM.69.3.1614-1622.2003

Pepe-Ranney, C., Campbell, A. N., Koechli, C. N., Berthrong, S., & Buckley, D. H. (2016). Unearthing the ecology of soil microorganisms using a high resolution DNA-SIP approach to explore cellulose and xylose metabolism in soil. *Frontiers in Microbiology*, *7*, 703.

Post, W. M., Izaurralde, R. C., West, T. O., Liebig, M. A., & King, A. W. (2012). Management opportunities for enhancing terrestrial carbon dioxide sinks. *Frontiers in Ecology and the Environment*, *10*(10), 554-561. https://doi.org/10.1890/120065

Prosser, J. I., Head, I. M., & Stein, L. Y. (2014). The Family *Nitrosomonadaceae*. In E. Rosenberg, E. F. DeLong, S. Lory, E. Stackebrandt, & F. Thompson (Eds.), *The Prokaryotes. Alphaproteobacteria and Betaproteobacteria* (pp. 901–918). Springer-Verlag.

Pruesse, E., Quast, C., Knittel, K., Fuchs, B. M., Ludwig, W., Peplies, J., & Glöckner, F. O. (2007). SILVA: a comprehensive online resource for quality checked and aligned ribosomal RNA sequence data compatible with ARB. *Nucleic Acids Research*, *35*(21), 7188-7196. https://doi.org/10.1093/nar/gkm864

R_Core_Team. (2020). *R: A language and environment for statistical computing. Vennia, Auatria*. In https://www.R-project.org/.

Rangel-Castro, J. I., Killham, K., Ostle, N., Nicol, G. W., Anderson, I. C., Scrimgeour, C. M., Ineson, P., Meharg, A., & Prosser, J. I. (2005). Stable isotope probing analysis of the influence of liming on root exudate utilization by soil microorganisms. *Environmental Microbiology*, *7*(6), 828-838.

Ravenek, J. M., Bessler, H., Engels, C., Scherer-Lorenzen, M., Gessler, A., Gockele, A., De Luca, E., Temperton, V. M., Ebeling, A., Roscher, C., Schmid, B., Weisser, W. W., Wirth, C., de Kroon, H., Weigelt, A., & Mommer, L. (2014). Long-term study of root biomass in a biodiversity experiment reveals shifts in diversity effects over time. *Oikos*, *123*(12), 1528-1536. https://doi.org/10.1111/oik.01502

RStudio_Team. (2020). *RStudio: Integrated Development for R. RStudio, PBC. Boston, MA*. In http://www.rstudio.com/

Ruamps, L. S., Nunan, N., Pouteau, V., Leloup, J., Raynaud, X., Roy, V., & Chenu, C. (2013). Regulation of soil organic C mineralisation at the pore scale. *FEMS Microbiology Ecology*, *86*(1), 26-35. https://doi.org/10.1111/1574-6941.12078

Sanderson, M. A., Adler, P. R., Boateng, A. A., Casler, M. D., & Sarath, G. (2006). Switchgrass as a biofuels feedstock in the USA. *Canadian Journal of Plant Science*, *86*(Special Issue), 1315-1325.

Schloss, P. D., Westcott, S. L., Ryabin, T., Hall, J. R., Hartmann, M., Hollister, E. B., Lesniewski, R. A., Oakley, B. B., Parks, D. H., Robinson, C. J., Sahl, J. W., Stres, B., Thallinger, G. G., Van Horn, D. J., & Weber, C. F. (2009). Introducing mothur: Open-Source, Platform-Independent, Community-Supported Software for Describing and Comparing Microbial Communities [Article]. *Applied and Environmental Microbiology*, *75*(23), 7537-7541. https://doi.org/10.1128/aem.01541-09

Sleutel, S., Bouckaert, L., Buchan, D., Van Loo, D., Cornelis, W. M., & Sanga, H. G. (2012). Manipulation of the soil pore and microbial community structure in soil mesocosm incubation studies. *Soil Biology and Biochemistry*, *45*, 40-48. https://doi.org/https://doi.org/10.1016/j.soilbio.2011.09.016

Sprunger, C. D., Oates, L. G., Jackson, R. D., & Robertson, G. P. (2017). Plant community composition influences fine root production and biomass allocation in perennial bioenergy cropping systems of the upper Midwest, USA. *Biomass and bioenergy*, *105*, 248-258. https://doi.org/https://doi.org/10.1016/j.biombioe.2017.07.007

Sprunger, C. D., & Robertson, G. P. (2018). Early accumulation of active fraction soil carbon in newly established cellulosic biofuel systems. *Geoderma*, *318*, 42-51. https://doi.org/10.1016/j.geoderma.2017.11.040

Štursová, M., Žifčáková, L., Leigh, M. B., Burgess, R., & Baldrian, P. (2012). Cellulose utilization in forest litter and soil: identification of bacterial and fungal decomposers. *FEMS microbiology ecology*, *80*(3), 735-746.

Tapia-García, E. Y., Hernández-Trejo, V., Guevara-Luna, J., Rojas-Rojas, F. U., Arroyo-Herrera, I., Meza-Radilla, G., Vásquez-Murrieta, M. S., & Estrada-de los Santos, P. (2020). Plant growth-promoting bacteria isolated from wild legume nodules and nodules of *Phaseolusvulgaris L.* trap plants in central and southern Mexico. *Microbiol Research*, *239*, 126522.

Verastegui, Y., Cheng, J., Engel, K., Kolczynski, D., Mortimer, S., Lavigne, J., Montalibet, J., Romantsov, T., Hall, M., McConkey, B. J., Rose, D. R., Tomashek, J. J., Scott, B. R., Charles, T. C., Neufeld, J. D., & Bailey, M. (2014). Multisubstrate Isotope Labeling and Metagenomic Analysis of Active Soil Bacterial Communities. *mBio*, *5*(4), e01157-01114. https://doi.org/doi:10.1128/mBio.01157-14

Verma, P., Yadav, A. N., Kazy, S. K., Saxena, A. K., & Suman, A. (2014). Evaluating the diversity and phylogeny of plant growth promoting bacteria associated with wheat (Triticum aestivum) growing in central zone of India. *Int J Curr Microbiol Appl Sci*, *3*(5), 432-447.

Waghmode, S., Suryavanshi, M., Sharma, D., & Satpute, S. K. (2020). Planococcus Species – An Imminent Resource to Explore Biosurfactant and Bioactive Metabolites for Industrial Applications [Mini Review]. *Frontiers in Bioengineering and Biotechnology*, *8*(996). https://doi.org/10.3389/fbioe.2020.00996

Wang, X., Zhang, W., Liu, Y., Jia, Z., Li, H., Yang, Y., Wang, D., He, H., & Zhang, X. (2021). Identification of microbial strategies for labile substrate utilization at phylogenetic classification using a microcosm approach. *Soil Biology and Biochemistry*, *153*, 107970.

Warnick, T. A., Methé, B. A., & Leschine, S. B. (2002). Clostridium phytofermentans sp. nov., a cellulolytic mesophile from forest soil. *International Journal of Systematic and Evolutionary Microbiology*, *52*(4), 1155-1160. https://doi.org/https://doi.org/10.1099/00207713-52-4-1155

West, T. O., & Post, W. M. (2002). Soil organic carbon sequestration rates by tillage and crop rotation: A global data analysis. *Soil Science Society of America Journal*, *66*, 1930-1946. https://doi.org/10.2136/sssaj2002.1930

Wickham, H. (2016). ggplot2: Create Elegant Data Visualisations Using the Grammar of Graphics. *Springer-Verlag New York*.

Wickham, H. (2021). *tidyr: Tidy Messy Data*. In (Version 1.1.4) https://CRAN.R-project.org/package=tidyr

Wickham, H., François, R., Henry, L., & Müller, K. (2021). *dplyr: A Grammar of Data Manipulation*. In (Version 1.0.7) https://CRAN.R-project.org/package=dplyr

Xia, Q., Rufty, T., & Shi, W. (2020). Soil microbial diversity and composition: Links to soil texture and associated properties. *Soil Biology and Biochemistry*, *149*, 107953. https://doi.org/https://doi.org/10.1016/j.soilbio.2020.107953

Xia, Q., Zheng, N., Heitman, J. L., & Shi, W. (2022). Soil pore size distribution shaped not only compositions but also networks of the soil microbial community. *Applied Soil Ecology*, *170*, 104273. https://doi.org/https://doi.org/10.1016/j.apsoil.2021.104273

Ye, Y., & Doak, T. G. (2009). A Parsimony Approach to Biological Pathway Reconstruction/Inference for Genomes and Metagenomes. *PLOS Computational Biology*, *5*(8), e1000465. https://doi.org/10.1371/journal.pcbi.1000465

Yuko Takada-Hoshino and Naoyuki, M. (2004). An Improved DNA Extraction Method Using Skim Milk from Soils That Strongly Adsorb DNA. *Microbes and Environments*, *19*(1), 13-19. https://doi.org/10.1264/jsme2.19.13

Zak, D. R., Holmes, W. E., White, D. C., Peacock, A. D., & Tilman, D. (2003). Plant diversity, soil microbial communities, and ecosystem function: Are there any links? *Ecology*, *84*(8), 2042-2050. https://doi.org/10.1890/02-0433

Zhang, C.-B., Wang, J., Liu, W.-L., Zhu, S.-X., Ge, H.-L., Chang, S. X., Chang, J., & Ge, Y. (2010). Effects of plant diversity on microbial biomass and community metabolic profiles in a full-scale constructed wetland. *Ecological Engineering*, *36*(1), 62-68. https://doi.org/https://doi.org/10.1016/j.ecoleng.2009.09.010

Zhang, H., Ding, W., Luo, J., Bolan, N., & Yu, H. (2015). The dynamics of glucose-derived 13C incorporation into aggregates of a sandy loam soil following two-decade compost or inorganic fertilizer amendments. *Soil and Tillage Research*, *148*, 14-19. https://doi.org/https://doi.org/10.1016/j.still.2014.11.010

Zhang, L., Zeng, G., Zhang, J., Chen, Y., Yu, M., Lu, L., Li, H., Zhu, Y., Yuan, Y., Huang, A., & He, L. (2015). Response of denitrifying genes coding for nitrite (*nirK* or *nirS*) and nitrous oxide (*nosZ*) reductases to different physico-chemical parameters during agricultural waste composting. *Applied Microbiology and Biotechnology*, *99*(9), 4059-4070. https://doi.org/10.1007/s00253-014-6293-3

Zhou, W., Qin, X., Lyu, D., & Qin, S. (2021). Effect of glucose on the soil bacterial diversity and function in the rhizosphere of Cerasus sachalinensis. *Horticultural Plant Journal*.

APPENDIX

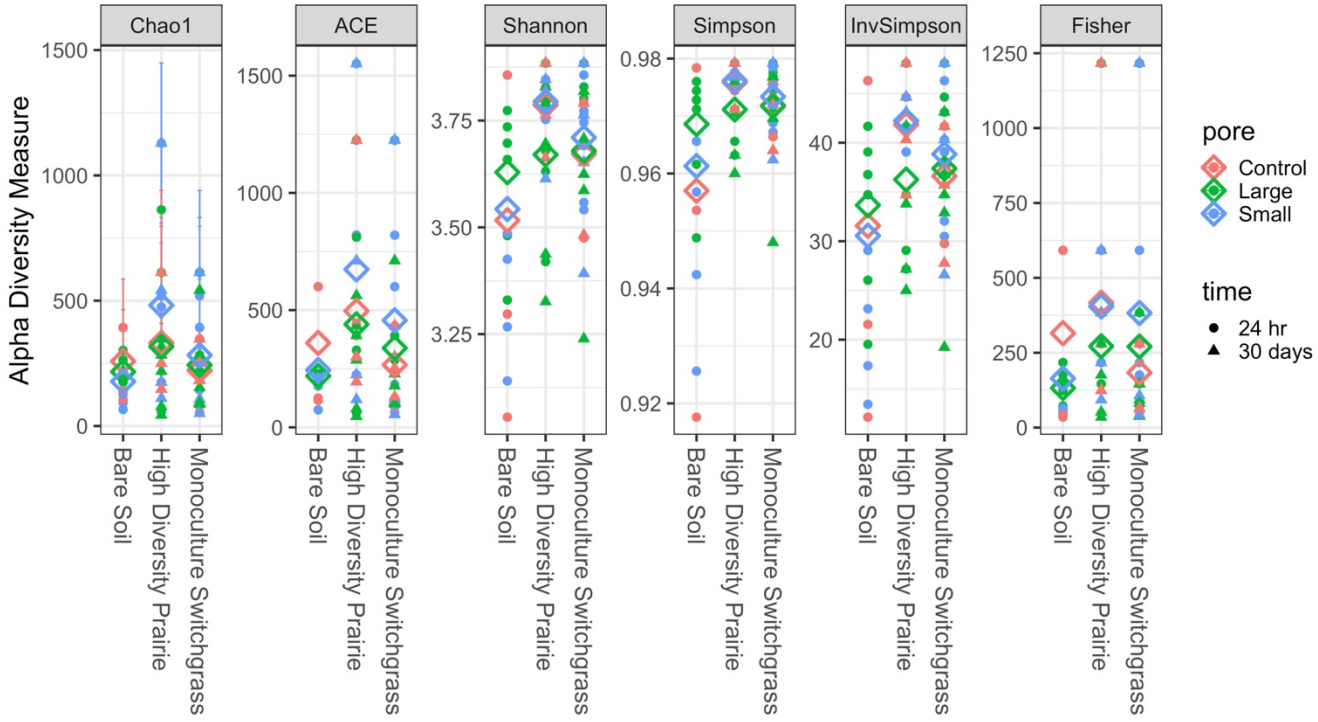

Figure A3.1 Alpha diversity assessed by richness (Chao1, ACE) and diversity (Shannon, Simpson, Inverse of Simpson and Fisher) for bare soil, high diversity prairie and monoculture switchgrass. Note: the hollow rhombus represents the means of the indices in control, large pore and small pore soils in each treatments.

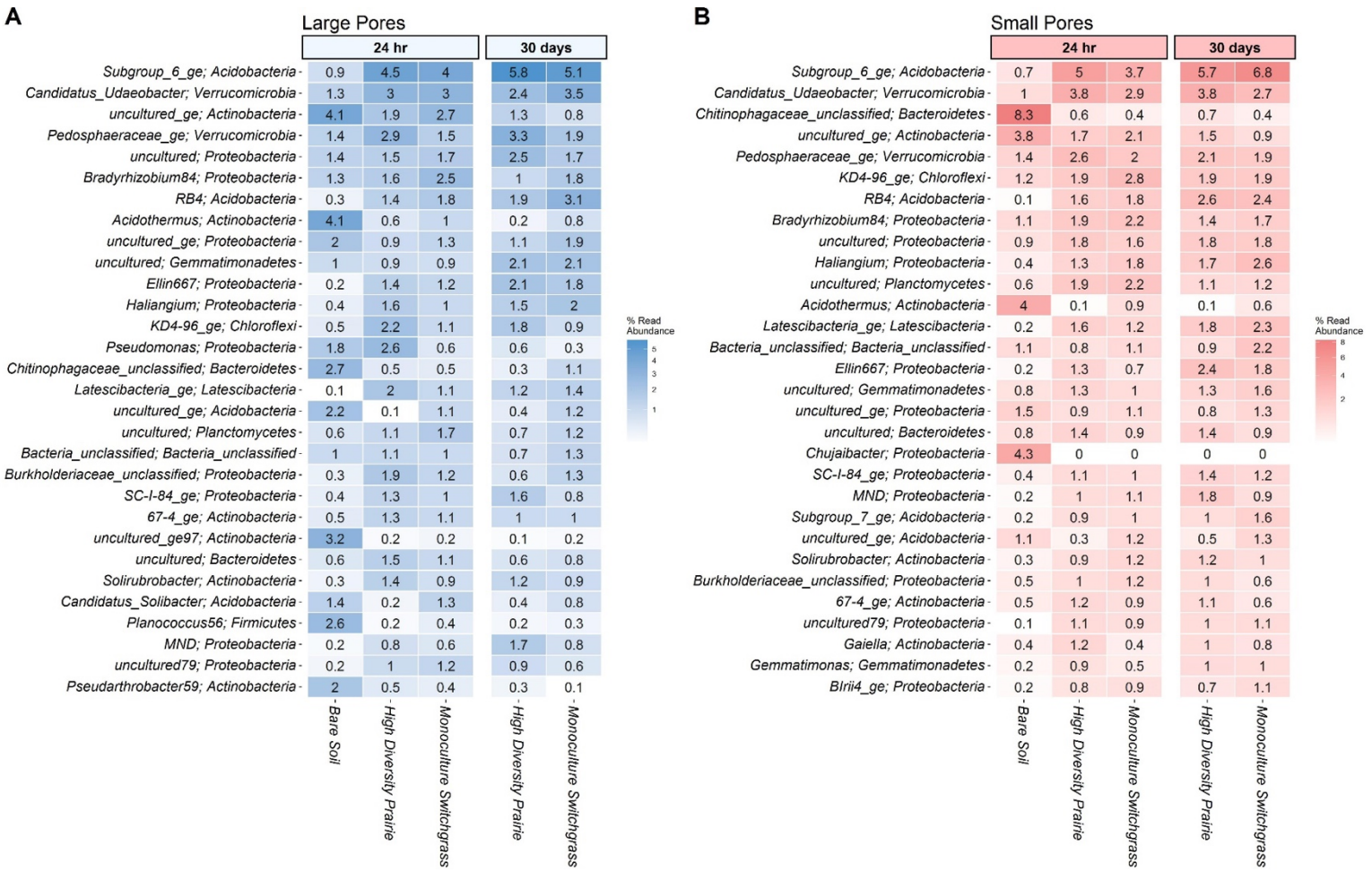

Figure A3.2 Heatmaps of thirty most abundant OTUs in the bare soil, monoculture switchgrass and high diversity prairie of large pores (A) and small pores (B) over the two incubation times.

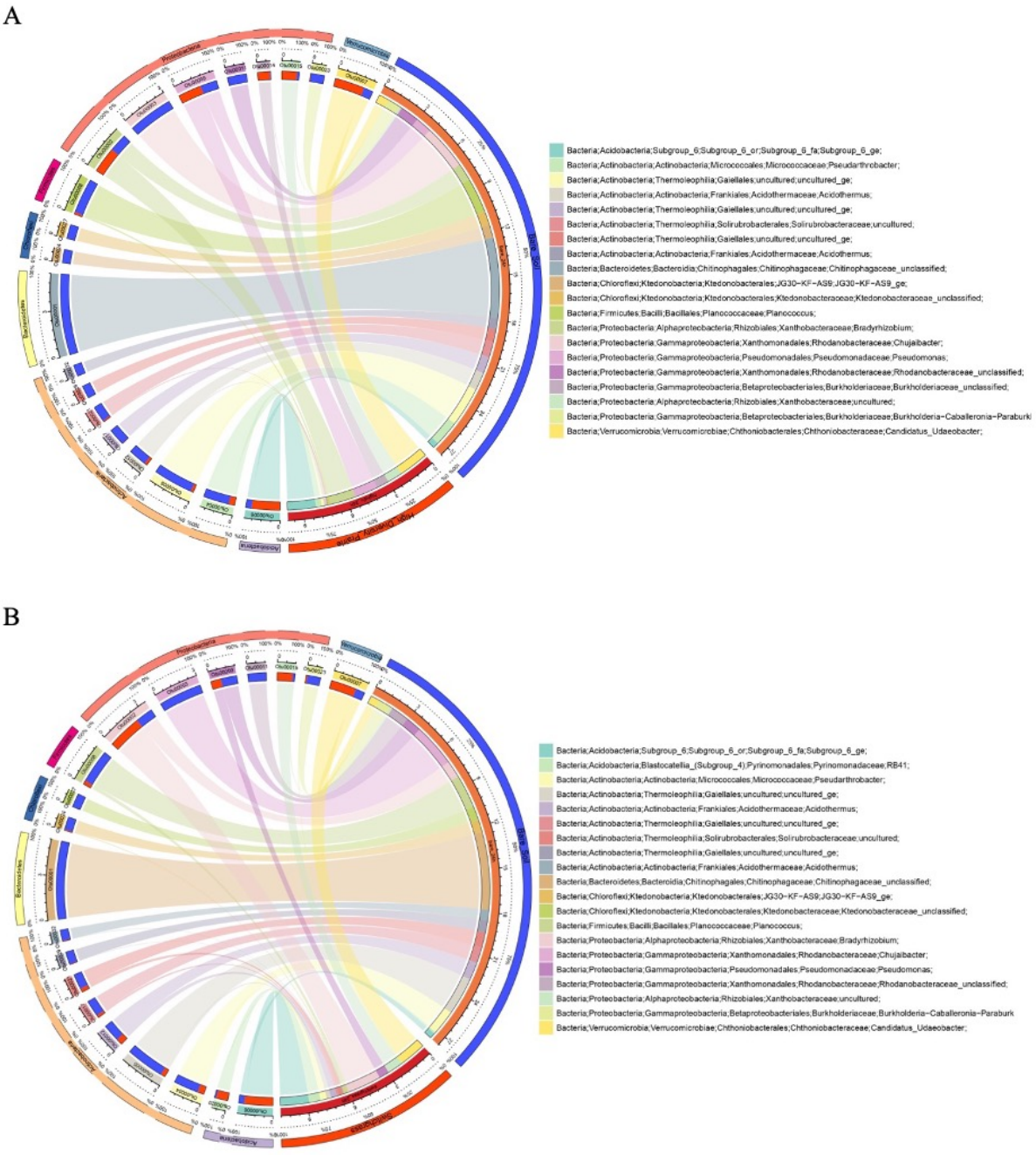

Figure A3.3 Chord diagrams illustrating the top 20 OTUs contributing to the differences of communities between bare soil and high diversity prairie incubated for 24 hr (A), bare soil and switchgrass incubated for 24 hr (B), switchgrass and high diversity prairie incubated for 24 hr (C) and switchgrass and high diversity prairie incubated for 30 days (D).

Figure A3.3 (cont'd)

C

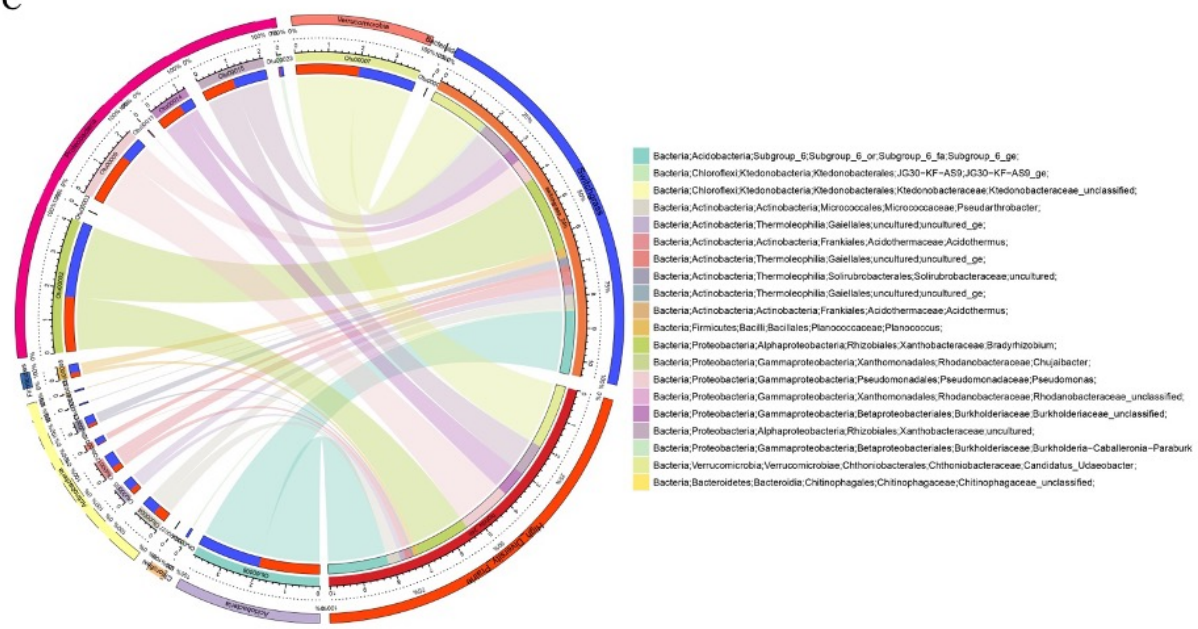

D

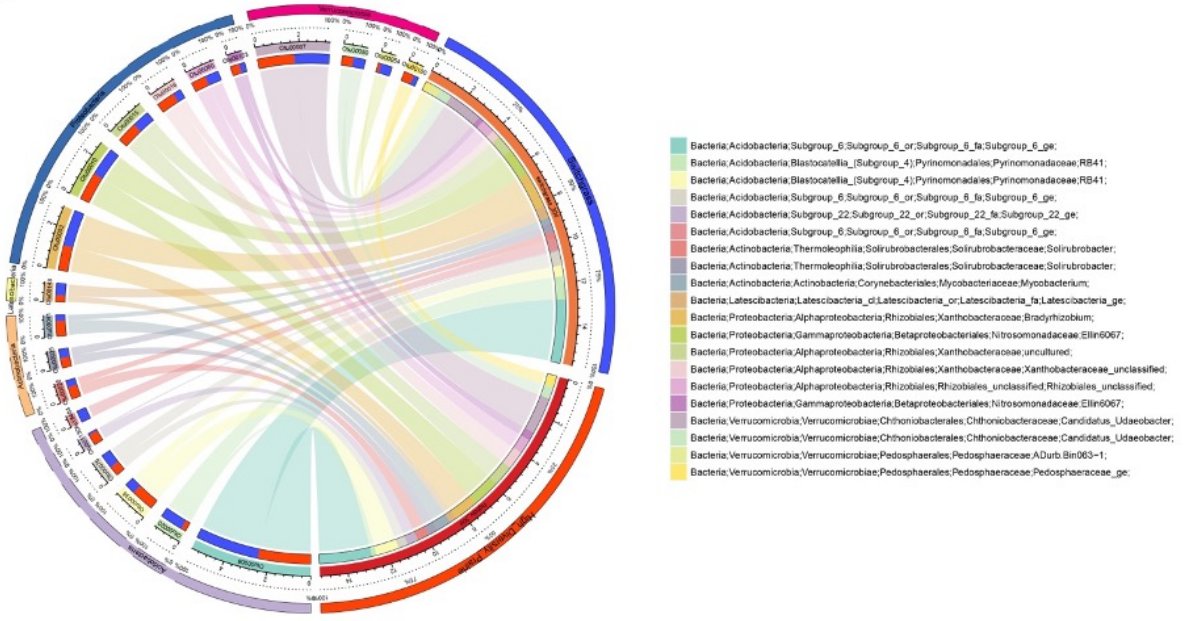

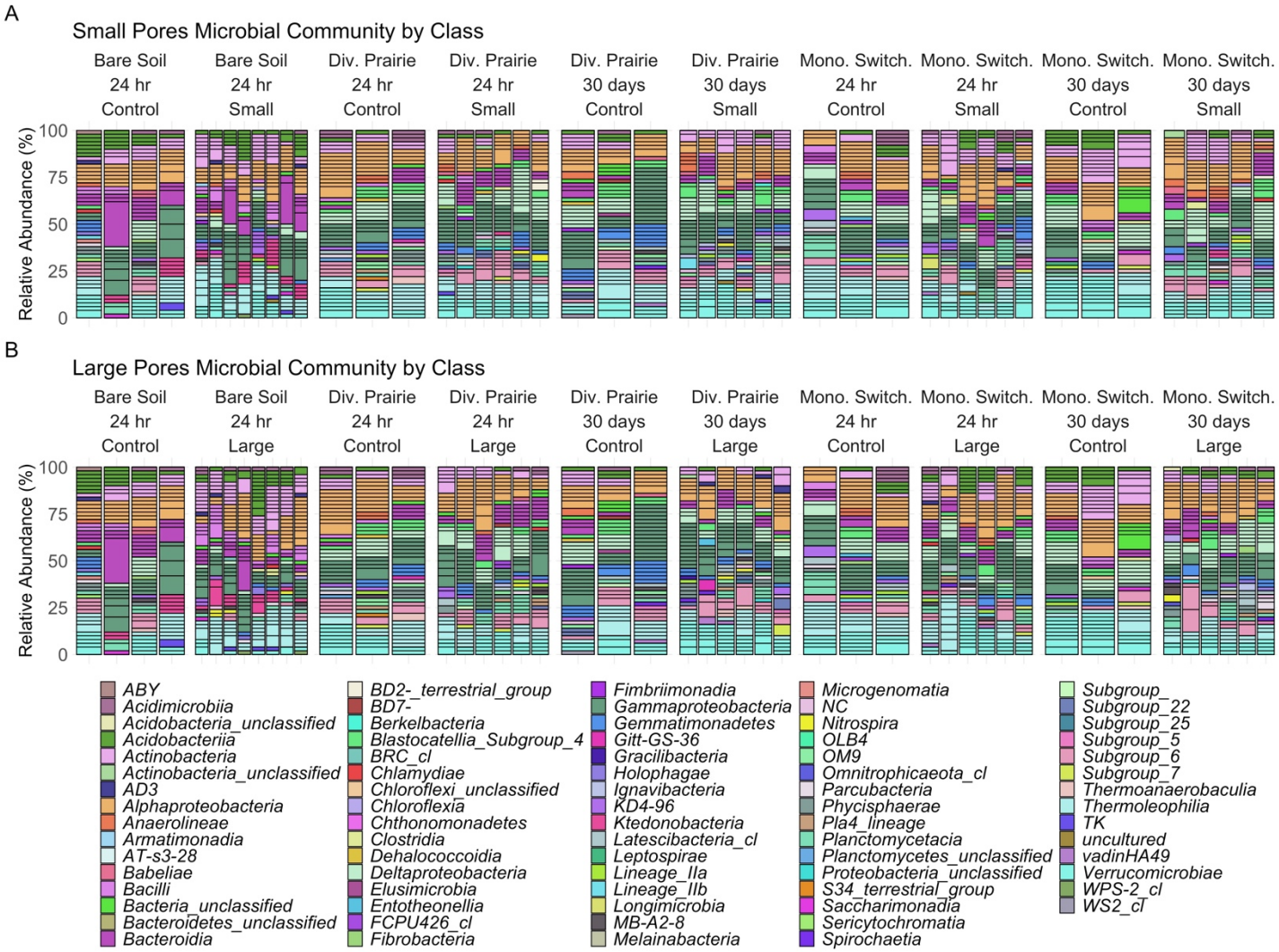

Figure A3.4 Relative abundance by class level for the treatments involving the small pore soils (A) and large pore soils (B) for the three treatments at two different incubation times.

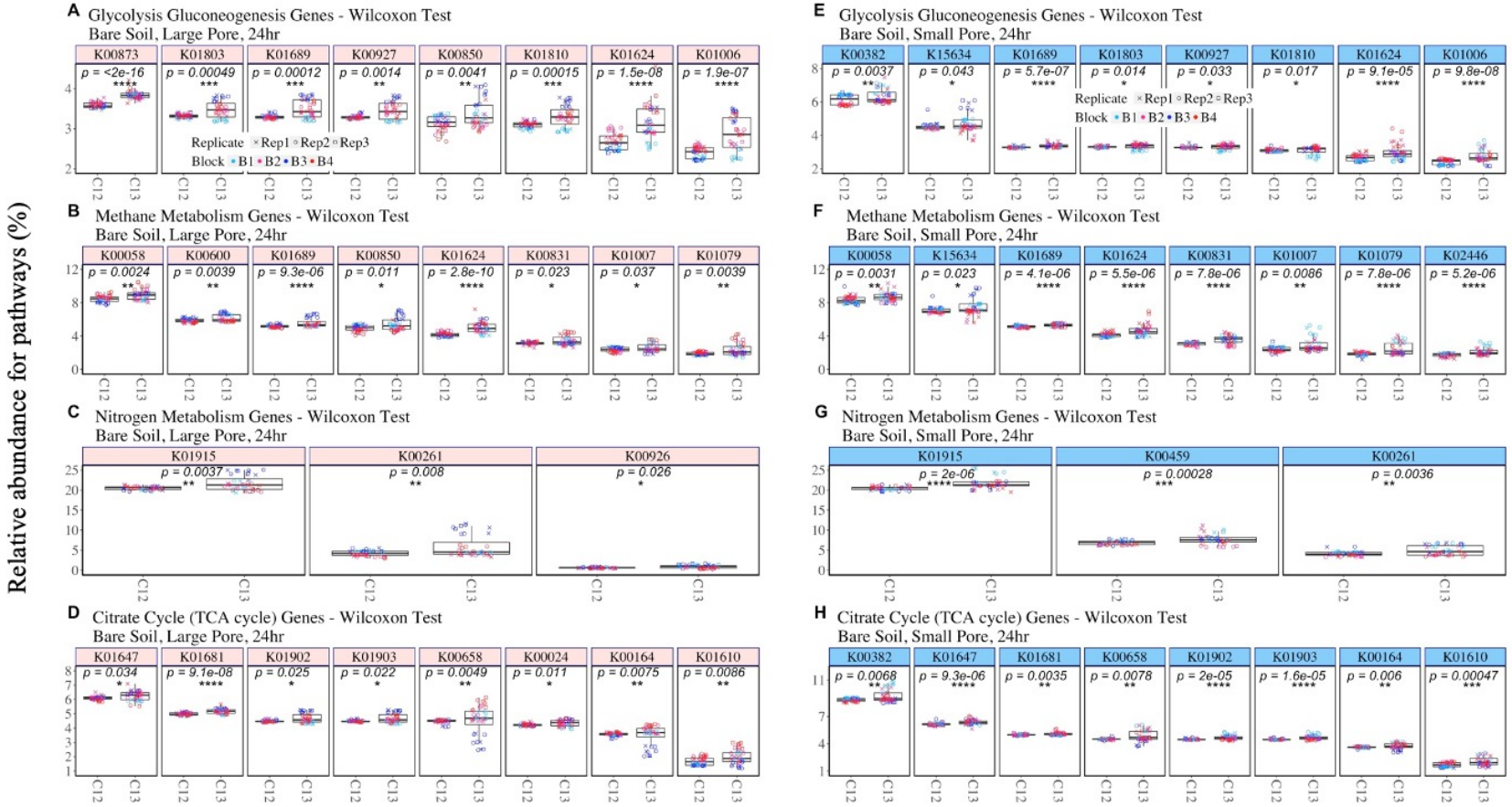

Figure A3.5 Genes statistically significantly enriched (Wilcoxon test, one sided, $p < 0.05$) in the bare soil incubated for 24 hr. Wilcoxon test one-sided p values of 0.0001, 0.001, 0.01, and 0.05 are represented by ****, ***, **, *. The eight most abundant for each treatment (A-H) are shown. In some cases, less than eight genes were significantly enriched.

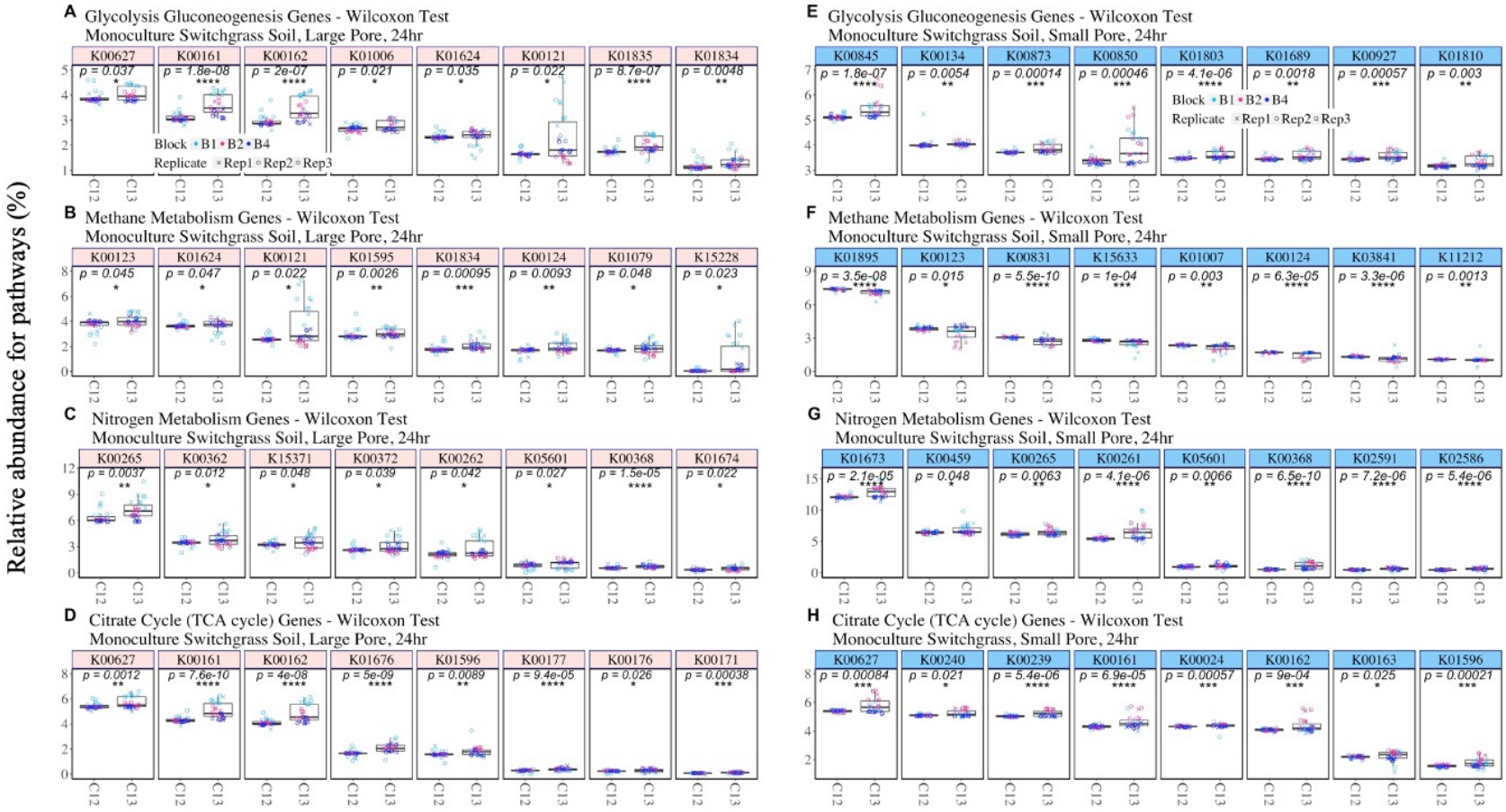

Figure A3.6 Genes statistically significantly enriched (Wilcoxon test, one sided, $p < 0.05$) in the monoculture switchgrass soil incubated for 24 hours. Wilcoxon test one-sided p values of 0.0001, 0.001, 0.01, and 0.05 are represented by ****, ***, **, *. The eight most abundant for each treatment (A-H) are shown.

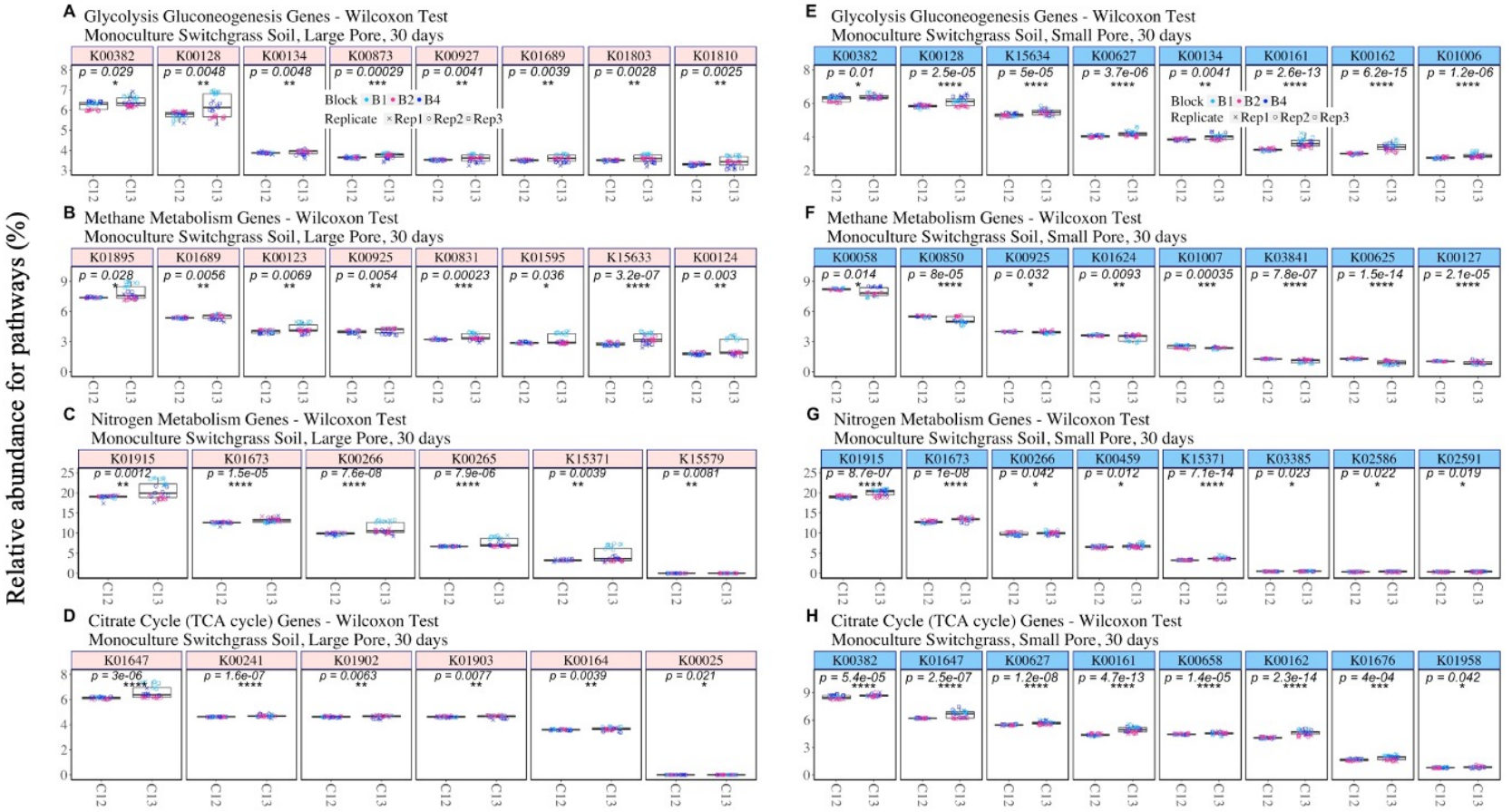

Figure A3.7 Genes statistically significantly enriched (Wilcoxon test, one sided, $p < 0.05$) in the monoculture switchgrass soil incubated for 30 days. Wilcoxon test one-sided p values of 0.0001, 0.001, 0.01, and 0.05 are represented by ****, ***, **, *. The eight most abundant for each treatment (A-H) are shown. In some cases, less than eight genes were significantly enriched.

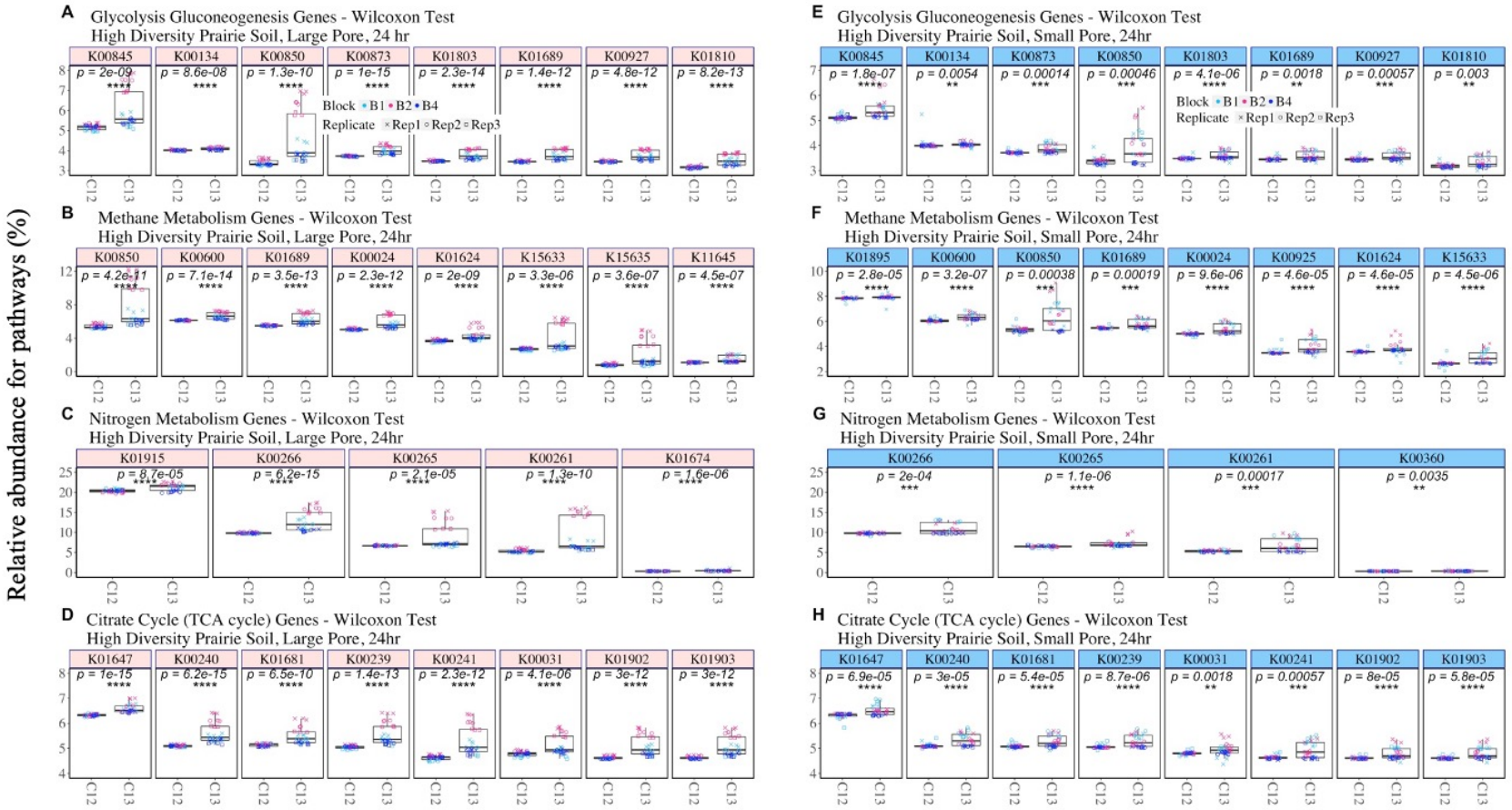

Figure A3.8 Genes statistically significantly enriched (Wilcoxon test, one sided, $p < 0.05$) in the high diversity prairie soil incubated for 24 hours. Wilcoxon test one-sided p values of 0.0001, 0.001, 0.01, and 0.05 are represented by ****, ***, **, *. The eight most abundant for each treatment (A-H) are shown. In some cases, less than eight genes were significantly enriched.

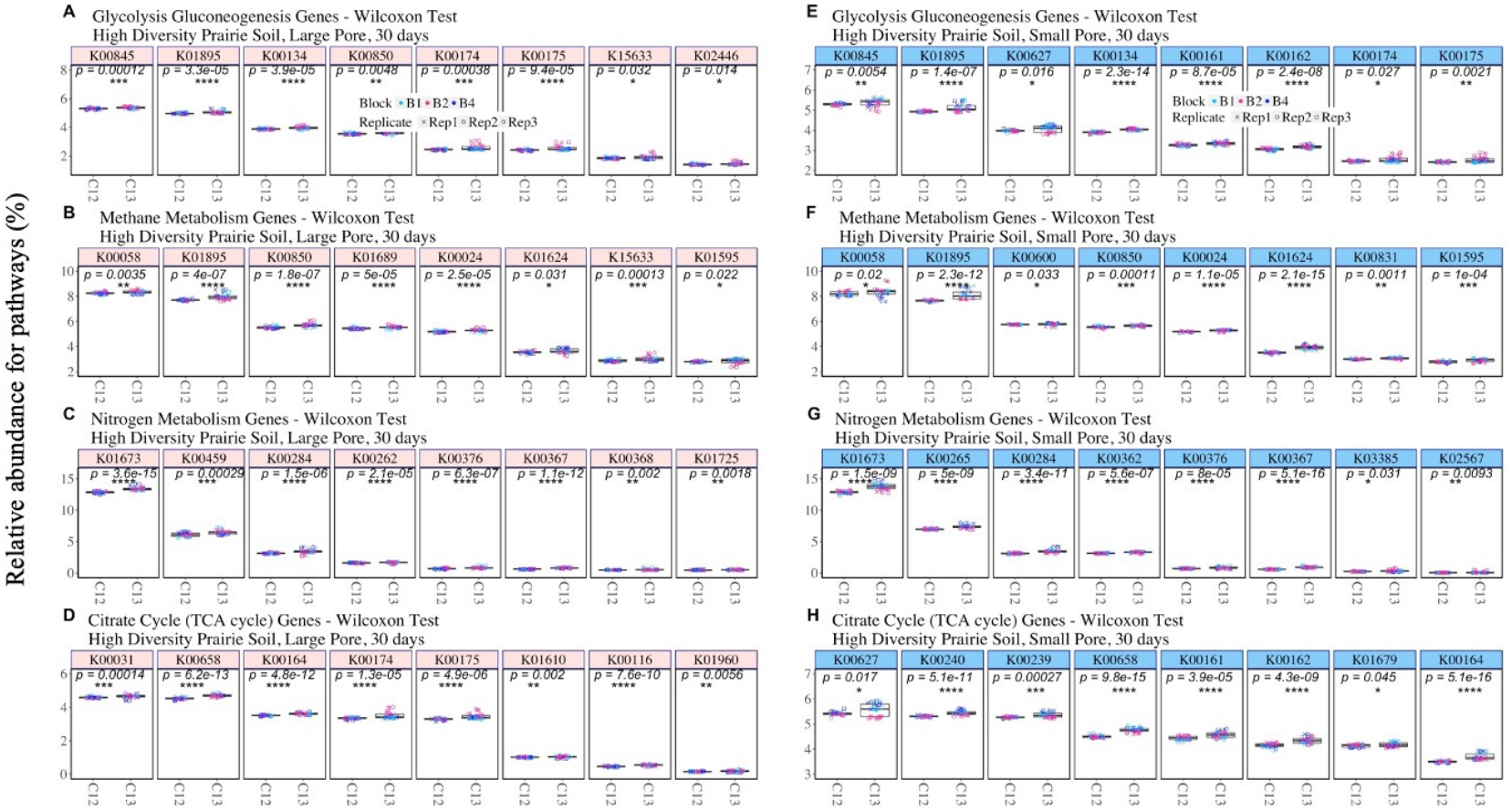

Figure A3.9 Genes statistically significantly enriched (Wilcoxon test, one sided, $p < 0.05$) in the high diversity prairie soil incubated for 30 days. Wilcoxon test one-sided p values of 0.0001, 0.001, 0.01, and 0.05 are represented by ****, ***, **, *. The eight most abundant for each treatment (A-H) are shown.

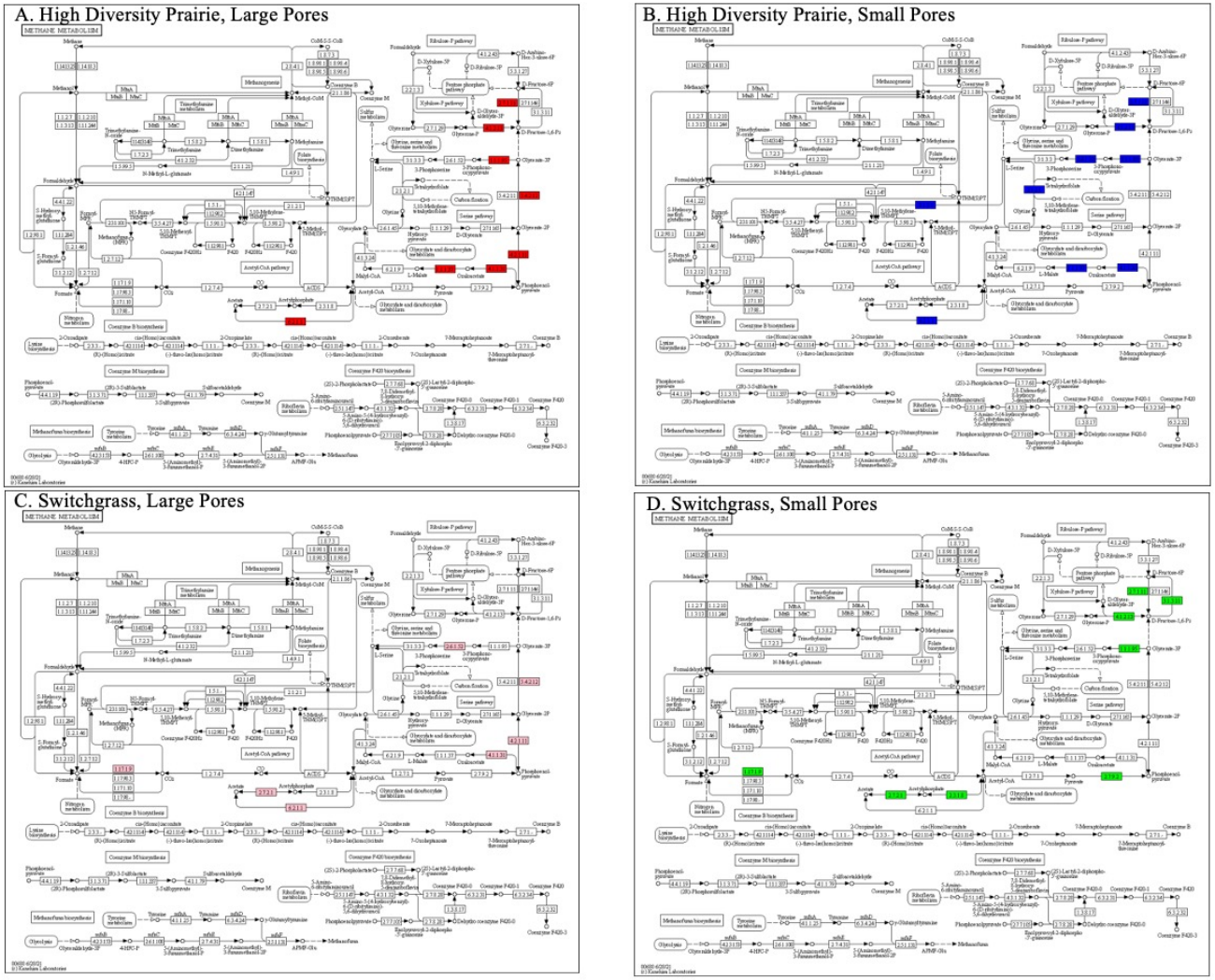

Figure A3.10 Genes enriched in methane metabolism pathway in the high diversity prairie soil (A, B) and in the switchgrass soil (C, D) after 30 days of incubation.

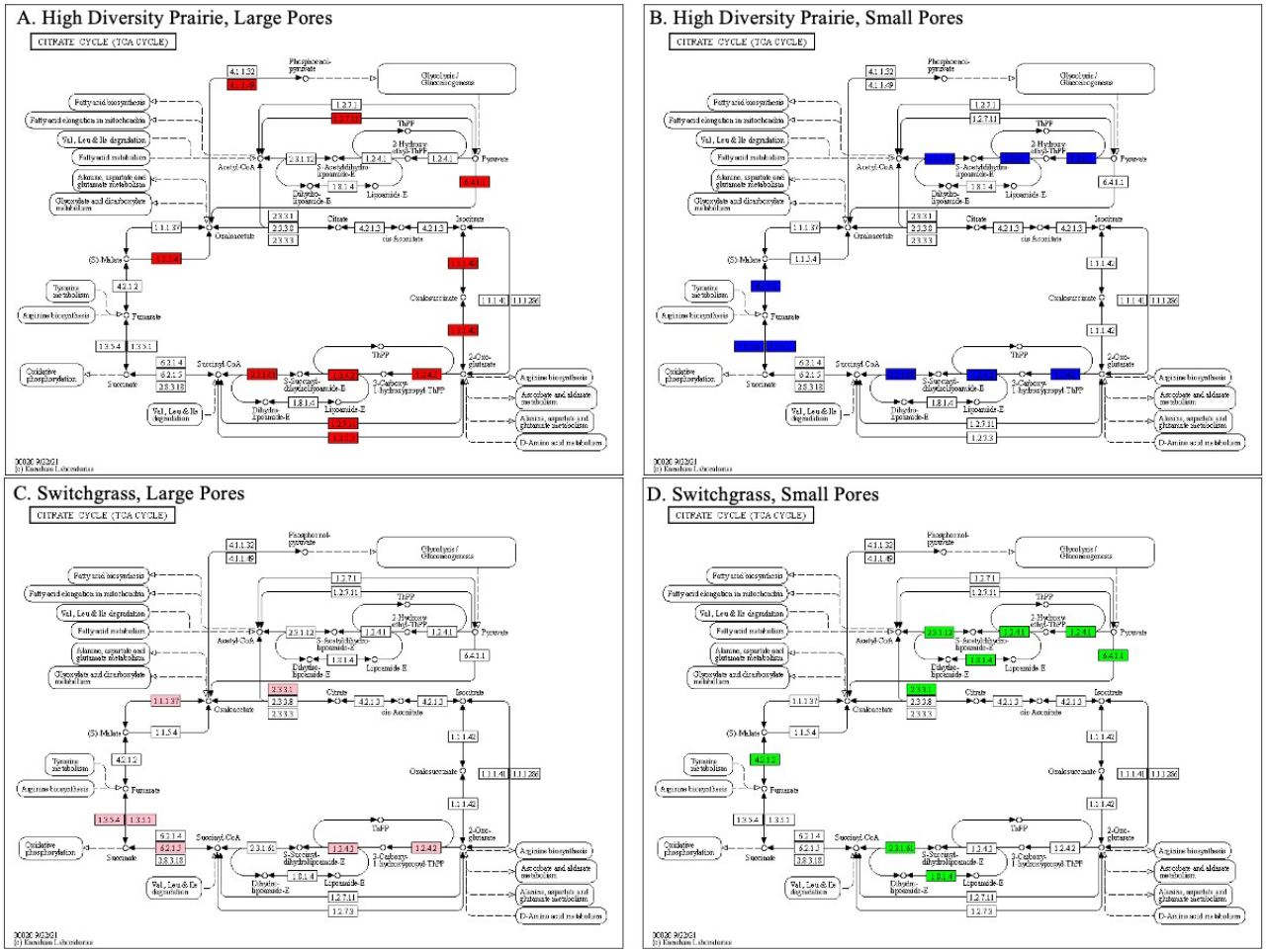

Figure A3.11 Genes enriched in the citrate cycle (TCA cycle) pathway in the high diversity prairie soil (A, B) and in the switchgrass soil (C, D) after 30 days of incubation.

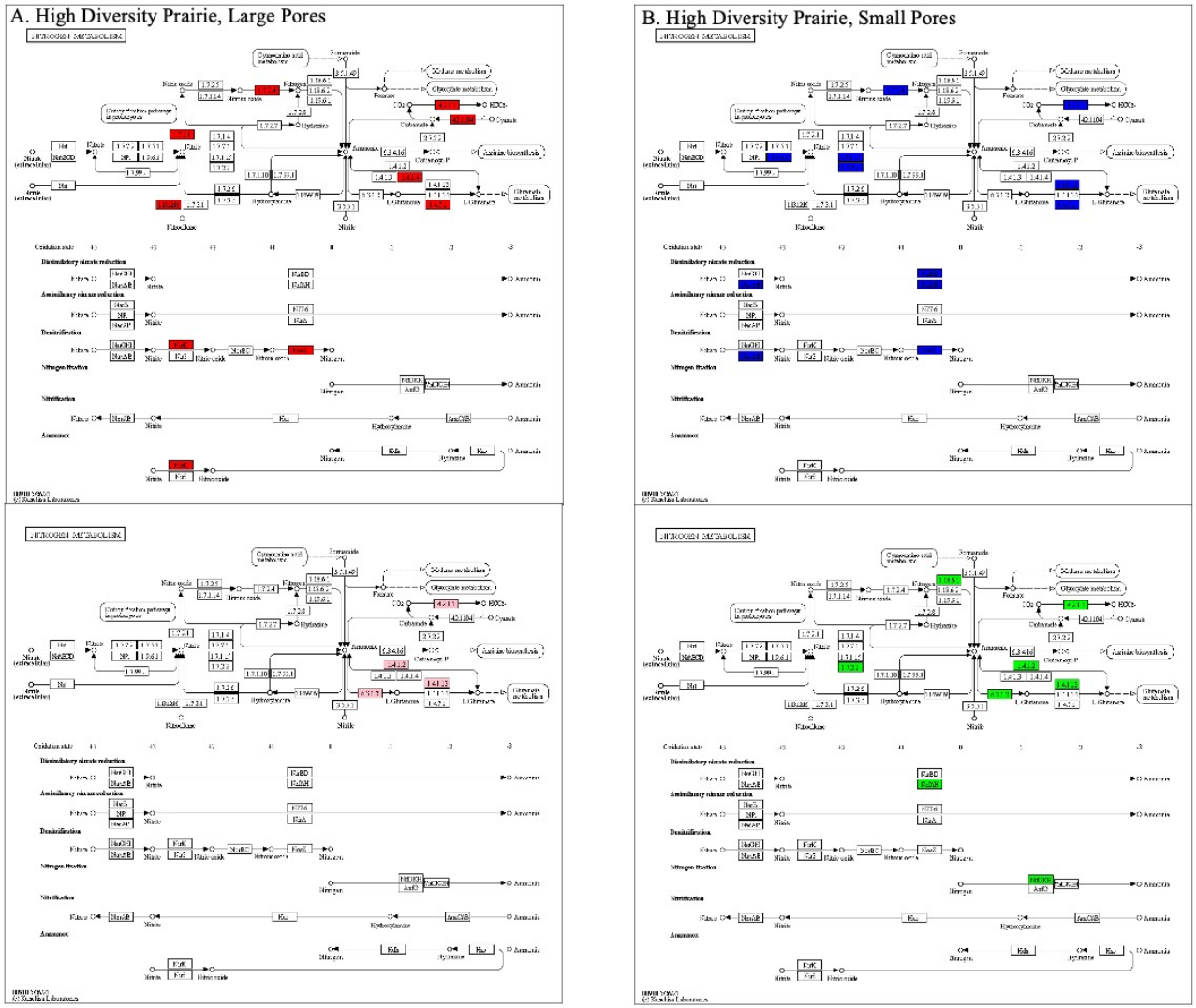

Figure A3.12 Genes enriched in nitrogen metabolism pathway in the high diversity prairie soil (A, B) and in the switchgrass soil (C, D) after 30 days of incubation.

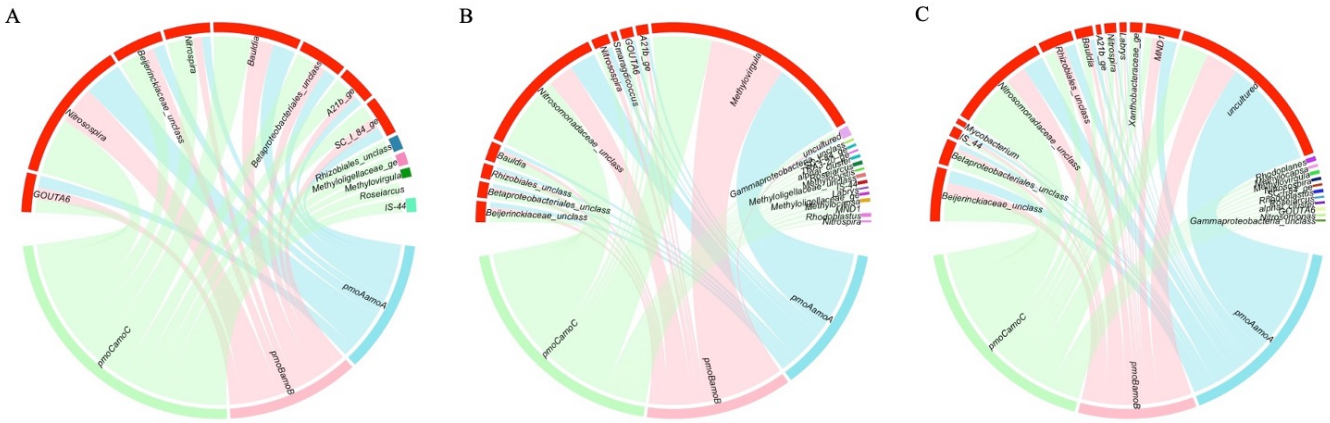

Figure A3.13 Phylotypes associated with methane/ammonia monooxygenase genes (*pmoA-amoA*, *pmoB-amoB* and *pmoC-amoC*) in the bare soil (A), switchgrass soil (B) and high diversity prairie soil (C) (both 24 hours and 30 days). To limit the number of phylotypes on each figure, the relative abundance threshold was set to > 0.008. Eight, ten and thirteen phylotypes (in red) contained all three genes for the bare soil (A), switchgrass (B) and high diversity prairie (C) samples, respectively.

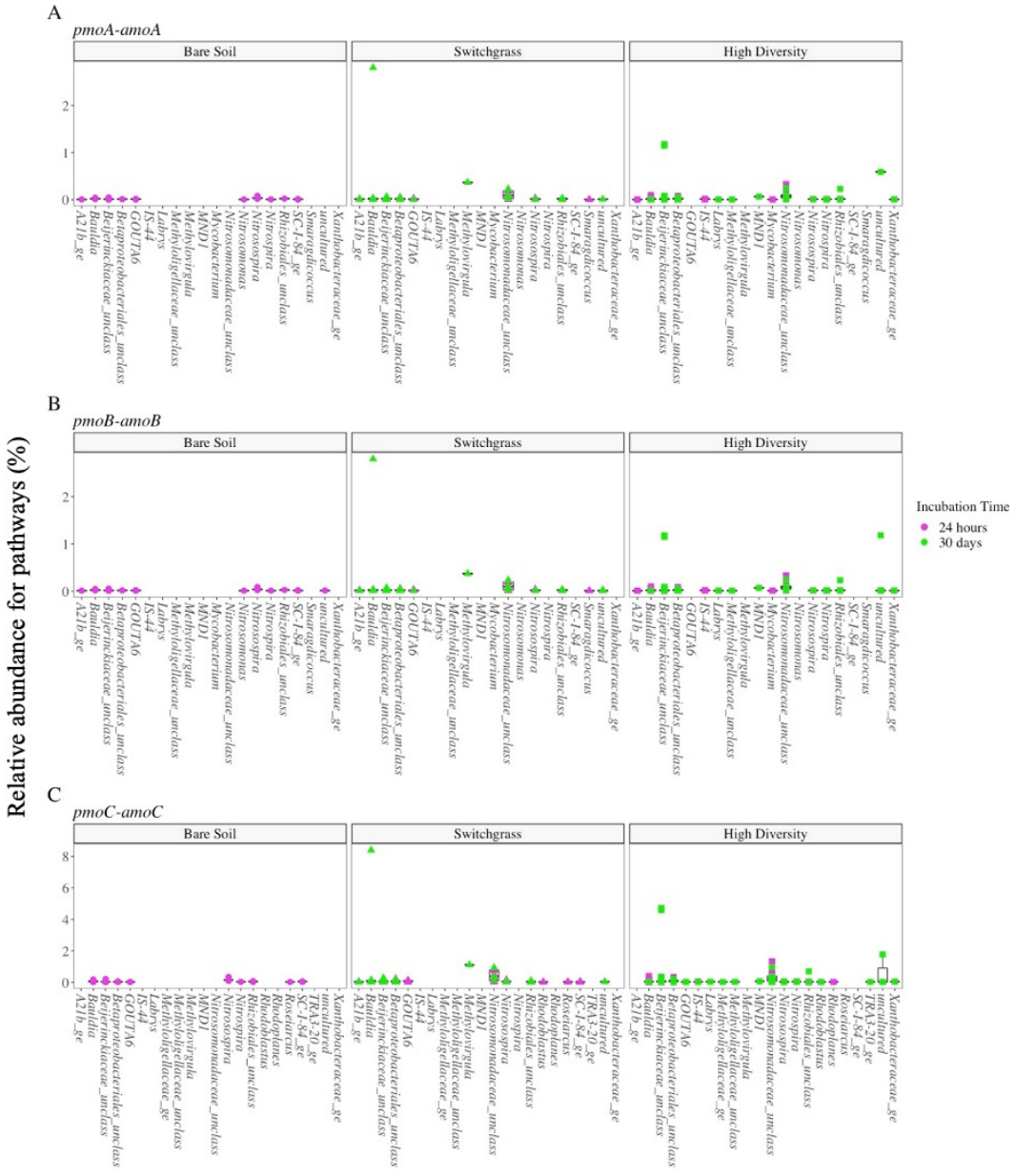

Figure A3.14 Phylotypes associated with methane/ammonia genes *pmoA-amoA* (A), *pmoB-amoB* (B) and *pmoC-amoC* (C) in the bare soil, switchgrass and high diversity prairie soils (incubated for 24 hours or 30 days). The relative abundance values were set to 0.008, 0.008 and 0.2 for *pmoA-amoA*, *pmoB-amoB*, and *pmoC-amoC,* respectively to limit the number of phylotypes shown.

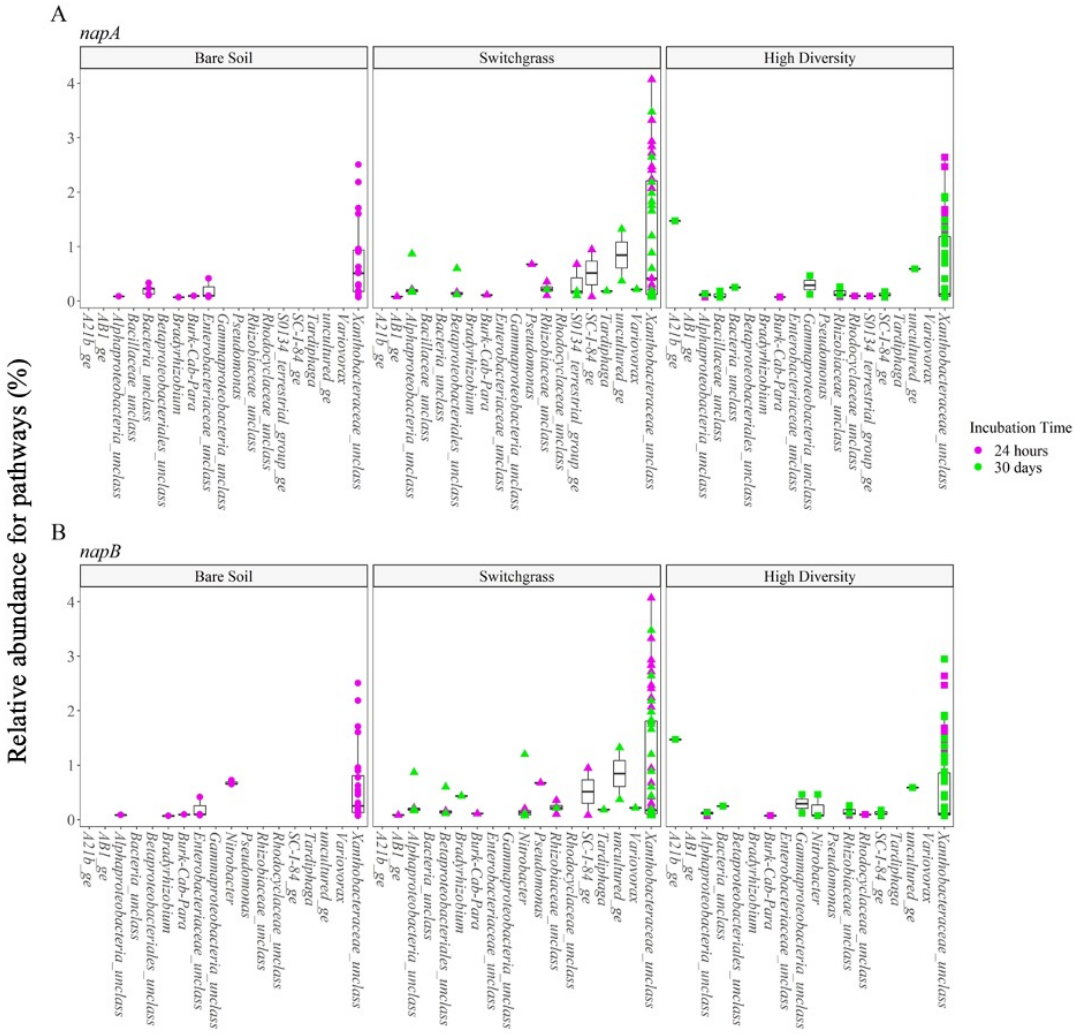

Figure A3.15 Phylotypes associated with nitrate reductase genes *napA* (A) and *napB* (B) in the bare soil, switchgrass and high diversity prairie soils (incubated for 24 hours or 30 days). The relative abundance values were set to 0.07 for both genes to limit the number of phylotypes shown.

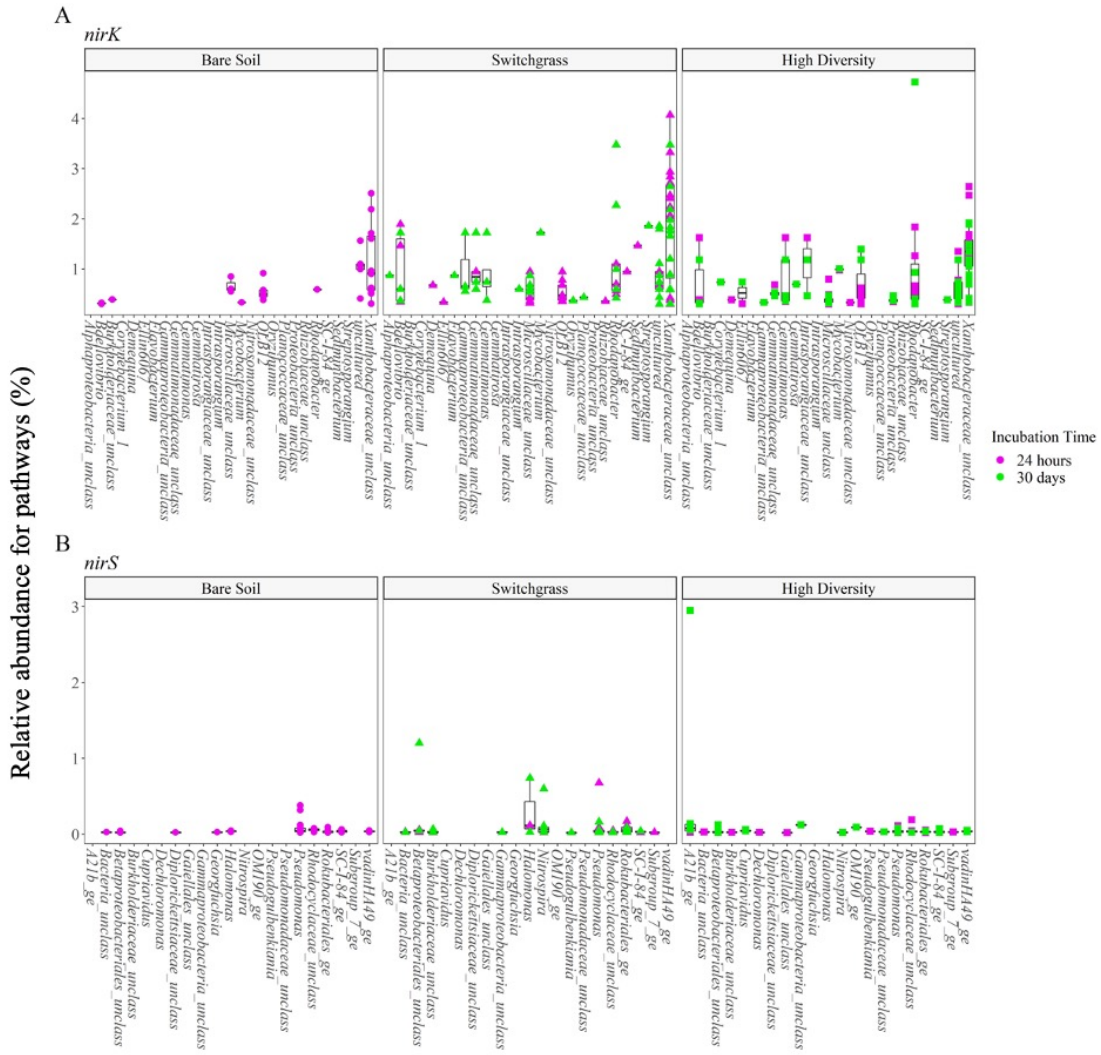

Figure A3.16 Phylotypes associated with nitrite reductase genes *nirK* (A) and *nirS* (B) in the bare soil, switchgrass and high diversity prairie soils (incubated for 24 hours or 30 days). The relative abundance values were set to 0.3 and 0.02 for *nirK* and *nirS,* respectively to limit the number of phylotypes shown.

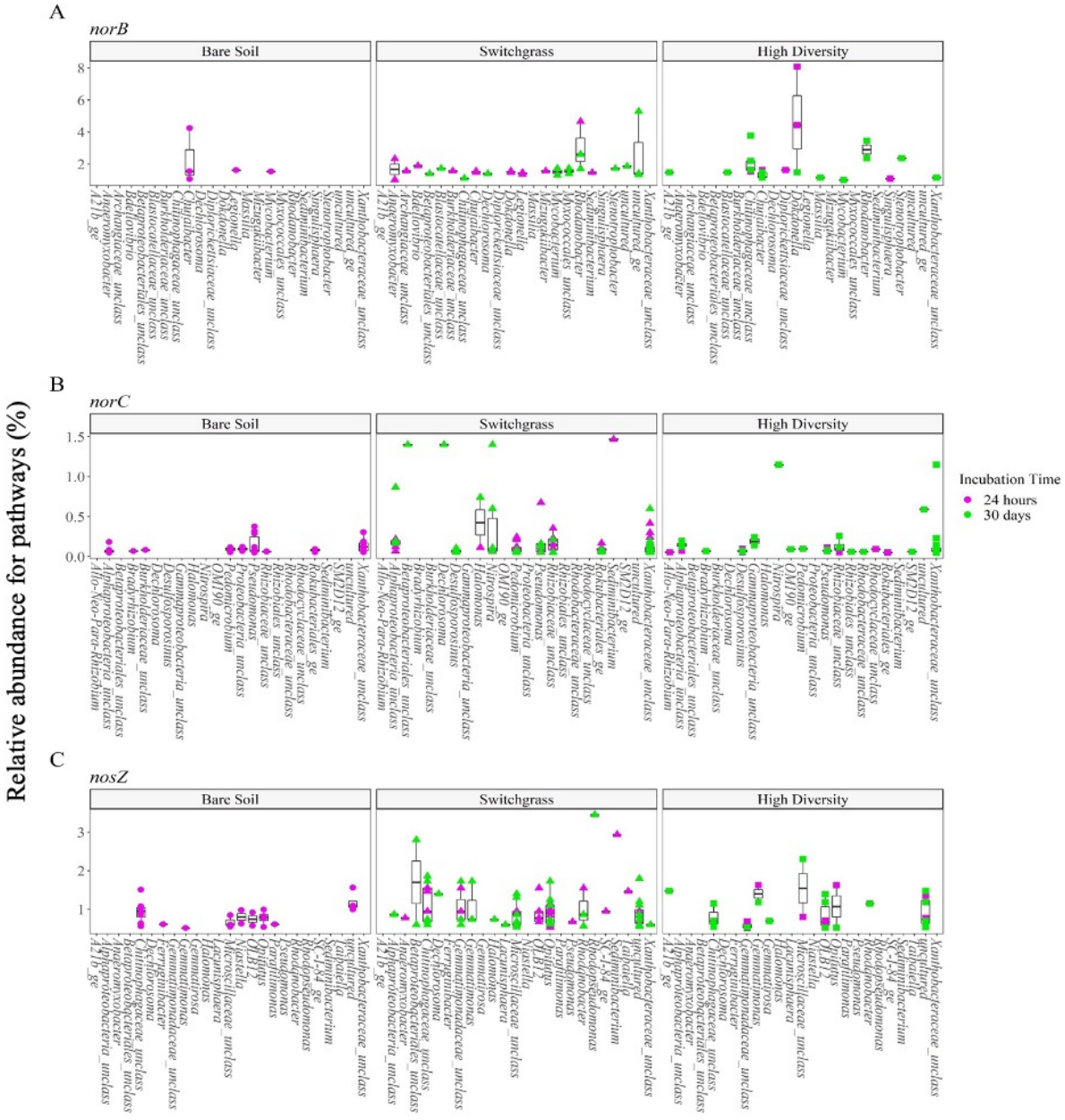

Figure A3.17. Phylotypes associated with nitric oxide reductase genes *norB* (A) and *norC* (B) and nitrous oxide reductase gene *nosZ* (C) in the bare soil, switchgrass and high diversity prairie soils (incubated for 24 hours or 30 days). The relative abundance values were set to 0.8, 0.05, and 0.5 for *norB, norC* and *nosZ*, respectively to limit the number of phylotypes

Table A3.1. Basic soil characteristics of the bare soil, switchgrass and high diversity prairie.

Treatment	pH	Phosphorus (ppm)	Potassium (ppm)	Magnesium (ppm)	Calcium (ppm)	% of Exchangeable Bases (K)	% of Exchangeable Bases (Mg)	% of Exchangeable Bases (Ca)	Organic Matter %
Switchgrass B1	6	13	83	157	783	3.9	24	72	2.3
Switchgrass B2	5	27	107	172	770	4.9	26	69	2
Switchgrass B4	6	25	80	116	775	4.1	19	77	2.4
High Div. B1	6	27	89	163	890	3.8	23	74	2.7
High Div. B2	6	55	154	173	1019	5.7	21	74	3.4
High Div. B4	6	46	213	177	1060	7.5	20	72	3.9
Bare soil B1	5	57	113	132	739	5.7	22	73	2

Table A3.2 P-values for statistical tests with the diversity indexes in large and small pores. "-" indicates the data was not collected and p-values in red indicate a significant difference ($p \leq 0.05$).

Index	Incubation time	Bare Soil			Switchgrass Monoculture			High Diversity Prairie		
		Large Pore	Small Pore	T-test (two-tailed)	Large Pore	Small Pore	T-test (two-tailed)	Large Pore	Small Pore	T-test (two-tailed)
Chao1	24 hr & 30 days	-	-	-	243.474	282.586	0.644	317.03	481.863	0.189
	30 days	-	-	-	197.832	326.655	0.393	214.542	486.143	0.14
	24 hr	216.588	177.688	0.382	289.117	245.863	0.69	419.517	477.583	0.762
ACE	24 hr & 30 days	-	-	-	338.283	456.402	0.485	439.475	673.704	0.208
	30 days	-	-	-	238.356	585.344	0.272	300.262	710.714	0.147
	24 hr	219.448	244.585	0.657	438.21	348.949	0.675	578.688	636.693	0.834
Shannon	24 hr & 30 days	-	-	-	3.679	3.71	0.663	**3.67**	**3.794**	**0.044**
	30 days	-	-	-	3.612	3.715	0.423	3.647	3.788	0.182
	24 hr	3.629	3.543	0.426	3.746	3.706	0.626	3.694	3.801	0.167
Simpson	24 hr & 30 days	-	-	-	0.972	0.973	0.575	**0.971**	**0.976**	**0.027**
	30 days	-	-	-	0.969	0.974	0.374	0.971	0.976	0.154
	24 hr	0.969	0.961	0.343	0.975	0.973	0.548	0.972	0.976	0.127
InvSimpson	24 hr & 30 days	-	-	-	37.384	38.848	0.643	**36.262**	**42.222**	**0.03**
	30 days	-	-	-	34.099	39.757	0.309	35.895	42.157	0.154
	24 hr	33.659	30.564	0.54	40.669	38.091	0.488	36.629	42.287	0.147
Fisher	24 hr & 30 days	-	-	-	270.508	382.604	0.248	271.475	404.614	0.299
	30 days	-	-	-	148.09	559.936	0.203	200.872	463.674	0.183
	24 hr	132.098	164.032	0.649	392.926	234.826	0.43	342.078	345.555	0.986

Table A3.3 P-values for statistical tests with the diversity indexes in different soil treatments. "-" indicates the data was not collected and p-values in red indicate a significant difference ($p \leq 0.05$).

					Bare vs High Div. vs Switchgrass	Bare vs High Div.	Bare vs Switchgrass	High Div.vs Switchgrass
		Bare Soil	High Diversity Prairie	Switchgrass	ANOVA	T-test (two-tailed)	T-test (two-tailed)	T-test (two-tailed)
Chao1	24 hr & 30 days	-	399.446	262.18	-	-	-	0.136
	30 days	-	350.343	256.388	-	-	-	0.401
	24 hr	197.14	448.55	267.49	**0.008**	**0.018**	0.219	0.096
ACE	24 hr & 30 days	-	556.589	394.774	-	-	-	0.29
	30 days	-	505.488	396.078	-	-	-	0.57
	24 hr	232.016	607.691	393.58	**0.013**	**0.015**	0.14	0.202
Shannon	24 hr & 30 days	-	3.732	3.694	-	-	-	0.541
	30 days	-	3.717	3.659	-	-	-	0.465
	24 hr	3.586	3.747	3.726	**0.025**	**0.017**	**0.038**	0.695
Simpson	24 hr & 30 days	-	0.974	0.973	-	-	-	0.723
	30 days	-	0.973	0.971	-	-	-	0.463
	24 hr	0.965	0.974	0.974	**0.029**	**0.034**	**0.031**	0.972
InvSimpson	24 hr & 30 days	-	39.242	38.084	-	-	-	0.775
	30 days	-	39.026	36.671	-	-	-	0.49
	24 hr	32.112	39.458	39.38	**0.022**	**0.022**	**0.022**	0.976
Fisher	24 hr & 30 days	-	338.045	324.119	-	-	-	0.912
	30 days	-	332.273	335.293	-	-	-	0.985
	24 hr	148.065	343.817	313.876	0.104	0.059	0.116	0.818

Table A3.4 Coefficients from the Permutational Multivariate Analysis of Variance (PERMANOVA) of the microbial communities in different soil treatments.

Coefficients for microbial communities based on pore size in bare soil incubated for 24 hr

	Df	SumsOfSqs	MeanSqs	F.Model	R2	Pr(>F)
pore	2	0.47	0.23	1.16	0.12	0.34
Residuals	17	3.43	0.20	NA	0.88	NA
Total	19	3.89	NA	NA	1.00	NA

Coefficients for microbial communities based on pore size in high diversity prairie incubated for 24 hr

	Df	SumsOfSqs	MeanSqs	F.Model	R2	Pr(>F)
pore	1	0.16	0.16	1.14	0.10	0.22
Residuals	10	1.43	0.14	NA	0.90	NA
Total	11	1.59	NA	NA	1.00	NA

Coefficients for microbial communities based on pore size in high diversity prairie incubated for 30 days.

	Df	SumsOfSqs	MeanSqs	F.Model	R2	Pr(>F)
pore	1	0.21	0.21	0.95	0.09	0.43
Residuals	10	2.15	0.22	NA	0.91	NA
Total	11	2.36	NA	NA	1.00	NA

Coefficients for microbial communities based on pore size in switchgrass incubated for 24 hr.

	Df	SumsOfSqs	MeanSqs	F.Model	R2	Pr(>F)
pore	1	0.14	0.14	0.60	0.06	0.91
Residuals	10	2.35	0.23	NA	0.94	NA
Total	11	2.49	NA	NA	1.00	NA

Table A3.4 (cont'd)

Coefficients for microbial communities based on pore size in switchgrass incubated for 30 days.

	Df	SumsOfSqs	MeanSqs	F.Model	R2	Pr(>F)
pore	1	0.21	0.21	0.62	0.06	1.00
Residuals	10	3.41	0.34	NA	0.94	NA
Total	11	3.62	NA	NA	1.00	NA

Coefficients for microbial communities based on incubation time in high diversity prairie (ignoring pore size).

	Df	SumsOfSqs	MeanSqs	F.Model	R2	Pr(>F)
time	1	0.28	0.28	1.53	0.07	0.12
Residuals	22	3.95	0.18	NA	0.93	NA
Total	23	4.22	NA	NA	1.00	NA

Coefficients for microbial communities based on soil treatment incubated for 24 hr (ignoring pore size).

	Df	SumsOfSqs	MeanSqs	F.Model	R2	Pr(>F)
treatment	2	3.45	1.72	9.21	0.33	**0.01**
Residuals	37	6.92	0.19	NA	0.67	NA
Total	39	10.37	NA	NA	1.00	NA

Coefficients for microbial communities based on soil treatment incubated for 30 days (ignoring pore size).

	Df	SumsOfSqs	MeanSqs	F.Model	R2	Pr(>F)
treatment	1.00	0.57	0.57	2.09	0.09	**0.02**
Residuals	22.00	5.97	0.27	NA	0.91	NA
Total	23.00	6.54	NA	NA	1.00	NA

Table A3.5 Coefficients from Pairwise comparison based on soil treatment incubated for 24 hr (ignoring pore size).

pairs	Df	SumsOfSqs	F.Model	R2	p.value	p.adjusted	sig
High Diversity Prairie vs Bare Soil	1	2.6	15.26	0.37	0.01	0.03	*
High Diversity Prairie vs Switchgrass	1	0.63	3.42	0.13	0.01	0.03	*
Bare Soil vs Switchgrass	1	1.78	8.66	0.25	0.01	0.03	*

Table A3.6 Summary of bacteria that contributed to 50% of the dissimilarity between the bare soil and high diversity prairie incubated for 24 hr, revealed by similarity percentage analyses. + represents more abundant, − represents less abundant.

	taxonomy	contribution	Bare_24h	High diversity prairie_24h
Phylum	*Proteobacteria*	18.15%	-	+
	Actinobacteria	13.08%	+	-
	Bacteroidetes	4.94%	+	-
	Acidobacteria	4.91%	+	-
	Verrucomicrobia	3.53%	-	+
	Chloroflexi	2.67%	+	-
	Firmicutes	1.73%	+	-
	Latescibacteria	0.43%	-	+
	Gemmatimonadetes	0.39%	+	-
	Nitrospirae	0.11%	-	+
	Planctomycetes	0.07%	-	+
Class	*Gammaproteobacteria*	8.98%	+	-
	Thermoleophilia	7.91%	+	-
	Alphaproteobacteria	7.60%	-	+
	Actinobacteria	5.00%	+	-
	Bacteroidia	4.94%	+	-
	Verrucomicrobiae	3.53%	-	+
	Acidobacteriia	2.21%	+	-
	Bacilli	1.64%	+	-
	Deltaproteobacteria	1.56%	-	+
	Ktedonobacteria	1.55%	+	-
	Subgroup_6	1.47%	-	+
	KD4-96	0.87%	-	+
	Blastocatellia_(Subgroup_4)	0.85%	-	+
	Latescibacteria_cl	0.43%	-	+
	Gemmatimonadetes	0.39%	+	-
	AD3	0.26%	+	-
	MB-A2-108	0.18%	-	+
	Subgroup_22	0.15%	-	+
	Subgroup_17	0.12%	-	+
	Nitrospira	0.11%	-	+
	Holophagae	0.11%	+	-
	Clostridia	0.09%	-	+
	Phycisphaerae	0.07%	-	+

Table A3.7 Summary of bacteria that contributed to 50% of the dissimilarity between the bare soil and switchgrass incubated for 24 hr, revealed by similarity percentage analyses. + represents more abundant, − represents less abundant.

	taxonomy	contribution	bare_24h	switchgrass_24h
Phylum	*Proteobacteria*	17.42%	-	+
	Actinobacteria	13.46%	+	-
	Acidobacteria	5.34%	-	+
	Bacteroidetes	4.99%	+	-
	Verrucomicrobia	3.02%	-	+
	Firmicutes	2.15%	+	-
	Chloroflexi	2.52%	+	-
	Latescibacteria	0.26%	-	+
	Gemmatimonadetes	0.57%	-	+
	Planctomycetes	0.28%	-	+
	Spirochaetes	0.09%	-	+
Class	*Gammaproteobacteria*	8.17%	+	-
	Thermoleophilia	7.51%	+	-
	Alphaproteobacteria	7.14%	-	+
	Actinobacteria	5.48%	+	-
	Bacteroidia	4.99%	+	-
	Verrucomicrobiae	3.02%	-	+
	Acidobacteriia	2.70%	+	-
	Deltaproteobacteria	2.11%	-	+
	Bacilli	1.57%	+	-
	Ktedonobacteria	1.47%	+	-
	Subgroup_6	1.41%	-	+
	vadinHA49	0.96%	-	+
	Blastocatellia_(Subgroup_4)	0.92%	-	+
	KD4-96	0.89%	-	+
	Clostridia	0.59%	-	+
	Gemmatimonadetes	0.57%	-	+
	Acidimicrobiia	0.29%	-	+
	Latescibacteria_cl	0.26%	-	+
	Holophagae	0.21%	-	+
	MB-A2-108	0.18%	-	+
	AD3	0.16%	+	-
	Subgroup_5	0.10%	-	+
	Planctomycetacia	0.10%	-	+

Table A3.8 Summary of bacteria that contributed to 50% of the dissimilarity between the switchgrass and high diversity prairie incubated for 24 hr, revealed by similarity percentage analyses. + represents more abundant, − represents less abundant.

	taxonomy	contribution	switchgrass_24h	high diversity prairie_24h
Phylum	Proteobacteria	18.15%	+	-
	Actinobacteria	11.60%	+	-
	Acidobacteria	6.31%	+	-
	Verrucomicrobia	4.50%	-	+
	Bacteroidetes	2.75%	-	+
	Chloroflexi	1.92%	+	-
	Gemmatimonadetes	1.05%	-	+
	Firmicutes	1.02%	+	-
	Latescibacteria	0.99%	-	+
	Planctomycetes	0.88%	+	-
	Bacteria_unclassified	0.28%	-	+
	Nitrospirae	0.27%	-	+
	Spirochaetes	0.10%	+	-
	Fibrobacteres	0.08%	+	-
	Elusimicrobia	0.08%	+	-
	Cyanobacteria	0.06%	+	-
Class	Gammaproteobacteria	7.84%	-	+
	Alphaproteobacteria	6.67%	+	-
	Thermoleophilia	6.45%	+	-
	Verrucomicrobiae	4.50%	-	+
	Actinobacteria	4.25%	+	-
	Deltaproteobacteria	3.64%	+	-
	Bacteroidia	2.67%	-	+
	Blastocatellia_(Subgroup_4)	1.88%	+	-
	Subgroup_6	1.80%	-	+
	Acidobacteriia	1.70%	+	-
	KD4-96	1.53%	-	+
	Gemmatimonadetes	1.05%	-	+
	Latescibacteria_cl	0.99%	-	+
	Clostridia	0.58%	+	-
	Acidimicrobiia	0.47%	+	-
	Bacilli	0.44%	+	-
	MB-A2-108	0.42%	-	+
	Subgroup_22	0.35%	-	+
	Bacteria_unclassified	0.28%	-	+

Table A3.8 (cont'd)

	taxonomy	contribution	switchgrass_24h	high diversity prairie_24h
	Nitrospira	0.27%	-	+
	OM190	0.24%	+	-
	Pla4_lineage	0.22%	+	-
	vadinHA49	0.17%	+	-
	Planctomycetacia	0.16%	+	-
	Anaerolineae	0.16%	+	-
	Ktedonobacteria	0.16%	+	-
	Subgroup_17	0.16%	+	-
	Thermoanaerobaculia	0.13%	+	-
Class	Holophagae	0.13%	+	-
	Spirochaetia	0.10%	+	-
	Phycisphaerae	0.10%	-	+
	Subgroup_5	0.09%	+	-
	Fibrobacteria	0.08%	+	-
	Lineage_IIa	0.08%	+	-
	Subgroup_11	0.07%	-	+
	Ignavibacteria	0.07%	-	+
	Melainabacteria	0.06%	+	-
	AD3	0.06%	+	-

Table A3.9 Summary of bacteria that contributed to 50% of the dissimilarity between the switchgrass and high diversity prairie incubated for 30 days, revealed by similarity percentage analyses. + represents more abundant, − represents less abundant.

	taxonomy	contribution	switchgrass_30d	high diversity prairie_30d
Phylum	*Proteobacteria*	19.74%	+	-
	Acidobacteria	7.89%	+	-
	Actinobacteria	6.50%	-	+
	Verrucomicrobia	5.77%	-	+
	Bacteroidetes	3.02%	+	-
	Chloroflexi	1.71%	-	+
	Gemmatimonadetes	1.64%	+	-
	Latescibacteria	1.02%	+	-
	Planctomycetes	0.99%	+	-
	Bacteria_unclassified	0.49%	+	-
	Firmicutes	0.35%	+	-
	Nitrospirae	0.35%	-	+
	Dependentiae	0.29%	-	+
	Rokubacteria	0.27%	-	+
	Entotheonellaeota	0.18%	-	+
	Fibrobacteres	0.15%	+	-
	Cyanobacteria	0.10%	+	-
	Patescibacteria	0.09%	+	-
	Chlamydiae	0.09%	+	-
Class	*Alphaproteobacteria*	8.06%	+	-
	Gammaproteobacteria	7.23%	-	+
	Verrucomicrobiae	5.77%	-	+
	Deltaproteobacteria	4.36%	+	-
	Thermoleophilia	3.47%	-	+
	Bacteroidia	2.92%	+	-
	Subgroup_6	2.78%	+	-
	Actinobacteria	2.75%	+	-
	Blastocatellia_(Subgroup_4)	2.73%	+	-
	Gemmatimonadetes	1.54%	+	-
	KD4-96	1.10%	-	+
	Latescibacteria_cl	1.02%	+	-
	Acidobacteriia	0.96%	+	-
	Bacteria_unclassified	0.49%	+	-
	Planctomycetacia	0.47%	+	-
	Holophagae	0.39%	+	-

Table A3.9 (cont'd)

	taxonomy	contribution	switchgrass_30d	high diversity prairie_30d
	Anaerolineae	0.37%	-	+
	Bacilli	0.35%	+	-
	Nitrospira	0.35%	-	+
	Subgroup_17	0.32%	-	+
	Subgroup_22	0.32%	-	+
	Babeliae	0.29%	-	+
	NC10	0.27%	-	+
	Subgroup_5	0.27%	-	+
	Gitt-GS-136	0.24%	-	+
	Phycisphaerae	0.23%	-	+
Class	*OM190*	0.20%	-	+
	MB-A2-108	0.19%	+	-
	Entotheonellia	0.18%	-	+
	Fibrobacteria	0.15%	+	-
	Thermoanaerobaculia	0.12%	+	-
	vadinHA49	0.10%	-	+
	Sericytochromatia	0.10%	+	-
	Ignavibacteria	0.09%	-	+
	Longimicrobia	0.09%	+	-
	Parcubacteria	0.09%	+	-
	Chlamydiae	0.09%	+	-
	Proteobacteria_unclassified	0.09%	+	-
	Actinobacteria_unclassified	0.09%	+	-

Table A3.10 KO numbers and gene descriptions for KEGG glycolysis gluconeogenesis pathway (PATHko00010).

Gene Name	Gene Description
K00114	exaA; alcohol dehydrogenase (cytochrome c) [EC:1.1.2.8]
K00121	frmA, ADH5, adhC; S-(hydroxymethyl) glutathione dehydrogenase / alcohol dehydrogenase [EC:1.1.1.284 1.1.1.1]
K00128	ALDH; aldehyde dehydrogenase (NAD+) [EC:1.2.1.3]
K00131	gapN; glyceraldehyde-3-phosphate dehydrogenase (NADP+) [EC:1.2.1.9]
K00134	GAPDH, gapA; glyceraldehyde 3-phosphate dehydrogenase [EC:1.2.1.12]
K00161	PDHA, pdhA; pyruvate dehydrogenase E1 component alpha subunit [EC:1.2.4.1]
K00162	PDHB, pdhB; pyruvate dehydrogenase E1 component beta subunit [EC:1.2.4.1]
K00171	porD; pyruvate ferredoxin oxidoreductase delta subunit [EC:1.2.7.1]
K00174	korA, oorA, oforA; 2-oxoglutarate/2-oxoacid ferredoxin oxidoreductase subunit alpha [EC:1.2.7.3 1.2.7.11]
K00175	korB, oorB, oforB; 2-oxoglutarate/2-oxoacid ferredoxin oxidoreductase subunit beta [EC:1.2.7.3 1.2.7.11]
K00382	DLD, lpd, pdhD; dihydrolipoamide dehydrogenase [EC:1.8.1.4]
K00627	DLAT, aceF, pdhC; pyruvate dehydrogenase E2 component (dihydrolipoamide acetyltransferase) [EC:2.3.1.12]
K00845	glk; glucokinase [EC:2.7.1.2]
K00850	pfkA, PFK; 6-phosphofructokinase 1 [EC:2.7.1.11]
K00873	PK, pyk; pyruvate kinase [EC:2.7.1.40]
K00886	ppgK; polyphosphate glucokinase [EC:2.7.1.63]
K00927	PGK, pgk; phosphoglycerate kinase [EC:2.7.2.3]
K01006	ppdK; pyruvate, orthophosphate dikinase [EC:2.7.9.1]
K01007	pps, ppsA; pyruvate, water dikinase [EC:2.7.9.2]
K01222	E3.2.1.86A, celF; 6-phospho-beta-glucosidase [EC:3.2.1.86]
K01223	E3.2.1.86B, bglA; 6-phospho-beta-glucosidase [EC:3.2.1.86]
K01596	E4.1.1.32, pckA, PCK; phosphoenolpyruvate carboxykinase (GTP) [EC:4.1.1.32]
K01610	E4.1.1.49, pckA; phosphoenolpyruvate carboxykinase (ATP) [EC:4.1.1.49]
K01624	FBA, fbaA; fructose-bisphosphate aldolase, class II [EC:4.1.2.13]
K01689	ENO, eno; enolase [EC:4.2.1.11]
K01785	galM, GALM; aldose 1-epimerase [EC:5.1.3.3]
K01792	E5.1.3.15; glucose-6-phosphate 1-epimerase [EC:5.1.3.15]
K01803	TPI, tpiA; triosephosphate isomerase (TIM) [EC:5.3.1.1]
K01810	GPI, pgi; glucose-6-phosphate isomerase [EC:5.3.1.9]
K01834	PGAM, gpmA; 2,3-bisphosphoglycerate-dependent phosphoglycerate mutase [EC:5.4.2.11]
K01835	pgm; phosphoglucomutase [EC:5.4.2.2]
K01895	ACSS1_2, acs; acetyl-CoA synthetase [EC:6.2.1.1]
K01905	acdA; acetate---CoA ligase (ADP-forming) subunit alpha [EC:6.2.1.13]
K02446	glpX; fructose-1,6-bisphosphatase II [EC:3.1.3.11]
K02777	crr; sugar PTS system EIIA component [EC:2.7.1.-]
K02791	malX; maltose/glucose PTS system EIICB component [EC:2.7.1.199 2.7.1.208]
K03841	FBP, fbp; fructose-1,6-bisphosphatase I [EC:3.1.3.11]

Table A3.10 (cont'd)

Gene Name	Gene Description
K04072	adhE; acetaldehyde dehydrogenase / alcohol dehydrogenase [EC:1.2.1.10 1.1.1.1]
K11532	glpX-SEBP; fructose-1,6-bisphosphatase II / sedoheptulose-1,7-bisphosphatase [EC:3.1.3.11 3.1.3.37]
K11645	fbaB; fructose-bisphosphate aldolase, class I [EC:4.1.2.13]
K13810	tal-pgi; transaldolase / glucose-6-phosphate isomerase [EC:2.2.1.2 5.3.1.9]
K13953	adhP; alcohol dehydrogenase, propanol-preferring [EC:1.1.1.1]
K13979	yahK; alcohol dehydrogenase (NADP+) [EC:1.1.1.2]
K15633	gpmI; 2,3-bisphosphoglycerate-independent phosphoglycerate mutase [EC:5.4.2.12]
K15634	gpmB; 2,3-bisphosphoglycerate-dependent phosphoglycerate mutase [EC:5.4.2.11]
K15635	apgM; 2,3-bisphosphoglycerate-independent phosphoglycerate mutase [EC:5.4.2.12]
K16370	pfkB; 6-phosphofructokinase 2 [EC:2.7.1.11]

Table A3.11 KO numbers and gene descriptions for the KEGG methane metabolism pathway (PATHko00680).

Gene Name	Gene Description
K00018	hprA; glycerate dehydrogenase [EC:1.1.1.29]
K00024	mdh; malate dehydrogenase [EC:1.1.1.37]
K00058	serA, PHGDH; D-3-phosphoglycerate dehydrogenase / 2-oxoglutarate reductase [EC:1.1.1.95 1.1.1.399]
K00121	frmA, ADH5, adhC; S-(hydroxymethyl)glutathione dehydrogenase / alcohol dehydrogenase [EC:1.1.1.284 1.1.1.1]
K00122	FDH; formate dehydrogenase [EC:1.17.1.9]
K00123	fdoG, fdhF, fdwA; formate dehydrogenase major subunit [EC:1.17.1.9]
K00124	fdoH, fdsB; formate dehydrogenase iron-sulfur subunit
K00126	fdsD; formate dehydrogenase subunit delta [EC:1.17.1.9]
K00127	fdoI, fdsG; formate dehydrogenase subunit gamma
K00169	porA; pyruvate ferredoxin oxidoreductase alpha subunit [EC:1.2.7.1]
K00170	porB; pyruvate ferredoxin oxidoreductase beta subunit [EC:1.2.7.1]
K00171	porD; pyruvate ferredoxin oxidoreductase delta subunit [EC:1.2.7.1]
K00172	porC, porG; pyruvate ferredoxin oxidoreductase gamma subunit [EC:1.2.7.1]
K00194	cdhD, acsD; acetyl-CoA decarbonylase/synthase, CODH/ACS complex subunit delta [EC:2.1.1.245]
K00196	cooF; anaerobic carbon-monoxide dehydrogenase iron sulfur subunit
K00197	cdhE, acsC; acetyl-CoA decarbonylase/synthase, CODH/ACS complex subunit gamma [EC:2.1.1.245]
K00198	cooS, acsA; anaerobic carbon-monoxide dehydrogenase catalytic subunit [EC:1.2.7.4]
K00200	fwdA, fmdA; formylmethanofuran dehydrogenase subunit A [EC:1.2.7.12]
K00201	fwdB, fmdB; formylmethanofuran dehydrogenase subunit B [EC:1.2.7.12]
K00202	fwdC, fmdC; formylmethanofuran dehydrogenase subunit C [EC:1.2.7.12]
K00317	dmd-tmd; dimethylamine/trimethylamine dehydrogenase [EC:1.5.8.1 1.5.8.2]
K00320	mer; 5,10-methylenetetrahydromethanopterin reductase [EC:1.5.98.2]
K00442	frhD; coenzyme F420 hydrogenase subunit delta
K00600	glyA, SHMT; glycine hydroxymethyltransferase [EC:2.1.2.1]
K00625	E2.3.1.8, pta; phosphate acetyltransferase [EC:2.3.1.8]
K00672	ftr; formylmethanofuran--tetrahydromethanopterin N-formyltransferase [EC:2.3.1.101]
K00830	AGXT; alanine-glyoxylate transaminase / serine-glyoxylate transaminase / serine-pyruvate transaminase [EC:2.6.1.44 2.6.1.45 2.6.1.51]
K00831	serC, PSAT1; phosphoserine aminotransferase [EC:2.6.1.52]
K00850	pfkA, PFK; 6-phosphofructokinase 1 [EC:2.7.1.11]
K00863	DAK, TKFC; triose/dihydroxyacetone kinase / FAD-AMP lyase (cyclizing) [EC:2.7.1.28 2.7.1.29 4.6.1.15]
K00918	pfkC; ADP-dependent phosphofructokinase/glucokinase [EC:2.7.1.146 2.7.1.147]
K00925	ackA; acetate kinase [EC:2.7.2.1]

Table A3.11 (cont'd)

Gene Name	Gene Description
K01079	serB, PSPH; phosphoserine phosphatase [EC:3.1.3.3]
K01007	pps, ppsA; pyruvate, water dikinase [EC:2.7.9.2]
K01070	frmB, ESD, fghA; S-formylglutathione hydrolase [EC:3.1.2.12]
K01499	mch; methenyltetrahydromethanopterin cyclohydrolase [EC:3.5.4.27]
K01595	ppc; phosphoenolpyruvate carboxylase [EC:4.1.1.31]
K01622	K01622; fructose 1,6-bisphosphate aldolase/phosphatase [EC:4.1.2.13 3.1.3.11]
K01623	ALDO; fructose-bisphosphate aldolase, class I [EC:4.1.2.13]
K01624	FBA, fbaA; fructose-bisphosphate aldolase, class II [EC:4.1.2.13]
K01689	ENO, eno; enolase [EC:4.2.1.11]
K01834	PGAM, gpmA; 2,3-bisphosphoglycerate-dependent phosphoglycerate mutase [EC:5.4.2.11]
K01895	ACSS1_2, acs; acetyl-CoA synthetase [EC:6.2.1.1]
K02203	thrH; phosphoserine / homoserine phosphotransferase [EC:3.1.3.3 2.7.1.39]
K02446	glpX; fructose-1,6-bisphosphatase II [EC:3.1.3.11]
K03388	hdrA2; heterodisulfide reductase subunit A2 [EC:1.8.7.3 1.8.98.4 1.8.98.5 1.8.98.6]
K03389	hdrB2; heterodisulfide reductase subunit B2 [EC:1.8.7.3 1.8.98.4 1.8.98.5 1.8.98.6]
K03390	hdrC2; heterodisulfide reductase subunit C2 [EC:1.8.7.3 1.8.98.4 1.8.98.5 1.8.98.6]
K03396	gfa; S-(hydroxymethyl)glutathione synthase [EC:4.4.1.22]
K03532	torC; trimethylamine-N-oxide reductase (cytochrome c), cytochrome c-type subunit TorC
K03533	torD; TorA specific chaperone
K03841	FBP, fbp; fructose-1,6-bisphosphatase I [EC:3.1.3.11]
K04041	fbp3; fructose-1,6-bisphosphatase III [EC:3.1.3.11]
K05299	fdhA; formate dehydrogenase (NADP+) alpha subunit [EC:1.17.1.10]
K05884	comC; L-2-hydroxycarboxylate dehydrogenase (NAD+) [EC:1.1.1.337]
K05979	comB; 2-phosphosulfolactate phosphatase [EC:3.1.3.71]
K06034	comD; sulfopyruvate decarboxylase subunit alpha [EC:4.1.1.79]
K06914	mfnD; tyramine---L-glutamate ligase [EC:6.3.4.24]
K07072	mfnF; (4-(4-[2-(gamma-L-glutamylamino)ethyl]phenoxymethyl)furan-2-yl)methanamine synthase [EC:2.5.1.131]
K07144	mfnE; 5-(aminomethyl)-3-furanmethanol phosphate kinase [EC:2.7.4.31]
K07811	torA; trimethylamine-N-oxide reductase (cytochrome c) [EC:1.7.2.3]
K07812	torZ; trimethylamine-N-oxide reductase (cytochrome c) [EC:1.7.2.3]
K08093	hxlA; 3-hexulose-6-phosphate synthase [EC:4.1.2.43]
K08094	hxlB; 6-phospho-3-hexuloisomerase [EC:5.3.1.27]
K08097	comA; phosphosulfolactate synthase [EC:4.4.1.19]
K08685	qhpA; quinohemoprotein amine dehydrogenase [EC:1.4.9.1]
K08691	mcl; malyl-CoA/(S)-citramalyl-CoA lyase [EC:4.1.3.24 4.1.3.25]

Table A3.11 (cont'd)

Gene Name	Gene Description
K08692	mtkB; malate-CoA ligase subunit alpha [EC:6.2.1.9]
K09733	mfnB; (5-formylfuran-3-yl)methyl phosphate synthase [EC:4.2.3.153]
K10713	fae; 5,6,7,8-tetrahydromethanopterin hydro-lyase [EC:4.2.1.147]
K10714	mtdB; methylene-tetrahydromethanopterin dehydrogenase [EC:1.5.1.-]
K10944	pmoA-amoA; methane/ammonia monooxygenase subunit A [EC:1.14.18.3 1.14.99.39]
K10945	pmoB-amoB; methane/ammonia monooxygenase subunit B
K10946	pmoC-amoC; methane/ammonia monooxygenase subunit C
K11212	cofD; LPPG:FO 2-phospho-L-lactate transferase [EC:2.7.8.28]
K11261	fwdE, fmdE; formylmethanofuran dehydrogenase subunit E [EC:1.2.7.12]
K11529	gck, gckA, GLYCTK; glycerate 2-kinase [EC:2.7.1.165]
K11532	glpX-SEBP; fructose-1,6-bisphosphatase II / sedoheptulose-1,7-bisphosphatase [EC:3.1.3.11 3.1.3.37]
K11645	fbaB; fructose-bisphosphate aldolase, class I [EC:4.1.2.13]
K11779	fbiC; FO synthase [EC:2.5.1.147 4.3.1.32]
K11780	cofG; 7,8-didemethyl-8-hydroxy-5-deazariboflavin synthase [EC:4.3.1.32]
K11781	cofH; 5-amino-6-(D-ribitylamino)uracil---L-tyrosine 4-hydroxyphenyl transferase [EC:2.5.1.147]
K12234	cofE; coenzyme F420-0:L-glutamate ligase / coenzyme F420-1:gamma-L-glutamate ligase [EC:6.3.2.31 6.3.2.34]
K13039	comE; sulfopyruvate decarboxylase subunit beta [EC:4.1.1.79]
K13788	pta; phosphate acetyltransferase [EC:2.3.1.8]
K13831	hps-phi; 3-hexulose-6-phosphate synthase / 6-phospho-3-hexuloisomerase [EC:4.1.2.43 5.3.1.27]
K14067	mtkA; malate-CoA ligase subunit beta [EC:6.2.1.9]
K14080	mtaA; [methyl-Co(III) methanol/glycine betaine-specific corrinoid protein]:coenzyme M methyltransferase [EC:2.1.1.246 2.1.1.377]
K14083	mttB; trimethylamine---corrinoid protein Co-methyltransferase [EC:2.1.1.250]
K14126	mvhA, vhuA, vhcA; F420-non-reducing hydrogenase large subunit [EC:1.12.99.- 1.8.98.5]
K14127	mvhD, vhuD, vhcD; F420-non-reducing hydrogenase iron-sulfur subunit [EC:1.12.99.- 1.8.98.5 1.8.98.6]
K14128	mvhG, vhuG, vhcG; F420-non-reducing hydrogenase small subunit [EC:1.12.99.- 1.8.98.5]
K14941	cofC, fbiD; 2-phospho-L-lactate/phosphoenolpyruvate guanylyltransferase [EC:2.7.7.68 2.7.7.105]
K15022	fdhB; formate dehydrogenase (NADP+) beta subunit [EC:1.17.1.10]
K15228	mauA; methylamine dehydrogenase light chain [EC:1.4.9.1]
K15229	mauB; methylamine dehydrogenase heavy chain [EC:1.4.9.1]

Table A3.11 (cont'd)

Gene Name	Gene Description
K15633	gpmI; 2,3-bisphosphoglycerate-independent phosphoglycerate mutase [EC:5.4.2.12]
K15634	gpmB; 2,3-bisphosphoglycerate-dependent phosphoglycerate mutase [EC:5.4.2.11]
K15635	apgM; 2,3-bisphosphoglycerate-independent phosphoglycerate mutase [EC:5.4.2.12]
K16254	mxaJ; mxaJ protein
K16256	mxaA; mxaA protein
K16257	mxaC; mxaC protein
K16258	mxaK; mxaK protein
K16259	mxaL; mxaL protein
K16260	mxaD; mxaD protein
K16306	K16306; fructose-bisphosphate aldolase / 2-amino-3,7-dideoxy-D-threo-hept-6-ulosonate synthase [EC:4.1.2.13 2.2.1.10]
K16370	pfkB; 6-phosphofructokinase 2 [EC:2.7.1.11]
K16792	aksD; methanogen homoaconitase large subunit [EC:4.2.1.114]
K16793	aksE; methanogen homoaconitase small subunit [EC:4.2.1.114]
K17067	mdo; formaldehyde dismutase / methanol dehydrogenase [EC:1.2.98.1 1.1.99.37]
K18277	tmm; trimethylamine monooxygenase [EC:1.14.13.148]

Table A3.12 KO numbers and gene descriptions for the KEGG nitrogen metabolism pathway (PATHko00680).

Gene Name	Gene Description
K00261	GLUD1_2, gdhA; glutamate dehydrogenase (NAD(P)+) [EC:1.4.1.3]
K00262	E1.4.1.4, gdhA; glutamate dehydrogenase (NADP+) [EC:1.4.1.4]
K00265	gltB; glutamate synthase (NADPH) large chain [EC:1.4.1.13]
K00266	gltD; glutamate synthase (NADPH) small chain [EC:1.4.1.13]
K00284	GLU, gltS; glutamate synthase (ferredoxin) [EC:1.4.7.1]
K00360	nasB; assimilatory nitrate reductase electron transfer subunit [EC:1.7.99.-]
K00362	nirB; nitrite reductase (NADH) large subunit [EC:1.7.1.15]
K00367	narB; ferredoxin-nitrate reductase [EC:1.7.7.2]
K00368	nirK; nitrite reductase (NO-forming) [EC:1.7.2.1]
K00372	nasA; assimilatory nitrate reductase catalytic subunit [EC:1.7.99.-]
K00376	nosZ; nitrous-oxide reductase [EC:1.7.2.4]
K00459	ncd2, npd; nitronate monooxygenase [EC:1.13.12.16]
K00926	arcC; carbamate kinase [EC:2.7.2.2]
K01673	cynT, can; carbonic anhydrase [EC:4.2.1.1]
K01674	cah; carbonic anhydrase [EC:4.2.1.1]
K01725	cynS; cyanate lyase [EC:4.2.1.104]
K01915	glnA, GLUL; glutamine synthetase [EC:6.3.1.2]
K02567	napA; nitrate reductase (cytochrome) [EC:1.9.6.1]
K02568	napB; nitrate reductase (cytochrome), electron transfer subunit
K02586	nifD; nitrogenase molybdenum-iron protein alpha chain [EC:1.18.6.1]
K02588	nifH; nitrogenase iron protein NifH
K02591	nifK; nitrogenase molybdenum-iron protein beta chain [EC:1.18.6.1]
K03385	nrfA; nitrite reductase (cytochrome c-552) [EC:1.7.2.2]
K05601	hcp; hydroxylamine reductase [EC:1.7.99.1]
K15371	GDH2; glutamate dehydrogenase [EC:1.4.1.2]
K15579	nrtD, cynD; nitrate/nitrite transport system ATP-binding protein
K15876	nrfH; cytochrome c nitrite reductase small subunit

Table A3.13 KO numbers and gene descriptions for the KEGG citrate cycle (TCA cycle) pathway (PATHko00020).

Gene Name	Gene Description
K00024	mdh; malate dehydrogenase [EC:1.1.1.37]
K00025	MDH1; malate dehydrogenase [EC:1.1.1.37]
K00030	IDH3; isocitrate dehydrogenase (NAD+) [EC:1.1.1.41]
K00031	IDH1, IDH2, icd; isocitrate dehydrogenase [EC:1.1.1.42]
K00116	mqo; malate dehydrogenase (quinone) [EC:1.1.5.4]
K00161	PDHA, pdhA; pyruvate dehydrogenase E1 component alpha subunit [EC:1.2.4.1]
K00162	PDHB, pdhB; pyruvate dehydrogenase E1 component beta subunit [EC:1.2.4.1]
K00163	aceE; pyruvate dehydrogenase E1 component [EC:1.2.4.1]
K00164	OGDH, sucA; 2-oxoglutarate dehydrogenase E1 component [EC:1.2.4.2]
K00171	porD; pyruvate ferredoxin oxidoreductase delta subunit [EC:1.2.7.1]
K00174	korA, oorA, oforA; 2-oxoglutarate/2-oxoacid ferredoxin oxidoreductase subunit alpha [EC:1.2.7.3 1.2.7.11]
K00175	korB, oorB, oforB; 2-oxoglutarate/2-oxoacid ferredoxin oxidoreductase subunit beta [EC:1.2.7.3 1.2.7.11]
K00176	korD, oorD; 2-oxoglutarate ferredoxin oxidoreductase subunit delta [EC:1.2.7.3]
K00177	korC, oorC; 2-oxoglutarate ferredoxin oxidoreductase subunit gamma [EC:1.2.7.3]
K00239	sdhA, frdA; succinate dehydrogenase / fumarate reductase, flavoprotein subunit [EC:1.3.5.1 1.3.5.4]
K00240	sdhB, frdB; succinate dehydrogenase / fumarate reductase, iron-sulfur subunit [EC:1.3.5.1 1.3.5.4]
K00241	sdhC, frdC; succinate dehydrogenase / fumarate reductase, cytochrome b subunit
K00245	frdB; fumarate reductase iron-sulfur subunit [EC:1.3.5.4]
K00246	frdC; fumarate reductase subunit C
K00247	frdD; fumarate reductase subunit D
K00382	DLD, lpd, pdhD; dihydrolipoamide dehydrogenase [EC:1.8.1.4]
K00627	DLAT, aceF, pdhC; pyruvate dehydrogenase E2 component (dihydrolipoamide acetyltransferase) [EC:2.3.1.12]
K00658	DLST, sucB; 2-oxoglutarate dehydrogenase E2 component (dihydrolipoamide succinyltransferase) [EC:2.3.1.61]
K01596	E4.1.1.32, pckA, PCK; phosphoenolpyruvate carboxykinase (GTP) [EC:4.1.1.32]
K01610	E4.1.1.49, pckA; phosphoenolpyruvate carboxykinase (ATP) [EC:4.1.1.49]
K01616	kgd; multifunctional 2-oxoglutarate metabolism enzyme [EC:2.2.1.5 4.1.1.71 1.2.4.2 2.3.1.61]
K01647	CS, gltA; citrate synthase [EC:2.3.3.1]
K01676	E4.2.1.2A, fumA, fumB; fumarate hydratase, class I [EC:4.2.1.2]

Table A3.13 (cont'd)

Gene Name	Gene Description
K01679	E4.2.1.2B, fumC, FH; fumarate hydratase, class II [EC:4.2.1.2]
K01681	ACO, acnA; aconitate hydratase [EC:4.2.1.3]
K01682	acnB; aconitate hydratase 2 / 2-methylisocitrate dehydratase [EC:4.2.1.3 4.2.1.99]
K01902	sucD; succinyl-CoA synthetase alpha subunit [EC:6.2.1.5]
K01903	sucC; succinyl-CoA synthetase beta subunit [EC:6.2.1.5]
K01958	PC, pyc; pyruvate carboxylase [EC:6.4.1.1]
K01960	pycB; pyruvate carboxylase subunit B [EC:6.4.1.1]

Table A3.14 Significantly enriched genes ($p < 0.05$) associated with the KEGG glycolysis gluconeogenesis pathway (X indicates the presence of the enriched genes).

Gene Name	Bare soil, 24 hr, large pores	Bare soil, 24 hr, small pores	High diversity prairie, 24 hr, large pores	High diversity prairie, 24 hr, small pores	High diversity prairie, 30 days, large pores	High diversity prairie, 30 days, small pores	Monoculture switchgrass, 24 hr, large pores	Monoculture switchgrass, 24 hr, small pores	Monoculture switchgrass, 30 days, large pores	Monoculture switchgrass, 30 days, small pores
K00114							X			X
K00121							X		X	X
K00128									X	X
K00131	X	X			X					X
K00134			X	X	X	X		X	X	X
K00161						X	X			X
K00162						X	X			X
K00171							X			
K00174			X	X	X	X		X		
K00175			X	X	X	X		X		
K00382		X							X	X
K00627						X	X			X
K00845			X	X	X	X		X		
K00850	X		X	X	X			X		
K00873	X		X	X				X	X	
K00886			X	X				X		X
K00927	X	X	X	X				X	X	
K01006	X	X	X	X			X	X	X	X
K01007		X		X				X		
K01222					X	X				
K01223	X									
K01596							X			
K01610	X	X			X					
K01624	X	X	X	X		X	X	X		

Table A3.14 (cont'd)

Gene Name	Bare soil, 24 hr, large pores	Bare soil, 24 hr, small pores	High diversity prairie, 24 hr, large pores	High diversity prairie, 24 hr, small pores	High diversity prairie, 30 days, large pores	High diversity prairie, 30 days, small pores	Monoculture switchgrass, 24 hr, large pores	Monoculture switchgrass, 24 hr, small pores	Monoculture switchgrass, 30 days, large pores	Monoculture switchgrass, 30 days, small pores
K01689	X	X	X	X				X	X	
K01785						X				
K01792					X		X			
K01803	X	X	X	X				X	X	
K01810	X	X	X	X				X	X	
K01834							X			X
K01835	X	X				X	X			
K01895					X	X				
K01905			X	X				X		
K02446	X	X			X	X				
K02777	X									
K02791	X				X					
K03841					X					
K04072										X
K11532							X		X	X
K11645			X						X	
K13810					X	X			X	
K13953		X			X	X				
K13979	X	X								
K15633	X		X	X	X			X	X	X
K15634		X								X
K15635			X	X				X		
K16370					X	X				X

Table A3.15 Significantly enriched genes ($p < 0.05$) associated with the KEGG methane metabolism pathway (X indicates the presence of the enriched genes).

Gene Name	Bare soil, 24 hr, large pores	Bare soil, 24 hr, small pores	High diversity prairie, 24 hr, large pores	High diversity prairie, 24 hr, small pores	High diversity prairie, 30 days, large pores	High diversity prairie, 30 days, small pores	Monoculture switchgrass, 24 hr, large pores	Monoculture switchgrass, 24 hr, small pores	Monoculture switchgrass, 30 days, large pores	Monoculture switchgrass, 30 days, small pores
K00018								X		X
K00024			X	X	X	X				
K00058	X				X	X				X
K00121						X	X			
K00122										X
K00123							X	X	X	
K00124							X	X	X	
K00126							X	X		
K00127								X		X
K00169								X		X
K00170								X		X
K00171							X			X
K00172								X		X
K00194							X			X
K00196								X		X
K00197							X			
K00198							X			X
K00200								X		X
K00201								X		X
K00202								X		X
K00317								X		X
K00320								X		X
K00442			X							

Table A3.15 (cont'd)

Gene Name	Bare soil, 24 hr, large pores	Bare soil, 24 hr, small pores	High diversity prairie, 24 hr, large pores	High diversity prairie, 24 hr, small pores	High diversity prairie, 30 days, large pores	High diversity prairie, 30 days, small pores	Monoculture switchgrass, 24 hr, large pores	Monoculture switchgrass, 24 hr, small pores	Monoculture switchgrass, 30 days, large pores	Monoculture switchgrass, 30 days, small pores
K00600	X		X	X		X				
K00625										X
K00672								X		X
K00830										X
K00831	X	X				X		X	X	
K00850	X		X	X	X	X				X
K00863										X
K00918										X
K00925				X					X	X
K01007	X	X		X	X			X		X
K01070								X	X	
K01079	X	X					X		X	
K01086								X		X
K01499								X		X
K01595					X	X	X		X	
K01622								X		
K01623								X		X
K01624	X	X	X	X	X	X	X			X
K01689	X	X	X	X	X				X	
K01834							X			
K01895				X	X	X		X	X	
K02203		X								X
K02446	X	X			X	X				
K03388							X			

Table A3.15 (cont'd)

Gene Name	Bare soil, 24 hr, large pores	Bare soil, 24 hr, small pores	High diversity prairie, 24 hr, large pores	High diversity prairie, 24 hr, small pores	High diversity prairie, 30 days, large pores	High diversity prairie, 30 days, small pores	Monoculture switchgrass, 24 hr, large pores	Monoculture switchgrass, 24 hr, small pores	Monoculture switchgrass, 30 days, large pores	Monoculture switchgrass, 30 days, small pores
K03396								X		X
K03532					X	X		X		X
K03533								X		X
K03841					X	X		X		X
K04041										X
K05299							X			X
K05884				X	X		X		X	
K05979					X	X				X
K06034								X		X
K06914										X
K07072								X		X
K07144	X							X		X
K07811								X		X
K07812								X		X
K08093								X		X
K08094								X		X
K08097					X	X		X		X
K08685							X			X
K08691										X
K08692								X		
K09733								X		X
K10713								X		X
K10714										X
K10944								X		X

Table A3.15 (cont'd)

Gene Name	Bare soil, 24 hr, large pores	Bare soil, 24 hr, small pores	High diversity prairie, 24 hr, large pores	High diversity prairie, 24 hr, small pores	High diversity prairie, 30 days, large pores	High diversity prairie, 30 days, small pores	Monoculture switchgrass, 24 hr, large pores	Monoculture switchgrass, 24 hr, small pores	Monoculture switchgrass, 30 days, large pores	Monoculture switchgrass, 30 days, small pores
K11212					X	X		X		
K11261							X			X
K11529										X
K11532							X	X	X	
K11645			X						X	
K11779					X	X				
K11780									X	
K11781									X	
K12234		X			X	X		X		
K13039								X		X
K13788		X			X	X				
K13831					X					X
K14067								X		
K14080								X		X
K14083								X		X
K14126										X
K14127						X				
K14128										X
K14941					X	X				
K15022										X
K15228							X			X
K15229							X			X
K15633			X	X	X			X	X	

Table A3.15 (cont'd)

Gene Name	Bare soil, 24 hr, large pores	Bare soil, 24 hr, small pores	High diversity prairie, 24 hr, large pores	High diversity prairie, 24 hr, small pores	High diversity prairie, 30 days, large pores	High diversity prairie, 30 days, small pores	Monoculture switchgrass, 24 hr, large pores	Monoculture switchgrass, 24 hr, small pores	Monoculture switchgrass, 30 days, large pores	Monoculture switchgrass, 30 days, small pores
K15634		X								
K15635			X	X						
K16257										X
K16258										X
K16259										X
K16260	X							X		
K16306								X		
K16370					X	X		X		
K16792								X		
K16793								X		
K17067								X		X
K18277								X		X

Table A3.16 Significantly enriched genes ($p < 0.05$) associated nitrogen metabolism (X indicates the presence of the enriched genes).

Gene Name	Bare soil, 24 hr, large pores	Bare soil, 24 hr, small pores	High diversity prairie, 24 hr, large pores	High diversity prairie, 24 hr, small pores	High diversity prairie, 30 days, large pores	High diversity prairie, 30 days, small pores	Monoculture switchgrass, 24 hr, large pores	Monoculture switchgrass, 24 hr, small pores	Monoculture switchgrass, 30 days, large pores	Monoculture switchgrass, 30 days, small pores
K00261	X	X	X	X				X		
K00262					X		X			
K00265			X	X		X	X	X		
K00266			X	X					X	X
K00284					X	X				
K00360				X				X		
K00362						X	X			
K00367					X	X				
K00368					X		X	X		
K00372							X			
K00376					X	X				
K00459		X			X			X	X	X
K00926	X									
K01673					X	X		X	X	X
K01674			X		X		X			
K01725					X					
K01915	X	X	X						X	X
K02567						X				
K02568						X				
K02586								X	X	X
K02588								X		
K02591								X	X	X

Table A3.16 (cont'd)

Gene Name	Bare soil, 24 hr, large pores	Bare soil, 24 hr, small pores	High diversity prairie, 24 hr, large pores	High diversity prairie, 24 hr, small pores	High diversity prairie, 30 days, large pores	High diversity prairie, 30 days, small pores	Monoculture switchgrass, 24 hr, large pores	Monoculture switchgrass, 24 hr, small pores	Monoculture switchgrass, 30 days, large pores	Monoculture switchgrass, 30 days, small pores
K03385						X		X	X	X
K05601							X	X		
K15371							X		X	X
K15579								X		
K15876									X	X

Table A3.17 Significantly enriched genes ($p < 0.05$) associated with the KEGG citrate cycle (TCA cycle) (X indicates the presence of the enriched genes).

Gene Name	Bare soil, 24 hr, large pores	Bare soil, 24 hr, small pores	High diversity prairie, 24 hr, large pores	High diversity prairie, 24 hr, small pores	High diversity prairie, 30 days, large pores	High diversity prairie, 30 days, small pores	Monoculture switchgrass, 24 hr, large pores	Monoculture switchgrass, 24 hr, small pores	Monoculture switchgrass, 30 days, large pores	Monoculture switchgrass, 30 days, small pores
K00024	X		X	X				X		
K00025									X	
K00030			X							
K00031			X	X	X					
K00116		X			X	X				
K00161						X	X	X		X
K00162						X	X	X		X
K00163								X		
K00164	X	X			X	X			X	
K00171							X			
K00174			X	X	X	X				
K00175			X	X	X	X				
K00176							X	X		
K00177							X	X		
K00239			X	X		X		X		
K00240			X	X		X		X		
K00241			X	X					X	
K00245			X	X		X				
K00246			X	X		X				
K00247		X								X
K00382		X								X
K00627						X	X	X		X
K00658	X	X	X	X	X	X				X
K01596							X	X		

Table A3.17 (cont'd)

Gene Name	Bare soil, 24 hr, large pores	Bare soil, 24 hr, small pores	High diversity prairie, 24 hr, large pores	High diversity prairie, 24 hr, small pores	High diversity prairie, 30 days, large pores	High diversity prairie, 30 days, small pores	Monoculture switchgrass, 24 hr, large pores	Monoculture switchgrass, 24 hr, small pores	Monoculture switchgrass, 30 days, large pores	Monoculture switchgrass, 30 days, small pores
K01610	X	X			X	X				
K01616							X	X		
K01647	X	X	X	X					X	X
K01676							X	X		X
K01679						X				
K01681	X	X	X	X						
K01682	X	X								
K01902	X	X	X	X					X	
K01903	X	X	X	X					X	
K01958										X
K01960					X					

CHAPTER 4: IMPACT OF YEAST EXTRACT AND BASAL SALTS MEDIUM ON 1,4-DIOXANE BIODEGRADATION RATES AND THE MICROORGANISMS INVOLVED IN CARBON UPTAKE FROM 1,4-DIOXANE

This chapter is a modified version of a published work in Environmental Pollution: Li, Z. and A. M. Cupples (2024). "Impact of Yeast Extract and Basal Salts Medium on 1,4-Dioxane Biodegradation Rates and the Microorganisms Involved in Carbon Uptake from 1,4-Dioxane." Environmental Pollution: 125014

4.1 Abstract

Conventional physical and chemical treatment technologies for 1,4-dioxane can be ineffective and consequently attention has focused on bioremediation. Towards this, the current research investigated the impact of basal salts medium (BSM) and yeast extract on 1,4-dioxane biodegradation rates in microcosms with different soil or sediment (agricultural soil, wetland sediment, sediment from an impacted site). Phylotypes responsible for carbon uptake from 1,4-dioxane were determined using stable isotope probing (SIP), both with and without BSM and yeast extract. Further, putative functional genes were investigated using 1) soluble di-iron monooxygenase (SDIMO) based amplicon sequencing, 2) qPCR targeting propane monooxygenase (large subunit, *prmA*) and 3) a predictive approach (PICRUSt2). The addition of BSM and yeast extract enhanced 1,4-dioxane removal rates in all three inocula, however, the differences were only significant for the agricultural soil and impacted site sediment microcosms. The phylotypes associated with carbon uptake varied across treatments and inocula. *Gemmatimonas* was important in the heavy SIP fractions of the wetland sediment microcosms. Unclassified *Solirubacteraceae*, *Solirubrobacter*, *Pseudonocardia* and *RB4* were dominant in the

heavy SIP fractions of the agricultural soil microcosms. The heavy SIP fractions of the impacted site microcosms were dominated by only two phylotypes, unclassified *Burkholderiaceae* and *oc3299*. SDIMO based amplicon sequencing detected three genes previously associated with 1,4-dioxane. The predicted functional gene analysis suggested the importance of propane monooxygenases associated with *Solirubrobacter* and *Pseudonocardia.* Overall, it is likely that a community of microorganisms were involved in carbon uptake from 1,4-dioxane in both the wetland and agricultural soil microcosms. In contrast, carbon uptake in the impacted site sediment microcosms was largely restricted to two phylotypes. Many of these microorganisms have not previously been associated with 1,4-dioxane removal. The results suggest amending with BSM and yeast extract, even at low levels, could be a promising approach for the enhancement of 1,4-dioxane biodegradation rates.

4.2 Introduction

1,4-Dioxane, a probable human carcinogen, commonly used as a solvent and stabilizer for the chlorinated solvents, has been detected in both surface water and groundwater (Derosa, Wilbur et al. 1996, USEPA 2013, Adamson, Piña et al. 2017, Dang, Kanitkar et al. 2018, Karges, Becker et al. 2018). The characteristics of 1,4-dioxane (high water solubility and low Henry's Law constant) pose challenges for remediation using conventional treatment techniques, such as air stripping or activated carbon (Zenker, Borden et al. 2003, Steffan, McClay et al. 2007, Zhang, Gedalanga et al. 2017, Godri Pollitt, Kim et al. 2019, Kikani, Satasiya et al. 2022). In the past decade, biologically mediated 1,4-dioxane removal has been used as alternative approach to clean up 1,4-dioxane contaminated sites (Lippincott, Streger et al. 2015, Horst, Bell et al. 2019, Bell, Wong et al. 2022, Divine, Bell et al. 2024).

Numerous microorganisms have been associated with metabolic or co-metabolic 1,4-

dioxane biodegradation. *Pseudonocardia dioxanivorans* CB1190 (Parales, Adamus et al. 1994, Mahendra and Alvarez-Cohen 2006), *Pseudonocardia* sp. D17 (Sei, Oyama et al. 2013), *Pseudonocardia* sp. N23 (Yamamoto, Saito et al. 2018), *Pseudonocardia benzenivorans* B5 (Mahendra and Alvarez-Cohen 2006), *Xanthobacter flavus* DT8 (Chen, Jin et al. 2016), *Mycobacterium* sp. PH-06 (Kim, Jeon et al. 2009), *Acinetobacter baumannii* DD1 (Huang et al. 2014) and *Rhodanobacter* AYS5 (Pugazhendi, Rajesh Banu et al. 2015) utilize 1,4-dioxane as a sole carbon source. Others degrade 1,4-dioxane co-metabolically, including: *Pseudonocardia* sp. ENV478 (Vainberg, McClay et al. 2006), *Pseudonocardia tetrahydrofuranoxydans* sp. K1 (Kohlweyer, Thiemer et al. 2000) and *Rhodococcus* sp. YYL (Yao, Lv et al. 2009) induced by tetrahydrofuran; *Rhodococcus* sp. RR1, *Burkholderia cepacia* G4, *Ralstonia pickettii* PKO1 and *Pseudomonas mendocina* KR1 (Mahendra and Alvarez-Cohen 2006) induced by toluene; and *Rhodococcus ruber* ENV425 (Lippincott, Streger et al. 2015), *Mycobacterium vaccae* JOB5 (Mahendra and Alvarez-Cohen 2006) and *Rhodococcus jostii* RHA1 (Hand, Wang et al. 2015) induced by propane.

The biochemical pathway for 1,4-dioxane biodegradation is initiated by soluble di-iron monooxygenases (SDIMOs). In general, SDIMOs have been classified into seven groups based on their substrate specificity and function (Notomista, Lahm et al. 2003, Coleman, Bui et al. 2006, Yang, Haritos et al. 2024). SDIMOs associated with the co-metabolic and metabolic biodegradation of 1,4-dioxane were previously summarized, being primarily in SDIMO groups 1, 2, 3, 5 and 6 (He, Mathieu et al. 2017). To date, the majority of 1,4-dioxane focused research has involved groups 5 and 6 SDIMOs, such as propane monooxygenase from *Mycobacterium dioxanotrophicus* PH-06 (group 6) (Deng, Li et al. 2018) and tetrahydrofuran monooxygenase from *Pseudonocardia dioxanivorans* CB1190 (group 5) (Sales, Mahendra et al. 2011, Sales,

Grostern et al. 2013), *Pseudonocardia* sp. strain ENV478 (group 5) (Masuda, McClay et al. 2012) and *Pseudonocardia tetrahydrofuranoxydans* K1 (group 5) (Sales, Grostern et al. 2013). Propane monooxygenase subunit sequences similar to *Rhodococcus* sp. RR1 *prmA* (group 5) were also linked to 1,4-dioxane biodegradation in mixed microbial communities (Eshghdoostkhatami and Cupples 2024).

Although much is known about the enzymes, genes and microorganisms associated with 1,4-dioxane biodegradation in pure culture, less is known about removal mechanisms in mixed microbial cultures. A valuable approach for examining contaminant biodegradation in mixed communities is known as stable isotope probing (SIP). SIP is a cultivation-independent method, tracking the incorporation of a stable isotope from a labeled chemical into DNA or RNA (Radajewski, Ineson et al. 2000, Cupples 2016, Kim, Hwangbo et al. 2023). This approach has been applied to characterize active degraders for various chemicals, such as ethane and propane (Farhan Ul Haque, Hernández et al. 2022), *n*-hexadecane (Liu, Zhang et al. 2019), phenanthrene (Thomas, Corre et al. 2019, Bao, Li et al. 2022), vinyl chloride (Paes, Liu et al. 2015), hexahydro-1,3,5-trinitro-1,3,5-triazine (Cho, Lee et al. 2013, Jayamani and Cupples 2015), methyl *tert*-butyl ether (Sun, Sun et al. 2012) and *cis*-dichloroethene (Dang and Cupples 2021). Previous studies used this approach to identify 1,4-dioxane degraders in sludge (Aoyagi, Morishita et al. 2018), groundwater (Bell, McDonough et al. 2016) and soils (Dang and Cupples 2021).

Optimizing bioremediation at contaminated sites often involves the addition of carbon sources to support *in situ* microbial communities. Various carbon sources have been evaluated as substrates to enhance 1,4-dioxane biodegradation, including tetrahydrofuran, 1,3,5-trioxane, ethylene glycol, diethylene glycol, 1,4-butanediol, butanone, acetone, 1-butanol, 2-butanol,

phenol, propanol, acetate, ethane, propane, methane and lactate (Sei, Kakinoki et al. 2010, Hatzinger, Banerjee et al. 2017, Xiong, Mason et al. 2019, Inoue, Hisada et al. 2020, Xiong, Mason et al. 2020, Dang and Cupples 2021, Miao, Heintz et al. 2021, Inoue, Hisada et al. 2022, Tawfik, Al-sayed et al. 2022). The current study examined the impact of adding yeast extract and basal salts medium (BSM) on 1,4-dioxane biodegradation rates. As yeast extract contains multiple growth factors, it has the potential to be beneficial to numerous microorganisms potentially linked to 1,4-dioxane biodegradation. Although yeast extract has previously been shown to enhance 1,4-dioxane biodegradation in pure cultures (Pugazhendi, Rajesh Banu et al. 2015, Chen, Jin et al. 2016), little is known about the impact in mixed communities. Also, in those studies, high yeast extract concentrations were used (20 mg/L and 100 mg/L) (Pugazhendi, Rajesh Banu et al. 2015, Chen, Jin et al. 2016), which is unlikely to be suitable at contaminated sites because of biofouling. Therefore, the current research examined the impact of lower yeast extract concentrations (60 μg/L) on 1,4-dioxane biodegradation rates. The objectives were to 1) examine the impact of yeast extract and BSM on 1,4-dioxane degradation rates in microcosms amended with different inocula (agricultural soil, wetland sediment and impacted site sediments), 2) identify the phylotypes involved in carbon uptake from 1,4-dioxane using SIP, and 3) determine the functional genes putatively associated with 1,4-dioxane biodegradation.

4.3 Methods

4.3.1 Chemicals, Inocula and Microcosm Setup

Unlabeled 1,4-dioxane (≥99.5%) and 1,4-dioxane-d_8 (≥99% isotopic purity) were purchased from Sigma-Aldrich (MO, USA). Labeled ^{13}C-1,4-dioxane ($(^{13}C)_4H_8O_2$, 99% isotopic purity) was purchased from Santa Cruz Biotechnology (TX, USA). The biodegradation of 1,4-dioxane was examined using three inocula, including wetland sediment (Lake Lansing, MI),

sediment from an impacted site in California (West Coast Naval Station) and agricultural soil. The agricultural soil was collected from six replicate plots of the Main Cropping System Experiment at the Kellogg Biological Station Long-Term Ecological Research, in southwest Michigan. This treatment (called Treatment 4) receives no chemical inputs, compost or manure. More details of this treatment can be found at https://lter.kbs.msu.edu/research/long-term-experiments/main-cropping-system-experiment/. All soils and sediments were stored at 4 °C in the dark before use. Laboratory microcosms were established with soil or sediment (10 g wet weight) and 30 mL of liquid (water or BSM with yeast extract) in 160 mL serum bottles. The BSM was modified from a previous recipe (Pugazhendi, Rajesh Banu et al. 2015) and contained NH_4Cl (1.0 g/L), K_2HPO_4 (3.24 g/L), NaH_2PO_4 (1.0 g/L), $MgSO_4$ (0.20 g/L), $FeSO_4$ (0.012 g/L), $MnSO_4$ (0.003 g/L), $ZnSO_4$ (0.003 g/L) and $CoCl_2$ (0.001 g/L). The final pH of the BSM was adjusted to 7.4 with 0.1N NaOH. The media also contained 60 μg/L yeast extract (Sigma-Aldrich, USA). For each inocula type, the experimental design included triplicate live microcosms amended with ^{13}C labeled 1,4-dioxane, triplicate live microcosms amended with ^{12}C 1,4-dioxane and triplicate abiotic microcosms (abiotic controls) amended with ^{12}C 1,4-dioxane. For each inocula type, the nine microcosms were either amended with water or were amended with BSM and yeast extract (eighteen microcosms for each in total). For all treatments, the abiotic controls were autoclaved daily for three consecutive days. All microcosms, sealed with a rubber stopper and aluminum crimp, were incubated at room temperature on a rotary bench-top shaker. The microcosms were opened for 0.5 hr every five days for aeration. The initial concentrations of 1,4-dioxane were ~2 mg/L in the live sample microcosms and abiotic controls.

4.3.2 1,4-Dioxane Analysis

A triple quadrupole Agilent 7010B GC/MS system (Agilent Technologies, CA, USA)

equipped with a VF-5ms column (length 30 m, inner diameter 0.25 mm, film thickness 0.25 μm) and solid phase micro extraction (SPME) (Sigma-Aldrich, MO, USA) was used to measure 1,4-dioxane concentrations in the liquid phase of the microcosms. The SPME fiber was assembled with 30 μm carboxen/polydimethylsiloxane layer, 50 μm divinylbenzene layer and a 24 Ga needle. At each sampling time-point, 1 mL of each sample was collected using a sterile syringe (3 mL) and needle (22 Ga 1.5 in.) and then filtered (0.22 μm nylon filter) (Biomed Scientific). An aliquot (500 μL) of the filtered samples or series of diluted external standards were added into amber glass vials (40 mL). Also, 500 μL of 200 μg/L 1,4-dioxane-d_8 was added into each vial as an internal standard. The vials were maintained at 40°C before the measurement. The SPME fiber was conditioned at 270 °C for 30 mins before each sequence run. For each sample, the fiber was inserted into the vials and exposed to the analytes for 2 mins. The analytes in the headspace adsorbed onto the fiber and then the fiber was exposed to the inlet. The initial oven temperature time was 40 °C and this was maintained for 4 mins. The oven temperature was then programmed to increase to 250 °C at a rate of 40 °C/min. The flow rate of carrier gas (helium) was 1.2 mL/min in constant flow mode.

4.3.3 DNA Extraction, Fractioning and MiSeq Illumina Sequencing

DNA was extracted, in triplicate, from the live ^{12}C 1,4-dioxane and ^{13}C labeled 1,4-dioxane amendment microcosms using the DNA extraction kit (DNeasy PowerLyzer PowerSoil Kit, Mo Bio, USA) according to the manual protocol. The concentration of DNA in each extract was quantified using the Quant-iT™ dsDNA High-Sensitivity Assay Kit. Ultracentrifugation and fractioning were performed as previously described (Dang and Cupples 2021, Li, Kravchenko et al. 2024). For each of the labeled and unlabeled 1,4-dioxane DNA extracts, twelve tubes were ultracentrifuged, including DNA from duplicate microcosms for both the H_2O treatment and the

BSM with yeast treatment, for impacted site, agricultural soil, and wetland sediment. In total, twenty-four tubes were ultracentrifuged (2 isotopes [^{12}C and ^{13}C] × 2 microcosms replicates × 2 treatments × 3 soil/sediment types). For each of the twenty-four ultracentrifugation runs, three heavy fractions (buoyant density ~1.73 to ~1.75 g/mL) and one light fraction (buoyant density ~1.7 g/mL) were selected. Although fractions of heavier buoyant density were collected, they did not meet the minimum DNA concentration required for 16S rRNA gene amplicon sequencing. In total, three 96-well plates (4 fractions, 3 replicates for each fraction, 2 isotopes, 2 microcosms replicates, 2 treatments, 3 soil types) were submitted to the Genomic Cores at the Research Technology Support Facility (RTSF) at Michigan State University (MSU).

The V4 region of 16S rRNA gene was targeted for amplification using primers 515f (5'-GTGCCAGCMGCCGCGGTAA-3') and 806r (5'-GGACTACHVGGGTWTCTAAT-3') following a previously described protocol (Kozich, Westcott et al. 2013). PCR products were batch normalized using Invitrogen SequalPrep DNA Normalization plates and the products recovered from the plates pooled. The pool was cleaned and concentrated using AmpureXP magnetic beads; then QC'd and quantified using a combination of Qubit dsDNA HS, Agilent 4200 TapeStation HS DNA1000, and Kapa Illumina Library Quantification qPCR assays. The pool was loaded onto an Illumina MiSeq v2 standard flow cell and sequencing was performed in a 2 × 250 bp paired end format using a MiSeq v2 500 cycle reagent cartridge. Custom sequencing and index primers were added to appropriate wells of the reagent cartridge. Base calling was performed by Illumina Real Time Analysis (RTA) v1.18.54 and RTA output demultiplexed and converted to FastQ format with Illumina Bcl2fastq v2.19.1. The raw sequences were summitted to NCBI under Bioproject PRJNA1073031 (accession numbers SAMN39784393 to SAMN39784676).

4.3.4 Microbial Community Analyses & the Identification of Phylotypes Incorporating 13C

Raw amplicon sequences in the fastq format were combined, trimmed, aligned and quality controlled using Mothur (Schloss, Westcott et al. 2009) on the High Performance Computing Cluster (HPCC) at MSU. The SILVA bacteria database (Release 138) for the V4 region (Pruesse, Quast et al. 2007) was used for the alignments and the sequences were then classified into operational taxonomic units (OTUs) at 97% similarity. The classification of OTUs into taxonomic levels and downstream analysis were conducted with two Mothur files (shared file and taxonomy file) with R (Version 4.2.1) (R Core Team 2018) in RStudio (Version 2022.12.0) (RStudio_Team 2020). The packages phyloseq (version 1.34.0) (McMurdie and Holmes 2013) and microbiome (version 1.12.0) (Lahti and Shetty 2012-2019) were used to 1) determine the relative abundance at the phyla level in the fractions, 2) generate barcharts for the most abundant families in the three soil samples, 3) perform the alpha diversity analysis (Chao1, ACE, Shannon's values, Simpson, Inverse of Simpson, and Fisher indices), and 4) conduct the Principal Coordinate Analysis (PCoA).

The statistically enriched phylotypes in the heavy fractions of the ^{13}C 1,4-dioxane amended samples (those responsible for carbon uptake from 1,4-dioxane) were determined using the R packages dplyr (version 1.1.3) (Wickham, Francois et al. 2023), tidyr (version 1.3.0) (Wickham, Vaughan et al. 2023), ggpubr (version 0.6.0) (Kassambara 2023) and rstatix (version 0.7.2) (Kassambara 2023). For this, the Wilcoxon Test (function wilcox_test) (one sided, $p < 0.05$) was used to determine which phylotypes exhibited a greater relative abundance in the ^{13}C 1,4-dioxane amended heavy fractions compared to the corresponding ^{12}C 1,4-dioxane amended heavy fractions. Following this, phylotypes statistically enriched in the light ^{13}C 1,4-dioxane amended fractions compared to the corresponding ^{12}C 1,4-dioxane amended light fractions were

removed from the list generated above to avoid possible false positives. The R packages ggplot2 (version 3.3.5) (Wickham 2016) and forcats (version 1.0.0) (Wickham 2023) were used to generate the boxplots for the top ten most abundant statistically enriched phylotypes. The packages dplyr (version 1.1.3) (Wickham, Francois et al. 2023) and ggplot2 (version 3.3.5) (Wickham 2016) were used to illustrate the number of enriched OTUs and families in the three soil types.

4.3.5 PICRUSt2 Monooxygenase Gene Predictions

PICRUSt2 (Douglas, Maffei et al. 2020) was utilized to analyze the Mothur generated files on the HPCC at MSU. The inputs to PICRUSt2 involved a fasta file and a biom file. PICRUSt2 predicts the functional potential of microbial communities based on marker gene (16S rRNA gene) sequencing profiles. PICRUSt2 was applied with EPA-NG (Barbera, Kozlov et al. 2019) and gappa (Czech, Barbera et al. 2020) for phylogenetic placement of reads, castor (Louca and Doebeli 2018) for hidden state prediction and MinPath (Ye and Doak 2009) for pathway inference. The PICRUSt2 generated files (pred_metagenome_contrib.tsv and pred_metagenome_contrib.tsv) were investigated (primarily using the R packages tidyr and dplyr) for the presence of genes associated with monooxygenases (from the KEGG database (Kanehisa 2002)) as well as the phylotypes associated with each. More information on the data within each file can be found in the following tutorial (https://github.com/picrust/picrust2/wiki/PICRUSt2-Tutorial-(v2.5.0)). Functional genes investigated (KEGG number in parenthesis) included: *prmA* propane 2-monooxygenase large subunit (K18223), *prmB* propane monooxygenase reductase component (K18225), *prmC* propane 2-monooxygenase small subunit (K18224), *prmD* (K18226) propane monooxygenase coupling protein, *pmoA-amoA* methane/ammonia monooxygenase subunit A (K10944), *pmoB-*

amoB methane/ammonia monooxygenase subunit B (K10945), *pmoC-amoC* methane/ammonia monooxygenase subunit C (K10946), *mmoX* methane monooxygenase component A alpha chain (K16157), *mmoY* methane monooxygenase component A beta chain (K16158), *mmoZ* methane monooxygenase component A gamma chain (K16159), *mmoB* methane monooxygenase regulatory protein B (K16160), *mmoC* methane monooxygenase component C (K16161), *mmoD* methane monooxygenase component D (K16162), *tmoA, tbuA1, touA* toluene monooxygenase system protein A (K15760), *tmoB, tbuU, touB* toluene monooxygenase system protein B (K15761), *tmoC, tbuB, touC* toluene monooxygenase system ferredoxin subunit (K15762), *tmoD, tbuV, touD* toluene monooxygenase system protein D (K15763), *tmoE, tbuA2, touE* toluene monooxygenase system protein E (K15764), *tmoF, tbuC, touF* toluene monooxygenase electron transfer component (K15765), *dmpK/poxA/tomA0* phenol/toluene 2-monooxygenase (NADH) P0/A0 (K16249), *dmpL/poxB/tomA1* phenol/toluene 2-monooxygenase (NADH) P1/A1 (K16243), *dmpM/ poxC/tomA2* phenol/toluene 2-monooxygenase (NADH) P2/A2 (K16244), *dmpN/poxD/tomA3* phenol/toluene 2-monooxygenase (NADH) P3/A3 (K16242), *dmpO/poxE/ tomA4* phenol/toluene 2-monooxygenase (NADH) P4/A4 (K16245) and *dmpP/poxF/tomA5* phenol/toluene 2-monooxygenase (NADH) P5/A5 (K16246).

RStudio on the HPCC at MSU was used to generate a file that contained which gene subunits and phylotypes were present using the PICRUSt2 output file pred_metagenome_contrib.tsv (unzipped). The approach involved combining this file with 1) a file containing gene numbers and descriptions and 2) a taxonomy file (from Mothur), using the R packages data.table (version 1.14.8) (Dowle and Srinivasan 2023), dplyr (version 1.1.3) (Wickham, Francois et al. 2023), tidyr (version 1.3.0) (Wickham, Vaughan et al. 2023), ggplot2 (Wickham 2016) and patchwork (version 1.1.3) (Pedersen 2023). Bar charts were generated for

each monooxygenase, faceted by the sample type and the gene subunits.

4.3.6 SDIMO Gene Amplicon Sequencing

A two-step library preparation was completed for sequencing, first involving PCR with target-specific primers with tags on the 5 prime ends (Fluidigm common oligos CS1/CS2) to facilitate the second PCR for barcoding. The target-specific primers included two degenerate primers previously designed to target conserved regions in the SDIMO alpha subunit gene (called NVC57 and NVC66, target size 420 bp, Table A4.1) (Coleman, Bui et al. 2006). The following steps were performed by the Genomics Core at RTSF at MSU. PCR amplicons were batch-normalized using Invitrogen SequalPrep DNA Normalization plates and the recovered product was pooled. The pool was QC'd and quantified using a combination of Qubit dsDNA HS, Agilent 4200 TapeStation HS DNA1000 and Invitrogen Collibri Library Quantification qPCR assays. This pool was loaded onto one (1) Illumina MiSeq v2 Standard flow cell and sequencing was carried out in a 2x250bp paired end format using a MiSeq v2 500 cycle reagent cartridge. Custom sequencing and index primers complementary to the Fluidigm CS1 and CS2 oligomers were added to appropriate wells of the reagent cartridge. Base calling was done by Illumina Real Time Analysis (RTA) v1.18.54 and output of RTA was demultiplexed and converted to FastQ format with Illumina Bcl2fastq v2.20.0. The raw sequences were summitted to NCBI under Bioproject PRJNA1073036 (accession numbers SAMN39784693 to SAMN39784716).

4.3.7 SDIMO Sequences Processing and Analysis

The amplicon sequencing files were processed on the HPCC at MSU using usearchv11 (Edgar 2010). The steps included an inspection of data quality and using the commands -fastx_info and fastq_eestats2. Sequences were then pooled using -fastq_mergepairs. Quality

filtering was achieved using -fastq_filter, with a maximum expected error threshold set to 1.0. Following this, sequences were dereplicated using -fastx_uniques. The command cluster_otus was used to complete 97% operational taxonomic units (OTU) clustering using the UPARSE-OTU (Edgar 2013) algorithm and to filter chimeras. The -otutab command was used to generate OTU tables with OTU abundance values.

To enable a comparison of the OTUs to genes previously associated with 1,4-dioxane metabolism and co-metabolism, twelve gene sequences previously associated with 1,4-dioxane biodegradation as summarized in (He, Mathieu et al. 2017) were obtained from NCBI. Each of the twelve gene sequence were then uploaded for a nucleotide-nucleotide blastn search to find highly similar sequences to create a blast database for each (Altschul, Gish et al. 1990). To ensure only highly similar sequences were selected, the resulting databases were filtered using a percent identity and query length threshold of greater than or equal to 95%. The occurrence of the gene sequences in each database was investigated in the usearch files generated by using blastn (BLAST/2.10.0-Linux_x86_64 on HPCC).

The results from the blastn search were downloaded from HPCC and were examined using R (Version 4.2.1) (R Core Team 2018) in RStudio (Version 2022.12.0) (RStudio_Team 2020). Specifically, the results were filtered to include matches of > 90% sequence identity (the sequence identity was reduced to capture a wide diversity of gene matches) and alignment length of more than 400 bps. The numbers of OTUs aligning to each gene database for each sample were determined and the datasets were used to construct phylogenetic trees (as described below). As only three (*Rhodococcus jostii* RHA1 *prmA* and *Rhodococcus* sp. RR1 *prmA*, *Pseudonocardia dioxanivorans* CB1190 plasmid pPSED02 Psed_6976) of the twelve genes were detected, only three trees were generated. Data manipulation, data analysis and the generation of

figures was completed with R (Version 4.2.1) (R Core Team 2018) in RStudio (Version 2022.12.0) (RStudio_Team 2020). For this, the following R packages were utilized: tidyverse (Version 1.3.1) (Wickham, Averick et al. 2019), ampir (Version 1.1.0) (Fingerhut L. and I. 2021), writexl (Version 1.4.2) (Ooms 2023), readxl (Version 1.4.2) (Wickham and Bryan 2023), writexl (Ooms 2023), ggplot2 (Wickham 2016) and phylotools (Version 0.2.2) (Zhang 2017).

4.3.8 Phylogenetic Trees

Sequences were first submitted for MAFFT (multiple alignment using fast Fourier transform) alignment using an online server (https://mafft.cbrc.jp/alignment/server/) (Katoh, Rozewicki et al. 2019) (Version 7). The alignments generated (using the Neighbor-Joining method and Jukes-Cantor model) were then exported in Newick format and uploaded to the Interactive Tree of Life (https://itol.embl.de) (Letunic and Bork 2021) (Version 6.7.2). The OTU abundance values for each sample were added using the datasets function called multi value bar chart.

4.3.9 Quantitative PCR on SIP Fractions

Gene copies of *Rhodococcus* sp. RR1 *prmA* were determined the SIP fractions using a previously developed qPCR assay (Eshghdoostkhatami and Cupples 2024) (Table A4.1). Quantitative PCR was performed with the CFX96™ Real-Time PCR System (Bio-Rad, Hercules, CA), using 20 µL total volume containing 10 µL PrimeTime™ Gene Expression Master Mix, 0.3 µM of each primer (IDT Integrated DNA Technologies, Coralville, IA), 0.2 µg/mL bovine serum albumin (Thermo Fisher Scientific), 0.15 µM of the probe (IDT Integrated Technologies), 6.4 µL of PCR grade water (IDT Integrated DNA Technologies), and 2 µL DNA extract or PCR grade water (for the negative controls). BSA was added as it has been shown to limit inhibition in environmental samples (Kreader 1996, Wang, Olson et al. 2007, Gedalanga,

Pornwongthong et al. 2014). The thermal cycler program involved an initial activation at 95°C for 10 minutes, followed by 40 cycles of denaturation at 95°C for 15 seconds, and annealing at 60°C for 1 minute. The target gene (*prmA*) was incorporated into a plasmid for use as qPCR standards (GenScript Biotech Corporation). Each qPCR assay was performed in triplicate with DNA templates, no template controls (NTCs), and 5-fold serial dilutions of the standards to create calibration curves. DNA extract concentrations (Table A4.2), as well as data concerning the qPCR assays (as suggested by MIQE guidelines) (Bustin, Benes et al. 2009) (Table A4.3) has been summarized.

4.3.10 Statistical Analysis

Differences in the 1,4-dioxane degradation rates and microbial alpha diversity values between inocula and treatments were investigated using one-way analysis of variance (ANOVA) and Welch's two-sided *t*-tests. If the *p*-value from the one-way ANOVA was smaller than 0.05, *t*-tests were used to compare the differences between inocula or treatments. The results of ANOVA and *t*-tests are provided (Tables A4.4-A4.11).

4.4 Results

4.4.1 1,4-Dioxane Biodegradation Rates

1,4-Dioxane concentrations in all live and control microcosms for all treatments were monitored over 50 days (Figure 4.1). For all live microcosms, the 95% confidence intervals (CIs) for the regression lines of ^{12}C 1,4-dioxane and ^{13}C 1,4-dioxane amended live samples overlapped entirely over the incubation, indicating the label did not impact removal rates. In contrast, the 95% CIs differed between the live samples and abiotic controls. The removal slopes were also significantly different between the live samples and corresponding abiotic controls ($p < 0.05$) (Tables A4.4-A4.7), indicating decreases in 1,4-dioxane concentrations were due to

biodegradation.

1,4-Dioxane removal rates were significantly different between the microcosms with the three inocula types (one-way ANOVA, $p < 0.05$) (Table A4.4). Treatment (water vs. yeast extract and BSM) differences between 1,4-dioxane removal rates also varied between the three inocula. Although the 1,4-dioxane removal rate was higher in the BSM and yeast extract treatment compared to the water treatment in the wetland sediment microcosms, the difference was not significant (t-tests, $p > 0.05$) (Table A4.5). However, the addition of BSM and yeast extract significantly increased 1,4-dioxane removal rates, compared to the water treatments, in both the agricultural soil and impacted site sediment microcosms (t-tests, $p <0.05$) (Tables A4.6 & A4.7).

4.4.2 Microbial Community Analyses

PCoA analysis indicated the microbial communities differed between the agricultural soils, wetland sediments and site sediments microcosms (Figure A4.1). Greater differentiations were observed between heavy and light fractions for the soil and wetland sediments microcosms (Figure A4.1B & C), compared to the site sediments microcosms (Figure A4.1D). The alpha diversity indices in the microcosms were significantly different (one-way ANOVA and *t*-tests) between the three soil/sediment types (Tables A4.8-4.10). For both the water and BSM and yeast treatments, the soil microcosms illustrated the highest alpha diversity and richness indices, followed by wetland sediment microcosms, then the impacted site sediment microcosms (Figure 4.2). For the soil microcosms, all the richness (Chao1, ACE) and diversity (Shannon, Simpson, Inverse of Simpson and Fisher) indices were significantly higher in the no yeast (water only) compared to the yeast with BSM treatment ($p < 0.05$; Table A4.11). Four indices (Chao1, ACE, Inverse of Simpson and Fisher) and three indices (Chao1, ACE and Fisher) were significantly

higher in the treatments with no yeast compared to those with yeast and BSM the for wetlandand impacted site sediment microcosms, respectively ($p < 0.05$; TableAA4.11).

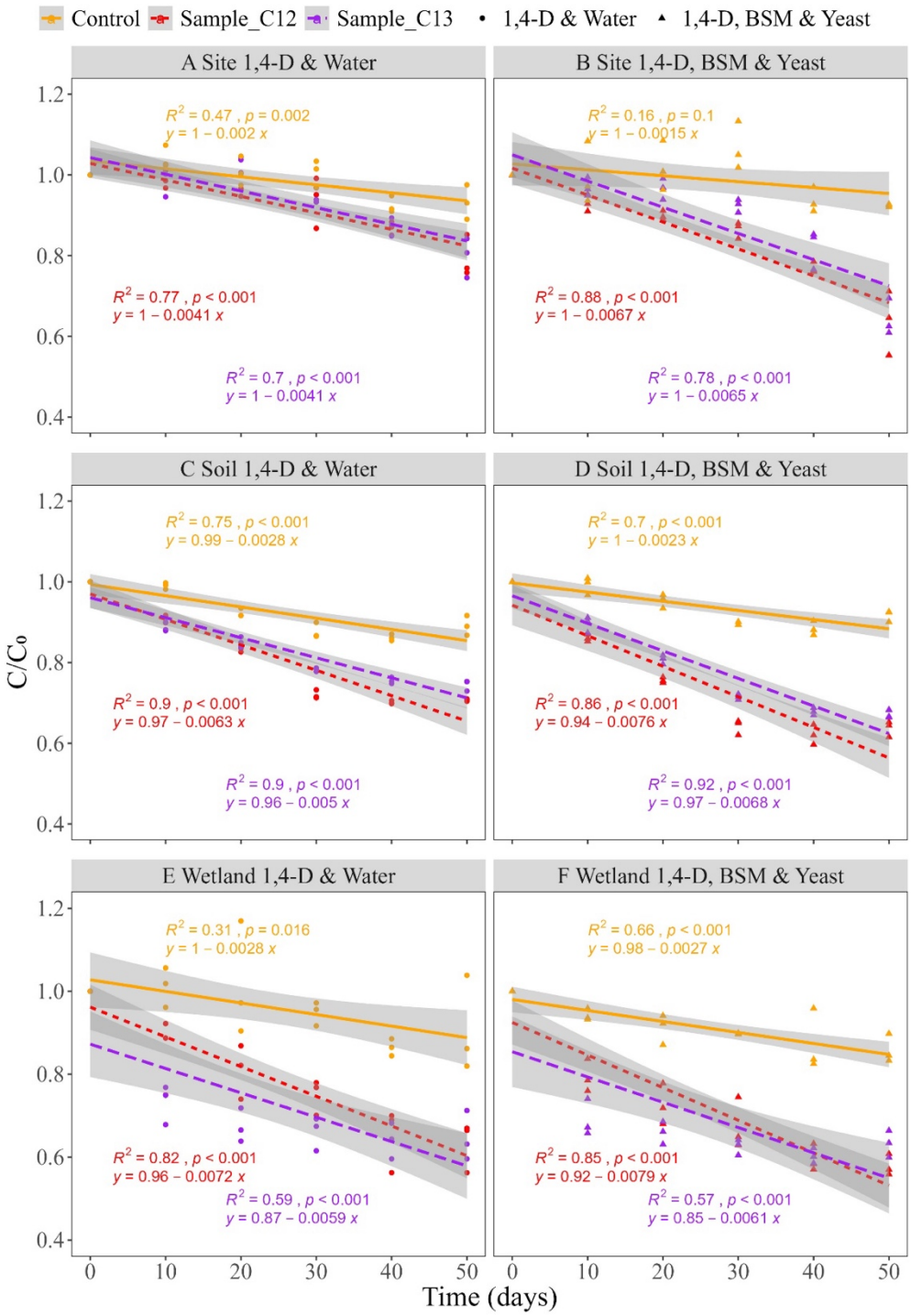

Figure 4.1 1,4-dioxane removal in triplicates of three different sample types (A, B for the site, C, D for the soil and E, F for the wetland microcosms) and triplicates of abiotic controls with a starting 1,4-dioxane concentration of approximately 2 mg/L. Graphs on the left represent microcosms amended with 1,4-dioxane and water, while graphs on the right represent those amended with basal salts media (BSM) and yeast extract. The grey areas represent 95% confidence intervals for the regression lines.

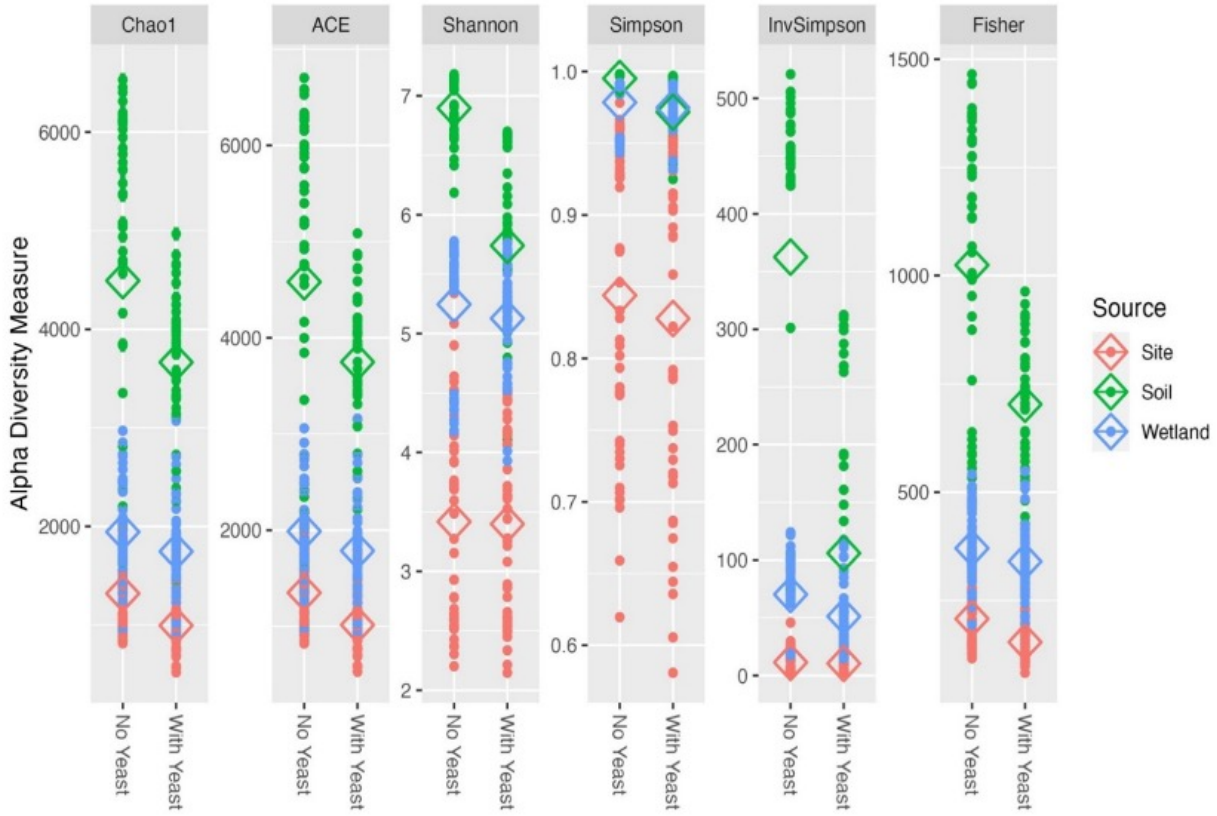

Figure 4.2 Alpha diversity analysis for all three sample types without yeast and with yeast and basal salts media. Note: the hollow diamonds represent the means of the indices, averaged across all the fractions.

4.4.3 Phyla and Phylotypes Responsible for Carbon Uptake from 1,4-Dioxane

The relative abundance of phyla in the ^{12}C and ^{13}C amended heavy and lights fractions were identified and compared (Figure 4.3). For the soil and wetland sediment microcosms, different phyla dominated in the heavy fractions compared to the light fractions. Specifically, *Firmicutes* and *Bacteroides* were dominant in the light fractions, while *Actinobacteria* and *Proteobacteria* were dominant in the heavy fractions. For impacted site sediment microcosms, the light and heavy fractions illustrated similar trends at the phylum level, with both being dominated by *Proteobacteria*.

The ten most abundant phylotypes statistically enriched in the heavy fractions of ^{13}C 1,4-dioxane amended samples compared to the ^{12}C 1,4-dioxane amended samples were determined using the Wilcoxon Rank test ($p < 0.05$) (Figure 4.4). The phylotypes associated with carbon uptake from 1,4-dioxane varied both across treatments (water vs. BSM and yeast) and inocula types (Figure 4.4). In the wetland microcosms with water only, the dominant phylotypes included an uncultured strain, *Gemmatimonas*, *Gemmata* and an unclassified *Alphaproteobacteria*. In the wetland microcosms with yeast and BSM, dominant phylotypes included *Massilia*, unclassified *Rhizobiales* as well as two *Gemmatimonas* strains. In the soil microcosms with water, the enriched phylotypes were dominated by *RB4, Udaeobacter, Subgroup 6* and *Ellin*. Whereas, in the soil microcosms with yeast and BSM, *Solirubacteraceae*, *Pseudonocardia*, *Solirubrobacter*, *Acidothermus* and *Gaiella* were primarily associated with label uptake. In contrast, the enriched phylotypes in the site microcosms were dominated by only one phylotype in each treatment, an unclassified *Burkholderiaceae* (water treatment) and *oc3299* (yeast and BSM treatment).

The datasets were also summarized to illustrated enrichment patterns for all statistically

enriched phylotypes across treatments and sample types (Figure 4.5). The largest number of OTUs and families were enriched in the wetland communities, followed by the agricultural soil, then the impacted site sediment (Figure 4.5A & B). In the comparison between yeast and no yeast treatments, the number of statistically enriched OTUs and families were similar for the impacted site sediments. However, for both soil and wetland sediments, the numbers of enriched families and OTUs were greater in the yeast treatment compared to the no yeast treatment.

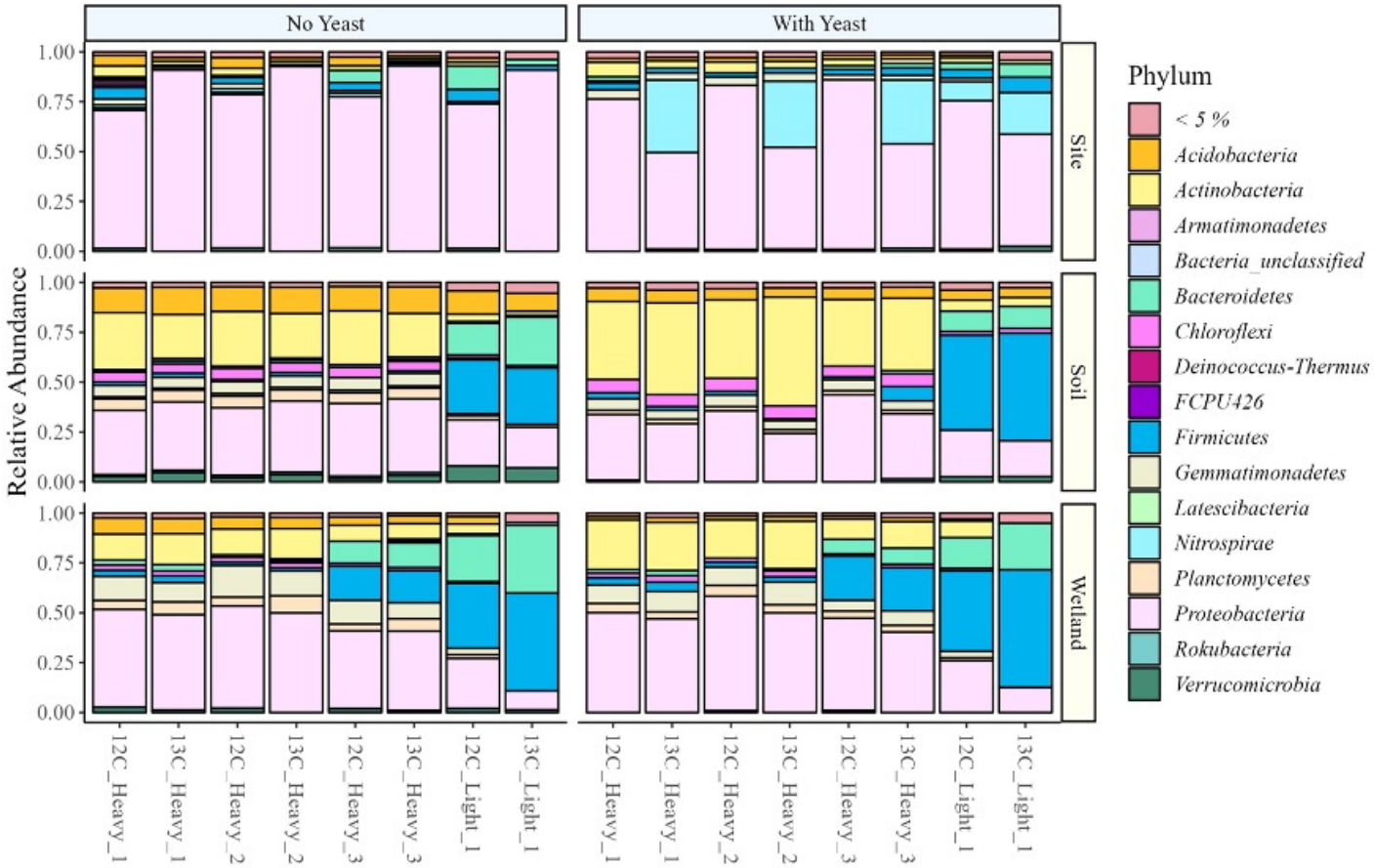

Figure 4.3 The relative abundance (%) of phyla in the light and heavy, ^{12}C 1,4-dioxane and ^{13}C 1,4-dioxane, amended fractions of both treatments (water only and basal salts media/yeast) and three sample types. Each column represents average values for three sequencing replicates.

Figure 4.4 Relative abundance (%) of significantly enriched phylotypes in the heavy fractions of ^{12}C and ^{13}C 1,4-dioxane amended microcosms inoculated with wetland sediment, agricultural soil and an impacted site sediment, without yeast and with yeast and basal salts media.

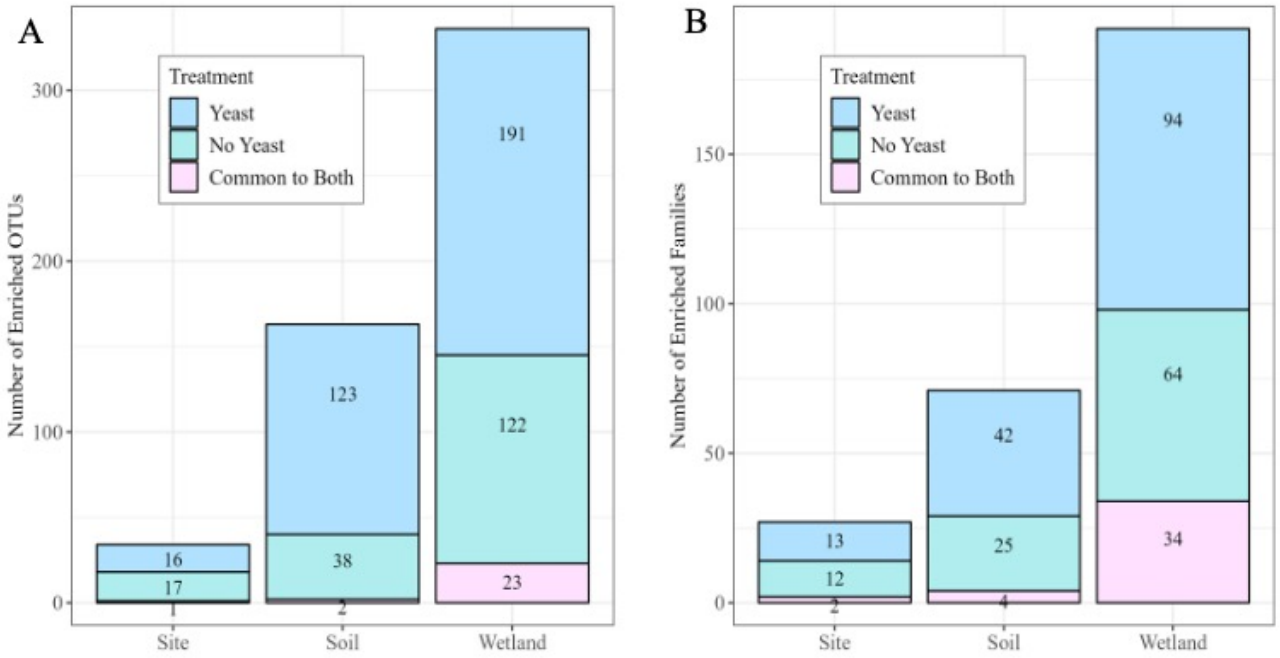

Figure 4.5 The number of statistically significantly enriched OTUs (A) and families (B) in the site sediment, soil and wetland sediment in the yeast and basal salts media amended samples, in the no yeast treatments and in both.

4.4.4 SDIMO Amplicon Sequencing and prmA Quantitative PCR Assay

The BLAST analysis compared the SDIMO amplicon sequencing OTUs to genes previously associated with 1,4-dioxane metabolism or co-metabolism. Three genes (*Rhodococcus jostii* RHA1 *prmA* and *Rhodococcus* sp. RR1 *prmA*, *Pseudonocardia dioxanivorans* CB1190 plasmid pPSED02 Psed_6976) were detected and aligned in the three soil/sediment types (Figure 4.6). The majority of alignments to both *Rhodococcus prmA* databases involved methane monooxygenases or propane monooxygenases from other *Rhodococcus* species. The numbers of alignments to both databases were the greatest for the wetland sediments, followed by the soil, then the impacted site sediments. The majority of the alignments to the *Pseudonocardia dioxanivorans* CB1190 plasmid pPSED02 Psed_6976 database were from the impacted site sediment microcosms (Figure 4.6C). The alignments were associated with genes encoding for tetrahydrofuran monooxygenase alpha subunit (*thmA*) from *Pseudonocardia*, *Rhodococcus*, *Arthrobacter* and *Acinetobacter*.

Gene copies of *Rhodococcus* sp. RR1 *prmA* were further investigated using qPCR in the ^{12}C and ^{13}C gradient fractions for the wetland sediments, soil and impacted site sediment microcosms. Only the fractions from the wetland microcosms illustrated an increase in buoyant density in the heavy fractions of the ^{13}C amended samples compared to the heavy fractions of the ^{12}C controls (Figure 4.7). The trends were similar for both replicates of both treatments (with and without yeast). In the no yeast treatment (Figure 4.7A), ^{13}C-labeled *prmA* genes peaked at heavier buoyant densities (BDs) (1.7382 and 1.7371 g/mL) compared to those of ^{12}C-labeled fractions (1.7360 and 1.7306 g/mL). In the yeast treatment (Figure 4.7B), ^{13}C-labeled *prmA* genes also peaked at heavier BDs (1.7393 and 1.7349 g/mL) compared to those of ^{12}C-labeled fractions (1.7328 and 1.7306 g/mL).

4.4.5 Prediction of 13C Enriched Monooxygenase Genes

PICRUSt2 predicted the phylotypes associated with monooxygenase genes for the three soil/sediment types (Figure 4.8, Figures A4.2-4.5). A number of microorganisms were associated with propane monooxygenase in the three sample types, however, only a small number were linked to all four subunits (*prmA*, *prmB*, *prmC* and *prmD*) (Figure 4.8). Specifically, in all three sample types, *Pseudonocardia*, unclassified *Pseudonocardiaceae, Solirubrobacter* and unclassified *Solirubrobacteraceae* were primarily associated with all four subunits. A number of phylotypes were linked to all six subunits of phenol/toluene 2-monooxygenase in all three sample types (Figure A4.2). The most dominant for the impacted site samples included unclassified *Burkholderiaceae*. The most dominant for the soil samples included *IS-44*, *oc32* (*Nitrosomonadaceae*), *Pseudomonas* and *SC-I_84*. For the wetland samples, *Acinetobacter* was associated with all six subunits (although the levels for three subunits were lower), as was *IS-44, MND1, oc32* and *SC-I_84*.

Dominant patterns for the other functional genes included Labrys (*Rhizobiales*) for the six subunits of toluene monooxygenase in the impacted site sediments (Figure A4.3), unclassified *Rhizobiales* for the three subunits of ammonia/particulate methane monooxygenase for all three sample types (Figure A4.4) and *Mycobacterium* for the five subunits of soluble methane monooxygenase for all three sample types (Figure A4.5).

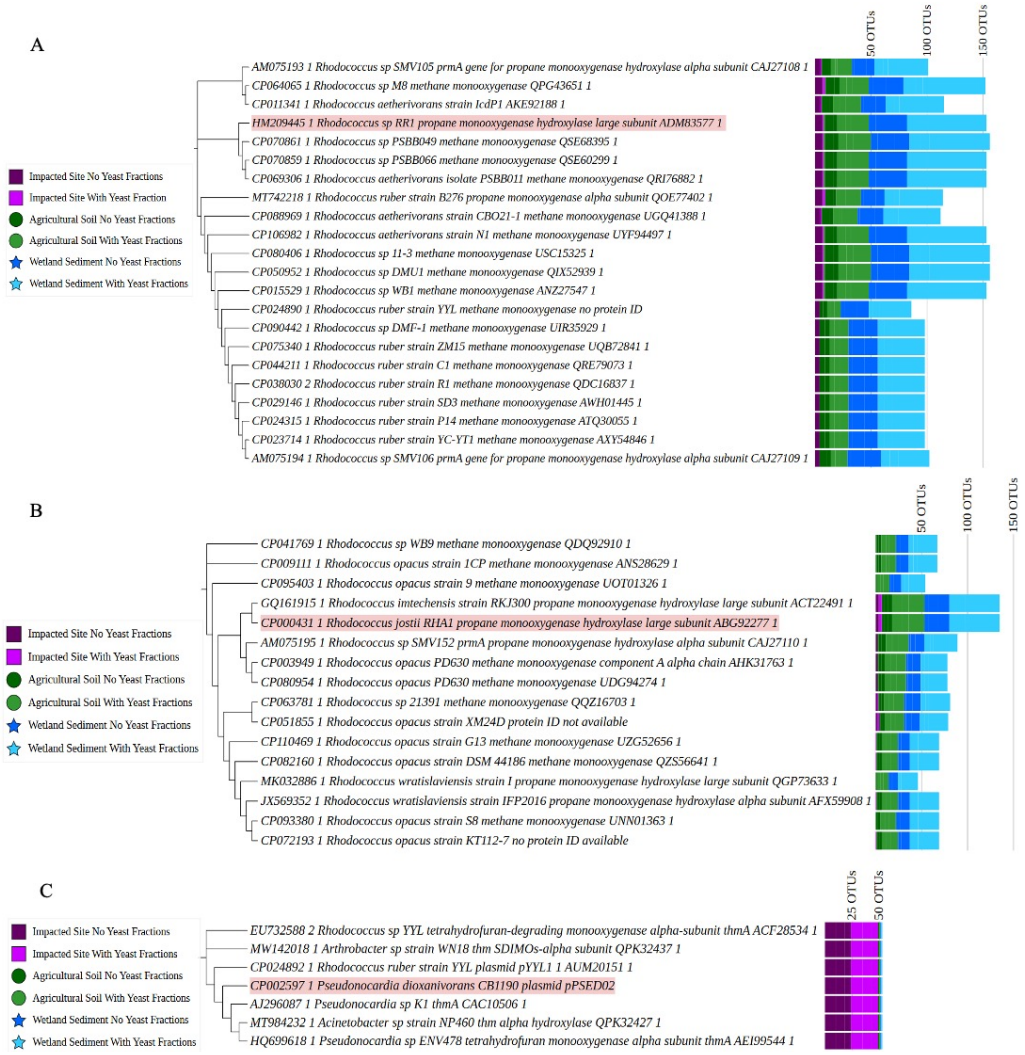

Figure 4.6 Number of OTUs aligning to sequences similar to *Rhodococcus* sp. RR1 *prmA* (A), *Rhodococcus jostii* RHA1 *prmA* (B) and *Pseudonocardia dioxanivorans* CB1190 plasmid pPSED02 Psed_6976 (dioxane monooxygenase) (C) in the heavy fractions of each sample type. The numbers at the end of each represent protein IDs.

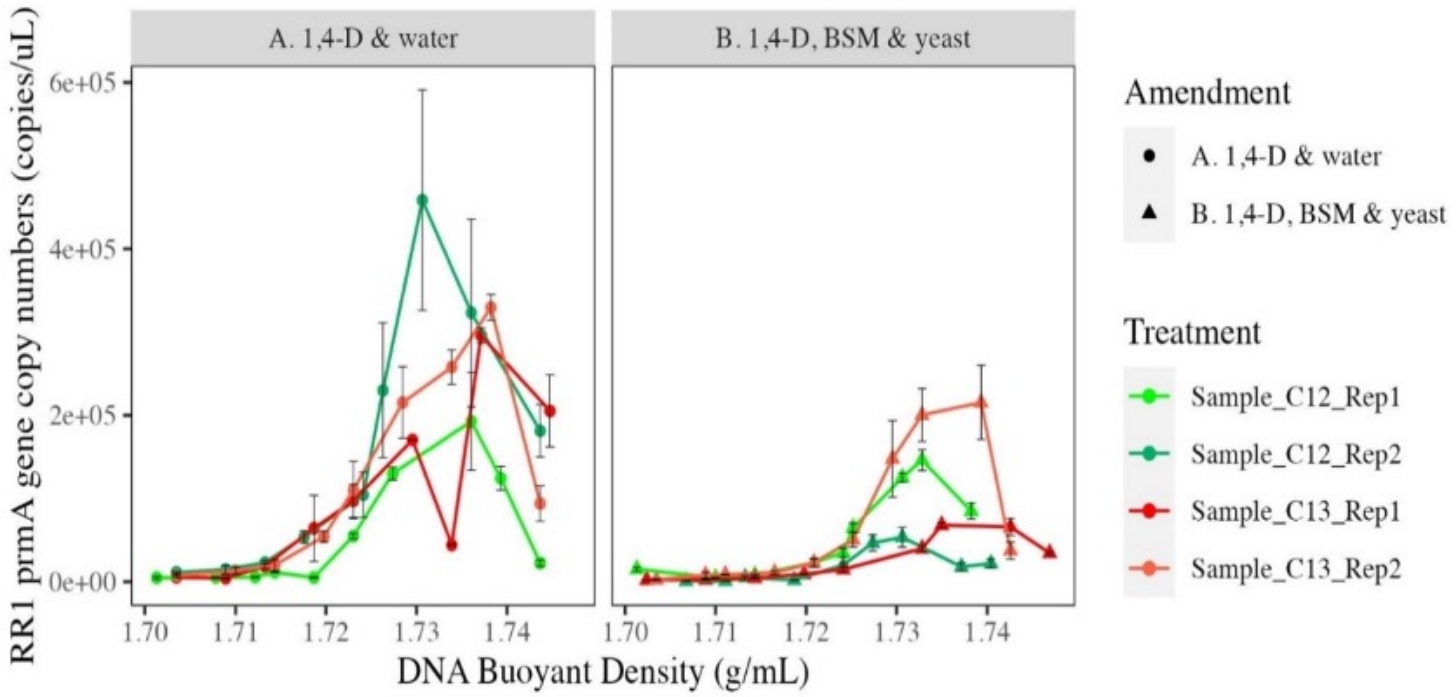

Figure 4.7 Gene copies of RR1 *prmA* in the SIP fractions from no yeast (water only) treatment (A) and the basal salts media and yeast treatment (B) of wetland sediments.

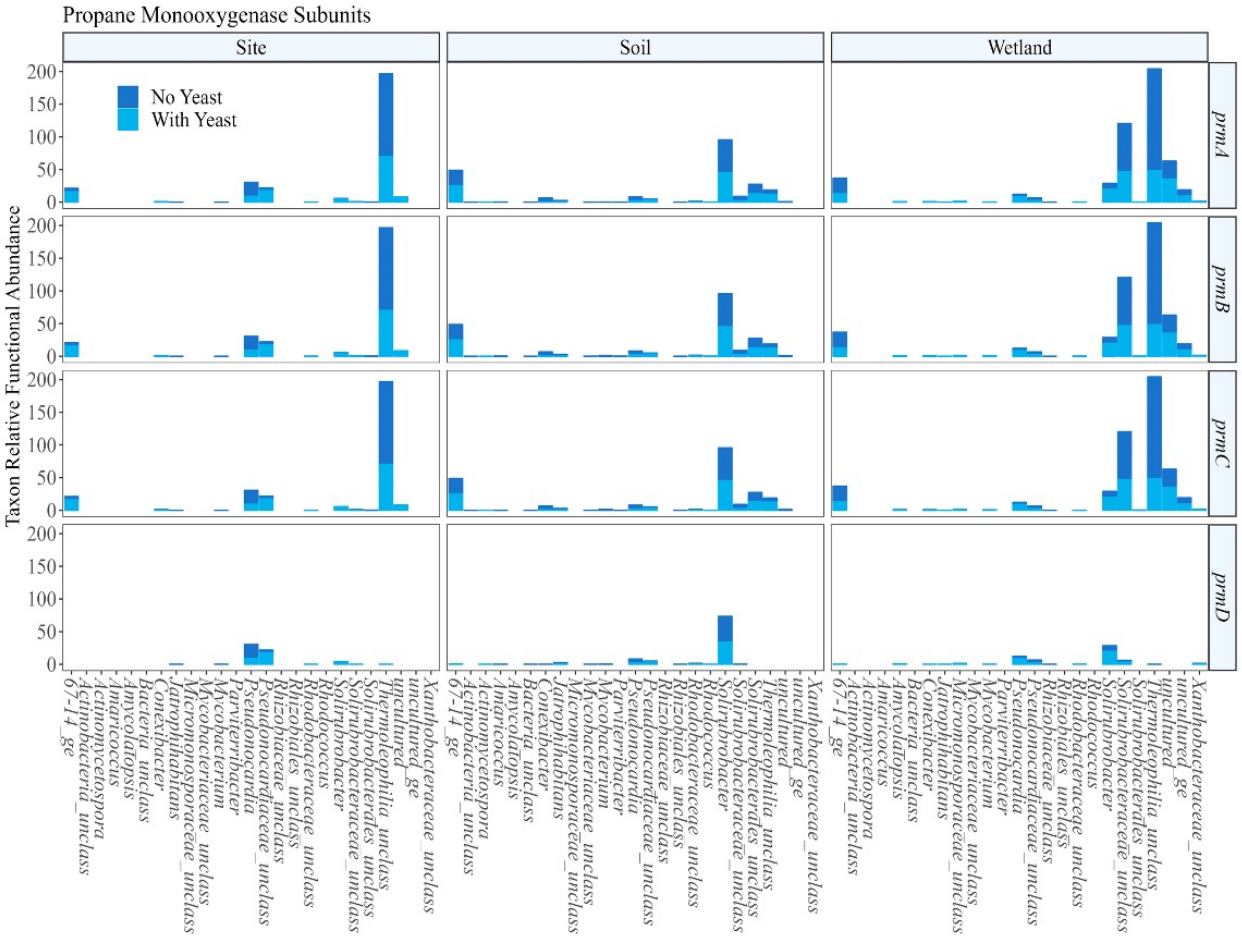

Figure 4.8 Relative abundance of taxa associated with all four subunits of propane monooxygenase, *prmA* (K18223), *prmB* (K18225), *prmC* (K18224) and *prmD* (K18226). Taxa without all four subunits were not included.

4.5 Discussion

This study examined the phylotypes and functional genes associated with 1,4-dioxane biodegradation in three mixed microbial communities. The impact of BSM and yeast extract on 1,4-dioxane biodegradation was also investigated as an easily available and non-hazardous substrate to potentially enhance removal rates *in situ*. Multiple molecular methods were utilized to ascertain the key biomarkers. The phylotypes responsible for the carbon uptake from 1,4-dioxane were identified using DNA-based SIP. The genes encoding for putative 1,4-dioxane degradative enzymes were investigated using 1) SDIMO based amplicon sequencing, 2) qPCR targeting *Rhodococcus* sp. RR1 *prmA* in the SIP fractions and 3) a predictive method (PICRUSt2) for the occurrence of oxygenase genes (Douglas, Maffei et al. 2020).

The impact of BSM and yeast extract on 1,4-dioxane biodegradation rates differed between the three microbial communities. The addition of BSM and yeast extract enhanced removal rates in all three inocula types, however, differences were only significant for the agricultural soil and impacted site sediment microcosms. A number of previous studies have added yeast extract while examining 1,4-dioxane biodegradation. One group added yeast extract to laboratory incubations with four river water samples, however, no 1,4-dioxane biodegradation was observed within the study period (29 days) (Sei, Kakinoki et al. 2010). Others have reported yeast extract accelerates 1,4-dioxane degradation rates by pure cultures (Pugazhendi, Rajesh Banu et al. 2015, Chen, Jin et al. 2016). *Rhodanobacter* AYS5 completely degraded 100 mg/L 1,4-dioxane in 4 days with 20 mg/L of yeast extract as an additional substrate (Pugazhendi, Rajesh Banu et al. 2015). *Xanthobacter flavus* DT8 degraded 100 mg/L 1,4-dioxane in less than 25 h with 100 mg/L of yeast extract (Chen, Jin et al. 2016). The biodegradation of tetrahydrofuran (a structural analog of 1,4-dioxane) by *Rhodococcus* strain YYL was also

improved by the addition of yeast extract (Yao, Lv et al. 2009). *Rhodococcus ruber* 219 sustained the degradation of low concentrations of 1,4-dioxane (<100 μg/L) to below health advisory levels (0.35 μg/L) when supplied with thiamine (Simmer, Richards et al. 2021). The researchers suggest that *in situ* biostimulation with growth supplements might result in efficient removal of 1,4-dioxane (Simmer, Richards et al. 2021). As yeast extract contains multiple growth factors, it has the potential to be beneficial to numerous microorganisms potentially linked to 1,4-dioxane biodegradation.

The results of the current study are not surprising as yeast extract has been associated with enhanced biodegradation of a large number of other contaminants, such as pyrene (by a bacterial consortium) (Wang, Qin et al. 2021), nonylphenol (in sediment and media) (Changa, Liua et al. 2008), methyl *tert*-butyl ether (by *Methylibium petroleiphilum* PM1) (Chen, Chen et al. 2009), petroleum hydrocarbons (by a bacterial consortium) (Al-Mur, Pugazhendi et al. 2021) and hexadecane (by *Burkholderia cepacia* GS3C) (Wu, Dang et al. 2011). For *B. cepacia* GS3C, researchers concluded amino acids were the active ingredients in yeast extract that caused the higher biodegradation rates and the trend was related to a greater level of cytochrome P450 activity (Wu, Dang et al. 2011).

In the current study, the different trends between the three microbial communities may be related to the nutritional requirements of the degradative microorganisms involved and/or the nutritional resources already present in the wetland sediment compared to the other two sample types. Given the practical implications, the most important trend is the enhancement of 1,4-dioxane biodegradation rates in the impacted site microcosms due to the addition of yeast extract and BSM. It is notable the effect was significant at an order of magnitude lower yeast extract concentration (60 μg/L) compared to the concentrations used in the pure culture studies. The

enhancement at low yeast extract concentrations is important because of the potential for biofouling *in situ* when biostimulation is practiced with high substrate concentrations.

SIP revealed different phylotypes were responsible for carbon uptake from 1,4-dioxane between the three mixed communities. *Gemmatimonas* was notably enriched in both wetland treatments. This genus belongs to the phylum *Gemmatimonadetes* and members of this phylum are widely distributed across various natural environments (Zhang, Sekiguchi et al. 2003, DeBruyn, Nixon et al. 2011, Hanada and Sekiguchi 2014). However, the physiology and environmental role of the members are largely unknown due to the limited number of cultivated species (Zeng, Selyanin et al. 2015). To our knowledge, members of this genus have not been previously associated with carbon uptake from 1,4-dioxane. However, *Gemmatimonas* was previously associated with benzoate biodegradation (Zhang, Sekiguchi et al. 2003) and was dominant in hydrocarbon-polluted soil (Sampaio, Almeida et al. 2017). *Gemmatimonas* was also associated with pyrene (Wang, Teng et al. 2018) and phenanthrene degradation in soil (Elyamine and Hu 2020, Dou, Sun et al. 2021, Wang, Wang et al. 2021).

Xanthobacteraceae (*Rhizobiales* order) and unclassified *Rhizobiales* were also responsible for carbon uptake from 1,4-dioxane in the wetland sediment microcosms. *Xanthobacteraceae* was previously linked to carbon uptake from 1,4-dioxane in soil microcosms (Dang and Cupples 2021). *Xanthobacteraceae* has also been associated with 1,4-dioxane biodegradation in activated sludge (Chen, Miao et al. 2021, Samadi, Kermanshahi-pour et al. 2023). Further, the 1,4-dioxane degraders *Xanthobacter flavus* DT8 (Chen, Jin et al. 2016) and *Xanthobacter* sp. YN2 (Ma, Wang et al. 2021) classify within the same family. Also consistent with the current study, genera classifying within the order *Rhizobiales* (*Hyphomicrobium* and *Chelativorans*) were enriched following 1,4-dioxane biodegradation compared to control

microcosms (no 1,4-dioxane) in agricultural soil microcosms (Ramalingam and Cupples 2020).

In the agricultural soil microcosms amended with BSM and yeast extract, both the genus *Solirubrobacter* and the family *Solirubacteraceae* were linked to carbon uptake from 1,4-dioxane. *Solirubrobacter* (*Solirubacteraceae* family) commonly exists in agricultural soil rhizospheres (Aguiar, Souza et al. 2020, Cordero Elvia, de Freitas et al. 2021, Lee, Kim et al. 2021). Members of this genus are difficult to cultivate and isolate due to their slow growth and the lack of specific media (Seki, Matsumoto et al. 2015). *Solirubrobacter* has previously been associated with the degradation of various substrates, such as 4-nonylphenol (Hung, Chen et al. 2022), coal (Wang, Wang et al. 2019), organic matter (Bukin, Pavlova et al. 2016) and petroleum hydrocarbons (Peng, Zi et al. 2015). To date, no 1,4-dioxane degrading *Solirubrobacter* isolate has been reported. *Pseudonocardia* was also associated with carbon uptake from 1,4-dioxane in the agricultural soil microcosms amended with BSM and yeast extract. This genus contains many well-known 1,4-dioxane degraders. For example, *Pseudonocardia dioxanivorans* CB1190 (Parales, Adamus et al. 1994, Mahendra and Alvarez-Cohen 2006), *Pseudonocardia* sp. D17 (Sei, Oyama et al. 2013), *Pseudonocardia* sp. N23 (Yamamoto, Saito et al. 2018) and *Pseudonocardia benzenivorans* B5 (Mahendra and Alvarez-Cohen 2006) can degrade 1,4-dioxane metabolically. *Pseudonocardia asaccharolytica* JCM 14343 (Inoue, Tsunoda et al. 2016), *Pseudonocardia* sp. ENV478 (Vainberg, McClay et al. 2006) and *Pseudonocardia tetrahydrofuranoxydans* sp. K1 (Kohlweyer, Thiemer et al. 2000) can degrade 1,4-dioxane co-metabolically when induced with tetrahydrofuran.

RB4 (*Pyrinomonadaceae* family) was notably enriched in the water only treatment of the agricultural soil microcosms. This is the first report of carbon uptake from 1,4-dioxane by this phylotype. Members of the same family were linked to phenanthrene degradation in oil field soil

with ryegrass root exudates (Li, Luo et al. 2019), with the degradation of cellulose, starch and xylan (Wüst, Foesel et al. 2016) and with the degradation of benzo [α] pyrene in soil (Lu, Sun et al. 2022).

Carbon uptake in the impacted site microcosms was dominated by two phylotypes, *oc3299* in the BSM and yeast extract treatment and *Burkholderiacae* in the water only treatment. *oc3299* classifies within a family (*Nitrosomonadaceae*) known to contain microorganisms with ammonia monooxygenases (Clark, Hughes et al. 2021, Cupples and Thelusmond 2022). This enzyme has been linked to the biodegradation of many environmental contaminants, such as 17 alpha-ethinylestradiol (Wang and Li 2023), 2-chlorophenol (Perez-Alfaro, Villaseca et al. 2023), micropollutants (Yu, Han et al. 2018) and trichloroethene (Alpaslan Kocamemi and Cecen 2007). Similar to the wetland sediment microcosms, *Gemmatimonas* was also responsible for carbon uptake in the impacted site microcosms amended with BSM and yeast extract. The family *Burkholderiacae* contains the genus *Burkholderia* which been associated with the biodegradation of many chemicals (Morya, Salvachua et al. 2020), such as hexadecane (Wu, Dang et al. 2011), phenol (Huang, Shao et al. 2022), naphthalene and phenanthrene (Kim, Lee et al. 2003), methyl parathion (Fernández-López, Popoca-Ursino et al. 2017, Castrejón-Godínez, Tovar-Sánchez et al. 2022) and polychlorinated biphenyls (Tillmann, Strömpl et al. 2005, Ponce, Latorre et al. 2011). Further, *Burkholderia cepacia* G4 degrades 1,4-dioxane co-metabolically when induced by toluene (Mahendra and Alvarez-Cohen 2006).

The current work investigated SDIMOs via amplicon-based sequencing. When the OTUs generated in the current work were compared to twelve genes previously associated with 1,4-dioxane metabolism and co-metabolism (as summarized (He, Mathieu et al. 2017)), three genes (*Rhodococcus jostii* RHA1 *prmA* and *Rhodococcus* sp. RR1 *prmA*, *Pseudonocardia*

dioxanivorans CB1190 plasmid pPSED02 Psed_6976) were detected in the three soil/sediment types. A similar trend of the dominance of the two *prmA* sequences in mixed microbial communities was also observed in previous work (Eshghdoostkhatami and Cupples 2024). Notably, in the current study, in all three mixed communities, the SIP results did not associate *Rhodococcus* with carbon uptake from 1,4-dioxane. Carbon uptake from microorganisms harboring *Rhodococcus* sp. RR1 *prmA*-like genes only occurred in the wetland sediments microcosms. The lack of *Rhodococcus* in the wetland SIP results could suggest other microorganisms may harbor similar genes.

The current study also revealed genes encoding for tetrahydrofuran monooxygenase alpha subunit *thmA* from *Pseudonocardia* were present in the impacted site sediments. However, SIP did not identify *Pseudonocardia* as a carbon consumer in the impacted site microcosms. The pattern suggests either these genes were not active, or biodegradation was co-metabolic and did not involve carbon uptake. The biomarker *thmA* has been associated with cometabolic 1,4-dioxane degradation by *Pseudonocardia tetrahydrofuran* K1, *Pseudonocardia* sp. ENV478 and *Rhodococcus* sp. YYL (Thiemer, Andreesen et al. 2003, Mahendra and Alvarez-Cohen 2006, Yao, Lv et al. 2009, Masuda, McClay et al. 2012). The current research suggests BSM and yeast extract could stimulate the co-metabolism of 1,4-dioxane in the impacted site sediments via tetrahydrofuran monooxygenase.

PICRUSt2 predicted the phylotypes and the functional genes associated with the 1,4-dioxane degradation. The identified degraders *Solirubrobacter* and *Pseudonocardia* (as discussed above) were predicted to be associated with all four subunits of propane monooxygenase (*prmA*, *prmB*, *prmC* and *prmD*) in all three soil types. Consistent with this, a NCBI search indicated *Solirubrobacter pauli* strain DSM 14954 contained the four propane

monooxygenase subunits (all located together and with the correct predicted length for each subunit). *Labrys* (*Rhizobiales*) and unclassified *Rhizobiales* were predicted to be associated with toluene monooxygenase (*tmo*/*tbu*/*tou*) and ammonia/particulate methane monooxygenase genes (*pmo*/*amo*) in all three samples. This order was also predicted to be a major phylotype associated with *pmo*/*amo* KEGG group in other soils (Cupples, Li et al. 2022). PICRUSt2 predicted *Mycobacterium* was associated with soluble methane monooxygenase genes in three soil types, however, this genus was not associated with carbon uptake from 1,4-dioxane. The trend indicates either sMMO was not involved in 1,4-dioxane degradation in the current study or the transformation did not result in any carbon uptake.

4.6 Conclusions

This research provides insight into the impact of BSM and yeast extract on 1,4-dioxane biodegradation rates as well as the microorganisms involved in carbon uptake during biodegradation. The addition of BSM and yeast extract enhanced removal rates in all three inocula types, however, differences were only significant for the agricultural soil and impacted site sediment microcosms. Numerous phylotypes were associated with carbon uptake across the three communities and two treatments. *Gemmatimonas* was particularly important in the heavy fractions of both treatments of the wetland sediment microcosms. Unclassified *Solirubacteraceae*, *Solirubrobacter*, *Pseudonocardia* and *RB4* were the dominant enriched phylotypes in the agricultural soil microcosms. The impacted site microcosms were dominated by only two phylotypes, unclassified *Burkholderiaceae* (water treatment) and *oc3299* (yeast and BSM treatment). To our knowledge, *Gemmatimonas*, *Solirubacteraceae*, *Solirubrobacter*, *RB4* and *oc3299* have not previously been linked to carbon uptake from 1,4-dioxane.

The SDIMO based amplicon sequencing detected three genes (*Rhodococcus jostii* RHA1

prmA and *Rhodococcus* sp. RR1 *prmA*, *Pseudonocardia dioxanivorans* CB1190 plasmid pPSED02 Psed_6976) in the mixed microbial communities. Although the genes were present, *prmA* was only linked to 1,4-dioxane biodegradation in one set of samples. The predicted functional gene analysis suggested the importance of propane monooxygenases associated with *Solirubrobacter* and *Pseudonocardia.* Overall, it is likely that a community of microorganisms is involved in 1,4-dioxane biodegradation in both the wetland and agricultural soil microcosms. In contrast, the carbon from 1,4-dioxane in the impacted site microcosms was largely restricted to two phylotypes. The results suggest that amending with BSM and yeast extract, even at low levels, could be a promising approach for the enhancement of 1,4-dioxane biodegradation.

Acknowledgements

Thanks to Stacey VanderWulp (MSU) for providing the agricultural soil samples from Kellogg Biological Station (KBS, MSU). Also, thanks to Anthony Danko and Michael Pound (NAVFAC) for providing the sediment samples from the contaminated site. This research was supported by a grant from NSF (Award Number 1902250). Support was also provided by the NSF Long-term Ecological Research Program (DEB 1832042) at the KBS and by MSU AgBioResearch.

REFERENCES

Adamson, D. T., E. A. Piña, A. E. Cartwright, S. R. Rauch, R. H. Anderson, T. Mohr and J. A. Connor (2017). "1, 4-Dioxane drinking water occurrence data from the third unregulated contaminant monitoring rule." Science of the Total Environment 596: 236-245.

Aguiar, L. M., M. d. F. Souza, M. L. de Laia, J. de Oliveira Melo, M. R. da Costa, J. F. Gonçalves, D. V. Silva and J. B. dos Santos (2020). "Metagenomic analysis reveals mechanisms of atrazine biodegradation promoted by tree species." Environmental Pollution 267: 115636.

Al-Mur, B. A., A. Pugazhendi and M. T. Jamal (2021). "Application of integrated extremophilic (halo-alkalo-thermophilic) bacterial consortium in the degradation of petroleum hydrocarbons and treatment of petroleum refinery wastewater under extreme condition." J Hazard Mater 413: 125351.

Alpaslan Kocamemi, B. and F. Cecen (2007). "Kinetic analysis of the inhibitory effect of trichloroethylene (TCE) on nitrification in cometabolic degradation." Biodegradation 18(1): 71-81.

Altschul, S. F., W. Gish, W. Miller, E. W. Myers and D. J. Lipman (1990). "Basic local alignment search tool." J Mol Biol 215(3): 403-410.

Aoyagi, T., F. Morishita, Y. Sugiyama, D. Ichikawa, D. Mayumi, Y. Kikuchi, A. Ogata, K. Muraoka, H. Habe and T. Hori (2018). "Identification of active and taxonomically diverse 1,4-dioxane degraders in a full-scale activated sludge system by high-sensitivity stable isotope probing." The ISME Journal 12(10): 2376-2388.

Bao, J., J. Li, L. Jiang, W. Mei, M. Song, D. Huang, C. Luo and G. Zhang (2022). "New insight into the mechanism underlying the effect of biochar on phenanthrene degradation in contaminated soil revealed through DNA-SIP." Journal of Hazardous Materials 438: 129466.

Barbera, P., A. M. Kozlov, L. Czech, B. Morel, D. Darriba, T. Flouri and A. Stamatakis (2019). "EPA-ng: Massively Parallel Evolutionary Placement of Genetic Sequences." Syst Biol 68(2): 365-369.

Bell, C., J. McDonough, K. S. Houston and K. Gerber (2016). "Stable Isotope Probing to Confirm Field-Scale Co-Metabolic Biodegradation of 1,4-Dioxane." Remediation Journal 27(1): 47-59.

Bell, C. H., J. Wong, K. Parsons, W. Semel, J. McDonough and K. Gerbe (2022). "First full-scale in situ propane biosparging for co-metabolic bioremediation of 1,4-dioxane." Ground Water Monitoring and Remediation 42: 54-66.

Bukin, S. V., O. N. Pavlova, A. Y. Manakov, E. A. Kostyreva, S. M. Chernitsyna, E. V. Mamaeva, T. V. Pogodaeva and T. I. Zemskaya (2016). "The Ability of Microbial Community of Lake Baikal Bottom Sediments Associated with Gas Discharge to Carry

Out the Transformation of Organic Matter under Thermobaric Conditions." Frontiers in Microbiology 7.

Bustin, S. A., V. Benes, J. A. Garson, J. Hellemans, J. Huggett, M. Kubista, R. Mueller, T. Nolan, M. W. Pfaffl and G. L. Shipley (2009). The MIQE guidelines: minimum information for publication of quantitative real-time PCR experiments, Oxford University Press.

Changa, B. V., C. L. Liua, S. Y. Yuana, C. Y. Chengb and W. H. Dingb (2008). "Biodegradation of nonylphenol in mangrove sediment." International Biodeterioration & Biodegradation 61: 325-330.

Chen, D., J. Chen and W. Zhong (2009). "Enhancement of methyl tert-butyl ether degradation by the addition of readily metabolizable organic substrates." Journal of Hazardous Materials 167(1): 860-865.

Chen, D.-Z., X.-J. Jin, J. Chen, J.-X. Ye, N.-X. Jiang and J.-M. Chen (2016). "Intermediates and substrate interaction of 1, 4-dioxane degradation by the effective metabolizer Xanthobacter flavus DT8." International Biodeterioration & Biodegradation 106: 133-140.

Chen, R., Y. Miao, Y. Liu, L. Zhang, M. Zhong, J. M. Adams, Y. Dong and S. Mahendra (2021). "Identification of novel 1, 4-dioxane degraders and related genes from activated sludge by taxonomic and functional gene sequence analysis." Journal of Hazardous Materials 412: 125157.

Cho, K.-C., D. G. Lee, H. Roh, M. E. Fuller, P. B. Hatzinger and K.-H. Chu (2013). "Application of 13C-stable isotope probing to identify RDX-degrading microorganisms in groundwater." Environmental Pollution 178: 350-360.

Clark, I. M., D. J. Hughes, Q. Fu, M. Abadie and P. R. Hirsch (2021). "Metagenomic approaches reveal differences in genetic diversity and relative abundance of nitrifying bacteria and archaea in contrasting soils." Scientific Reports 11(1): 15905.

Coleman, N. V., N. B. Bui and A. J. Holmes (2006). "Soluble di-iron monooxygenase gene diversity in soils, sediments and ethene enrichments." Environmental Microbiology 8(7): 1228-1239.

Cordero Elvia, J., J. R. de Freitas and J. J. Germida (2021). "Bacterial Microbiomes Associated with the Rhizosphere, Root Interior, and Aboveground Plant Organs of Wheat and Canola at Different Growth Stages." Phytobiomes Journal 5(4): 442-451.

Cupples, A. M. (2016). "Contaminant-Degrading Microorganisms Identified Using Stable Isotope Probing." Chemical Engineering & Technology 39(9): 1593-1603.

Cupples, A. M., Z. Li, F. P. Wilson, V. Ramalingam and A. Kelly (2022). "In silico analysis of soil, sediment and groundwater microbial communities to predict biodegradation potential." Journal of Microbiological Methods 202: 106595.

Cupples, A. M. and J.-R. Thelusmond (2022). "Predicting the occurrence of monooxygenases and their associated phylotypes in soil microcosms." Journal of Microbiological Methods 193: 106401.

Czech, L., P. Barbera and A. Stamatakis (2020). "Genesis and Gappa: processing, analyzing and visualizing phylogenetic (placement) data." Bioinformatics 36(10): 3263-3265.

Dang, H. and A. M. Cupples (2021). "Identification of the phylotypes involved in cis-dichloroethene and 1,4-dioxane biodegradation in soil microcosms." Science of The Total Environment 794: 148690.

Dang, H., Y. H. Kanitkar, R. D. Stedtfeld, P. B. Hatzinger, S. A. Hashsham and A. M. Cupples (2018). "Abundance of chlorinated solvent and 1,4-dioxane degrading microorganisms at five chlorinated solvent contaminated sites determined via shotgun sequencing." Environmental Science & Technology 52(23): 13914-13924.

DeBruyn, J. M., L. T. Nixon, M. N. Fawaz, A. M. Johnson and M. Radosevich (2011). "Global biogeography and quantitative seasonal dynamics of Gemmatimonadetes in soil." Appl Environ Microbiol 77(17): 6295-6300.

Deng, D. Y., F. Li and M. Y. Li (2018). "A novel propane monooxygenase initiating degradation of 1,4-dioxane by Mycobacterium dioxanotrophicus PH-06." Environmental Science and Technolology Letters 5(2): 86-91.

Derosa, C. T., S. Wilbur, J. Holler, P. Richter and Y.-W. Stevens (1996). "Health Evaluation of 1,4-Dioxane." Toxicology and Industrial Health 12(1): 1-43.

Divine, C., C. H. Bell, M. B. Heintz, A. Lorenz, P. Vallin, D. Favero, K. Gerber, C. Zheng and B. Rittmann (2024). "Advances in remediation solutions: new developments and opportunities in 1,4- dioxane biological treatment." Groundwater Monitoring & Remediation: DOI10.1111/gwmr.12649.

Dou, R., J. Sun, J. Lu, F. Deng, C. Yang, G. Lu and Z. Dang (2021). "Bacterial communities and functional genes stimulated during phenanthrene degradation in soil by bio-microcapsules." Ecotoxicology and Environmental Safety 212: 111970.

Douglas, G. M., V. J. Maffei, J. R. Zaneveld, S. N. Yurgel, J. R. Brown, C. M. Taylor, C. Huttenhower and M. G. I. Langille (2020). "PICRUSt2 for prediction of metagenome functions." Nat Biotechnol 38(6): 685-688.

Dowle, M. and A. Srinivasan (2023). data.table: Extension of `data.frame`. R package version 1.14.8.

Edgar, R. C. (2010). "Search and clustering orders of magnitude faster than BLAST." Bioinformatics 26(19): 2460-2461.

Edgar, R. C. (2013). "UPARSE: highly accurate OTU sequences from microbial amplicon reads." Nat Methods 10(10): 996-998.

Elyamine, A. M. and C. Hu (2020). "Earthworms and rice straw enhanced soil bacterial diversity and promoted the degradation of phenanthrene." Environmental Sciences Europe 32(1): 124.

Eshghdoostkhatami, Z. and A. M. Cupples (2024). "Occurrence of Rhodococcus sp. RR1 prmA and Rhodococcus jostii RHA1 prmA across microbial communities and their enumeration during 1,4-dioxane biodegradation." J Microbiol Methods 219: 106908.

Farhan Ul Haque, M., M. Hernández, A. T. Crombie and J. C. Murrell (2022). "Identification of active gaseous-alkane degraders at natural gas seeps." The ISME Journal 16(7): 1705-1716.

Fingerhut L. and C. I. (2021). "ampir Predict Antimicrobial Peptides_. R package version 1.1.0." <https://CRAN.R-project.org/package=ampir>.

Gedalanga, P. B., P. Pornwongthong, R. Mora, S. Y. D. Chiang, B. Baldwin, D. Ogles and S. Mahendra (2014). "Identification of bomarker genes to predict biodegradation of 1,4-dioxane." Applied and Environmental Microbiology 80(10): 3209-3218.

Godri Pollitt, K. J., J.-H. Kim, J. Peccia, M. Elimelech, Y. Zhang, G. Charkoftaki, B. Hodges, I. Zucker, H. Huang, N. C. Deziel, K. Murphy, M. Ishii, C. H. Johnson, A. Boissevain, E. O'Keefe, P. T. Anastas, D. Orlicky, D. C. Thompson and V. Vasiliou (2019). "1,4-Dioxane as an emerging water contaminant: State of the science and evaluation of research needs." Science of The Total Environment 690: 853-866.

Hanada, S. and Y. Sekiguchi (2014). The phylum Gemmatimonadetes. The Prokaryotes. E. Rosenberg, E. F. DeLong, S. Lory, E. Stackebrandt and Thompson.F. Springer, Berlin, Heidelberg. 11: 677–681.

Hand, S., B. Wang and K.-H. Chu (2015). "Biodegradation of 1,4-dioxane: Effects of enzyme inducers and trichloroethylene." Science of The Total Environment 520: 154-159.

Hatzinger, P. B., R. Banerjee, R. Rezes, S. H. Streger, K. McClay and C. E. Schaefer (2017). "Potential for cometabolic biodegradation of 1,4-dioxane in aquifers with methane or ethane as primary substrates." Biodegradation 28(5): 453-468.

He, Y., J. Mathieu, Y. Yang, P. Yu, M. L. B. da Silva and P. J. J. Alvarez (2017). "1,4-Dioxane biodegradation by Mycobacterium dioxanotrophicus PH-06 is associated with a group-6 soluble di-iron monooxygenase." Environmental Science and Technolology Letters 4(11): 494–499.

Horst, J. F., C. H. Bell, A. Lorenz, M. Heintz, Y. Miao, J. Saling, D. Favero and S. Mahendra (2019). "Bioremediation of 1,4- dioxane: Successful demonstration of in situ and ex situ approaches." Groundwater Monitoring & Remediation 39: 15-24.

Hung, C.-M., C.-W. Chen, C.-P. Huang and C.-D. Dong (2022). "Degradation of 4-nonylphenol in marine sediments using calcium peroxide activated by water hyacinth (Eichhornia crassipes)-derived biochar." Environmental Research 211: 113076.

Inoue, D., K. Hisada and M. Ike (2022). "Effectiveness of tetrahydrofuran at enhancing the 1,4-dioxane degradation ability of activated sludge lacking prior exposure to 1,4-dioxane." Water Science and Technology 86(7): 1707-1718.

Inoue, D., K. Hisada, T. Okumura, Y. Yabuki, G. Yoshida, M. Kuroda and M. Ike (2020). "Carbon sources that enable enrichment of 1,4-dioxane-degrading bacteria in landfill leachate." Biodegradation 31(1): 23-34.

Inoue, D., T. Tsunoda, K. Sawada, N. Yamamoto, Y. Saito, K. Sei and M. Ike (2016). "1,4-Dioxane degradation potential of members of the genera Pseudonocardia and Rhodococcus." Biodegradation 27(4): 277-286.

Jayamani, I. and A. M. Cupples (2015). "Stable isotope probing reveals the importance of Comamonas and Pseudomonadaceae in RDX degradation in samples from a Navy detonation site." Environmental Science and Pollution Research 22(13): 10340-10350.

Karges, U., J. Becker and W. Püttmann (2018). "1, 4-Dioxane pollution at contaminated groundwater sites in western Germany and its distribution within a TCE plume." Science of the Total Environment 619: 712-720.

Kassambara, A. (2023). "ggpubr: 'ggplot2' Based Publication Ready Plots. R package version 0.6.0."

Kassambara, A. (2023). "rstatix: Pipe-Friendly Framework for Basic Statistical Tests. R package version 0.7.2."

Katoh, K., J. Rozewicki and K. D. Yamada (2019). "MAFFT online service: multiple sequence alignment, interactive sequence choice and visualization." Brief Bioinform 20(4): 1160-1166.

Kikani, M., G. V. Satasiya, T. P. Sahoo, P. S. Kumar and M. A. Kumar (2022). "Remedial strategies for abating 1,4-dioxane pollution-special emphasis on diverse biotechnological interventions." Environmental Research 214: 113939.

Kim, J., M. Hwangbo, C.-H. Shih and K.-H. Chu (2023). "Advances and perspectives of using stable isotope probing (SIP)-based technologies in contaminant biodegradation." Water Research X 20: 100187.

Kim, Y.-M., J.-R. Jeon, K. Murugesan, E.-J. Kim and Y.-S. Chang (2009). "Biodegradation of 1, 4-dioxane and transformation of related cyclic compounds by a newly isolated Mycobacterium sp. PH-06." Biodegradation 20(4): 511-519.

Kohlweyer, U., B. Thiemer, T. Schräder and J. R. Andreesen (2000). "Tetrahydrofuran degradation by a newly isolated culture of Pseudonocardia sp. strain K1." FEMS microbiology letters 186(2): 301-306.

Kozich, J. J., S. L. Westcott, N. T. Baxter, S. K. Highlander and P. D. Schloss (2013). "Development of a Dual-Index Sequencing Strategy and Curation Pipeline for Analyzing

Amplicon Sequence Data on the MiSeq Illumina Sequencing Platform." Applied and Environmental Microbiology 79(17): 5112-5120.

Kreader, C. A. (1996). "Relief of amplification inhibition in PCR with bovine serum albumin or T4 gene 32 protein." Applied and Environmental Microbiology 62(3): 1102-1106.

Lahti, L. and S. Shetty (2012-2019). microbiome R package.

Lee, S. A., H. S. Kim, M. K. Sang, J. Song and H. Y. Weon (2021). "Effect of Bacillus mesonae H20-5 Treatment on Rhizospheric Bacterial Community of Tomato Plants under Salinity Stress." Plant Pathol J 37(6): 662-672.

Letunic, I. and P. Bork (2021). "Interactive Tree Of Life (iTOL) v5: an online tool for phylogenetic tree display and annotation." Nucleic Acids Res 49(W1): W293-W296.

Li, J., C. Luo, D. Zhang, X. Cai, L. Jiang, X. Zhao and G. Zhang (2019). "Diversity of the active phenanthrene degraders in PAH-polluted soil is shaped by ryegrass rhizosphere and root exudates." Soil Biology and Biochemistry 128: 100-110.

Li, Z., A. N. Kravchenko, A. Cupples, A. K. Guber, Y. Kuzyakov, G. Philip Robertson and E. Blagodatskaya (2024). "Composition and metabolism of microbial communities in soil pores." Nature Communications 15(1): 3578.

Lippincott, D., S. H. Streger, C. E. Schaefer, J. Hinkle, J. Stormo and R. J. Steffan (2015). "Bioaugmentation and propane biosparging for in situ biodegradation of 1,4-dioxane." Ground Water Monitoring and Remediation 35(2): 81-92.

Liu, J.-F., K. Zhang, B. Liang, Z.-C. Zhou, S.-Z. Yang, W. Li, Z.-W. Hou, X.-L. Wu, J.-D. Gu and B.-Z. Mu (2019). "Key players in the methanogenic biodegradation of n-hexadecane identified by DNA-Stable isotope probing." International Biodeterioration & Biodegradation 143: 104709.

Louca, S. and M. Doebeli (2018). "Efficient comparative phylogenetics on large trees." Bioinformatics 34(6): 1053-1055.

Lu, Q., X. Sun, Z. Jiang, Y. Cui, X. Li and J. Cui (2022). "Effects of Comamonas testosteroni on dissipation of polycyclic aromatic hydrocarbons and the response of endogenous bacteria for soil bioremediation." Environmental Science and Pollution Research 29(54): 82351-82364.

Ma, F., Y. Wang, J. Yang, H. Guo, D. Su and L. Yu (2021). "Degradation of 1, 4-Dioxane by Xanthobacter sp. YN2." Current Microbiology 78: 992-1005.

Mahendra, S. and L. Alvarez-Cohen (2006). "Kinetics of 1, 4-dioxane biodegradation by monooxygenase-expressing bacteria." Environmental science & technology 40(17): 5435-5442.

Masuda, H., K. McClay, R. J. Steffan and G. J. Zylstra (2012). "Biodegradation of tetrahydrofuran and 1,4-dioxane by soluble diiron monooxygenase in Pseudonocardia sp. strain ENV478." J Mol Microbiol Biotechnol 22(5): 312-316.

McMurdie, P. J. and S. Holmes (2013). "phyloseq: An R Package for Reproducible Interactive Analysis and Graphics of Microbiome Census Data." PLOS ONE 8(4): e61217.

Miao, Y., M. B. Heintz, C. H. Bell, N. W. Johnson, A. L. Polasko, D. Favero and S. Mahendra (2021). "Profiling microbial community structures and functions in bioremediation strategies for treating 1,4-dioxane-contaminated groundwater." Journal of Hazardous Materials 408: 124457.

Morya, R., D. Salvachua and I. S. Thakur (2020). "Burkholderia: an untapped but promising bacterial genus for the conversion of aromatic compounds." Trends Biotechnol 38(9): 963-975.

Notomista, E., A. Lahm, A. Di Donato and A. Tramontano (2003). "Evolution of Bacterial and Archaeal Multicomponent Monooxygenases." Journal of Molecular Evolution 56(4): 435-445.

Ooms, J. (2023). "writexl: Export Data Frames to Excel 'xlsx' Format_. R package version 1.4.2." <https://CRAN.R-project.org/package=writexl>.

Paes, F., X. Liu, T. E. Mattes and A. M. Cupples (2015). "Elucidating carbon uptake from vinyl chloride using stable isotope probing and Illumina sequencing." Applied Microbiology and Biotechnology 99(18): 7735-7743.

Parales, R., J. Adamus, N. White and H. May (1994). "Degradation of 1, 4-dioxane by an actinomycete in pure culture." Applied and Environmental Microbiology 60(12): 4527-4530.

Pedersen, T. L. (2023). "patchwork: The Composer of Plots. R package version 1.1.3.".

Peng, M., X. Zi and Q. Wang (2015). "Bacterial community diversity of oil-contaminated soils assessed by high throughput sequencing of 16S rRNA genes." International Journal of Environmental Research and Public Health 12(10): 12002-12015.

Perez-Alfaro, J. E., A. Villaseca, R. Gaytan, M. A. Martinez-Jardines, G. Buitron, A. C. Texier and F. M. Cuervo-Lopez (2023). "Nitrification activity in the presence of 2-chlorophenol using whole nitrifying cells and cell-free extracts: batch and SBR assays." 3 Biotech 13(11): 364.

Pruesse, E., C. Quast, K. Knittel, B. M. Fuchs, W. Ludwig, J. Peplies and F. O. Glöckner (2007). "SILVA: a comprehensive online resource for quality checked and aligned ribosomal RNA sequence data compatible with ARB." Nucleic Acids Research 35(21): 7188-7196.

Pugazhendi, A., J. Rajesh Banu, J. Dhavamani and I. T. Yeom (2015). "Biodegradation of 1,4-dioxane by Rhodanobacter AYS5 and the role of additional substrates." Annals of Microbiology 65(4): 2201-2208.

R Core Team (2018). R: A language and environment for statistical computing, R Foundation for Statistical Computing, Vienna, Austria. .

Radajewski, S., P. Ineson, N. R. Parekh and J. C. Murrell (2000). "Stable-isotope probing as a tool in microbial ecology." Nature 403(6770): 646-649.

Ramalingam, V. and A. M. Cupples (2020). "Enrichment of novel Actinomycetales and the detection of monooxygenases during aerobic 1,4-dioxane biodegradation with uncontaminated and contaminated inocula." Applied Microbiology and Biotechnology 104(5): 2255-2269.

RStudio_Team (2020). RStudio: Integrated Development for R. RStudio, PBC. Boston, MA URL http://www.rstudio.com/.

Sales, C. M., A. Grostern, J. V. Parales, R. E. Parales and L. Alvarez-Cohen (2013). "Oxidation of the cyclic ethers 1,4-dioxane and tetrahydrofuran by a monooxygenase in two Pseudonocardia species." Appl Environ Microbiol 79(24): 7702-7708.

Sales, C. M., S. Mahendra, A. Grostern, R. E. Parales, L. A. Goodwin, T. Woyke, M. Nolan, A. Lapidus, O. Chertkov, G. Ovchinnikova, A. Sczyrba and L. Alvarez-Cohen (2011). "Genome sequence of the 1,4-dioxane-degrading Pseudonocardia dioxanivorans strain CB1190." J Bacteriol 193(17): 4549-4550.

Samadi, A., A. Kermanshahi-pour, S. M. Budge, Y. Huang and R. Jamieson (2023). "Biodegradation of 1,4-dioxane by a native digestate microbial community under different electron accepting conditions." Biodegradation 34(3): 283-300.

Sampaio, D. S., J. R. B. Almeida, H. E. de Jesus, A. S. Rosado, L. Seldin and D. Jurelevicius (2017). "Distribution of Anaerobic Hydrocarbon-Degrading Bacteria in Soils from King George Island, Maritime Antarctica." Microbial Ecology 74(4): 810-820.

Schloss, P. D., S. L. Westcott, T. Ryabin, J. R. Hall, M. Hartmann, E. B. Hollister, R. A. Lesniewski, B. B. Oakley, D. H. Parks, C. J. Robinson, J. W. Sahl, B. Stres, G. G. Thallinger, D. J. Van Horn and C. F. Weber (2009). "Introducing mothur: Open-Source, Platform-Independent, Community-Supported Software for Describing and Comparing Microbial Communities." Applied and Environmental Microbiology 75(23): 7537-7541.

Sei, K., T. Kakinoki, D. Inoue, S. Soda, M. Fujita and M. Ike (2010). "Evaluation of the biodegradation potential of 1,4-dioxane in river, soil and activated sludge samples." Biodegradation 21(4): 585-591.

Sei, K., M. Oyama, T. Kakinoki, D. Inoue and M. Ike (2013). "Isolation and characterization of tetrahydrofuran- degrading bacteria for 1,4-dioxane-containing wastewater treatment by co-metabolic degradation." Journal of Water and Environment Technology 11(1): 11-19.

Seki, T., A. Matsumoto, S. Ōmura and Y. Takahashi (2015). "Distribution and isolation of strains belonging to the order Solirubrobacterales." J Antibiot (Tokyo) 68(12): 763-766.

Simmer, R. A., P. M. Richards, J. M. Ewald, C. Schwarz, M. L. B. da Silva, J. Jacques Mathieu, P. J. J. Alvarez and J. L. Schnoor (2021). "Rapid metabolism of 1,4-dioxane to below health advisory levels by thiamine-amended Rhodococcus ruber Strain 219." Environmental Science & Technology Letters 8 (11): 975-980

Steffan, R. J., K. R. McClay, H. Masuda and G. J. Zylstra (2007). "Biodegradatdion of 1,4-dioxane." Strategic Environmental Research and Development Program: ER-1422 Final Report.

Sun, W., X. Sun and A. M. Cupples (2012). "Anaerobic methyl tert-butyl ether-degrading microorganisms identified in wastewater treatment plant samples by stable isotope probing." Appl Environ Microbiol 78(8): 2973-2980.

Tawfik, A., A. Al-sayed, G. K. Hassan, M. Nasr, S. A. El-Shafai, N. S. Alhajeri, M. S. Khan, M. S. Akhtar, Z. Ahmad, P. Rojas and J. L. Sanz (2022). "Electron donor addition for stimulating the microbial degradation of 1,4 dioxane by sequential batch membrane bioreactor: A techno-economic approach." Chemosphere 306: 135580.

Thiemer, B., J. R. Andreesen and T. Schräder (2003). "Cloning and characterization of a gene cluster involved in tetrahydrofuran degradation in Pseudonocardia sp. strain K1." Archives of microbiology 179: 266-277.

Thomas, F., E. Corre and A. Cébron (2019). "Stable isotope probing and metagenomics highlight the effect of plants on uncultured phenanthrene-degrading bacterial consortium in polluted soil." The ISME Journal 13(7): 1814-1830.

USEPA (2013). Integrated Risk Information System (IRIS) on 1,4-Dioxane. Washington DC, National Center for Environmental Assessment Office of Research and Development.

Vainberg, S., K. McClay, H. Masuda, D. Root, C. Condee, G. J. Zylstra and R. J. Steffan (2006). "Biodegradation of ether pollutants by Pseudonocardia sp. strain ENV478." Applied and environmental microbiology 72(8): 5218-5224.

Wang, B., Y. Teng, Y. Xu, W. Chen, W. Ren, Y. Li, P. Christie and Y. Luo (2018). "Effect of mixed soil microbiomes on pyrene removal and the response of the soil microorganisms." Science of the total environment 640: 9-17.

Wang, B., Y. Wang, X. Cui, Y. Zhang and Z. Yu (2019). "Bioconversion of coal to methane by microbial communities from soil and from an opencast mine in the Xilingol grassland of northeast China." Biotechnology for Biofuels 12(1): 236.

Wang, D., L. Qin, E. Liu, G. Chai, Z. Su, J. Shan, Z. Yang, Z. Wang, H. Wang, H. Meng, X. Zheng, H. Li, J. Li and Y. Lin (2021). "Biodegradation performance and diversity of enriched bacterial consortia capable of degrading high-molecular-weight polycyclic aromatic hydrocarbons." Environ Technol: 1-12.

Wang, L. and A. Li (2023). "Ammonia monooxygenase-mediated transformation of 17alpha-ethinylestradiol: Underlying molecular mechanism." Environ Res 237(Pt 1): 116930.

Wang, M. Y., B. H. Olson and J. S. Chang (2007). "Improving PCR and qPCR detection of hydrogenase A (hydA) associated with Clostridia in pure cultures and environmental sludges using bovine serum albumin." Applied Microbiology and Biotechnology 77(3): 645-656.

Wang, Y.-Q., M.-X. Wang, Y.-Y. Chen, C.-M. Li and Z.-F. Zhou (2021). "Microbial community structure and co-occurrence are essential for methanogenesis and its contribution to phenanthrene degradation in paddy soil." Journal of Hazardous Materials 417: 126086.

Wickham, H. (2016). "ggplot2: Create Elegant Data Visualisations Using the Grammar of Graphics." Springer-Verlag New York.

Wickham, H. (2016). " ggplot2: Elegant Graphics for Data Analysis. Springer-Verlag New York, 2016." https://ggplot2.tidyverse.org.

Wickham, H. (2023). forcats: Tools for Working with Categorical Variables (Factors). R package version 1.0.0.

Wickham, H., , and J. Bryan (2023). " readxl: Read Excel Files_. R package version 1.4.2,." <https://CRAN.R-project.org/package=readxl>.

Wickham, H., M. Averick, J. Bryan, W. Chang, L. D. A. McGowan, R. François, G. Grolemund, A. Hayes, L. Henry, J. Hester, M. Kuhn, T. L. Pedersen, E. Miller, S. M. Bache, K. Müller, J. Ooms, D. Robinson, D. P. Seidel, V. Spinu, K. Takahashi, D. Vaughan, C. Wilke, K. Woo and H. Yutani (2019). "Welcome to the Tidyverse." Journal of Open Source Software 4(43), 1686,.

Wickham, H., R. Francois, L. Henry, K. Müller and D. Vaughan (2023). "dplyr: A Grammar of Data Manipulation. R package version 1.1.3.".

Wickham, H., D. Vaughan and M. Girlich (2023). "tidyr: Tidy Messy Data. R package version 1.3.0.".

Wu, R. R., Z. Dang, X. Y. Yi, C. Yang, G. N. Lu, C. L. Guo and C. Q. Liu (2011). "The effects of nutrient amendment on biodegradation and cytochrome P450 activity of an n-alkane degrading strain of Burkholderia sp. GS3C." J Hazard Mater 186(2-3): 978-983.

Wüst, P. K., B. U. Foesel, A. Geppert, K. J. Huber, M. Luckner, G. Wanner and J. Overmann (2016). "Brevitalea aridisoli, B. deliciosa and Arenimicrobium luteum, three novel species of Acidobacteria subdivision 4 (class Blastocatellia) isolated from savanna soil and description of the novel family Pyrinomonadaceae." International Journal of Systematic and Evolutionary Microbiology 66(9): 3355-3366.

Xiong, Y., O. U. Mason, A. Lowe, Z. Zhang, C. Zhou, G. Chen, M. J. Villalonga and Y. Tang (2020). "Investigating promising substrates for promoting 1, 4-dioxane biodegradation:

effects of ethane and tetrahydrofuran on microbial consortia." Biodegradation 31: 171-182.

Xiong, Y., O. U. Mason, A. Lowe, C. Zhou, G. Chen and Y. Tang (2019). "Microbial community analysis provides insights into the effects of tetrahydrofuran on 1, 4-dioxane biodegradation." Applied and Environmental Microbiology 85(11): e00244-00219.

Yamamoto, N., Y. Saito, D. Inoue, K. Sei and M. Ike (2018). "Characterization of newly isolated Pseudonocardia sp. N23 with high 1,4-dioxane-degrading ability." Journal of Bioscience and Bioengineering 125(5): 552-558.

Yang, S. N. N., V. Haritos, M. A. Kertesz and N. V. Coleman (2024). "A novel soluble di-iron monooxygenase from the soil bacterium Solimonas soli." Environ Microbiol 26(2): e16567.

Yao, Y., Z. Lv, H. Min, Z. Lv and H. Jiao (2009). "Isolation, identification and characterization of a novel Rhodococcus sp. strain in biodegradation of tetrahydrofuran and its medium optimization using sequential statistics-based experimental designs." Bioresource Technology 100(11): 2762-2769.

Ye, Y. and T. G. Doak (2009). "A parsimony approach to biological pathway reconstruction/inference for genomes and metagenomes." PLoS Comput Biol 5(8): e1000465.

Yu, Y., P. Han, L. J. Zhou, Z. Li, M. Wagner and Y. Men (2018). "Ammonia monooxygenase-mediated cometabolic biotransformation and hydroxylamine-mediated abiotic transformation of micropollutants in an AOB/NOB coculture." Environ Sci Technol 52(16): 9196-9205.

Zeng, Y., V. Selyanin, M. Lukes, J. Dean, D. Kaftan, F. Feng and M. Koblizek (2015). "Characterization of the microaerophilic, bacteriochlorophyll a-containing bacterium Gemmatimonas phototrophica sp. nov., and emended descriptions of the genus Gemmatimonas and Gemmatimonas aurantiaca." Int J Syst Evol Microbiol 65(8): 2410-2419.

Zenker, M. J., R. C. Borden and M. A. Barlaz (2003). "Occurrence and treatment of 1,4-dioxane in aqueous environments." Environmental Engineering Science 20(5): 423-432.

Zhang, H., Y. Sekiguchi, S. Hanada, P. Hugenholtz, H. Kim, Y. Kamagata and K. Nakamura (2003). "Gemmatimonas aurantiaca gen. nov., sp. nov., a gram-negative, aerobic, polyphosphate-accumulating micro-organism, the first cultured representative of the new bacterial phylum Gemmatimonadetes phyl. nov." Int J Syst Evol Microbiol 53(Pt 4): 1155-1163.

Zhang, J. (2017). "phylotools: Phylogenetic Tools for Eco-Phylogenetics_. R package version 0.2.2." <https://CRAN.R-project.org/package=phylotools>.

Zhang, S., P. B. Gedalanga and S. Mahendra (2017). "Advances in bioremediation of 1,4-dioxane-contaminated waters." Journal of Environmental Management 204: 765-774.

APPENDIX

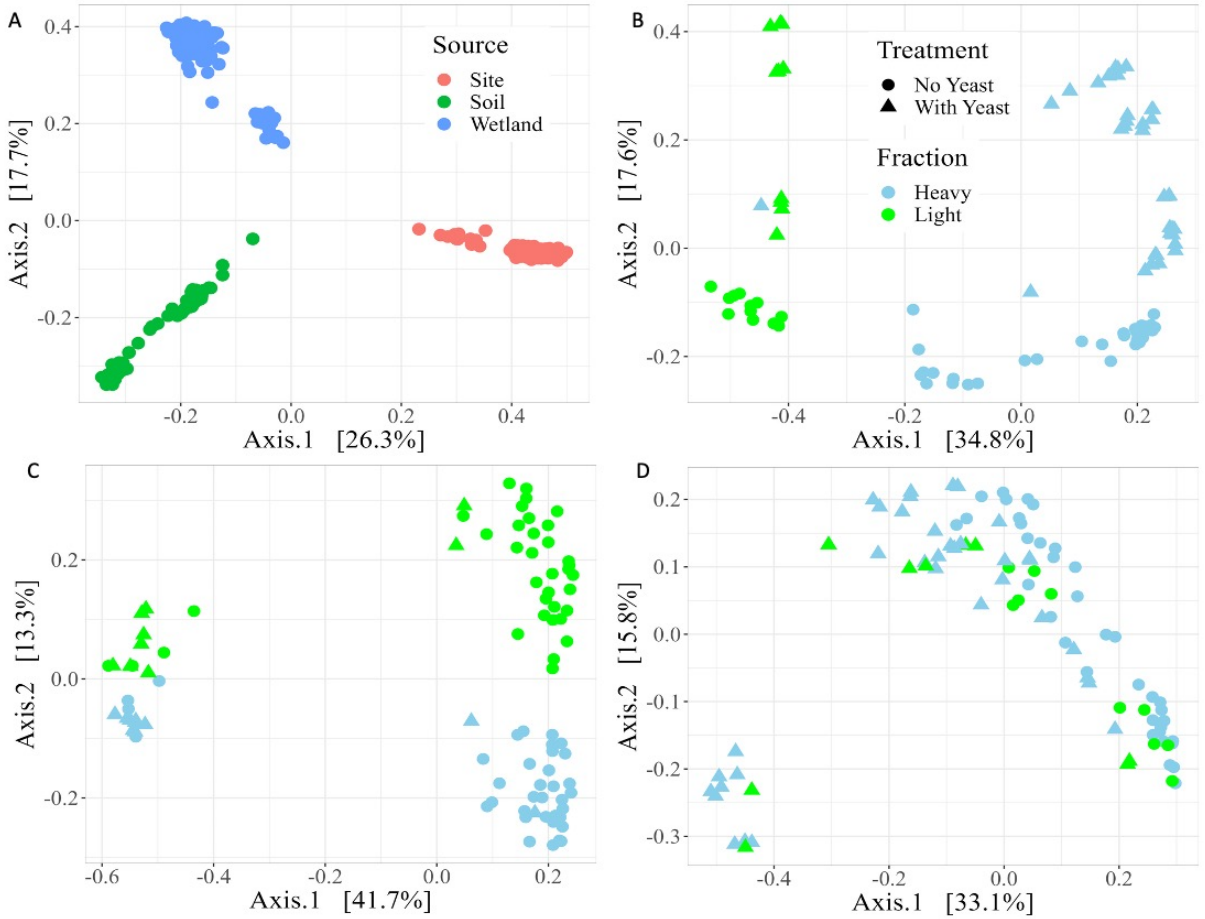

Figure A4.1 Principal coordinate analysis for all three sample types together (A), for the soil only (B), wetland sediments only (C) and site sediments only (D), separated by treatment and fraction type.

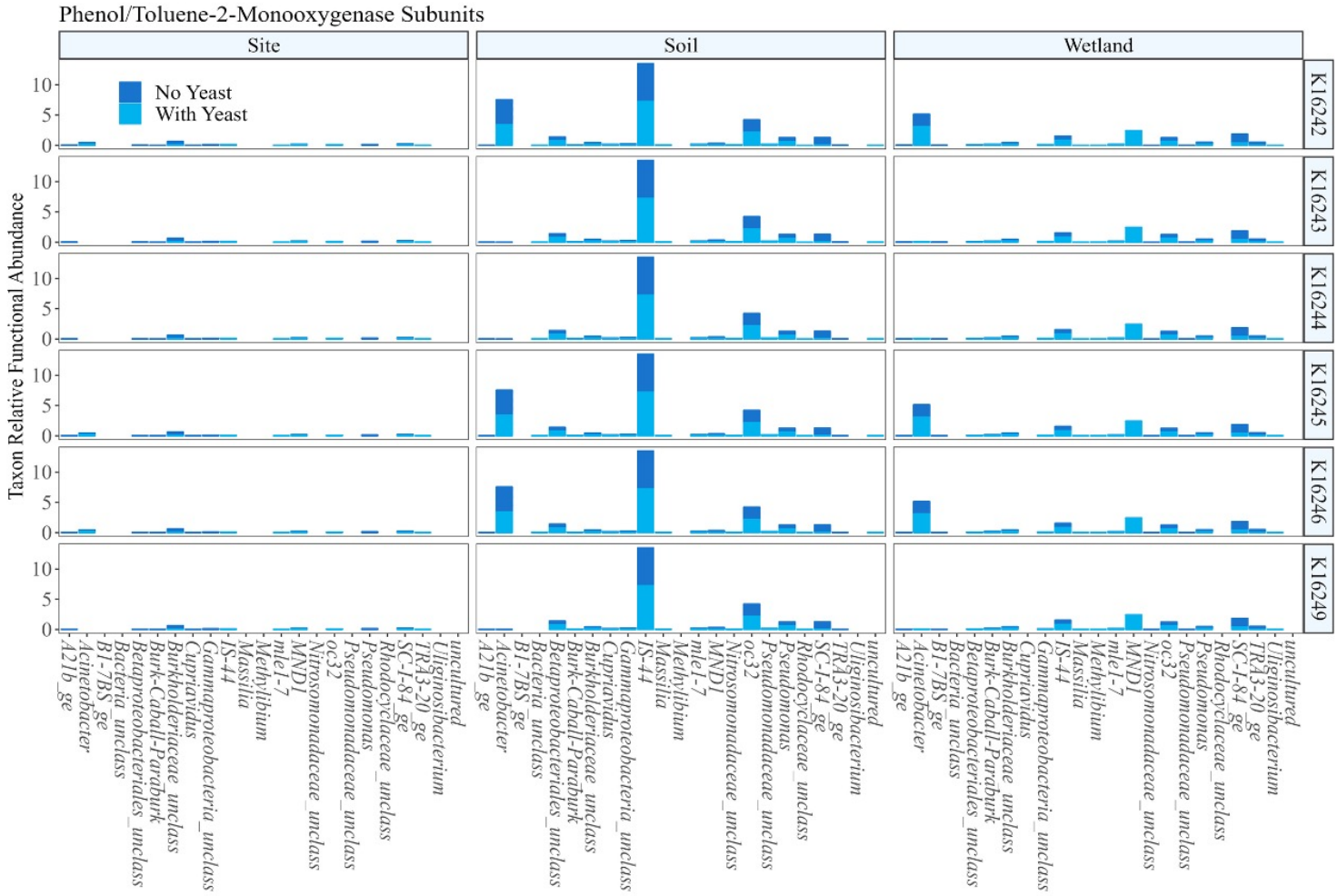

Figure A4.2 Relative abundance of taxa associated with the six subunits of phenol/toluene 2-monooxygenase, *dmpK/poxA/tomA0* (K16249), *dmpL/poxB/tomA1* (K16243), *dmpM/ poxC/tomA2* (K16244), *dmpN/poxD/tomA3* (K16242), *dmpO/poxE/ tomA4* (K16245) and *dmpP/poxF/tomA5* (K16246). Taxa without all six subunits were removed.

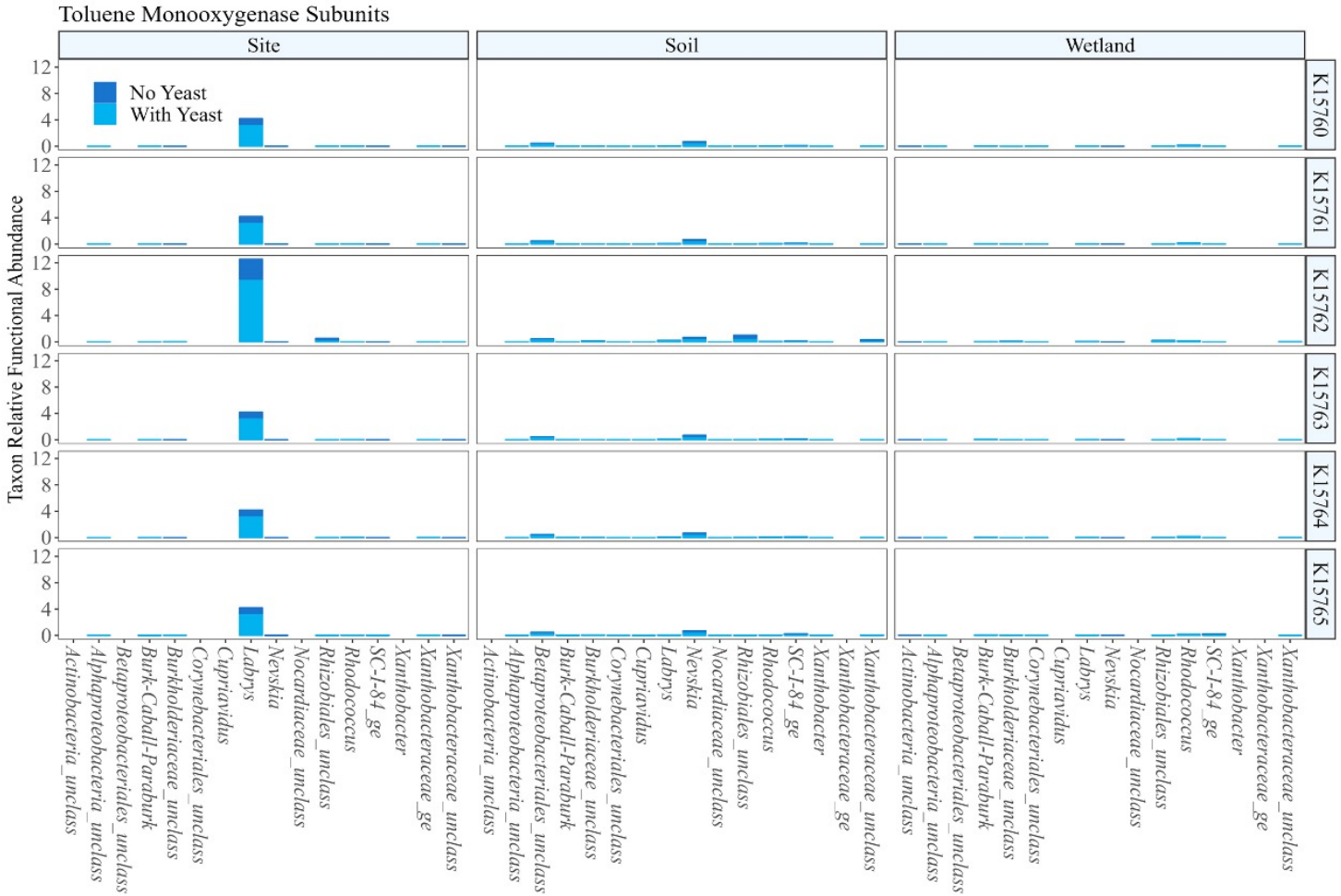

Figure A4.3 Relative abundance of taxa associated with the six subunits of toluene monooxygenase, *tmoA/tbuA1/touA* (K15760), *tmoB/tbuU/touB* (K15761), *tmoC/tbuB/touC* (K15762), *tmoD/tbuV/touD* (K15763), *tmoE/tbuA2/touE* (K15764) and *tmoF/tbuC/touF* (K15765). Taxa without all six subunits were removed.

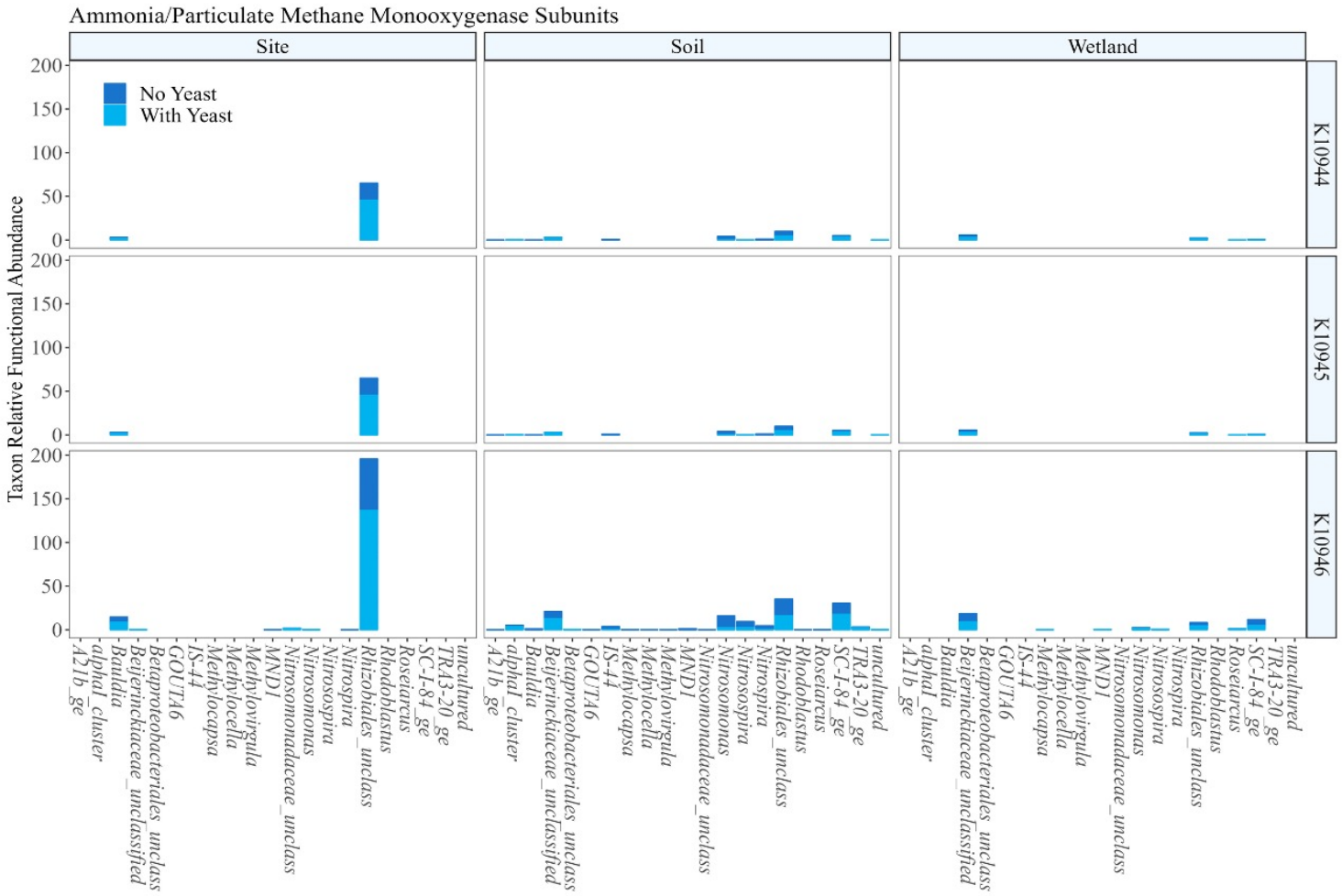

Figure A4.4 Relative abundance of taxa associated with the three subunits of ammonia/particulate methane monooxygenase, *pmoA/amoA* (K10944), *pmoB/amoB* (K10945), *pmoC/amoC* (K10946). Taxa without all three subunits were removed.

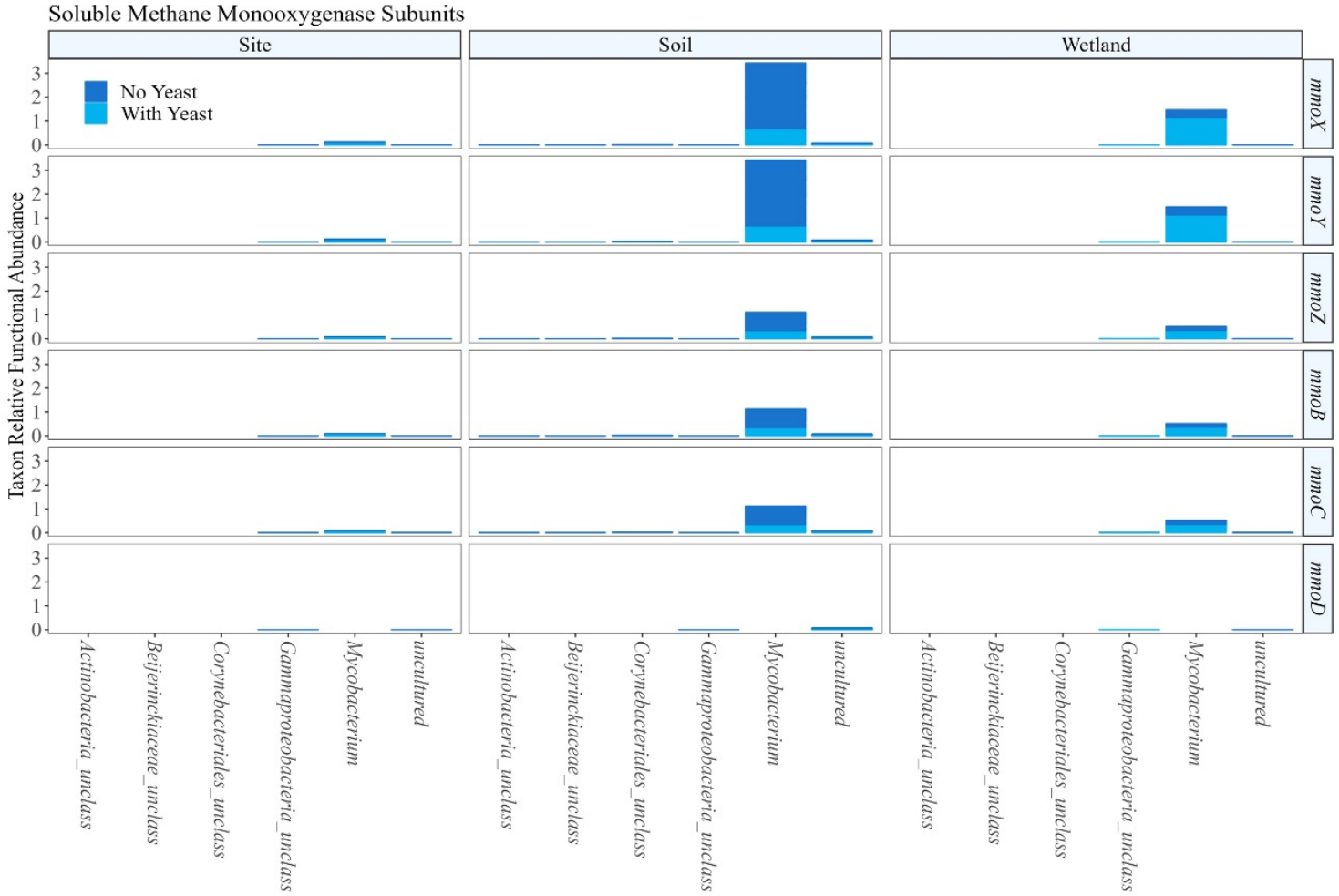

Figure A4.5 Relative abundance of taxa associated with the six subunits of soluble methane monooxygenase. Taxa without five (except *mmoD*) or six subunits were removed.

Table A4.1 Target genes, primer names, primer/probe sequences, product sizes and references for the primers used in this study.

Target gene	***Primer name***	***Sequences (5'-3')***	***Amplicon size (bp)***	***Reference***
Rhodococcus sp. RR1 prmA	RR1 prmA forward	TTCCCGGAGATCTCGGCGGCC	141	(Eshghdoostkhatami and Cupples 2024)
	RR1 prmA reverse	GAGCTTCTTGAGGTTCATCTGGATCGT	141	As above
	RR1 prmA probe	FAM/TGGATCTCG/ZEN/GGGTTGGGCACC/ABkFQ/		As above
Monooxygenase Genes	CS1-TS-F-NV57	CAGTCNGAYGARKCSCGN CAYAT	420	(Coleman, Bui et al. 2006)
	CS2-TS-R-NVC66	CCANCCNGGRTAYTTRTTYTCRAACCA	420	As above

Table A4.2 DNA concentration in DNA extracts, as measured with Qubit.

Sample type	***DNA concentration (ng/μL)***
wetland H_2O 12C replicate 1 heavy fraction 1	4.68
wetland H_2O 12C replicate 1 heavy fraction 2	21.00
wetland H_2O 12C replicate 1 heavy fraction 3	51.40
wetland H_2O 12C replicate 1 fraction 4	65.00
wetland H_2O 12C replicate 1 fraction 5	2.46
wetland H_2O 12C replicate 1 fraction 6	38.20
wetland H_2O 12C replicate 1 fraction 7	12.60
wetland H_2O 12C replicate 1 fraction 8	12.00
wetland H_2O 12C replicate 1 fraction 9	11.44
wetland H_2O 12C replicate 1 light fraction 1	5.14
wetland BSM yeast 12C replicate 1 heavy fraction 1	7.96
wetland BSM yeast 12C replicate 1 heavy fraction 2	17.68
wetland BSM yeast 12C replicate 1 heavy fraction 3	23.40
wetland BSM yeast 12C replicate 1 fraction 4	12.12
wetland BSM yeast 12C replicate 1 fraction 5	9.50
wetland BSM yeast 12C replicate 1 fraction 6	6.68
wetland BSM yeast 12C replicate 1 fraction 7	6.72
wetland BSM yeast 12C replicate 1 fraction 8	8.12
wetland BSM yeast 12C replicate 1 light fraction 1	3.04
wetland H_2O 12C replicate 2 heavy fraction 1	4.92
wetland H_2O 12C replicate 2 heavy fraction 2	15.44
wetland H_2O 12C replicate 2 heavy fraction 3	23.20
wetland H_2O 12C replicate 2 fraction 4	25.20
wetland H_2O 12C replicate 2 fraction 5	16.20
wetland H_2O 12C replicate 2 fraction 6	7.24
wetland H_2O 12C replicate 2 fraction 7	5.96
wetland H_2O 12C replicate 2 fraction 8	4.98
wetland H_2O 12C replicate 2 light fraction 1	3.20
wetland BSM yeast 12C replicate 2 heavy fraction 1	3.96
wetland BSM yeast 12C replicate 2 fraction	0.91
wetland BSM yeast 12C replicate 2 heavy fraction 2	7.16
wetland BSM yeast 12C replicate 2 heavy fraction 3	16.74
wetland BSM yeast 12C replicate 2 fraction 4	4.32
wetland BSM yeast 12C replicate 2 fraction 5	0.53
wetland BSM yeast 12C replicate 2 fraction 6	5.86
wetland BSM yeast 12C replicate 2 fraction 7	0.66
wetland BSM yeast 12C replicate 2 light fraction 1	2.26

Table A4.2 (cont'd)

Sample type	*DNA concentration (ng/µL)*
wetland H_2O 13C replicate 1 heavy fraction 1	15.48
wetland H_2O 13C replicate 1 heavy fraction 2	55.4
wetland H_2O 13C replicate 1 heavy fraction 3	4.76
wetland H_2O 13C replicate 1 fraction 4	43.8
wetland H_2O 13C replicate 1 fraction 5	28.8
wetland H_2O 13C replicate 1 fraction 6	61.6
wetland H_2O 13C replicate 1 fraction 7	11.62
wetland H_2O 13C replicate 1 fraction 8	4.46
wetland H_2O 13C replicate 1 light fraction 1	5.88
wetland BSM yeast 13C replicate 2 heavy fraction 1	8.52
wetland BSM yeast 13C replicate 2 heavy fraction 2	15.24
wetland BSM yeast 13C replicate 2 heavy fraction 3	21.00
wetland BSM yeast 13C replicate 2 fraction 4	19.74
wetland BSM yeast 13C replicate 2 fraction 5	8.04
wetland BSM yeast 13C replicate 2 fraction 6	6.06
wetland BSM yeast 13C replicate 2 fraction 7	6.98
wetland BSM yeast 13C replicate 2 fraction 8	4.74
wetland BSM yeast 13C replicate 2 light fraction 1	2.36
wetland H_2O 13C replicate 2 heavy fraction 1	2.08
wetland H_2O 13C replicate 2 heavy fraction 2	6.94
wetland H_2O 13C replicate 2 heavy fraction 3	23.00
wetland H_2O 13C replicate 2 fraction 4	19.42
wetland H_2O 13C replicate 2 fraction 5	11.96
wetland H_2O 13C replicate 2 fraction 6	6.64
wetland H_2O 13C replicate 2 fraction 7	6.26
wetland H_2O 13C replicate 2 fraction 8	8.14
wetland H_2O 13C replicate 2 light fraction 1	4.32
wetland BSM yeast 13C replicate 2 heavy fraction 1	1.96
wetland BSM yeast 13C replicate 2 heavy fraction 2	11.60
wetland BSM yeast 13C replicate 2 heavy fraction 3	13.88
wetland BSM yeast 13C replicate 2 fraction 4	45.80
wetland BSM yeast 13C replicate 2 fraction 5	67.80
wetland BSM yeast 13C replicate 2 fraction 6	46.40
wetland BSM yeast 13C replicate 2 fraction 7	22.60
wetland BSM yeast 13C replicate 2 fraction 8	6.26
wetland BSM yeast 13C replicate 2 fraction 9	16.96
wetland BSM yeast 13C replicate 2 light fraction 1	4.10

Table A4.3 QPCR parameters based on MIQE guidelines (Bustin, Benes et al. 2009).

Target gene	Experiment	Primer concentration (µM)	QPCR linear range (gene copies/reaction)	QPCR efficiency	Y-intercept
Rhodococcus sp. RR1 prmA	Wetland 12C H_2O and 12C BSM & yeast replicate 1	0.3	98 - 98×10^5	73.32 ± 2.18	47.04 ± 0.62
Rhodococcus sp. RR1 prmA	Wetland 12C H_2O and 12C BSM & yeast replicate 2	0.3	98 - 98×10^5	76.69 ± 7.90	45.32 ± 1.56
Rhodococcus sp. RR1 prmA	Wetland 13C H_2O and 13C BSM & yeast replicate 1	0.3	98 - 98×10^5	74.98 ± 1.75	45.80 ± 0.36
Rhodococcus sp. RR1 prmA	Wetland 13C H_2O and 13C BSM & yeast replicate 2	0.3	98 - 98×10^5	77.91 ± 4.66	45.24 ± 0.77

Table A4.4 P-values for one-way ANOVA with the slopes of 1,4-dioxane degradation plots between different treatments for each soil/sediment types. P-values in bold indicate a significant difference ($p \leq 0.05$).

Soil types	P-values
Wetland sediments	**8.64E-07**
Agricultural soil	**7.91E-12**
Site sediments	**1.32E-04**

Table A4.5 P-values for the *t*-test with the slopes of 1,4-dioxane degradation plots between different treatments for wetland sediment microcosms. P-values in bold indicate a significant difference ($p \leq 0.05$).

	12C BSM& yeast	13C BSM& yeast	Abiotic 12C H_2O	Abiotic 12C BSM& yeast
12C H_2O	1.02E-01	-	**2.23E-03**	-
13C H_2O	-	4.59E-01	**4.74E-03**	-
12C BSM& yeast	-	-	-	**8.07E-05**
13C BSM& yeast	-	-	-	**3.00E-04**

Table A4.6 P-values for the *t*-test with the slopes of 1,4-dioxane degradation plots between different treatments for agricultural soil microcosms. P-values in bold indicate a significant difference ($p \leq 0.05$).

	12C BSM& yeast	13C BSM& yeast	Abiotic 12C H_2O	Abiotic 12C BSM& yeast
12C H_2O	**4.17E-03**	-	**3.20E-06**	-
13C H_2O	-	**6.01E-05**	**5.10E-05**	-
12C BSM& yeast	-	-	-	**6.76E-04**
13C BSM& yeast	-	-	-	**9.08E-04**

Table A4.7 P-values for the *t*-test with the slopes of 1,4-dioxane degradation plots between different treatments for the impacted site sediment microcosms. P-values in bold indicate a significant difference ($p \leq 0.05$).

	12C BSM& yeast	13C BSM& yeast	Abiotic 12C H_2O	Abiotic 12C BSM& yeast
12C H_2O	**1.80E-02**	-	**7.32E-03**	-
13C H_2O	-	**1.57E-02**	**7.94E-03**	-
12C BSM& yeast	-	-	-	**1.11E-03**
13C BSM& yeast	-	-	-	**5.79E-04**

Table A4.8 P-values for one-way ANOVA with alpha diversity indices between three soil/sediment types of the water or BSM and yeast treatments. P-values in bold indicate a significant difference ($p \leq 0.05$).

	Chao1	ACE	Shannon	Simpson	Inverse of Simpson	Fisher
Water	**1.14E-30**	**5.74E-30**	**4.52E-56**	**1.87E-25**	**2.82E-37**	**2.52E-42**
BSM and yeast	**1.16E-50**	**8.79E-50**	**9.20E-35**	**3.19E-20**	**2.38E-09**	**1.08E-53**

Table A4.9 P-values for the *t* test with alpha diversity indices between three soil/sediment types of the water treatment. P-values in bold indicate a significant difference ($p \leq 0.05$).

	Chao1	ACE	Shannon	Simpson	Inverse of Simpson	Fisher
Soil vs Site	**2.02E-21**	**6.02E-21**	**1.72E-44**	**5.61E-17**	**4.34E-25**	**6.37E-29**
Soil vs Wetland	**4.32E-16**	**1.10E-15**	**2.26E-33**	**1.03E-09**	**6.15E-20**	**1.48E-22**
Site vs Wetland	**6.59E-11**	**7.33E-11**	**2.29E-20**	**6.34E-14**	**1.53E-19**	**5.38E-18**

Table A4.10 P-values for the *t* test with alpha diversity indices between three soil/sediment types of the BSM and yeast treatment. P-values in bold indicate a significant difference ($p \leq 0.05$).

	Chao1	ACE	Shannon	Simpson	Inverse of Simpson	Fisher
Soil vs Site	**4.13E-39**	**2.27E-38**	**8.99E-26**	**2.52E-12**	**8.12E-08**	**1.67E-40**
Soil vs Wetland	**2.34E-26**	**8.77E-26**	**3.50E-06**	2.32E-01	**9.10E-04**	**7.36E-26**
Site vs Wetland	**4.81E-15**	**5.65E-15**	**3.77E-23**	**7.32E-13**	**4.86E-15**	**9.00E-24**

Table A4.11 P-values for the *t* test with the alpha diversity indices between water and yeast treatments for the three soil/sediment types. P-values in bold indicate a significant difference ($p \leq 0.05$).

	Chao1	ACE	Shannon	Simpson	Inverse of Simpson	Fisher
Soil	**1.79E-03**	**2.38E-03**	**7.35E-17**	**2.89E-10**	**9.98E-14**	**2.87E-08**
Site	**2.69E-06**	**2.39E-06**	4.56E-01	2.46E-01	3.00E-01	**1.47E-05**
Wetland	**2.28E-02**	**2.35E-02**	1.39E-01	1.28E-01	**2.37E-03**	**3.04E-02**

CHAPTER 5: BIODEGRADATION OF 1,4-DIOXANE AT LOW CONCENTRATIONS IN SITE SEDIMENTS USING YEAST AMENDMENT AND BIOAUGMENTATION

5.1 Abstract

1,4-Dioxane was commonly used as a stabilizer in 1,1,1-trichloroethane formulations and is now frequently detected at sites where chlorinated solvents are present. A major challenge in addressing 1,4-dioxane contamination concerns chemical characteristics that result in migration and persistence. The objectives of this study were to 1) examine the effectiveness of yeast extract in supporting growth and prompting 1,4-dioxane biodegradation in mixed microbial communities at low 1,4-dioxane concentrations, 2) identify phylotypes that may utilize 1,4-dioxane and/or metabolites to support growth and 3) evaluate the impact of bioaugmentation with agricultural soil microorganisms on 1,4-dioxane removal rates in impacted site sediments. For this, 1,4-dioxane biodegradation was examined in microcosms amended with sediment from three impacted sites and four agricultural soils. 1,4-Dioxane biodegradation trends differed between inocula sources and treatments. Amending microcosms with basal salts medium (BSM) and yeast extract improved 1,4-dioxane biodegradation rates in sediment with indigenous 1,4-dioxane degraders. 1,4-Dioxane biodegradation did not occur in two of the three impacted sites studied, suggesting an absence of degraders at these sites. Bioaugmentation with agricultural soils led to 1,4-dioxane biodegradation in the impacted site sediments lacking 1,4-dioxane degraders. Differentially abundant phylotypes were determined via DESeq2 analysis by comparing live sample microcosms and live controls (no 1,4-dioxane) and included those previously associated with 1,4-dioxane biodegradation (*Rhodococcus*, *Rhizobiales*, *Gemmatimonas*, *Flavobacterium* and *Chitinophagaceae*). PICRUSt2 analysis indicated a group

of enriched phylotypes were also associated with ammonia/particulate monooxygenase and propane monooxygenase subunits. Notably, Rhodococcus was associated with methane/ammonia degradation exclusively in the three treatments containing BSM, and with propane monooxygenase subunits only in the treatments containing both BSM and yeast extract in Site 1 sediment microcosms. These findings suggest that Rhodococcus may contribute to 1,4-dioxane degradation via cometabolism. Overall, the results indicate yeast extract and BSM may be beneficial for promoting 1,4-dioxane biodegradation at sites with indigenous 1,4-dioxane degradations. Further, at sites without 1,4-dioxane degraders, bioaugmentation with agricultural soil microorganisms may represent a feasible remediation strategy.

5.2 Introduction

1,4-Dioxane, a synthetic cyclic ether, was utilized as a stabilizer and is commonly detected at sites contaminated with chlorinated solvents (Derosa, Wilbur et al. 1996, USEPA 2013, Dang, Kanitkar et al. 2018, Mohr, DiGuiseppi et al. 2020). The US Environmental Protection Agency (USEPA) has classified 1,4-dioxane as a likely human carcinogen and established a health advisory level of 0.35 μg/L in drinking water based on a one-in-one million cancer risk assessment (USEPA 2013). Due to its high solubility and mobility in water (low Henry's law constant, low K_{ow} and low K_{oc}) (USEPA 2013), 1,4-dioxane is widespread in surface water and groundwater worldwide (USEPA 2013, Stepien, Diehl et al. 2014, Sun, Lopez-Velandia et al. 2016, Adamson, Piña et al. 2017), making it a challenging contaminant to remediate. Traditional technologies such as air stripping, thermal desorption, and soil vapor extraction have been less effective for 1,4-dioxane remediation (Chiang, Anderson et al. 2016, Mohr, DiGuiseppi et al. 2020) Alternative strategies for remediating 1,4-dioxane-impacted sites include advanced oxidation processes (Barndõk, Merayo et al. 2016, Ikehata, Wang-Staley et al.

2016), phytoremediation (Aitchison, Kelley et al. 2000, Kelley, Aitchison et al. 2001) and microbial remediation (Mahendra and Alvarez-Cohen 2006, Sei, Oyama et al. 2013).

Both metabolic and co-metabolic 1,4-dioxane biodegradation have been reported. Numerous metabolic 1,4-dioxane degraders can utilize 1,4-dioxane as a sole source of carbon and energy to support growth (Mahendra and Alvarez-Cohen 2006, Kim, Jeon et al. 2009, Huang, Shen et al. 2014, Pugazhendi, Rajesh Banu et al. 2015, Chen, Jin et al. 2016, Yamamoto, Saito et al. 2018). Metabolic strains, such as *Pseudonocardia dioxanivorans* CB1190 and *Mycobacterium* sp. PH-06, are known for their ability to mineralize 1,4-dioxane and avoid the accumulation of harmful byproducts (Mahendra, Petzold et al. 2007, Kim, Jeon et al. 2009). However, half-saturation Monod constants (Ks) of metabolic degraders are typically high and their growth can be slow unless at very high 1,4-dioxane concentrations (>100 mg/L) (Mahendra and Alvarez-Cohen 2006, Kim, Jeon et al. 2009, Chen, Jin et al. 2016). Consequently, metabolic degraders may not be able to grow effectively or degrade 1,4-dioxane at environmental relevant low concentrations, as the available carbon substrates may be insufficient for growth and enzyme induction (Barajas-Rodriguez and Freedman 2018).

Other strains can degrade 1,4-dioxane co-metabolically while growing on other carbon substrates (e.g., propane, toluene and tetrahydrofuran) to induce enzymes (Kohlweyer, Thiemer et al. 2000, Vainberg, McClay et al. 2006, Yao, Lv et al. 2009, Hand, Wang et al. 2015, Lippincott, Streger et al. 2015). Co-metabolic degraders, which generate metabolic energy from other primary substrates (i.e., propane), may perform better at low 1,4-dioxane concentrations.

Most 1,4-dioxane-contaminated plumes are below 1000 μg/L (Adamson, Mahendra et al. 2014, Gedalanga, Madison et al. 2016). However, the majority of research on 1,4-dioxane biodegradation by metabolic strains has been conducted at higher concentrations (Huang, Shen

et al. 2014, Pugazhendi, Rajesh Banu et al. 2015, Chen, Jin et al. 2016, Inoue, Tsunoda et al. 2016, Yamamoto, Saito et al. 2018). There are limited metabolic studies conducted at μg/L concentrations (He, Mathieu et al. 2018, Simmer, Richards et al. 2021). *Mycobacterium* sp. PH-06, *Pseudonocardia* sp. CB1190 and two microbial consortia (with *Mycobacterium* as the dominant genus) degraded 300 μg/L 1,4-dioxane to below 5 μg/L when bioaugmented into groundwater from a dioxane-impacted site (He, Mathieu et al. 2018). In another study, rapid metabolic 1,4-dioxane degradation was observed for *Rhodococcus ruber* strain 219, which degraded ~100 μg/L 1,4-dioxane to < 0.35 μg/L when supplied with thiamine (vitamin B1) (Simmer, Richards et al. 2021).

Several studies reported co-metabolic 1,4-dioxane degradation at environmentally relevant concentrations (Lippincott, Streger et al. 2015, Chu, Bennett et al. 2018, Li, Deng et al. 2021). *Azoarcus* sp. DD4 co-metabolically degraded 1,4-dioxane from 20 μg/L to below 0.4 μg/L when supplemented with propane (Li, Deng et al. 2021). One field study reported indigenous microbial populations in the groundwater achieved 1,4-dioxane removal from 60 μg/L to below 3 μg/L when stimulated with propane and oxygen (Chu, Bennett et al. 2018). Another field study demonstrated that bioaugmentation with propanotroph *Rhodococcus ruber* ENV425, induced by propane amendment, can reduce low levels of 1,4-dioxane in a deep aquifer (Lippincott, Streger et al. 2015). However, some inducing substrate (i.e., tetrahydrofuran) at high concentrations may increase the lag period for 1,4-dioxane removal due to competitive inhibition (Li, Liu et al. 2017).

Contaminated sites have demonstrated intrinsic 1,4-dioxane biodegradation potential (Chiang, Mora et al. 2012, Li, Mathieu et al. 2013, Li, Mathieu et al. 2014, Li, Van Orden et al. 2015, Gedalanga, Madison et al. 2016, Li, Liu et al. 2017). Various 1,4-dioxane-degrading

monooxygenase genes were detected in Arctic groundwater impacted by 1,4-dioxane (Li, Mathieu et al. 2013, Li, Mathieu et al. 2014). Moreover, microcosms prepared with the source zone groundwater demonstrated 1,4-dioxane degradation at a rate of 13 μg/L per week with initial concentrations of approximately 250 μg/L (Li, Mathieu et al. 2013). In comparison, unamended microcosms prepared with soils and groundwater samples from the same site were able to degrade 1,4-dioxane at a rate of 9.8 μg/L per week with an initial concentration of 500 μg/L (Li, Fiorenza et al. 2010). Even at an initial concentration as low as 7.5 μg/L, complete 1,4-dioxane degradation was achieved at a rate of 0.3 μg/L per week in the microcosms inoculated with contaminated groundwater and aquifer materials (Li, Van Orden et al. 2015).

1,4-Dioxane-degrading bacteria with natural attenuation capacities widely exist in uncontaminated soils and thus offer potential for 1,4-dioxane remediation (He, Mathieu et al. 2018, Ramalingam and Cupples 2020, Dang and Cupples 2021, Tang, Wang et al. 2023). For instance, two 1,4-dioxane-degrading bacteria consortia enriched from uncontaminated garden soils removed 1,4-dioxane from 300 μg/L to below 5 μg/L within three days in impacted groundwater without known intrinsic biodegradation potential (He, Mathieu et al. 2018). In another enrichment study using uncontaminated garden soils, three consecutive doses of 300 μg/L of 1,4-dioxane were quickly degraded to below 80 μg/L within three days (Tang, Wang et al. 2023).

Metabolic degradation of 1,4-dioxane at low concentrations by thiamine-grown *Rhodococcus* ruber 219 suggests that *in situ* biostimulation with growth supplements might reduce 1,4-dioxane to health advisory levels (Simmer, Richards et al. 2021). As yeast extract contains multiple growth factors (amino acids, peptides, and water-soluble vitamins, and carbohydrates), various microorganisms involved in 1,4-dioxane biodegradation could

potentially benefit. Previous studies applied yeast extract to enhance 1,4-dioxane degradation at high concentrations (100 mg/L) by pure cultures of metabolic strains *Rhodanobacter* AYS5 and *Xanthobacter flavus* DT8 (Pugazhendi, Rajesh Banu et al. 2015, Chen, Jin et al. 2016). Another study discovered that the amendment of basal salts medium (BSM) and yeast extract significantly enhanced the 1,4-dioxane degradation (2 mg/L) in the mixed communities from impacted site sediments and agricultural soils (manuscript in progress, Li et al.). However, little is known about the impact of yeast on the 1,4-dioxane degradation at low concentrations (<500 μg/L), especially in mixed microbial communities. To fill the knowledge gap, the objectives of this study were to 1) examine the impact of varying concentrations of yeast extract on biodegradation kinetics of 1,4-dioxane at low concentrations in mixed microbial communities; 2) investigate the phylotypes deriving a growth benefit from the 1,4-dioxane of low concentration of 1,4-dioxane and 3) examine the impact of bioaugmentation with agricultural soil microorganisms on 1,4-dioxane removal rates in site sediments.

5.3 Methods

5.3.1 Chemicals and Inocula

1,4-Dioxane (≥99.5%) and 1,4-dioxane-d_8 (≥99% isotopic purity) were purchased from Sigma-Aldrich (MO, USA) and Santa Cruz Biotechnology (TX, USA), respectively. Sediments from three contaminated sites and soils from four agricultural systems were utilized to inoculate microcosms. This included sediments from an impacted site at a West Coast Naval Station in California (herein called Site 1), sediments from a site contaminated with tetrachloroethene, trichloroethylene, 1,4-dioxane and hexavalent chromium from a former latex product manufacturing facility in California (herein called Site 2), sediments from a low pH site in New Jersey (herein called Site 3) and agricultural soils from Main Cropping System Experiment at the

Kellogg Biological Station Long-Term Ecological Research (KBS LTER) in southwest Michigan. The agricultural soils were collected from six replicate plots for four treatments (referred to as Soil 1, Soil 2, Soil 3 and Soil 4). The Soil 1 and Soil 2 receive conventional levels of chemical inputs, but with chisel plow and no-till management, respectively. The Soil 3 receives reduced chemical input and the Soil 4 receives no chemical inputs. More details of the agricultural soils can be found at https://lter.kbs.msu.edu/research/long-term-experiments/main-cropping-system-experiment/. Remediation of Site 2 included In Situ Chemical Oxidation followed by Enhanced Reductive Dechlorination (ERD), using molasses and emulsified vegetable oil. As a result of ERD, it was likely the sediments from Site 2 were anaerobic. Due to privacy concerns, no other information is available on the other sites.

5.3.2 Microcosms Setup

To investigate the impact of yeast extract on 1,4-dioxane degradation, a series of experiments were performed as summarized in Table 5.1. The initial experiment involved a higher concentration of 1,4-dioxane (2 mg/L), 10 g wet-weight sediments from site 1 and 30 mL of liquid (160 mL serum bottles). The liquid amendments included water with 300 μg/L yeast extract (Sigma-Aldrich, USA), BSM only and BSM with 300 μg/L yeast extract. The BSM contained NH_4Cl (1.0 g/L), K_2HPO_4 (3.24 g/L), NaH_2PO_4 (1.0 g/L), $MgSO_4$ (0.20 g/L), $FeSO_4$ (0.012 g/L), $MnSO_4$ (0.003 g/L), $ZnSO_4$ (0.003 g/L) and $CoCl_2$ (0.001 g/L) and was adjusted to 7.4 with 0.1N NaOH, modified from a previous recipe (Pugazhendi, Rajesh Banu et al. 2015).

All other microcosm studies were established to evaluate 1,4-dioxane degradation with low initial concentrations. For each inoculum, the experimental design included triplicate live microcosms, triplicate abiotic control microcosms and triplicate live control microcosms. The abiotic controls were autoclaved daily for three consecutive days. Live controls were also

included to evaluate changes in microbial communities with and without 1,4-dioxane. The live controls were treated in the same manner as live microcosms except no 1,4-dioxane was added.

The first experiment involved 10 g wet-weight sediments from Site 1 and Site 2 suspended in 30 mL of water or media in 160 mL serum bottles. The amendments examined included water, BSM, BSM with 100 μg/L yeast extract and BSM with 1000 μg/L yeast extract (Sigma-Aldrich, USA) with approximately 50 μg/L, 100 μg/L or 500 μg/L 1,4-dioxane. The second experiment involved soil microcosms with 10 g wet-weight sediments from site 2 and site 3 as well as 30 mL of liquid in 160 mL serum bottles. The amendments included water, BSM with 100 μg/L yeast extract and BSM with 1000 μg/L yeast extract with approximately 50 μg/L 1,4-dioxane.

The third low 1,4-dioxane concentration experiment was designed to evaluate the impact of bioaugmentation with agricultural soil microorganisms on 1,4-dioxane biodegradation in site sediments. Sediment from Site 2 was selected for this because no removal was noted in the Site 2 microcosms described above. This involved soil microcosms with 5 g wet-weight sediments from Site 2 inoculated with 5 g wet-weight soils from Soil 1, Soil 2 or Soil 3, and 30 mL of water or media in 160 mL serum bottles. Two amendments examined included water and BSM with 1000 μg/L yeast extract with approximately 50 μg/L 1,4-dioxane.

5.3.3 1,4-Dioxane Analysis

1,4-Dioxane concentrations were measured by a triple quadrupole Agilent 7010B GC/MS system (Agilent Technologies, CA, USA) equipped with solid phase micro extraction (SPME) (Sigma-Aldrich, MO, USA). Each sample was collected by extracting 1 mL from the liquid phase using a 3 mL sterile syringe and 22 Ga 1.5 in. needle. The extracted samples were then filtered through 0.22 μm nylon filters (Biomed Scientific). An aliquot (500 μL) of the filtered

samples or series of diluted external standards were injected into 40 mL amber glass vials. Also, 500 μL of 200 μg/L 1,4-dioxane-d_8 was added to each vial as an internal standard for subsequent GC/MS analysis. The vials were kept at 40°C before the analysis, with the SPME fiber conditioned at 270 °C for 30 mins before each sequence run. For each sample, the SPME fiber was inserted into the vials and exposed to the analytes for 2 mins. The analytes in the headspace adsorbed onto the fiber and then the fiber was exposed to the inlet. Initially, the oven temperature time was set at 40 °C for 4 mins, followed by a programmed increase to 250 °C at a rate of 40 °C/min. The detection limit was approximately 1 μg/L.

5.3.4 DNA Extraction, 16S rRNA Gene Sequencing and Microbial Analysis

DNA was extracted from the live sample microcosms and live control microcosms using the DNA extraction kit (DNeasy PowerLyzer PowerSoil Kit, Qiagen, USA) as per the manual protocol. The DNA concentrations were quantified using the Quant-iT™ dsDNA High-Sensitivity Assay Kit. Then DNA extracts were submitted for 16S rRNA gene amplicon sequencing to the Genomic Cores at the Research Technology Support Facility (RTSF) at Michigan State University (MSU). The V4 region of the 16S rRNA gene was targeted for amplification using primers 515f (5' GTGCCAGCMGCCGCGGTAA-3') and 806r (5'-GGACTACHVGGGTWTCTAAT-3') following a previous protocol (Kozich, Westcott et al. 2013). The PCR products were normalized using Invitrogen SequalPrep DNA Normalization plates, followed by pooling of the normalized products. The pool was then cleaned and concentrated using AmpureXP magnetic beads. Quality control (QC) and quantification were performed using a combination of Qubit dsDNA HS for concentration, Agilent 4200 TapeStation HS DNA1000 for sizing, and Kapa Illumina Library Quantification qPCR assays. The pooled library was loaded onto an Illumina MiSeq v2 standard flow cell for sequencing, using a 2 × 250

bp paired-end format with a MiSeq v2 500-cycle reagent cartridge. Custom sequencing and index primers were added to the appropriate wells of the reagent cartridge. Base calling was carried out with Illumina Real Time Analysis (RTA) v1.18.54, and the RTA output was demultiplexed and converted into FastQ format using Illumina Bcl2fastq v2.19.1. The raw sequences were submitted to NCBI under Bioproject PRJNA1183415, with accession numbers SAMN44626197 to SAMN44626290.

Raw amplicon sequences in fastq format were processed using Mothur (Schloss, Westcott et al. 2009) using the Mothur Miseq SOP (accessed July 2024) on the High-Performance Computing Cluster (HPCC) at MSU. This process included combining, trimming, aligning, and quality-controlling the sequences. For alignments, the SILVA bacteria database (Release 138.2) specific to the V4 region was used (Pruesse, Quast et al. 2007). Sequences was then be classified into operational taxonomic units (OTUs) at 97% similarity. The classification of OTUs into taxonomic levels and downstream analysis were performed using the shared and taxonomy files generated by Mothur, with R (Version 4.4.1) (R Core Team 2018) in RStudio (Version 2024.09.0) (RStudio_Team 2020). The differentially abundant taxa between the samples and live controls were determined by the Wald test coupled with a parametric model using the R packages DESeq2 (Love, Huber et al. 2014) and microbiome (version 1.26.0) (Lahti and Shetty 2012-2019). The packages phyloseq (version 1.48.0) (McMurdie and Holmes 2013) and microbiome (version 1.26.0) (Lahti and Shetty 2012-2019) were used to determine the relative abundance at the phyla level in the soil microcosms.

5.3.5 PICRUSt2 Monooxygenase Gene Predictions

PICRUSt2 (Douglas, Maffei et al. 2020) was employed to predict the functional potential of microbial communities from 16S rRNA gene sequencing data. Input files for PICRUSt2

included a fasta file and a biom file. The analysis incorporated EPA-NG (Barbera, Kozlov et al. 2019) and gappa (Czech, Barbera et al. 2020) for the phylogenetic placement of reads, castor (Louca and Doebeli 2018) for hidden state prediction and MinPath (Ye and Doak 2009) for pathway inference. The PICRUSt2 generated files (pred_metagenome_contrib.tsv and pred_metagenome_contrib.tsv) were investigated (primarily using the R packages tidyr and dplyr) to identify the genes associated with monooxygenases (from the KEGG database (Kanehisa 2002)) as well as the phylotypes associated with each. More information on the data within each file can be found in the following tutorial (https://github.com/picrust/picrust2/wiki/PICRUSt2-Tutorial-(v2.5.0)). Functional genes investigated (KEGG number in parenthesis) included: *prmA* propane 2-monooxygenase large subunit (K18223), *prmB* propane monooxygenase reductase component (K18225), *prmC* propane 2-monooxygenase small subunit (K18224), *prmD* (K18226) propane monooxygenase coupling protein, *pmoA-amoA* methane/ammonia monooxygenase subunit A (K10944), *pmoB-amoB* methane/ammonia monooxygenase subunit B (K10945), *pmoC-amoC* methane/ammonia monooxygenase subunit C (K10946), *tmoA, tbuA1, touA* toluene monooxygenase system protein A (K15760), *tmoB, tbuU, touB* toluene monooxygenase system protein B (K15761), *tmoC, tbuB, touC* toluene monooxygenase system ferredoxin subunit (K15762), *tmoD, tbuV, touD* toluene monooxygenase system protein D (K15763), *tmoE, tbuA2, touE* toluene monooxygenase system protein E (K15764) and *tmoF, tbuC, touF* toluene monooxygenase electron transfer component (K15765).

RStudio on the HPCC at MSU was used to generate a file that contained which gene subunits and phylotypes were present using the PICRUSt2 output file pred_metagenome_contrib.tsv (unzipped). The approach involved combining this file with 1) a

file containing gene numbers and descriptions and 2) a taxonomy file (from Mothur), using the R packages data.table (version 1.16.2) (Dowle and Srinivasan 2023), dplyr (version 1.1.4) (Wickham, Francois et al. 2023), tidyr (version 1.3.1) (Wickham, Vaughan et al. 2023), ggplot2 (version 3.5.1) (Wickham 2016) and patchwork (version 1.3.0) (Pedersen 2023). Bar charts were generated for each monooxygenase, faceted by the sample type and the gene subunits.

5.4 Results

5.4.1 1,4-Dioxane Biodegradation rates

1,4-Dioxane degradation rates with an initial concentration of 2 mg/L were investigated in the Site 1 microcosms (Figure A5.1). A two-phase degradation pattern was observed in all three treatments, with an initial lag phase followed by a rapid decline. During the lag phase, the 1,4-dioxane removal rates were notably faster in the treatment of BSM and yeast extract compared to treatments of water and yeast extract or BSM only. This trend suggests the amendment of BSM and yeast extract may provide sufficient growth substrates for the microbial population, thus initiating the 1,4-dioxane degradation in a shorter time.

The potential of 1,4-dioxane degradation at low concentrations (100 μg/L) was further evaluated with microcosms inoculated with Site 1 sediment (Figure 5.1). 1,4-Dioxane removal rates have been summarized in Table 5.2. The BSM and yeast extract treatments resulted in higher 1,4-dioxane biodegradation rates (0.23 ± 0.10 μg/L per day for BSM/100 μg/L yeast extract, 0.32 ± 0.02 μg/L per day for BSM/1000 yeast extract μg/L) (Figure 5.2C and D), compared to the water only (0.13 ± 0.03 μg/L per day) treatment (Figure 5.2A) or the BSM only treatment (0.14 ± 0.01 μg/L per day) (Figure 5.2B). Also, there was no significant difference in biodegradation rates between the water treatment and the BSM only treatment, indicating that BSM alone does not improve 1,4-dioxane removal.

1,4-Dioxane biodegradation was also evaluated at two other concentrations (~50 µg/L and ~500 µg/L) for Site 1 sediment inoculated microcosms (Figures 5.3 & 5.4). At ~50 µg/L, the BSM and yeast extract treatments resulted in higher 1,4-dioxane biodegradation rates (0.22 ± 0.003 µg/L per day for BSM/100 µg/L yeast extract, 0.2 ± 0.02 µg/L per day for BSM/1000 yeast extract µg/L) (Figure 5.3B and C), compared to the water only (0.08 ± 0.03 µg/L per day) (Figure 3A). At ~500 µg/L, the BSM and yeast extract treatments resulted in higher 1,4-dioxane biodegradation rates (1.1 ± 0.16 µg/L per day for BSM/100 µg/L yeast extract, 1.16 ± 0.34 µg/L per day for BSM/1000 yeast extract µg/L) (Figure 5.3B and C), compared to the water only (0.19 ± 0.13 µg/L per day) (Figure 5.3A). The amendment of BSM and yeast extract was also reported to significantly accelerate the 1,4-dioxane degradation rates in the microcosms inoculated with Site 1 sediments and Soil 4 at ~2 mg/L 1,4-dioxane (Li and Cupples 2024). As shown in Table 5.2, 1,4-dioxane degradation rates greatly increased with increasing initial concentrations for site 1 sediments. The 1,4-dioxane degradation rates at ~2 mg/L were more than one order of magnitude lower than those observed at low concentrations for Site 1 sediments and Soil 4.

The biodegradation of 1,4-dioxane was also evaluated at concentrations of ~50 µg/L, ~100 µg/L, and ~500 µg/L in Site 2 microcosms (Figures A5.2 & A5.3) and at ~50 µg/L in Site 3 microcosms (Figure A5.4). No degradation was observed in any of the treatments for these sites, indicating a lack of intrinsic degradation capabilities. In contrast to the results from the microcosms inoculated with Site 2 and Site 3 sediments, the microcosms inoculated with Soil 4 illustrated 1,4-dioxane biodegradation. In the Soil 4 microcosms, 1,4-dioxane at ~50 µg/L degraded in all treatments (Figure A5.5), As shown in Table 5.2, Soil 4 exhibited higher degradation rates than those noted in the Site 1 microcosms with the same 1,4-dioxane concentration and amendment.

Table 5.1 Soil microcosm treatments spiked with dioxane of different concentrations.

Experiment	Soil type	Initial 1,4-dioxane concentrations (μg/L)	Treatments
Initial	Site 1	2000	Water/yeast extract 300 μg/L BSM/yeast extract 300 μg/L Only BSM
1st experiment	Site 1	50, 100, 500	Water BSM BSM/yeast extract 100 μg/L BSM/yeast extract 1000 μg/L
	Site 2	50, 100, 500	
2nd experiment	Site 3	50	Water BSM BSM/yeast extract 100 μg/L BSM/yeast extract 1000 μg/L
	T4	50	
3rd experiment	Site 2/T1	50	Water BSM/yeast extract 1000 μg/L
	Site 2/T2	50	
	Site 2/T3	50	

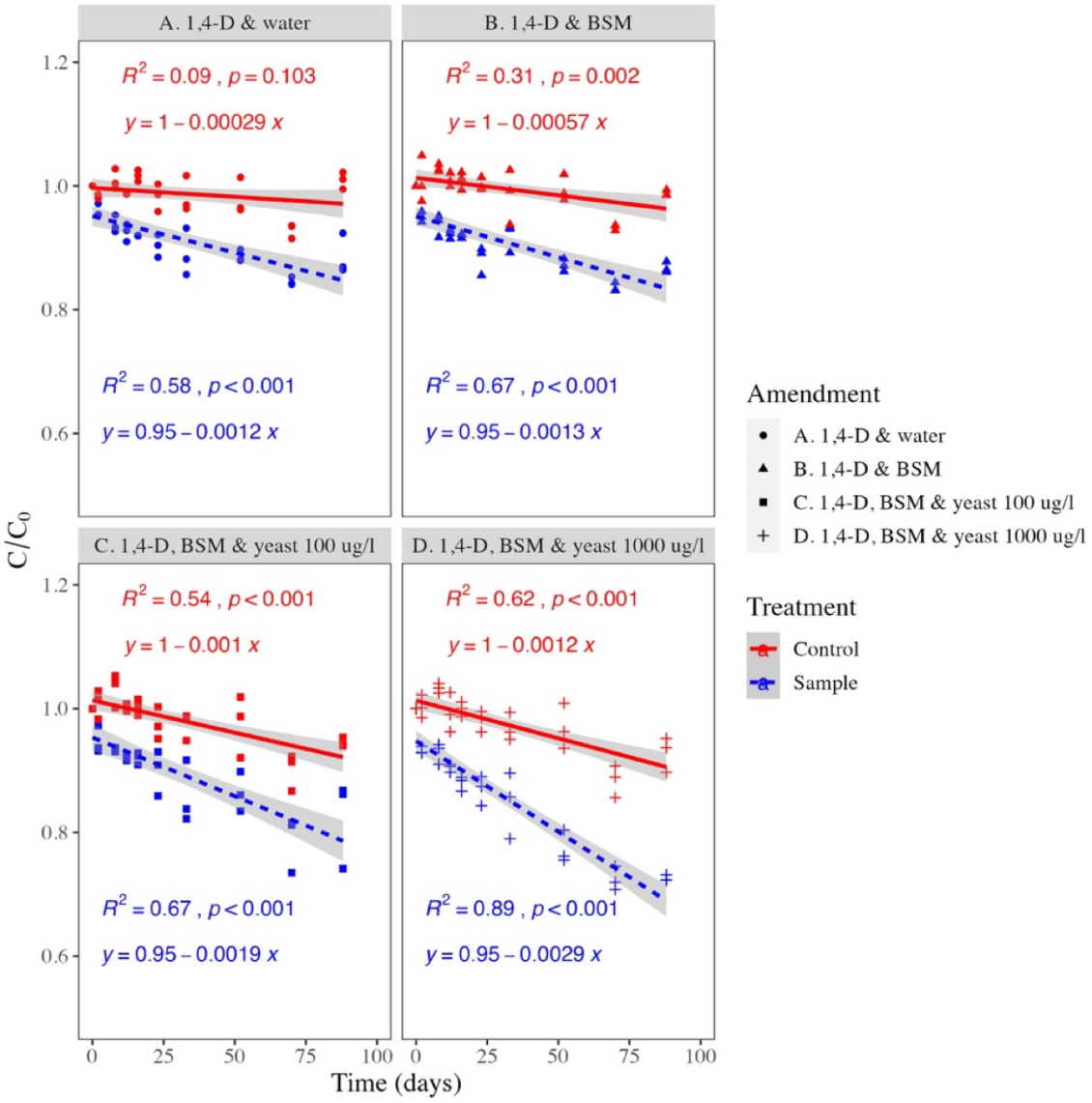

Figure 5.1 1,4-Dioxane concentrations over time in microcosms inoculated with Site 1 sediments with four treatments. The initial concentration was approximately 100 µg/L 1,4-dioxane.

Sediments from Site 2 were used to investigate the feasibility of 1,4-dioxane remediation by bioaugmentation with agricultural soils. As discussed above, no 1,4-dioxane biodegradation was observed in microcosms amended with Site 2 sediment. In contrast, when Site 2 sediment was mixed with different agricultural soils, biodegradation was observed. At ~50 μg/L, Site 2 sediments demonstrated 1,4-dioxane biodegradation inoculated with Soil 1, Soil 2 and Soil 3 (Figure 5.3). The mixed soil microcosms resulted in approximately half of the degradation rates compared to microcosms with Soil 4 (Table 5.2). This suggests that the 1,4-dioxane degraders in the agricultural soils can adapt to the mixed soil environments and further enhance the 1,4-dioxane degradation at low levels.

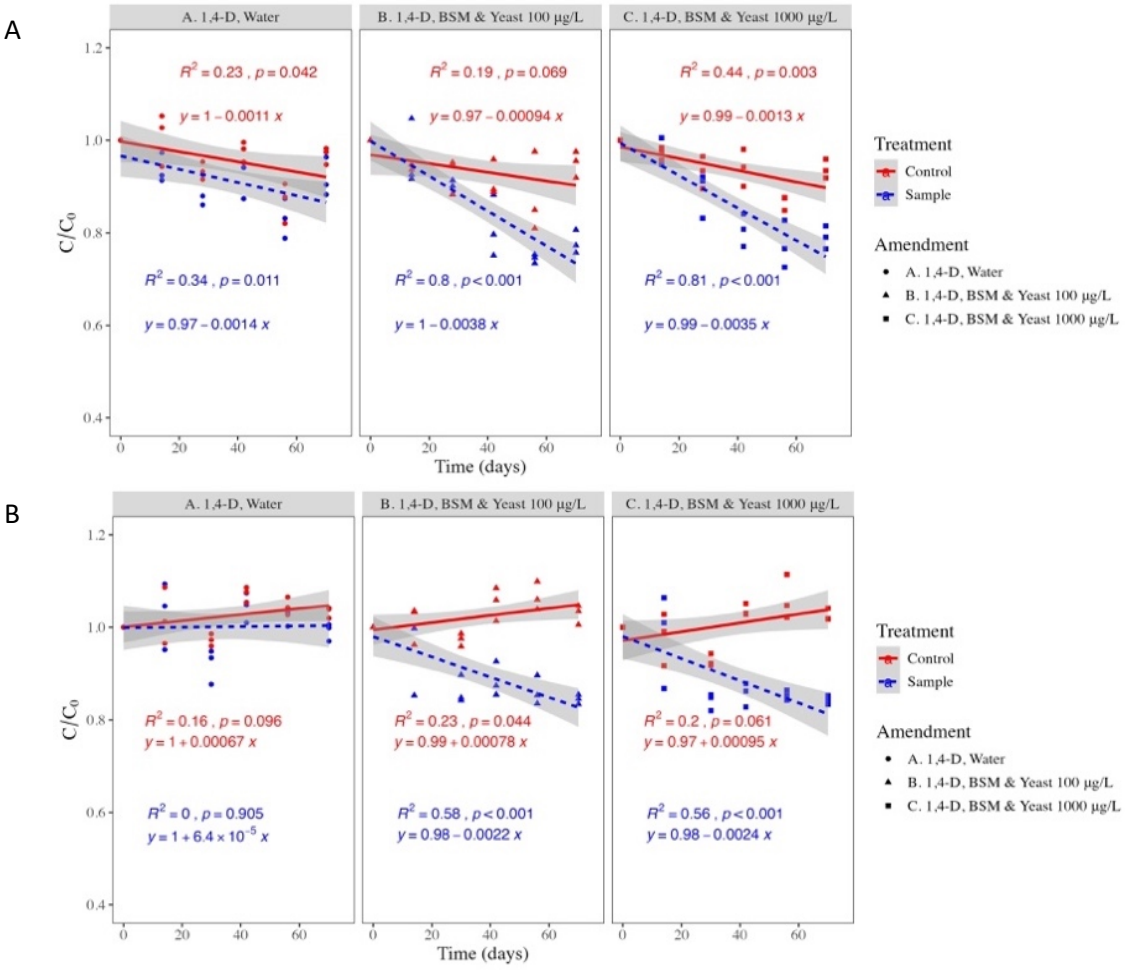

Figure 5.2 1,4-Dioxane concentrations over time (C/C_0) in microcosms inoculated with Site 1 sediments, three treatments and two initial 1,4-dioxane concentrations (approximately 50 µg/L (A) and approximately 500 µg/L 1,4-dioxane (B)).

Table 5.2 Removal rates (µg/L per day) for 1,4-dioxane biodegradation.

Soil type	Initial 1,4-dioxane concentration (µg/L)	Treatments					References
		Water	BSM	BSM/yeast extract 100 µg/L	BSM/yeast extract 1000 µg/L	BSM/yeast extract 60 µg/L	
Site 1	50	0.08± 0.03	-	0.22± 0.003	0.2± 0.02	-	This study
Site 1	100	0.13± 0.03	0.14± 0.01	0.23± 0.08	0.32± 0.02	-	This study
Site 1	500	0.19± 0.13	-	1.1± 0.16	1.16± 0.34	-	This study
T4	50	0.93± 0.04	0.84± 0.04	0.87± 0.02	0.78± 0.05	-	This study
Site 2/T1	50	0.44± 0.01	-	-	0.49± 0.02	-	This study
Site 2/T2	50	0.46± 0.03	-	-	0.45± 0.02	-	This study
Site 2/T3	50	0.5± 0.09	-	-	0.51± 0.07	-	This study
Site 1	2000	8.42± 1.68	-	-	-	14.91± 2.87	(Li and Cupples 2024)
T4	2000	12.69± 0.12	-	-	-	15.76± 1.27	(Li and Cupples 2024)
Wetland	2000	13.83± 2.33	-	-	-	20.4± 2.52	(Li and Cupples 2024)

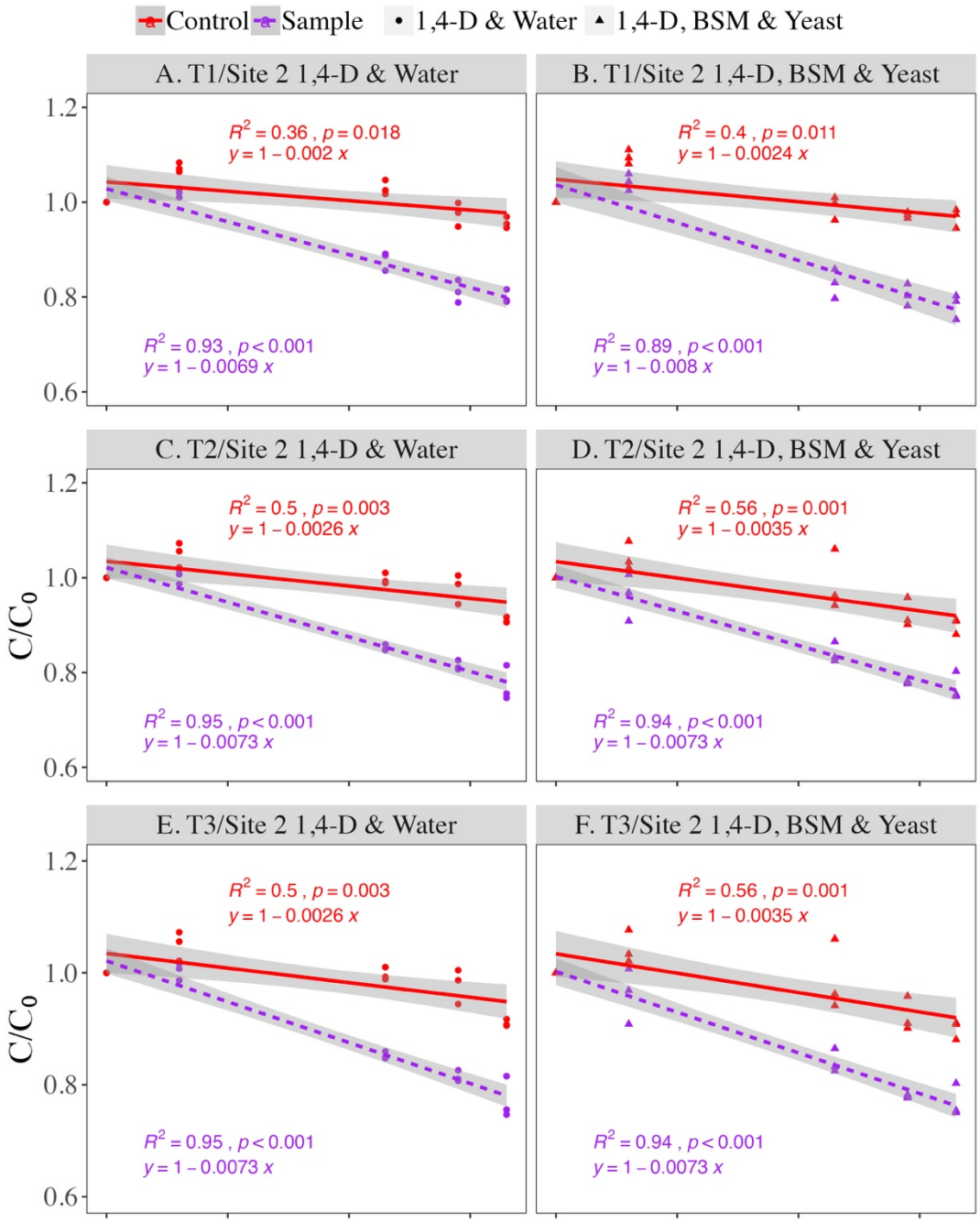

Figure 5.3 1,4-Dioxane concentrations over time in microcosms inoculated with agricultural soils T1 (A, B), T2 (C, D) and T3 (E, F) with two treatments. The initial concentration was approximately 50 µg/L 1,4-dioxane.

5.4.2 Microbial Community Analyses

The composition of microbial communities in soil microcosms was characterized at the phylum level across various treatment conditions (Figure A5.6). For Site 1 sediment microcosms, *Proteobacteria* represented over 75% of the community in the water treatment, while alternative phyla were more prominent in treatments with BSM (Figure A5.6A). Notably, *Proteobacteria* and *Nitrospira* dominated in the treatment with BSM and 1000 μg/L yeast extract. For the soil microcosms, *Proteobacteria* was more enriched in the treatment with BSM and yeast extract compared to that in water treatment (Figure A5.6B). For the agricultural soil microcosms mixed with Site 2 sediments, *Acidobacteria* and *Verrucomicrobia* were more abundant in the water treatment compared to the treatment with BSM and yeast extract.

To further elucidate differential abundances between samples and live controls (without 1,4-dioxane), DESeq analysis was conducted to determine significantly differentiated phylotypes (p<0.05) (Figures 5.4–5.6, Figures A5.7–A5.11). A group of phylotypes were enriched in Site 1 microcosms amended with 1,4-dioxane compared to the live controls (no 1,4-dioxane). At a concentration of ~100 μg/L, samples of Site 1 sediment microcosms displayed a significant enrichment of phylotypes from *Proteobacteria*, *Actinobacteria*, and *Gemmatimonadetes*, including genera such as *Gemmatimonas*, *Hydrogenophaga*, *Phyllobacterium*, *Dietzia*, unclassified *Rhizobiales*, and *Rhodococcus* (Figure 5.4). At ~50 μg/L, enriched phylotypes in the samples included representatives from *Gemmatimonadetes*, *Actinobacteria*, *Firmicutes*, *Proteobacteria*, and *Bacteroidetes*, specifically *Gemmatimonas*, *Rhodococcus*, *Geobacillus*, *Streptococcus*, unclassified *Rhizobiales*, and *Flavobacterium* (Figure 5.5). At ~500 μg/L, *Geobacillus* (phylum *Firmicutes*) was significantly more abundant in Site 1 sediment sample microcosms compared to the live controls (Figure 5.6).

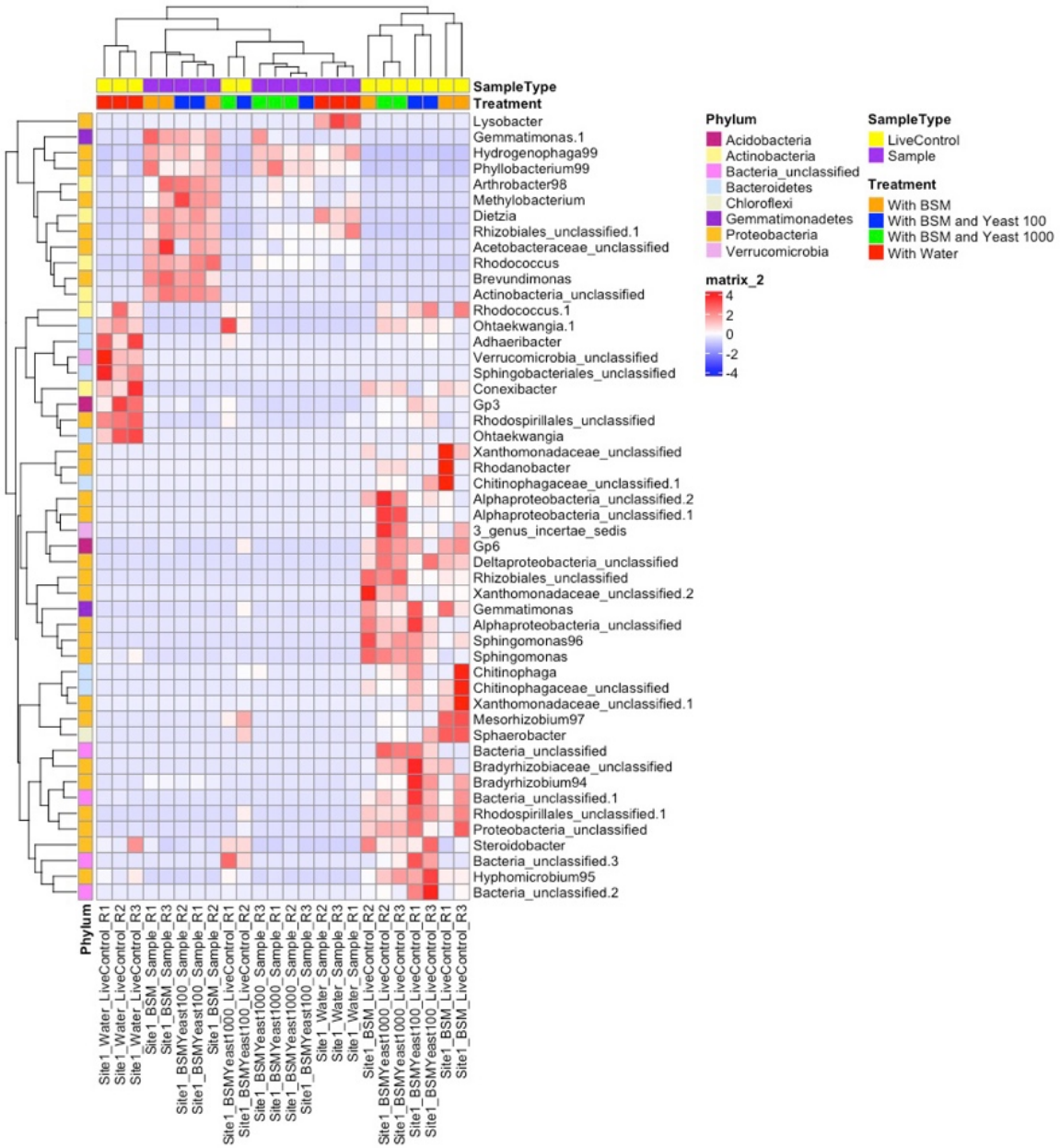

Figure 5.4 The top 50 differentially abundant taxa between the samples amended with 1,4-dioxane (100 µg/L) and the live controls (as determined by DESeq2 analysis) for Site 1 sediments microcosms.

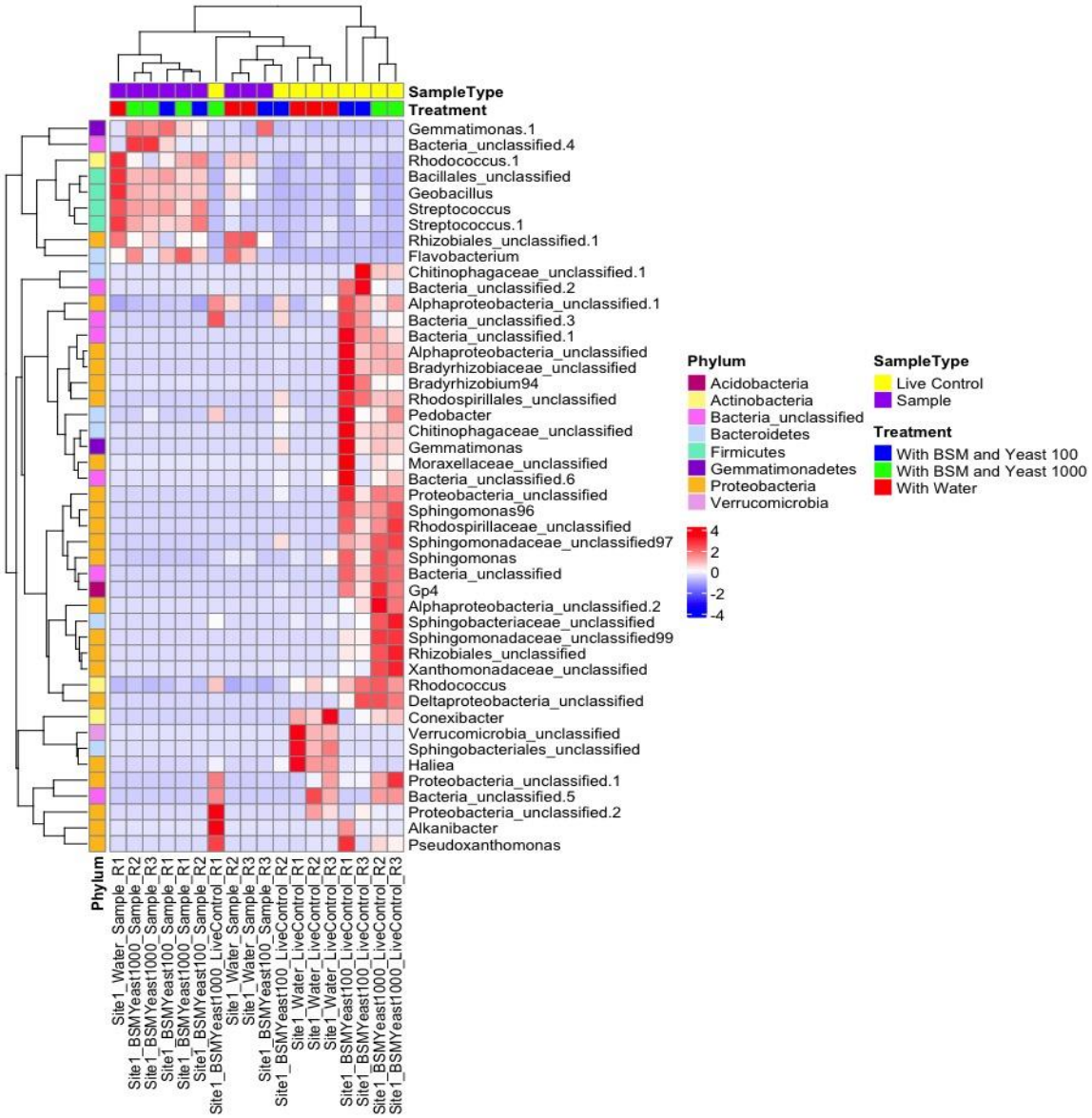

Figure 5.5 Differentially abundant taxa (46 in total) between the samples amended with 1,4-dioxane (50 µg/L) and the live controls (as determined by DESeq2 analysis) for Site 1 sediments microcosms.

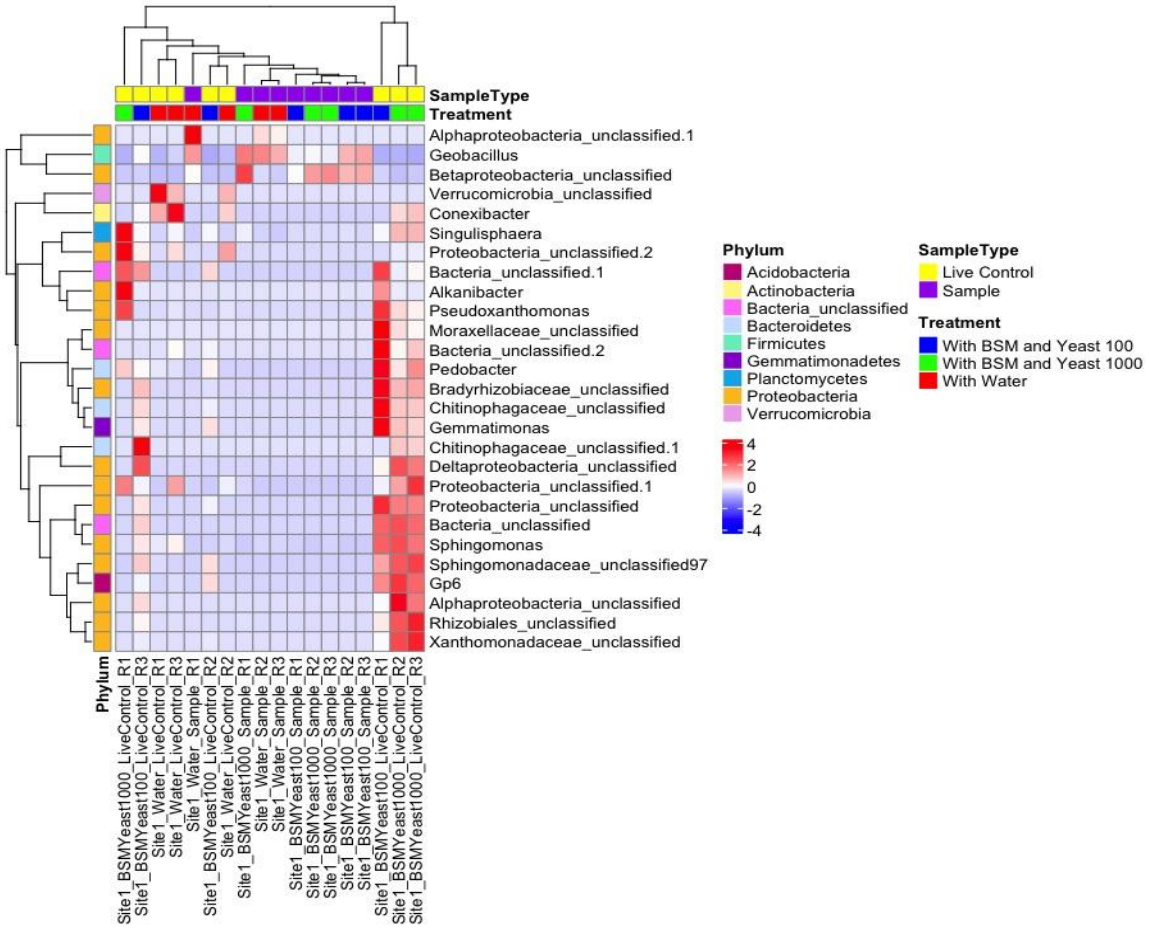

Figure 5.6 Differentially abundant taxa (27 in total) between the samples amended with 1,4-dioxane (500 µg/L) and the live controls (as determined by DESeq2 analysis) for Site 1 sediments microcosms.

In the agricultural soil microcosms, a limited number of phylotypes were significantly enriched in the samples compared to live controls (Figures A5.7-A5.11). Specifically, in Soil 2 microcosms inoculated with Site 2 sediments, the water treatment led to significant enrichment of unclassified *Chitinophagaceae* and unclassified *Bacteroidetes* in the samples compared to live controls (Figure A5.8). The treatment with BSM and yeast extract resulted in the enrichment of unclassified Bacteria, unclassified *Ktedonobacterales*, unclassified *Myxococcales* and *Gp*. For the Soil 3 microcosms inoculated with Site 2 sediments, unclassified *Chitinophagaceae*, unclassified *Bacteroidetes*, unclassified *Myxococcales* and unclassified *Bacteria* were differentially abundant in the water treatment compared to live controls (Figure A5.9). Due to the unsuccessful sequencing of one replicate, DESeq analysis was not performed for the samples treated with BSM and yeast extract in Soil 3 microcosms. For Soil 4 microcosms, enriched phylotypes in water treatment included unclassified *Alphaproteobacteria*, unclassified *Betaproteobacteria*, unclassified *Myxococcales*, unclassified *Chitinophagaceae*, *Nitrospira*, unclassified *Bacteroidetes*, unclassified *Firmicutes*, *3_genus_incertae* and unclassified *Bacteria* (Figure A5.10). In contrast, only unclassified *Bacteria* and unclassified *Gammaproteobacteria* were differentially abundant in the treatment of BSM and yeast extract (Figure A5.11).

5.4.3 Prediction of Monooxygenase Genes

PICRUSt2 predicted the enriched phylotypes (identified by DESeq analysis) associated with monooxygenase genes for the Site 1 and agricultural soil microcosms (Figure 5.7 and Figures A5.12-A5.16). A number of microorganisms were associated with monooxygenase genes in the different sample types. In the Site 1 sediment microcosms, dominant phylotypes associated with methane/ammonia monooxygenase subunits included unclassified *Rhizobiales*, unclassified *Betaproteobacteria* and unclassified *Bacteria* for all four treatments (Figure 5.7).

Notably, *Rhodococcus* was associated with methane/ammonia only in the three treatments with BSM. In the Site 1 sediment microcosms, unclassified *Acetobacteraceae* was the most abundant phylotype associated with propane monooxygenase subunits in all four treatments. Interestingly, *Rhodococcus* was found to be associated with propane subunits only in the treatments with BSM and yeast extract. The main phylotypes predicted to be associated with methane/ammonia monooxygenase subunits, including unclassified *Rhizobiales*, unclassified *Betaproteobacteria*, and unclassified *Bacteria*, showed higher abundance in samples compared to live controls (Figure A5.12).

In the Site 2 sediment and agricultural soil microcosms combined, most of the enriched phylotypes identified by DESeq analysis were predicted to be associated with methane/ammonia and propane monooxygenase subunits (Figures A5.13 &A5.14). In particular, *Nitrospira* exhibited higher abundances in water treatment compared to the treatment with BSM and yeast extract (Figures A5.13). Unclassified *Ktedonobacterales* were associated three subunits of propane monooxygenase (*prmA*, *prmB* and *prmC*) only in live samples compared to live controls. In addition, the relative abundance of enriched phylotypes associated with toluene monooxygenase subunits is also presented (Figures A5.15 &A5.16). Rare phylotypes were predicted to be associated with the monooxygenase genes in the untreated Site 2 sediment (Figures A5.12- A5.16).

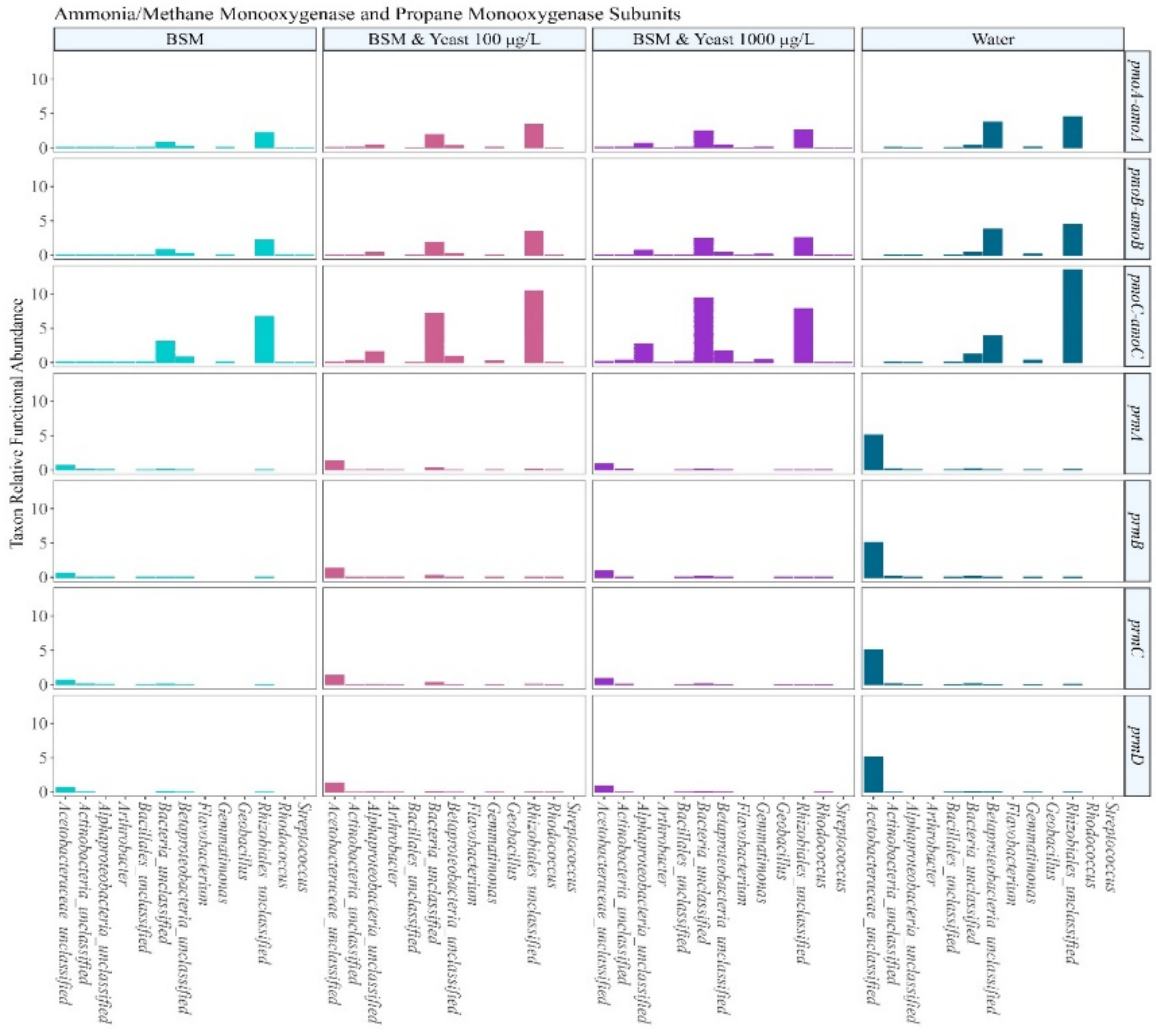

Figure 5.7 Relative abundance of enriched taxa (identified by DESeq analysis) associated with methane/ammonia monooxygenase subunits *pmoA-amoA* (K10944), *pmoB-amoB* (K10945) and *pmoC-amoC* (K10946) as well as taxa associated with all four propane monooxygenase subunits, *prmA* (K18223), *prmB* (K18225), *prmC* (K18224) and *prmD* (K18226) in the Site 1 sediment microcosms.

5.5 Discussion

This study examined the effectiveness of yeast extract for sustaining microbial growth and facilitating 1,4-dioxane biodegradation within mixed microbial communities at low 1,4-dioxane concentrations. Differentially enriched phylotypes that benefited from low 1,4-dioxane concentrations were identified using DESeq analysis. Functional monooxygenase genes involved in the 1,4-dioxane degradation were predicted by PICRUSt2 (Douglas, Maffei et al. 2020). The impact of bioaugmentation with agricultural soil microorganisms on 1,4-dioxane removal rates in site sediments were also evaluated.

Amending microcosms with BSM and yeast extract improved 1,4-dioxane biodegradation rates in sediment with indigenous 1,4-dioxane degraders. Yeast extract was previously found to accelerate the degradation rates by pure cultures of *Rhodanobacter* AYS5 and *Xanthobacter* flavus DT8 at a high 1,4-dioxane concentration (100 mg/L) (Pugazhendi, Rajesh Banu et al. 2015, Chen, Jin et al. 2016). *Rhodococcus ruber* 219 demonstrated the ability to effectively degrade 1,4-dioxane to levels below the health advisory threshold (0.35 μg/L) when supplied with thiamine at low 1,4-dioxane concentrations (below 100 μg/L), (Simmer, Richards et al. 2021). Due to the multiple growth factors contained in yeast extract, it is reasonable that yeast extract can enhance the 1,4-dioxane degradation at low 1,4-dioxane concentrations.

No degradation was observed in any of the treatments for Site 2 and Site 3, indicating a lack of intrinsic degradation capabilities. A consistent lack of 1,4-dioxane degradation activity at low concentrations was observed in site samples down gradient from the source zone (Li, Van Orden et al. 2015). This could be due to the absence or low population of 1,4-dioxane degraders in these site samples. In addition, the low 1,4-dioxane concentrations may be insufficient to induce the activity of degrading populations (Adamson, Mahendra et al. 2014). These findings

suggest the need for bioaugmentation to enhance the degradation of 1,4-dioxane at low concentrations in these site samples.

Uncontaminated agricultural soils have demonstrated 1,4-dioxane degradation potential (Ramalingam and Cupples 2020, Dang and Cupples 2021, Li and Cupples 2024). In microcosms amended with four different agricultural soils, over 50% 1,4-dioxane was removed within 40 days (Ramalingam and Cupples 2020). Concurrent degradation of 1,4-dioxane and *cis*-dichloroethene was also observed in agricultural soil microcosms (Dang and Cupples 2021). Functional propane monooxygenase genes were detected in agricultural soils (Eshghdoostkhatami and Cupples 2024, Li and Cupples 2024). In addition, genes potentially associated with 1,4-dioxane degradation were predicted to exist in agricultural soils through PICRUSt2 analysis (Cupples, Li et al. 2022).

Other researchers have also highlighted the 1,4-dioxane degradation potential at environmental relevant concentrations by bacteria consortia enriched from uncontaminated garden soils (He, Mathieu et al. 2018, Tang, Wang et al. 2023). In one study, bacteria consortia dominated by *Mycobacterium* degraded 300 µg/L 1,4-dioxane to below 5 µg/L within three days (He, Mathieu et al. 2018). In another study, bacteria consortia dominated by *Pseudonocardia* degraded three consecutive doses of 300 µg/L of 1,4-dioxane to below 80 µg/L within 3 days (Tang, Wang et al. 2023). Both *Pseudonocardia* and *Mycobacterium* are well-known 1,4-dioxane degraders (Parales, Adamus et al. 1994, Mahendra and Alvarez-Cohen 2006, Kim, Jeon et al. 2009). In addition, the 1,4-dioxane degrading consortia in the above two studies were enriched by amending 100 mg/L 1,4-dioxane to the soil suspension mixture.

Differentially abundant phylotypes identified via DESeq2 analysis between the samples and live controls provide insights into microbial taxa potentially involved in 1,4-dioxane

degradation. These phylotypes may contribute to the initial breakdown of 1,4-dioxane and/or benefit from the consumption of its biodegradation products (Ramalingam and Cupples 2020). In the current study, *Rhodococcus* was differentially enriched in the Site 1 sediment microcosms. However, A prior study using yeast extract amendments did not associate *Rhodococcus* with carbon uptake from 1,4-dioxane in the sediment microcosms from same site (Li and Cupples 2024). This suggests that *Rhodococcus* may be involved in 1,4-dioxane degradation without directly utilizing it as a carbon source.

Within the *Rhodococcus* genus, strains such as *Rhodococcus ruber* 219 and *Rhodococcus aetherivorans* JCM 14343 have been reported to utilize 1,4-dioxane as the sole carbon and energy source (Bernhardt and Diekmann 1991, Inoue, Tsunoda et al. 2016). Additionally, several members of this genus, such as *Rhodococcus* sp. YYL, *Rhodococcus* sp. RR1, *Rhodococcus jostii* RHA1, *Rhodococcus* ENV425, *Rhodococcus rhodochrous* strain ATCC 21198, *Rhodococcus. ruber* T1 and T5, and *Rhodococcus aetherivorans* JCM 14343, are capable of degrading 1,4-dioxane co-metabolically in the presence of tetrahydrofuran, propane, toluene, isobutane or 1,4-butanediol (Mahendra and Alvarez-Cohen 2006, Vainberg, McClay et al. 2006, Yao, Lv et al. 2009, Sei, Oyama et al. 2013, Hand, Wang et al. 2015, Inoue, Tsunoda et al. 2018, Rolston, Hyman et al. 2019).

Gemmatimonas benefited from 1,4-dioxane degradation in the Site 1 sediment microcosms. This genus was first reported to be responsible for carbon uptake in the contaminated Site 1 sediment and lake wetland microcosms (Li and Cupples 2024). In addition, *Gemmatimonas* was previously associated with benzoate, pyrene and phenanthrene degradation (Zhang, Sekiguchi et al. 2003, Wang, Teng et al. 2018, Wang, Wang et al. 2021).

Rhizobiales also benefited from the presence of 1,4-dioxane in Site 1 sediments.

Consistent with the current study, members of the *Rhizobiales* order (*Hyphomicrobium, Bartonella* and *Chelativorans*) have been shown to thrive in response to 1,4-dioxane degradation in agricultural soil microcosms (Ramalingam and Cupples 2020). This order has been associated with carbon uptake from 1,4-dioxane in the lake wetland microcosms (Li and Cupples 2024) and was dominant in microbial consortia across successive 1,4-dioxane degradation cycles (Tian, Zhang et al. 2024). Furthermore, the family *Xanthobacteraceae*, which belongs to the *Rhizobiales* order, as well as *Xanthobacter flavus* DT8 and *Xanthobacter sp.*, which are classified within the *Xanthobacteraceae* family, are known 1,4-dioxane degraders (Chen, Jin et al. 2016, Chen, Miao et al. 2021, Ma, Wang et al. 2021, Samadi, Kermanshahi-pour et al. 2023).

Other enriched phylotypes include Flavobacterium in Site 1 sediments. *Flavobacterium* is known to co-metabolically degrades 1,4-dioxane in the presence of tetrahydrofuran (Sun, Ko et al. 2011) and has been detected in contaminated site sediments during the 1,4-dioxane degradation period (Ramalingam and Cupples 2020). This genus is also recognized for its ability to degrade a range of compounds, including diesel, polysaccharide, cellulose, dichlorvos, and paracetamol (Ning, Gang et al. 2012, Nedashkovskaya, Balabanova et al. 2014, Palma, Donaldben et al. 2018, Chaudhary, Kim et al. 2019, Kim and Yu 2020).

Chitinophagaceae was enriched in the water treatment of agricultural soil microcosms. This family was also notably enriched in the uncontaminated garden soil (Tang, Wang et al. 2023) and activated sludge (Chen, Miao et al. 2021), which exhibited 1,4-dioxane degradation capacity. Additionally, the *Chitinophagales* order was consistently increased during the 1,4-dioxane degradation process in sludge (Samadi, Kermanshahi-pour et al. 2023). The *Chitinophagaceae* family has also been suggested to play an role in the biodegradation of other compounds, such as 1,1,1-trichloroethane, lindane, anthracene, hydrocarbon, 2-methylisoborneol

and benzo[a]pyrene (Zhang, Wang et al. 2011, Aburto-Medina, Adetutu et al. 2012, Song, Luo et al. 2015, Du, Zhou et al. 2017, Tusher, Inoue et al. 2022, Wu, Chang et al. 2022).

PICRUSt2 analysis revealed a subset of the enriched phylotypes associated with monooxygenase subunits. *Rhodococcus* was associated with methane/ammonia degradation exclusively in the three treatments containing BSM and be linked to propane monooxygenase subunits only in the treatments containing both BSM and yeast extract in Site 1 sediment microcosms. *Rhodococcus* sp. RR1 is known for its ability to catabolize a wide range of compounds due to its diverse metabolic pathways (McLeod, Warren et al. 2006). In particular, the initiation of 1,4-dioxane biodegradation by *Rhodococcus* species has been associated with various groups of soluble di-iron monooxygenases (SDIMOs), including *Rhodococcus* sp. strain YYL *thmA* (group 5) (Yao, Lv et al. 2009), *Rhodococcus* jostii RHA1 *prmA* (group 5) (Sharp, Sales et al. 2007, Hand, Wang et al. 2015), *Rhodococcus* sp. RR1 *prmA* (group 5) (Sharp, Sales et al. 2007). Despite the absence of propane, *Rhodococcus* community may survive by extracting energy from co-metabolic intermediates of 1,4-dioxane (Miao, Heintz et al. 2021). Further, *Rhodococcus* may acquire dioxane degradation gene via horizontal transfer, as indicated by its significant correlation with *prmA* gene, which encodes the alpha subunit of propane monooxygenase (Li, Deng et al. 2023). SDIMO analysis also detected that *Rhodococcus* species were detected in relation to *Rhodococcus jostii* RHA1 *prmA* and *Rhodococcus* sp. RR1 *prmA* in the Site 1 sediments (Li and Cupples 2024). Overall, these findings suggest that *Rhodococcus* may participate in 1,4-dioxane degradation in Site 1 sediments through cometabolism involving multiple monooxygenases.

5.6 Conclusions

This study demonstrates the potential for 1,4-dioxane biodegradation in contaminated

sediments and highlights the efficacy of agricultural soils for bioaugmentation. While yeast extract enhanced biodegradation rates in certain treatments, particularly in sediments containing indigenous degraders, its impact was limited in two of the three impacted sites (which lacked indigenous degraders). Bioaugmentation with agricultural soils successfully facilitated 1,4-dioxane removal in sediments that lacked native degraders. These results suggest that agricultural soils could provide a promising strategy for the bioremediation of 1,4-dioxane, particularly at low concentrations. Furthermore, a subset of the differentially abundant phylotypes (determined via DESeq analysis) between the samples and the live controls were previously associated with 1,4-dioxane biodegradation (*Rhodococcus*, *Rhizobiales*, *Gemmatimonas*, *Flavobacterium*, and *Chitinophagaceae*). PICRUSt2 analysis indicated some of the enriched phylotypes were associated with ammonia/particulate monooxygenase and propane monooxygenase subunits.

Acknowledgment

Thanks to Stacey VanderWulp (MSU) for providing the agricultural soil samples from Kellogg Biological Station (KBS, MSU). Thanks to Anthony Danko and Michael Pound (NAVFAC), Dr. Vidhya Ramalingam (Tetra Tech) as well as Paul Hatzinger (APTIM) for providing the sediment samples from the impacted site. Also, thanks to James O'Keefe, Dr. Casey Johnny, and Dr. Tony Schilmiller at the Mass Spectrometry Laboratory at the RTSF (MSU) for 1,4-dioxane analytical method support. This research was supported by a grant from NSF (Award Number 1902250) and SERDP (Grant Number ER23-3590). Support was also provided by the NSF Long-term Ecological Research Program (DEB 1832042) at the KBS and by MSU AgBioResearch.

REFERENCES

Aburto-Medina, A., E. M. Adetutu, S. Aleer, J. Weber, S. S. Patil, P. J. Sheppard, A. S. Ball and A. L. Juhasz (2012). "Comparison of indigenous and exogenous microbial populations during slurry phase biodegradation of long-term hydrocarbon-contaminated soil." Biodegradation 23(6): 813-822.

Adamson, D. T., S. Mahendra, K. L. Walker Jr, S. R. Rauch, S. Sengupta and C. J. Newell (2014). "A multisite survey to identify the scale of the 1, 4-dioxane problem at contaminated groundwater sites." Environmental Science & Technology Letters 1(5): 254-258.

Adamson, D. T., E. A. Piña, A. E. Cartwright, S. R. Rauch, R. H. Anderson, T. Mohr and J. A. Connor (2017). "1, 4-Dioxane drinking water occurrence data from the third unregulated contaminant monitoring rule." Science of the Total Environment 596: 236-245.

Aitchison, E. W., S. L. Kelley, P. J. J. Alvarez and J. L. Schnoor (2000). "Phytoremediation of 1,4-Dioxane by hybrid poplar trees." Water Environment Research 72(3): 313-321.

Barajas-Rodriguez, F. J. and D. L. Freedman (2018). "Aerobic biodegradation kinetics for 1,4-dioxane under metabolic and cometabolic conditions." Journal of Hazardous Materials 350: 180-188.

Barbera, P., A. M. Kozlov, L. Czech, B. Morel, D. Darriba, T. Flouri and A. Stamatakis (2019). "EPA-ng: Massively Parallel Evolutionary Placement of Genetic Sequences." Syst Biol 68(2): 365-369.

Barndõk, H., N. Merayo, L. Blanco, D. Hermosilla and Á. Blanco (2016). "Application of on-line FTIR methodology to study the mechanisms of heterogeneous advanced oxidation processes." Applied Catalysis B: Environmental 185: 344-352.

Bernhardt, D. and H. Diekmann (1991). "Degradation of dioxane, tetrahydrofuran and other cyclic ethers by an environmental Rhodococcus strain." Applied Microbiology and Biotechnology 36(1): 120-123.

Chaudhary, D. K., D.-U. Kim, D. Kim and J. Kim (2019). "Flavobacterium petrolei sp. nov., a novel psychrophilic, diesel-degrading bacterium isolated from oil-contaminated Arctic soil." Scientific Reports 9(1): 4134.

Chen, D.-Z., X.-J. Jin, J. Chen, J.-X. Ye, N.-X. Jiang and J.-M. Chen (2016). "Intermediates and substrate interaction of 1,4-dioxane degradation by the effective metabolizer Xanthobacter flavus DT8." International Biodeterioration & Biodegradation 106: 133-140.

Chen, R., Y. Miao, Y. Liu, L. Zhang, M. Zhong, J. M. Adams, Y. Dong and S. Mahendra (2021). "Identification of novel 1, 4-dioxane degraders and related genes from activated sludge by taxonomic and functional gene sequence analysis." Journal of Hazardous Materials 412: 125157.

Chiang, S.-Y. D., R. Mora, W. H. Diguiseppi, G. Davis, K. Sublette, P. Gedalanga and S. Mahendra (2012). "Characterizing the intrinsic bioremediation potential of 1, 4-dioxane and trichloroethene using innovative environmental diagnostic tools." Journal of Environmental Monitoring 14(9): 2317-2326.

Chiang, S. Y., R. Anderson, M. Wilken and C. Walecka-Hutchison (2016). "Practical perspectives of 1, 4-dioxane investigation and remediation." Remediation Journal 27(1): 7-27.

Chu, M. Y. J., P. J. Bennett, M. E. Dolan, M. R. Hyman, A. D. Peacock, A. Bodour, R. H. Anderson, D. M. Mackay and M. N. Goltz (2018). "Concurrent treatment of 1, 4-dioxane and chlorinated aliphatics in a groundwater recirculation system via aerobic cometabolism." Groundwater Monitoring & Remediation 38(3): 53-64.

Cupples, A. M., Z. Li, F. P. Wilson, V. Ramalingam and A. Kelly (2022). "In silico analysis of soil, sediment and groundwater microbial communities to predict biodegradation potential." Journal of Microbiological Methods 202: 106595.

Czech, L., P. Barbera and A. Stamatakis (2020). "Genesis and Gappa: processing, analyzing and visualizing phylogenetic (placement) data." Bioinformatics 36(10): 3263-3265.

Dang, H. and A. M. Cupples (2021). "Identification of the phylotypes involved in cis-dichloroethene and 1,4-dioxane biodegradation in soil microcosms." Science of The Total Environment 794: 148690.

Dang, H., Y. H. Kanitkar, R. D. Stedtfeld, P. B. Hatzinger, S. A. Hashsham and A. M. Cupples (2018). "Abundance of Chlorinated Solvent and 1,4-Dioxane Degrading Microorganisms at Five Chlorinated Solvent Contaminated Sites Determined via Shotgun Sequencing." Environmental Science & Technology 52(23): 13914-13924.

Derosa, C. T., S. Wilbur, J. Holler, P. Richter and Y.-W. Stevens (1996). "Health Evaluation of 1,4-Dioxane." Toxicology and Industrial Health 12(1): 1-43.

Douglas, G. M., V. J. Maffei, J. R. Zaneveld, S. N. Yurgel, J. R. Brown, C. M. Taylor, C. Huttenhower and M. G. I. Langille (2020). "PICRUSt2 for prediction of metagenome functions." Nat Biotechnol 38(6): 685-688.

Dowle, M. and A. Srinivasan (2023). data.table: Extension of `data.frame`. R package version 1.14.8.

Du, K., B. Zhou and R. Yuan (2017). "Biodegradation of 2-methylisoborneol by single bacterium in culture media and river water environment." International Journal of Environmental Studies 74(3): 399-411.

Eshghdoostkhatami, Z. and A. M. Cupples (2024). "Occurrence of Rhodococcus sp. RR1 prmA and Rhodococcus jostii RHA1 prmA across microbial communities and their enumeration during 1,4-dioxane biodegradation." Journal of Microbiological Methods: 106908.

Gedalanga, P., A. Madison, Y. Miao, T. Richards, J. Hatton, W. H. DiGuiseppi, J. Wilson and S. Mahendra (2016). "A Multiple Lines of Evidence Framework to Evaluate Intrinsic Biodegradation of 1,4-Dioxane." Remediation Journal 27(1): 93-114.

Hand, S., B. Wang and K.-H. Chu (2015). "Biodegradation of 1,4-dioxane: Effects of enzyme inducers and trichloroethylene." Science of The Total Environment 520: 154-159.

He, Y., J. Mathieu, M. L. B. da Silva, M. Li and P. J. J. Alvarez (2018). "1,4-Dioxane-degrading consortia can be enriched from uncontaminated soils: prevalence of Mycobacterium and soluble di-iron monooxygenase genes." Microbial Biotechnology 11(1): 189-198.

Huang, H., D. Shen, N. Li, D. Shan, J. Shentu and Y. Zhou (2014). "Biodegradation of 1, 4-dioxane by a novel strain and its biodegradation pathway." Water, Air, & Soil Pollution 225: 1-11.

Ikehata, K., L. Wang-Staley, X. Qu and Y. Li (2016). "Treatment of Groundwater Contaminated with 1,4-Dioxane, Tetrahydrofuran, and Chlorinated Volatile Organic Compounds Using Advanced Oxidation Processes." Ozone: Science & Engineering 38(6): 413-424.

Inoue, D., T. Tsunoda, K. Sawada, N. Yamamoto, Y. Saito, K. Sei and M. Ike (2016). "1,4-Dioxane degradation potential of members of the genera Pseudonocardia and Rhodococcus." Biodegradation 27(4): 277-286.

Inoue, D., T. Tsunoda, N. Yamamoto, M. Ike and K. Sei (2018). "1,4-Dioxane degradation characteristics of Rhodococcus aetherivorans JCM 14343." Biodegradation 29(3): 301-310.

Kelley, S. L., E. W. Aitchison, M. Deshpande, J. L. Schnoor and P. J. Alvarez (2001). "Biodegradation of 1, 4-dioxane in planted and unplanted soil: effect of bioaugmentation with Amycolata sp. CB1190." Water Research 35(16): 3791-3800.

Kim, H. and S. M. Yu (2020). "Flavobacterium nackdongense sp. nov., a cellulose-degrading bacterium isolated from sediment." Archives of microbiology 202(3): 591-595.

Kim, Y.-M., J.-R. Jeon, K. Murugesan, E.-J. Kim and Y.-S. Chang (2009). "Biodegradation of 1, 4-dioxane and transformation of related cyclic compounds by a newly isolated Mycobacterium sp. PH-06." Biodegradation 20(4): 511-519.

Kohlweyer, U., B. Thiemer, T. Schräder and J. R. Andreesen (2000). "Tetrahydrofuran degradation by a newly isolated culture of Pseudonocardia sp. strain K1." FEMS microbiology letters 186(2): 301-306.

Kozich, J. J., S. L. Westcott, N. T. Baxter, S. K. Highlander and P. D. Schloss (2013). "Development of a Dual-Index Sequencing Strategy and Curation Pipeline for Analyzing Amplicon Sequence Data on the MiSeq Illumina Sequencing Platform." Applied and Environmental Microbiology 79(17): 5112-5120.

Lahti, L. and S. Shetty (2012-2019). microbiome R package.

Li, F., D. Deng, A. Wadden, P. Parvis, D. Cutt and M. Li (2023). "Effective removal of trace 1,4-dioxane by biological treatments augmented with propanotrophic single culture versus synthetic consortium." Journal of Hazardous Materials Advances 9: 100246.

Li, F., D. Deng, L. Zeng, S. Abrams and M. Li (2021). "Sequential anaerobic and aerobic bioaugmentation for commingled groundwater contamination of trichloroethene and 1, 4-dioxane." Science of the Total Environment 774: 145118.

Li, M., S. Fiorenza, J. R. Chatham, S. Mahendra and P. J. J. Alvarez (2010). "1,4-Dioxane biodegradation at low temperatures in Arctic groundwater samples." Water Research 44(9): 2894-2900.

Li, M., Y. Liu, Y. He, J. Mathieu, J. Hatton, W. DiGuiseppi and P. J. J. Alvarez (2017). "Hindrance of 1,4-dioxane biodegradation in microcosms biostimulated with inducing or non-inducing auxiliary substrates." Water Research 112: 217-225.

Li, M., J. Mathieu, Y. Liu, E. T. Van Orden, Y. Yang, S. Fiorenza and P. J. J. Alvarez (2014). "The Abundance of Tetrahydrofuran/Dioxane Monooxygenase Genes (thmA/dxmA) and 1,4-Dioxane Degradation Activity Are Significantly Correlated at Various Impacted Aquifers." Environmental Science & Technology Letters 1(1): 122-127.

Li, M., J. Mathieu, Y. Yang, S. Fiorenza, Y. Deng, Z. He, J. Zhou and P. J. Alvarez (2013). "Widespread distribution of soluble di-iron monooxygenase (SDIMO) genes in Arctic groundwater impacted by 1,4-dioxane." Environ Sci Technol 47(17): 9950-9958.

Li, M., E. T. Van Orden, D. J. DeVries, Z. Xiong, R. Hinchee and P. J. Alvarez (2015). "Bench-scale biodegradation tests to assess natural attenuation potential of 1,4-dioxane at three sites in California." Biodegradation 26(1): 39-50.

Li, Z. and A. M. Cupples (2024). "Impact of Yeast Extract and Basal Salts Medium on 1,4-Dioxane Biodegradation Rates and the Microorganisms Involved in Carbon Uptake from 1,4-Dioxane." Environmental Pollution: 125014.

Lippincott, D., S. H. Streger, C. E. Schaefer, J. Hinkle, J. Stormo and R. J. Steffan (2015). "Bioaugmentation and propane biosparging for in situ biodegradation of 1, 4-dioxane." Groundwater Monitoring & Remediation 35(2): 81-92.

Louca, S. and M. Doebeli (2018). "Efficient comparative phylogenetics on large trees." Bioinformatics 34(6): 1053-1055.

Love, M. I., W. Huber and S. Anders (2014). "Moderated estimation of fold change and dispersion for RNA-seq data with DESeq2." Genome Biology 15(12): 550.

Ma, F., Y. Wang, J. Yang, H. Guo, D. Su and L. Yu (2021). "Degradation of 1, 4-Dioxane by Xanthobacter sp. YN2." Current Microbiology 78: 992-1005.

Mahendra, S. and L. Alvarez-Cohen (2006). "Kinetics of 1,4-Dioxane Biodegradation by Monooxygenase-Expressing Bacteria." Environmental Science & Technology 40(17): 5435-5442.

Mahendra, S., C. J. Petzold, E. E. Baidoo, J. D. Keasling and L. Alvarez-Cohen (2007). "Identification of the Intermediates of in Vivo Oxidation of 1,4-Dioxane by Monooxygenase-Containing Bacteria." Environmental Science & Technology 41(21): 7330-7336.

McLeod, M. P., R. L. Warren, W. W. Hsiao, N. Araki, M. Myhre, C. Fernandes, D. Miyazawa, W. Wong, A. L. Lillquist and D. Wang (2006). "The complete genome of Rhodococcus sp. RHA1 provides insights into a catabolic powerhouse." Proceedings of the National Academy of Sciences 103(42): 15582-15587.

McMurdie, P. J. and S. Holmes (2013). "phyloseq: An R Package for Reproducible Interactive Analysis and Graphics of Microbiome Census Data." PLOS ONE 8(4): e61217.

Miao, Y., M. B. Heintz, C. H. Bell, N. W. Johnson, A. L. Polasko, D. Favero and S. Mahendra (2021). "Profiling microbial community structures and functions in bioremediation strategies for treating 1,4-dioxane-contaminated groundwater." Journal of Hazardous Materials 408: 124457.

Mohr, T. K., W. DiGuiseppi, J. Hatton and J. Anderson (2020). Environmental investigation and remediation: 1, 4-dioxane and other solvent stabilizers, CRC Press.

Nedashkovskaya, O. I., L. A. Balabanova, N. V. Zhukova, S.-J. Kim, I. Y. Bakunina and S.-K. Rhee (2014). "Flavobacterium ahnfeltiae sp. nov., a new marine polysaccharide-degrading bacterium isolated from a Pacific red alga." Archives of microbiology 196: 745-752.

Ning, J., G. Gang, Z. Bai, Q. Hu, H. Qi, A. Ma, X. Zhuan and G. Zhuang (2012). "In situ enhanced bioremediation of dichlorvos by a phyllosphere Flavobacterium strain." Frontiers of Environmental Science & Engineering 6: 231-237.

Palma, T. L., M. N. Donaldben, M. C. Costa and J. D. Carlier (2018). "Putative role of Flavobacterium, Dokdonella and Methylophilus strains in paracetamol biodegradation." Water, Air, & Soil Pollution 229: 1-23.

Parales, R., J. Adamus, N. White and H. May (1994). "Degradation of 1, 4-dioxane by an actinomycete in pure culture." Applied and Environmental Microbiology 60(12): 4527-4530.

Pedersen, T. L. (2023). "patchwork: The Composer of Plots. R package version 1.1.3.".

Pruesse, E., C. Quast, K. Knittel, B. M. Fuchs, W. Ludwig, J. Peplies and F. O. Glöckner (2007). "SILVA: a comprehensive online resource for quality checked and aligned ribosomal RNA sequence data compatible with ARB." Nucleic Acids Research 35(21): 7188-7196.

Pugazhendi, A., J. Rajesh Banu, J. Dhavamani and I. T. Yeom (2015). "Biodegradation of 1,4-dioxane by Rhodanobacter AYS5 and the role of additional substrates." Annals of Microbiology 65(4): 2201-2208.

R Core Team (2018). R: A language and environment for statistical computing, R Foundation for Statistical Computing, Vienna, Austria. .

Ramalingam, V. and A. M. Cupples (2020). "Anaerobic 1,4-dioxane biodegradation and microbial community analysis in microcosms inoculated with soils or sediments and different electron acceptors." Applied Microbiology and Biotechnology 104(9): 4155-4170.

Ramalingam, V. and A. M. Cupples (2020). "Enrichment of novel Actinomycetales and the detection of monooxygenases during aerobic 1,4-dioxane biodegradation with uncontaminated and contaminated inocula." Applied Microbiology and Biotechnology 104(5): 2255-2269.

Rolston, H. M., M. R. Hyman and L. Semprini (2019). "Aerobic cometabolism of 1,4-dioxane by isobutane-utilizing microorganisms including Rhodococcus rhodochrous strain 21198 in aquifer microcosms: Experimental and modeling study." Science of The Total Environment 694: 133688.

RStudio_Team (2020). RStudio: Integrated Development for R. RStudio, PBC. Boston, MA URL http://www.rstudio.com/.

Samadi, A., A. Kermanshahi-pour, S. M. Budge, Y. Huang and R. Jamieson (2023). "Biodegradation of 1,4-dioxane by a native digestate microbial community under different electron accepting conditions." Biodegradation 34(3): 283-300.

Schloss, P. D., S. L. Westcott, T. Ryabin, J. R. Hall, M. Hartmann, E. B. Hollister, R. A. Lesniewski, B. B. Oakley, D. H. Parks, C. J. Robinson, J. W. Sahl, B. Stres, G. G. Thallinger, D. J. Van Horn and C. F. Weber (2009). "Introducing mothur: Open-Source, Platform-Independent, Community-Supported Software for Describing and Comparing Microbial Communities." Applied and Environmental Microbiology 75(23): 7537-7541.

Sei, K., M. Oyama, T. Kakinoki, D. Inoue and M. Ike (2013). "Isolation and Characterization of Tetrahydrofuran- Degrading Bacteria for 1,4-Dioxane-Containing Wastewater Treatment by Co-Metabolic Degradation." Journal of Water and Environment Technology 11(1): 11-19.

Sharp, J. O., C. M. Sales, J. C. LeBlanc, J. Liu, T. K. Wood, L. D. Eltis, W. W. Mohn and L. Alvarez-Cohen (2007). "An inducible propane monooxygenase is responsible for N-nitrosodimethylamine degradation by Rhodococcus sp. strain RHA1." Applied and environmental microbiology 73(21): 6930-6938.

Simmer, R. A., P. M. Richards, J. M. Ewald, C. Schwarz, M. L. B. da Silva, J. Jacques Mathieu, P. J. J. Alvarez and J. L. Schnoor (2021). "Rapid metabolism of 1,4-dioxane to below

health advisory levels by thiamine-amended Rhodococcus ruber Strain 219." Environmental Science & Technology Letters 8 (11): 975-980

Simmer, R. A., P. M. Richards, J. M. Ewald, C. Schwarz, M. L. B. da Silva, J. Mathieu, P. J. J. Alvarez and J. L. Schnoor (2021). "Rapid Metabolism of 1,4-Dioxane to below Health Advisory Levels by Thiamine-Amended Rhodococcus ruber Strain 219." Environmental Science & Technology Letters 8(11): 975-980.

Song, M., C. Luo, L. Jiang, D. Zhang, Y. Wang and G. Zhang (2015). "Identification of Benzo[a]pyrene-Metabolizing Bacteria in Forest Soils by Using DNA-Based Stable-Isotope Probing." Applied and Environmental Microbiology 81(21): 7368-7376.

Stepien, D. K., P. Diehl, J. Helm, A. Thoms and W. Püttmann (2014). "Fate of 1,4-dioxane in the aquatic environment: From sewage to drinking water." Water Research 48: 406-419.

Sun, B., K. Ko and J. A. Ramsay (2011). "Biodegradation of 1, 4-dioxane by a Flavobacterium." Biodegradation 22: 651-659.

Sun, M., C. Lopez-Velandia and D. R. Knappe (2016). "Determination of 1,4-Dioxane in the Cape Fear River Watershed by Heated Purge-and-Trap Preconcentration and Gas Chromatography-Mass Spectrometry." Environ Sci Technol 50(5): 2246-2254.

Tang, Y., M. Wang, C.-S. Lee, A. K. Venkatesan and X. Mao (2023). "Characterization of 1,4-dioxane degrading microbial community enriched from uncontaminated soil." Applied Microbiology and Biotechnology 107(2): 955-969.

Tian, K., Y. Zhang, D. Yao, D. Tan, X. Fu, R. Chen, M. Zhong, Y. Dong and Y. Liu (2024). "Synergistic interactions in core microbiome Rhizobiales accelerate 1,4-dioxane biodegradation." Journal of Hazardous Materials 476: 135098.

Tusher, T. R., C. Inoue and M.-F. Chien (2022). "Efficient biodegradation of 1, 4-dioxane commingled with additional organic compound: Role of interspecies interactions within consortia." Chemosphere 308: 136440.

USEPA (2013). Integrated Risk Information System (IRIS) on 1,4-Dioxane. Washington DC, National Center for Environmental Assessment Office of Research and Development.

Vainberg, S., K. McClay, H. Masuda, D. Root, C. Condee, G. J. Zylstra and R. J. Steffan (2006). "Biodegradation of ether pollutants by Pseudonocardia sp. strain ENV478." Applied and environmental microbiology 72(8): 5218-5224.

Wang, B., Y. Teng, Y. Xu, W. Chen, W. Ren, Y. Li, P. Christie and Y. Luo (2018). "Effect of mixed soil microbiomes on pyrene removal and the response of the soil microorganisms." Science of the total environment 640: 9-17.

Wang, Y.-Q., M.-X. Wang, Y.-Y. Chen, C.-M. Li and Z.-F. Zhou (2021). "Microbial community structure and co-occurrence are essential for methanogenesis and its contribution to phenanthrene degradation in paddy soil." Journal of Hazardous Materials 417: 126086.

Wickham, H. (2016). " ggplot2: Elegant Graphics for Data Analysis. Springer-Verlag New York, 2016." https://ggplot2.tidyverse.org.

Wickham, H., R. Francois, L. Henry, K. Müller and D. Vaughan (2023). "dplyr: A Grammar of Data Manipulation. R package version 1.1.3.".

Wickham, H., D. Vaughan and M. Girlich (2023). "tidyr: Tidy Messy Data. R package version 1.3.0.".

Wu, S. C., B.-S. Chang and Y.-Y. Li (2022). "Effect of the coexistence of endosulfan on the lindane biodegradation by Novosphingobium barchaimii and microbial enrichment cultures." Chemosphere 297: 134063.

Yamamoto, N., Y. Saito, D. Inoue, K. Sei and M. Ike (2018). "Characterization of newly isolated Pseudonocardia sp. N23 with high 1,4-dioxane-degrading ability." Journal of Bioscience and Bioengineering 125(5): 552-558.

Yao, Y., Z. Lv, H. Min, Z. Lv and H. Jiao (2009). "Isolation, identification and characterization of a novel Rhodococcus sp. strain in biodegradation of tetrahydrofuran and its medium optimization using sequential statistics-based experimental designs." Bioresource Technology 100(11): 2762-2769.

Ye, Y. and T. G. Doak (2009). "A parsimony approach to biological pathway reconstruction/inference for genomes and metagenomes." PLoS Comput Biol 5(8): e1000465.

Zhang, H., Y. Sekiguchi, S. Hanada, P. Hugenholtz, H. Kim, Y. Kamagata and K. Nakamura (2003). "Gemmatimonas aurantiaca gen. nov., sp. nov., a Gram-negative, aerobic, polyphosphate-accumulating micro-organism, the first cultured representative of the new bacterial phylum Gemmatimonadetes phyl. nov." International Journal of Systematic and Evolutionary Microbiology 53(4): 1155-1163.

Zhang, S.-y., Q.-f. Wang, R. Wan and S.-g. Xie (2011). "Changes in bacterial community of anthracene bioremediation in municipal solid waste composting soil." Journal of Zhejiang University SCIENCE B 12: 760-768.

APPENDIX

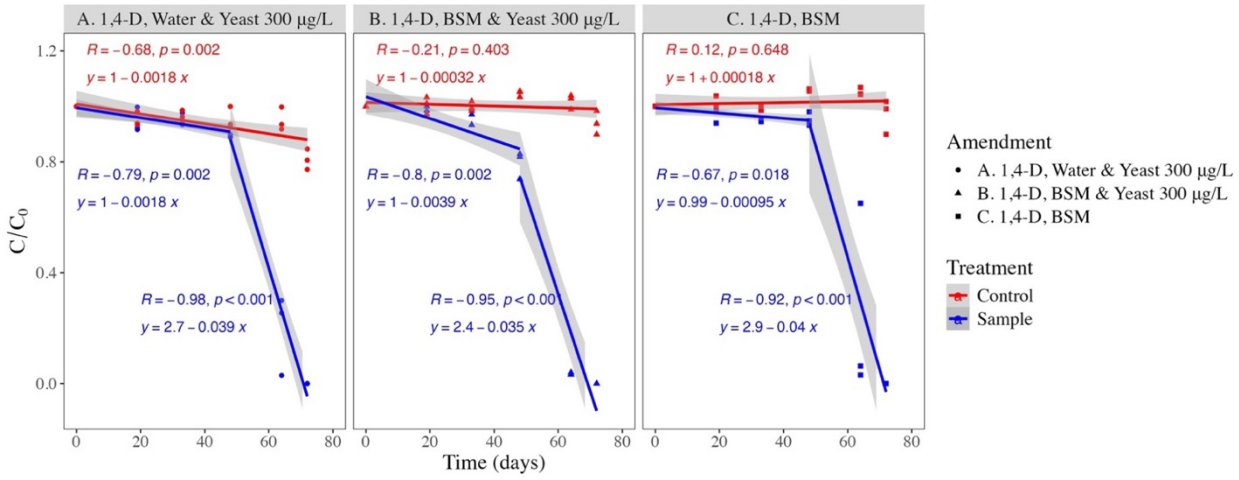

Figure A5.1 1,4-Dioxane concentrations over time in microcosms inoculated with Site 1 sediments with three treatments. The initial concentration was approximately 2 mg/L 1,4-dioxane. Dioxane concentrations lower than the detection limit (i.e., 1 µg/L) were denoted as 0 in the graphs.

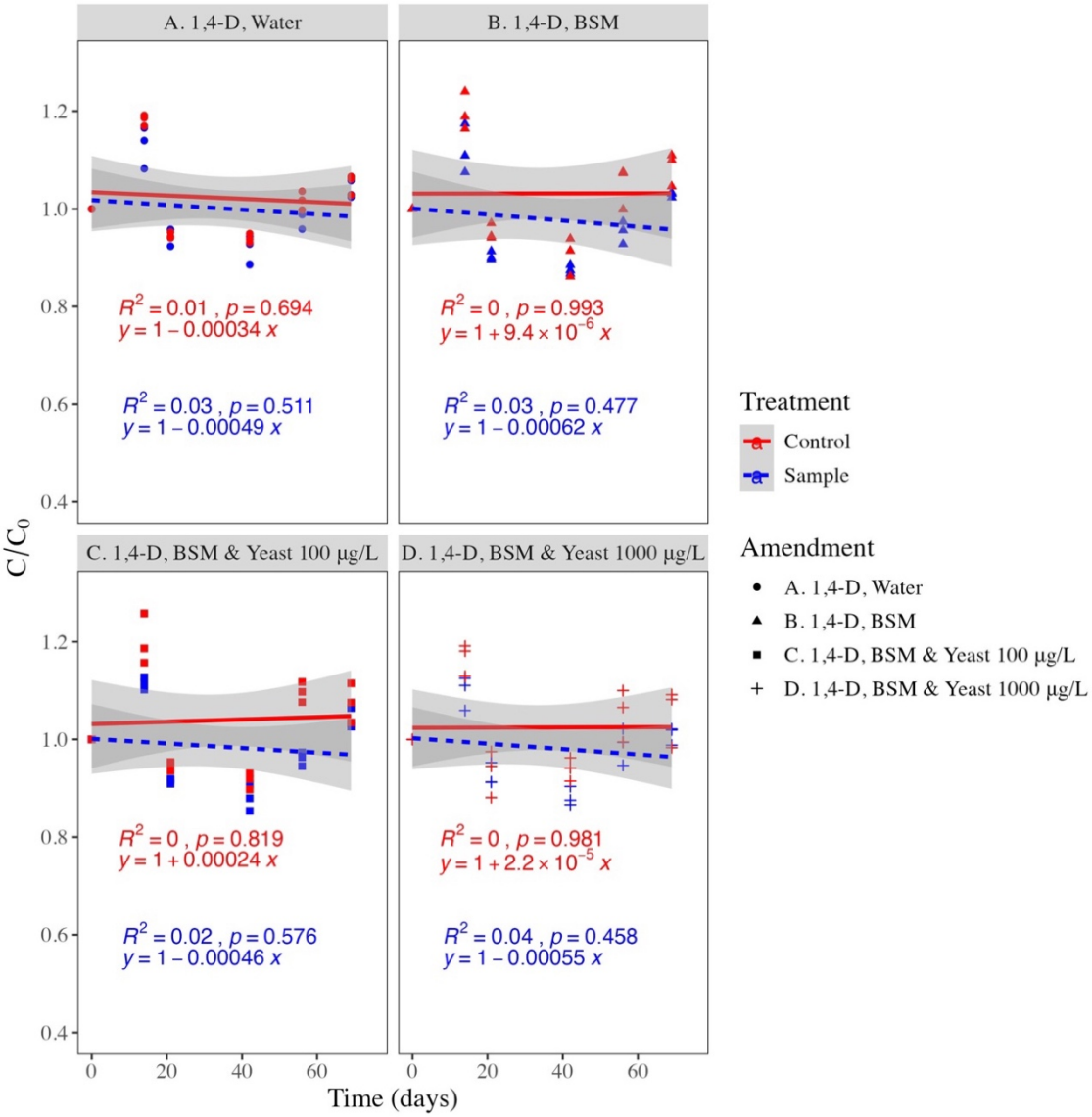

Figure A5.2 1,4-Dioxane concentrations over time (C/C_0) in microcosms inoculated with Site 2 sediments with four treatments. The initial concentration was approximately 100 µg/L 1,4-dioxane.

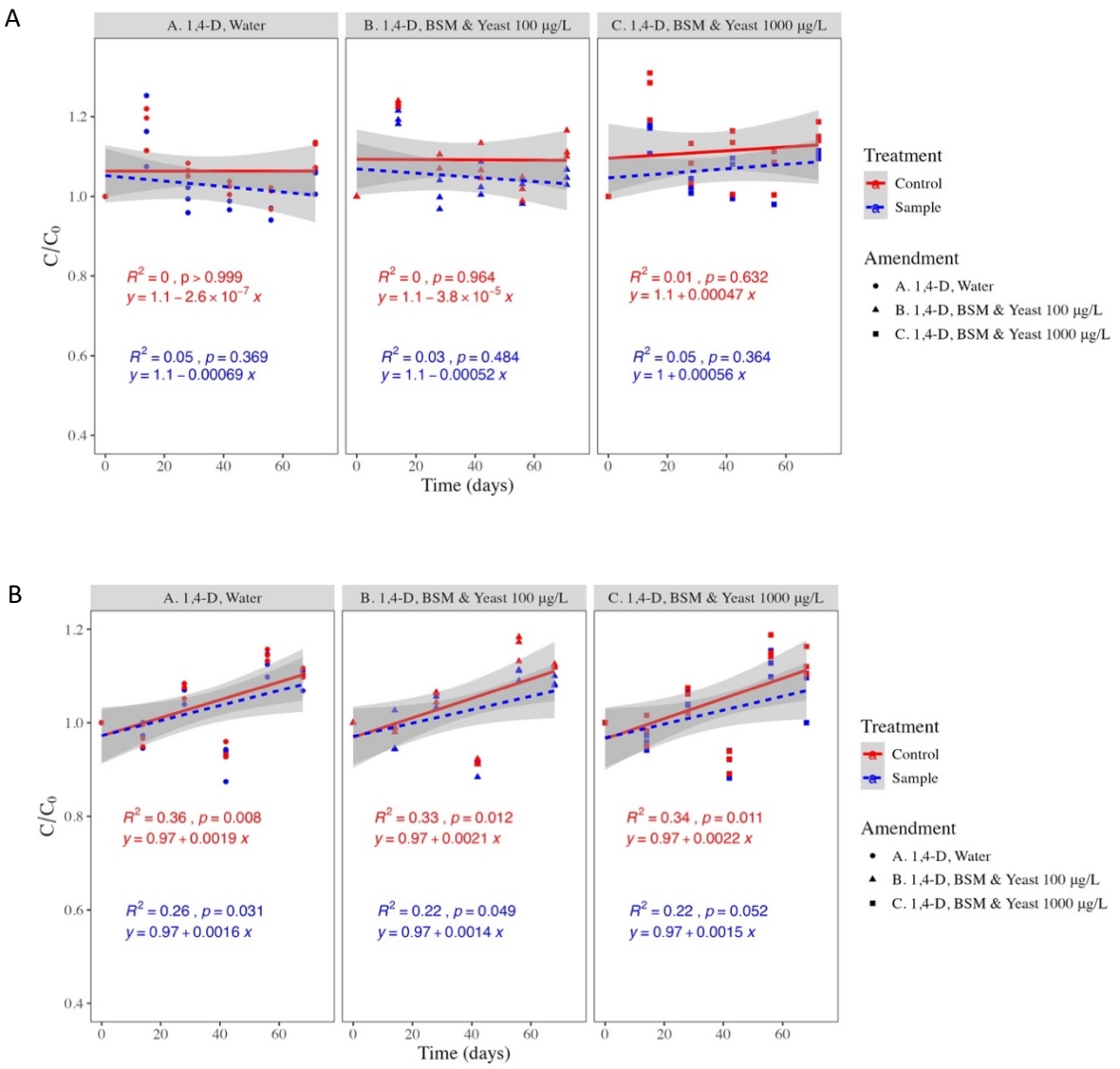

Figure A5.3 1,4-Dioxane concentrations over time (C/C_0) in microcosms inoculated with Site 2 sediments with three treatments. The initial concentration was approximately (A) 50 µg/L and (B) 500 µg/L 1,4-dioxane.

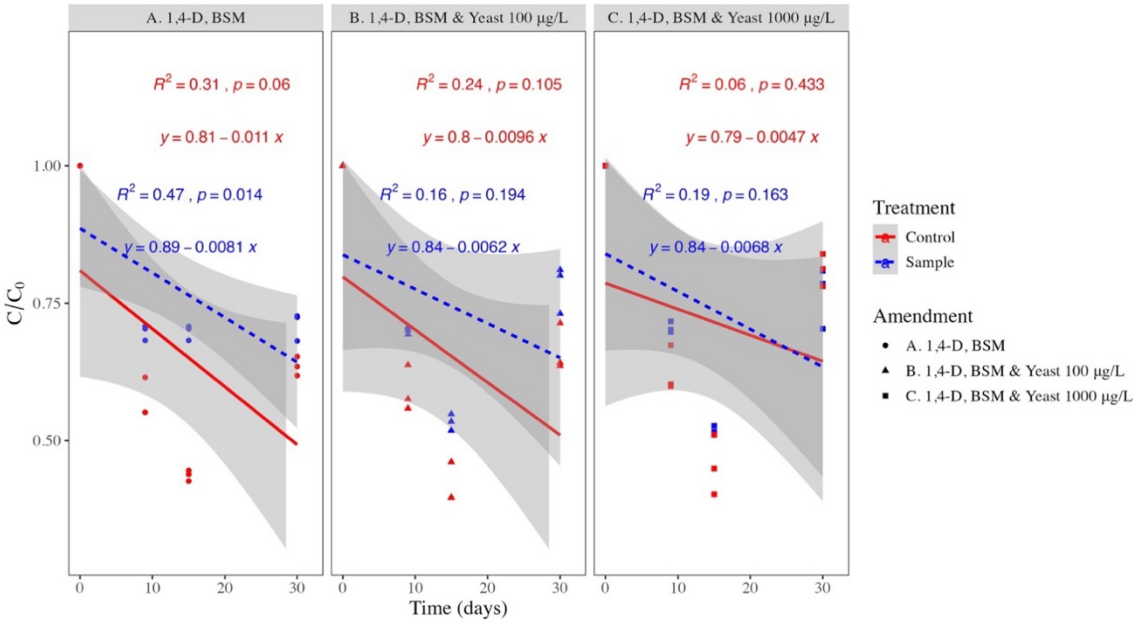

Figure A5.4 1,4-Dioxane concentrations over time (C/C_0) in microcosms inoculated with Site 3 sediments with four treatments. The initial concentration was approximately 50 µg/L 1,4-dioxane. Dioxane concentrations lower than the detection limit (1.72 µg/L) were denoted as 0 in the graphs.

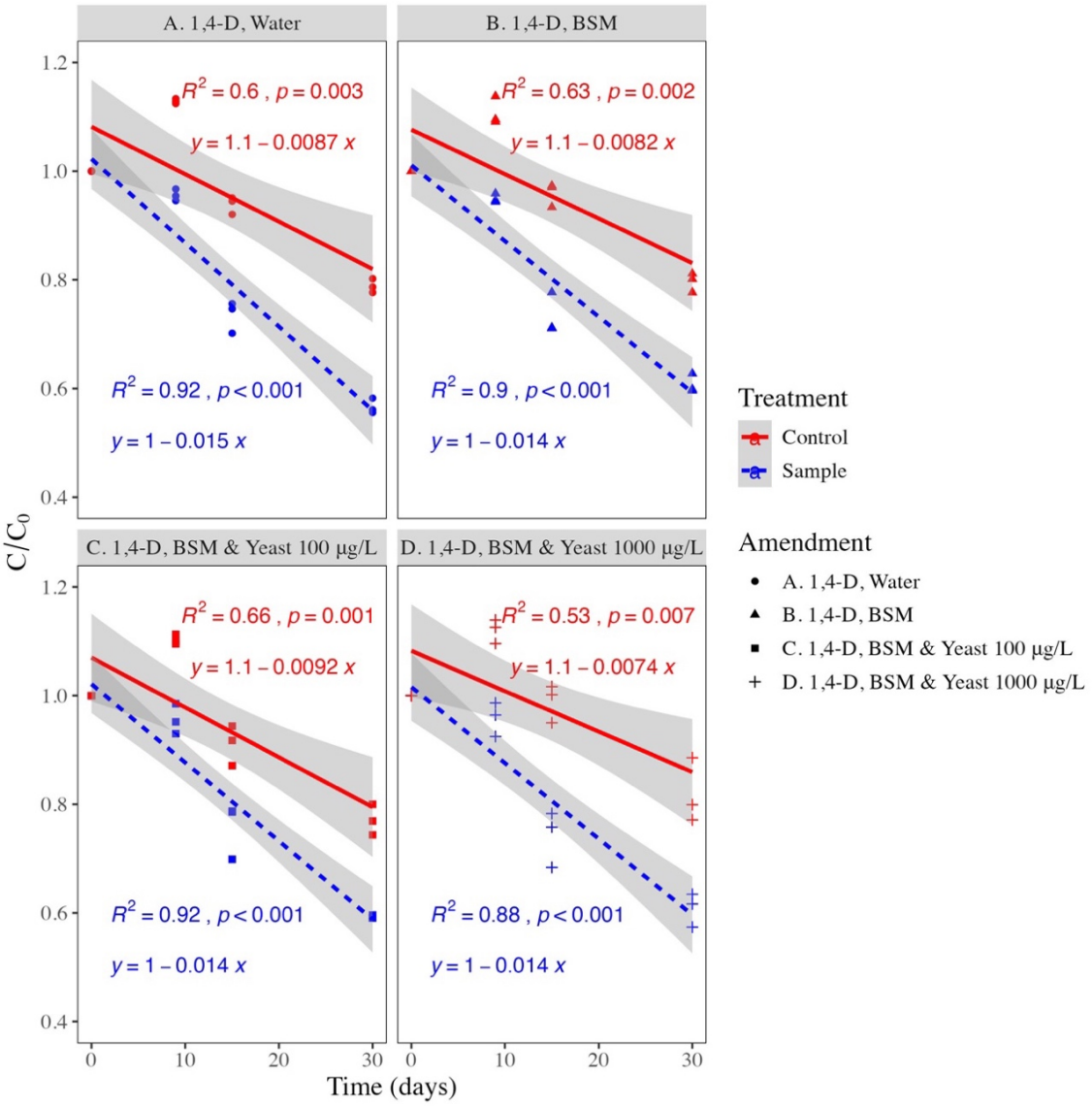

Figure A5.5 1,4-Dioxane concentrations over time (C/C_0) in microcosms inoculated with agricultural Soil 4 with four treatments. The initial concentration was approximately 50 µg/L 1,4-dioxane.

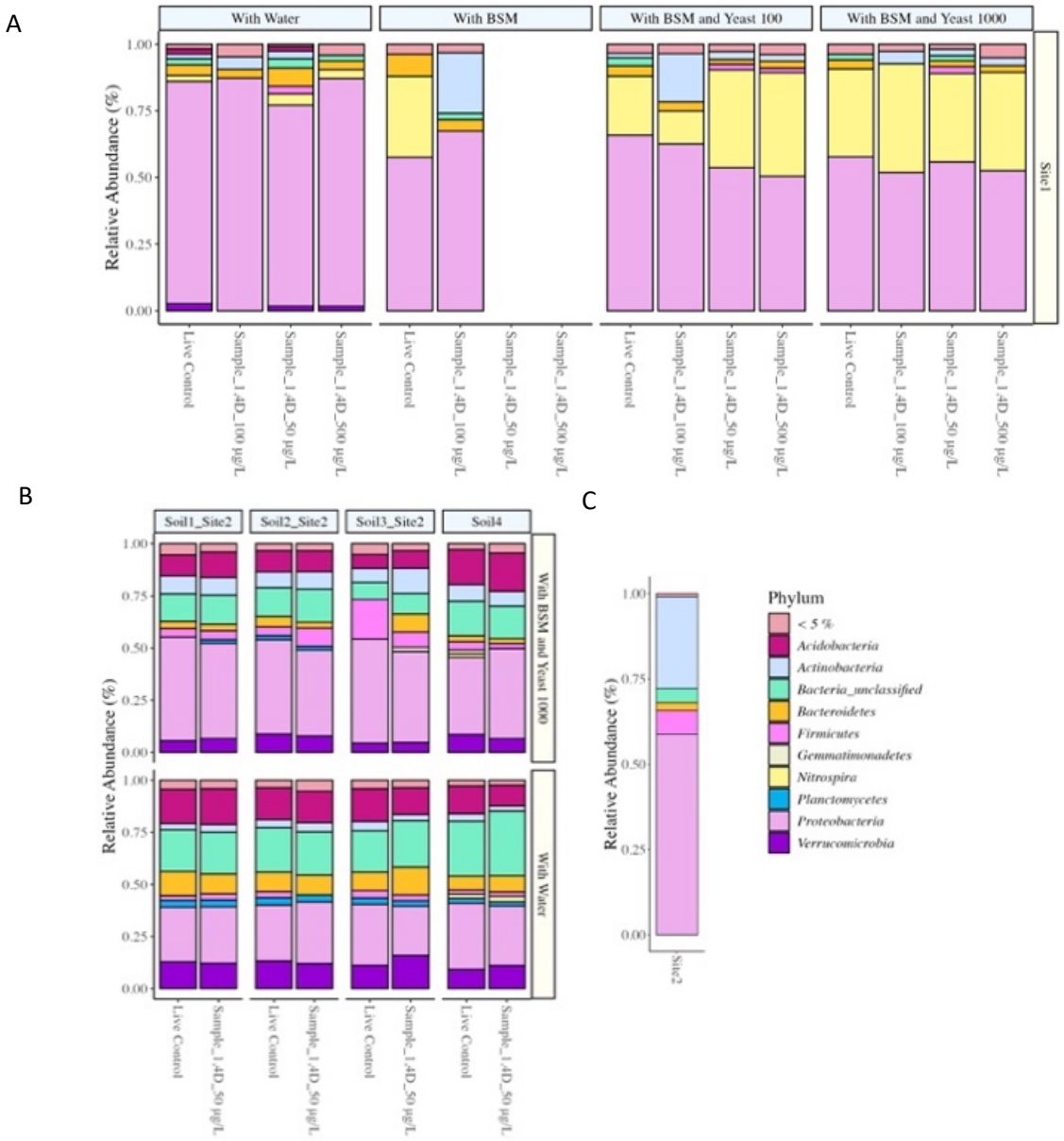

Figure A5.6 The relative abundance (%) of phyla in the (A) Site 1 sediments microcosms, (B) Agricultural soil microcosms and (C) untreated Site 2 microcosms. Each column represents average values for three sequencing replicates.

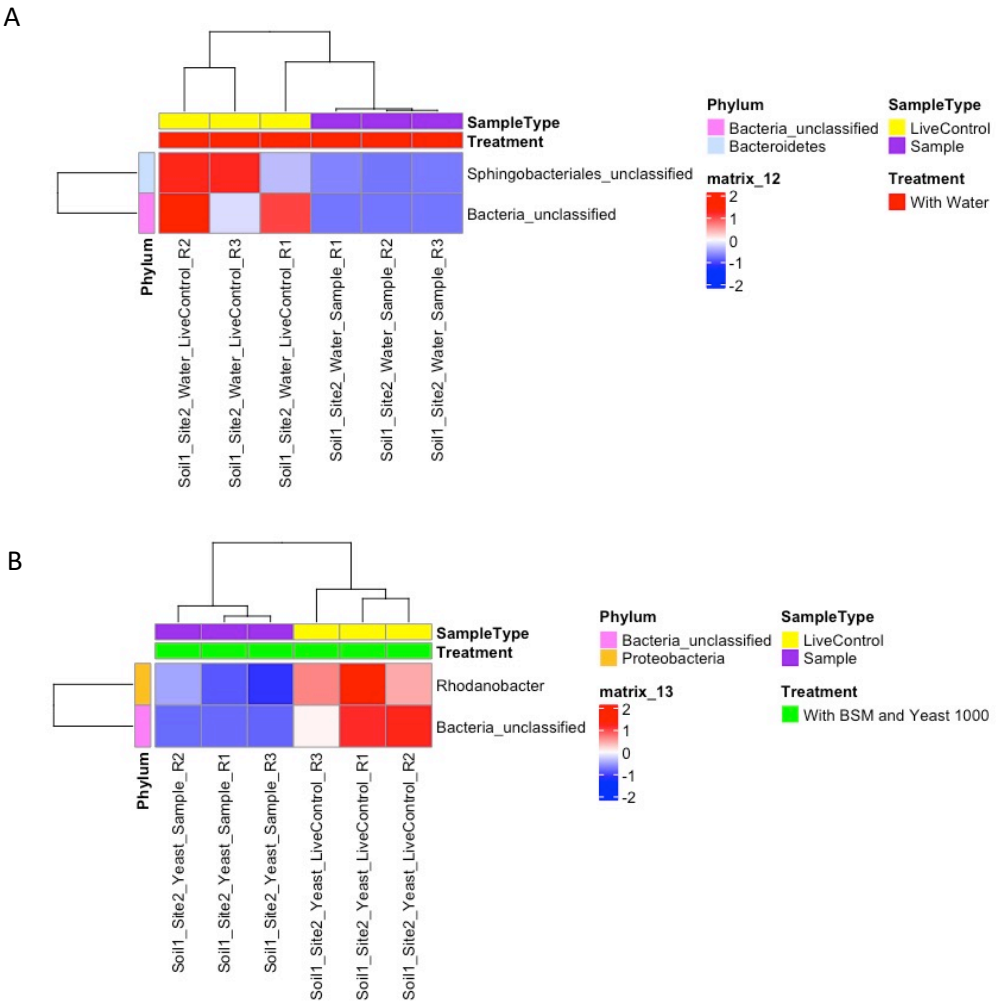

Figure A5.7 Top 50 differentially abundant taxa between the samples and live controls using DESeq2 analysis for the water treatment (A) and the BSM and yeast treatment (B) in Site 2 sediments microcosms inoculated with agricultural Soil 1. Note: "Soil 2_Site2_Yeast" is an abbreviation for "Soil2_Site2_BSMYeast1000." The column names were abbreviated to fit the visual constraints of the heatmap.

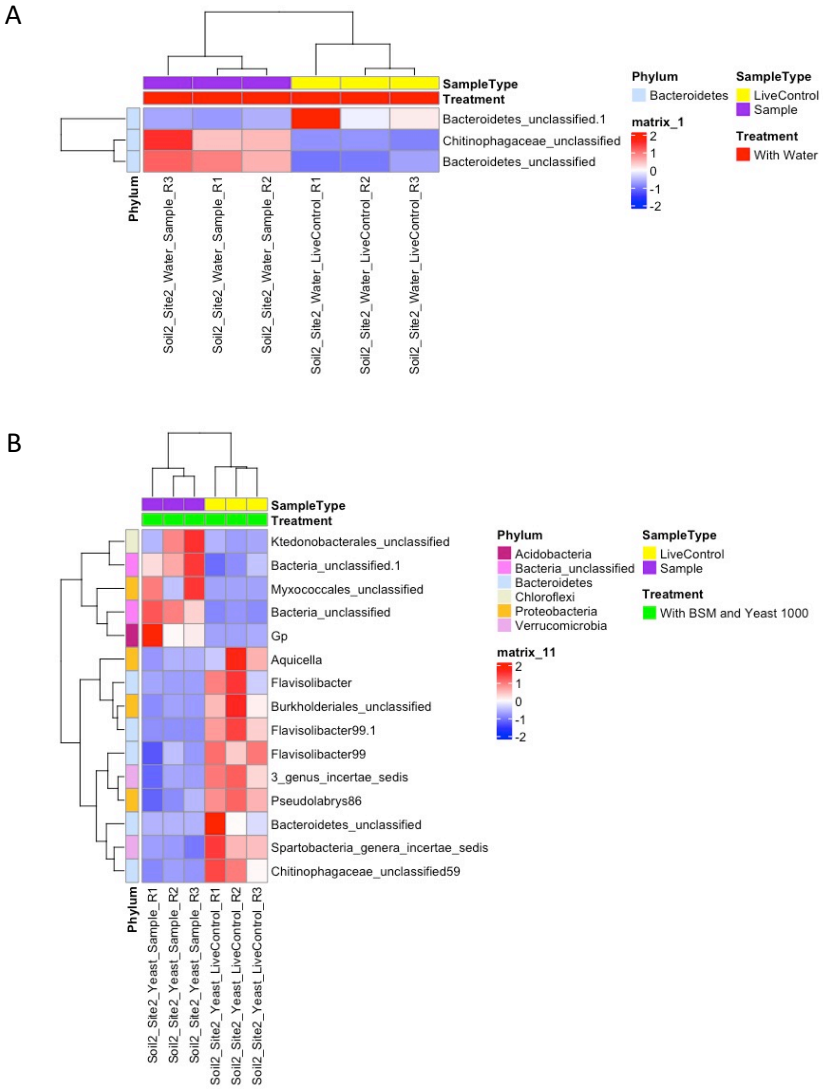

Figure A5.8 Top 50 differentially abundant taxa between the live samples and live controls using DESeq2 analysis for the water treatment (A) and the BSM and yeast treatment (B) in Site 2 sediments microcosms inoculated with agricultural Soil 2. Note: "Soil 2_Site2_Yeast" is an abbreviation for "Soil2_Site2_BSMYeast1000." The column names were abbreviated to fit the visual constraints of the heatmap.

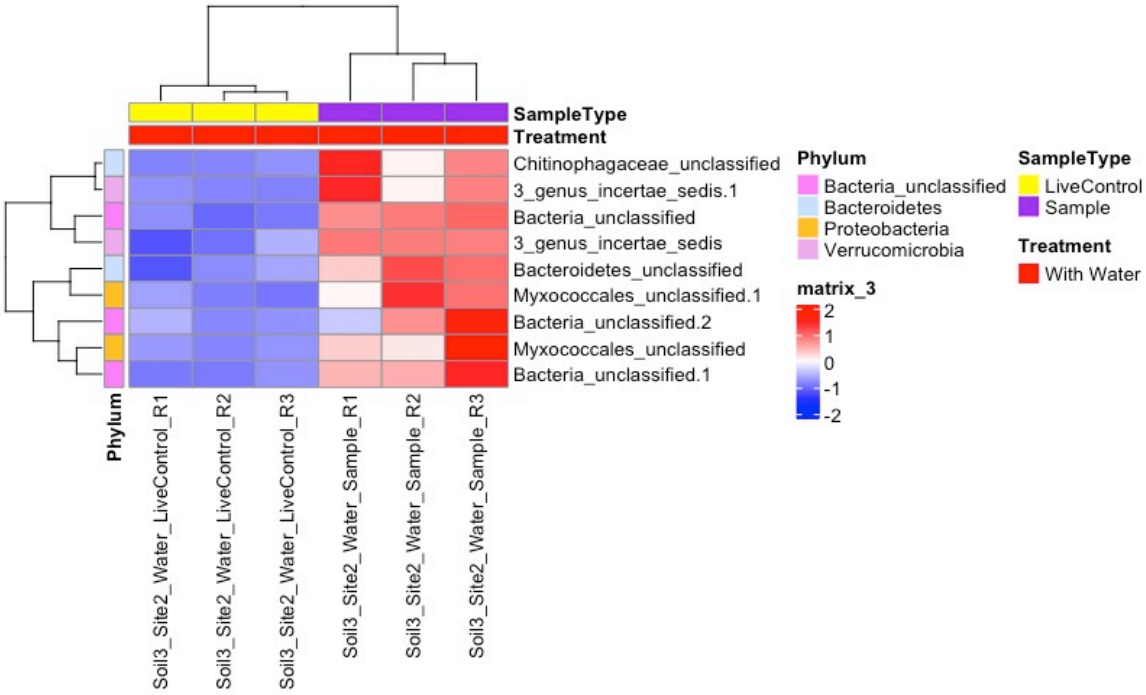

Figure A5.9 Top 50 differentially abundant taxa between the live samples and live controls using DESeq2 analysis for the water treatment in Site 2 sediments microcosms inoculated with agricultural Soil 3. There was no differentially expressed abundant taxa for the BSM and yeast treatment.

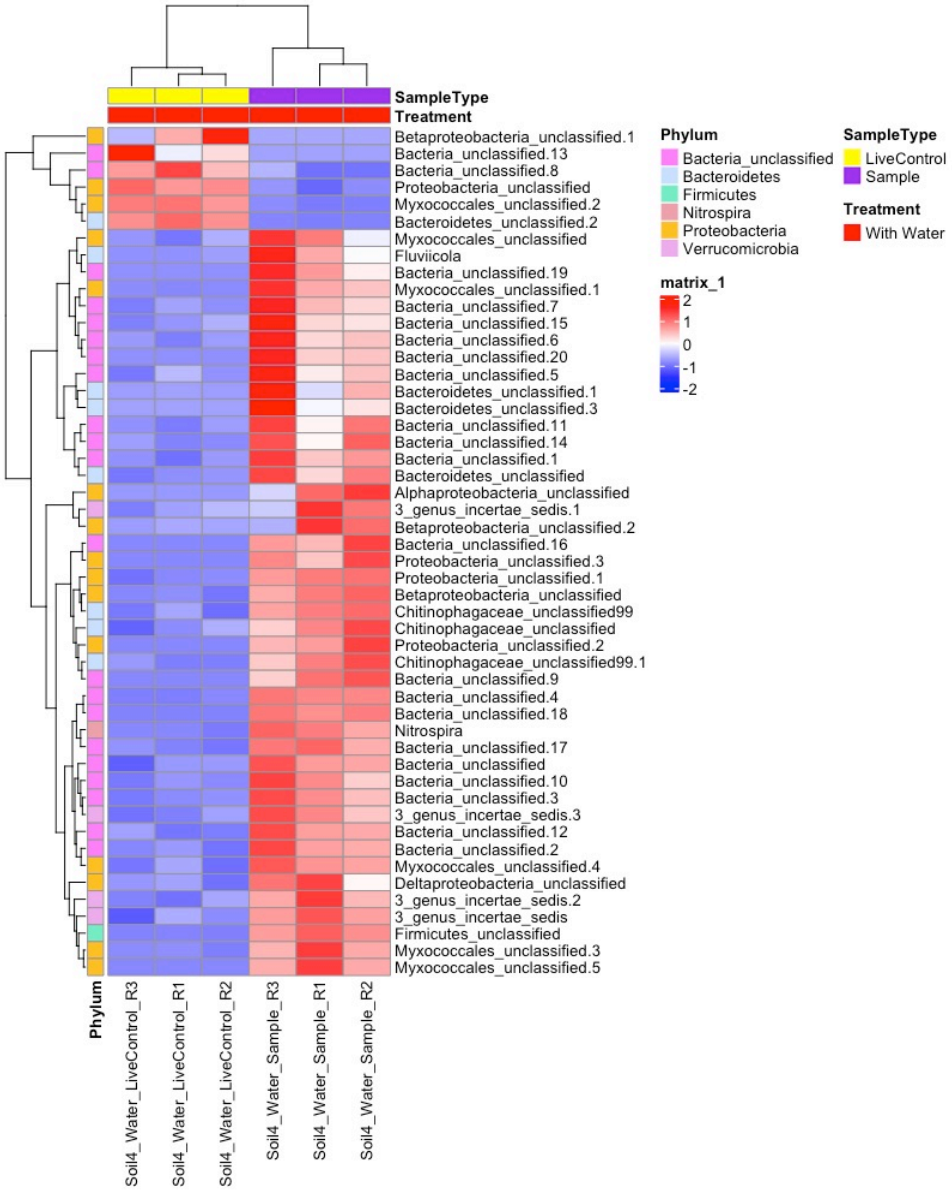

Figure A5.10. Top 50 differentially abundant taxa between the live samples and live controls using DESeq2 analysis for water treatment in agricultural Soil 4 microcosms.

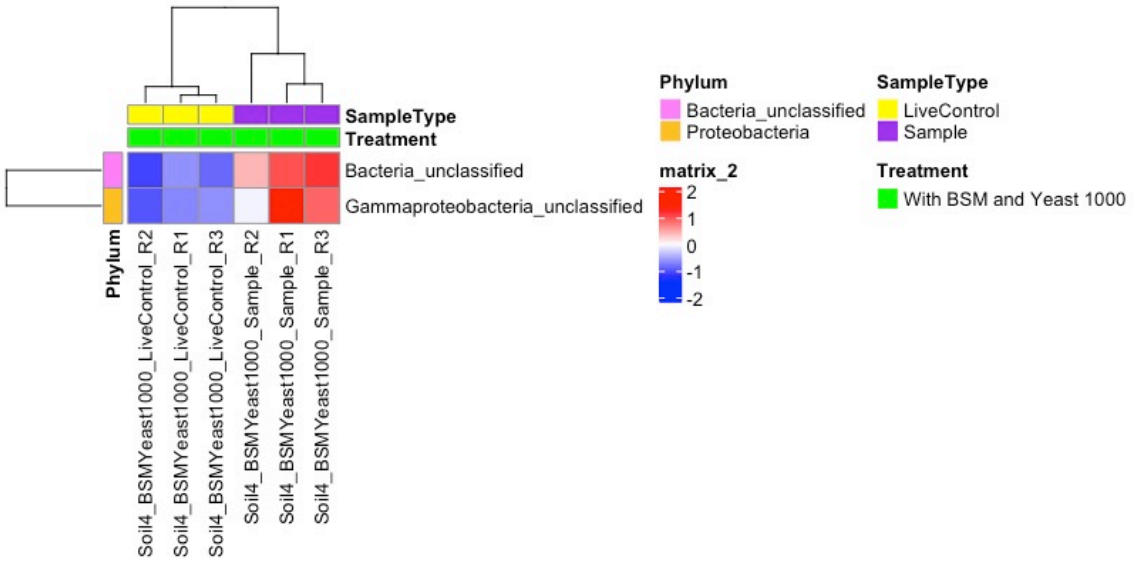

Figure A5.11 Top 50 differentially abundant taxa between the live samples and live controls using DESeq2 analysis for BSM and yeast treatment in agricultural Soil 4 microcosms.

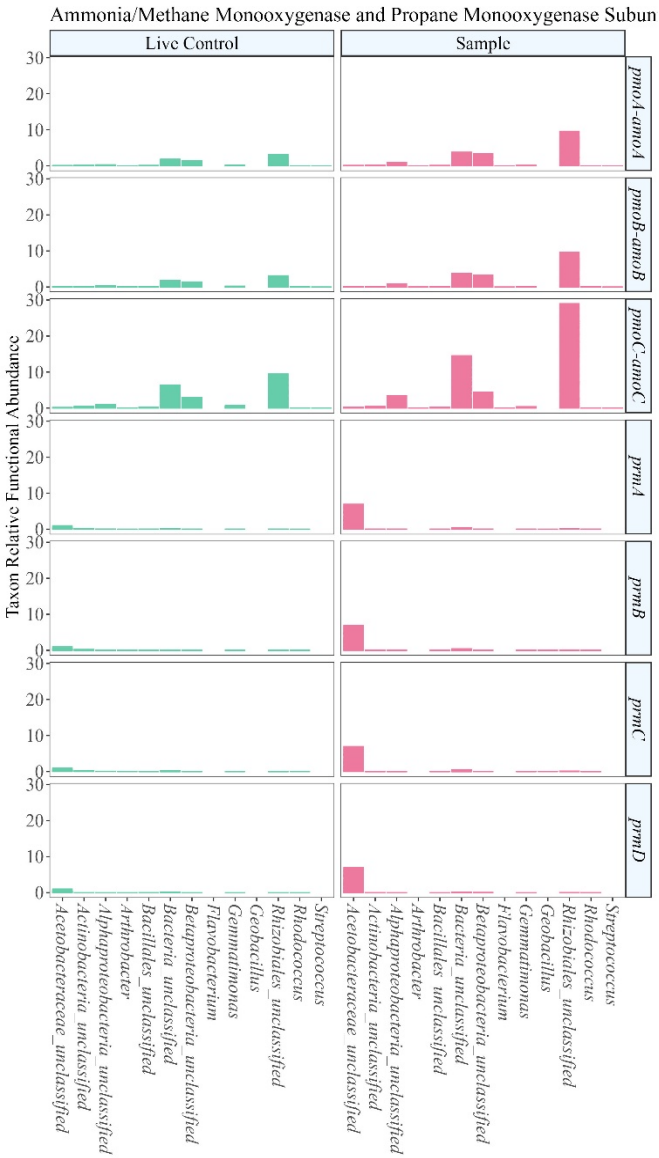

Figure A5.12 Relative abundance of enriched taxa (identified by DESeq analysis) associated with methane/ammonia monooxygenase subunits *pmoA-amoA* (K10944), *pmoB-amoB* (K10945) and *pmoC-amoC* (K10946) as well as taxa associated with all four subunits of propane monooxygenase *prmA* (K18223), *prmB* (K18225), *prmC* (K18224) and *prmD* (K18226) in the Site 1 microcosms.

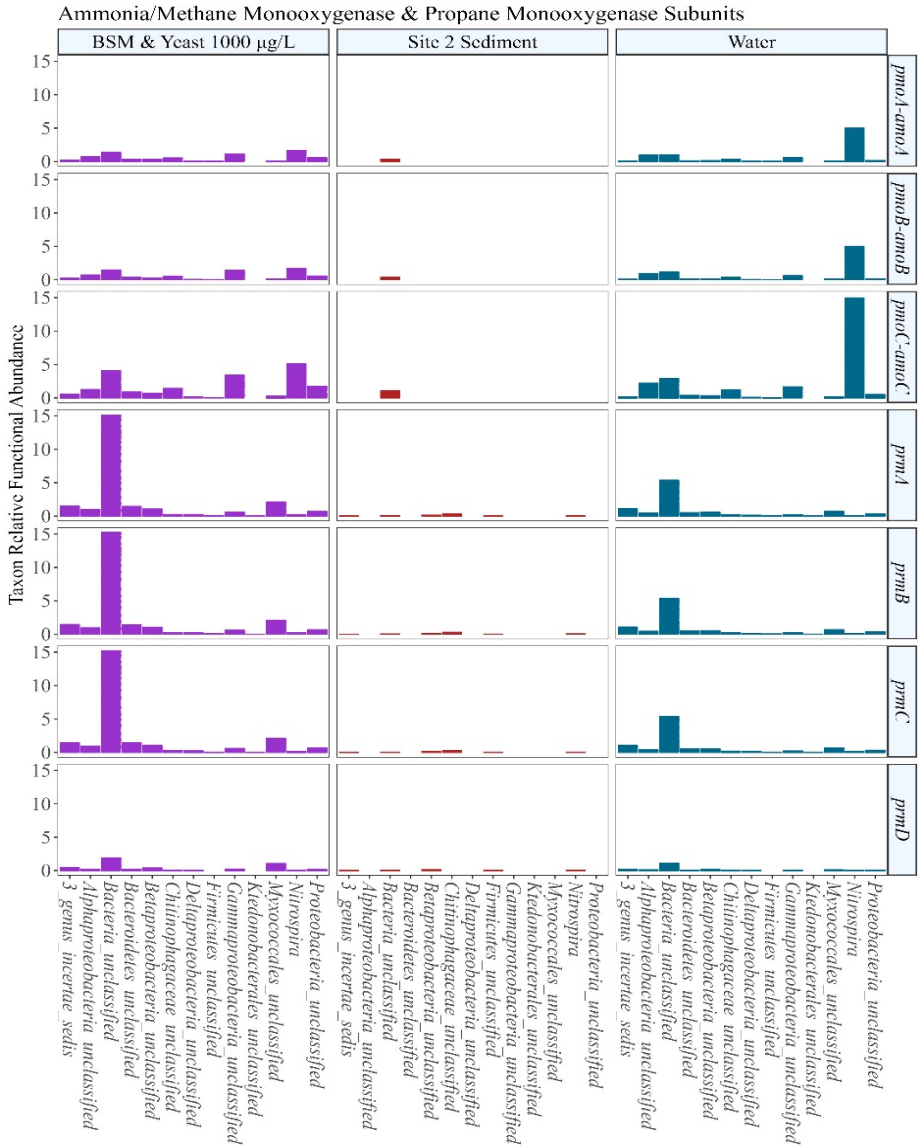

Figure A5.13 Relative abundance of enriched taxa (identified by DESeq analysis) associated with methane/ammonia monooxygenase subunits *pmoA-amoA* (K10944), *pmoB-amoB* (K10945) and *pmoC-amoC* (K10946) as well as taxa associated with all four subunits of propane monooxygenase *prmA* (K18223), *prmB* (K18225), *prmC* (K18224) and *prmD* (K18226) in the Site 2 sediment and agricultural soil microcosms combined.

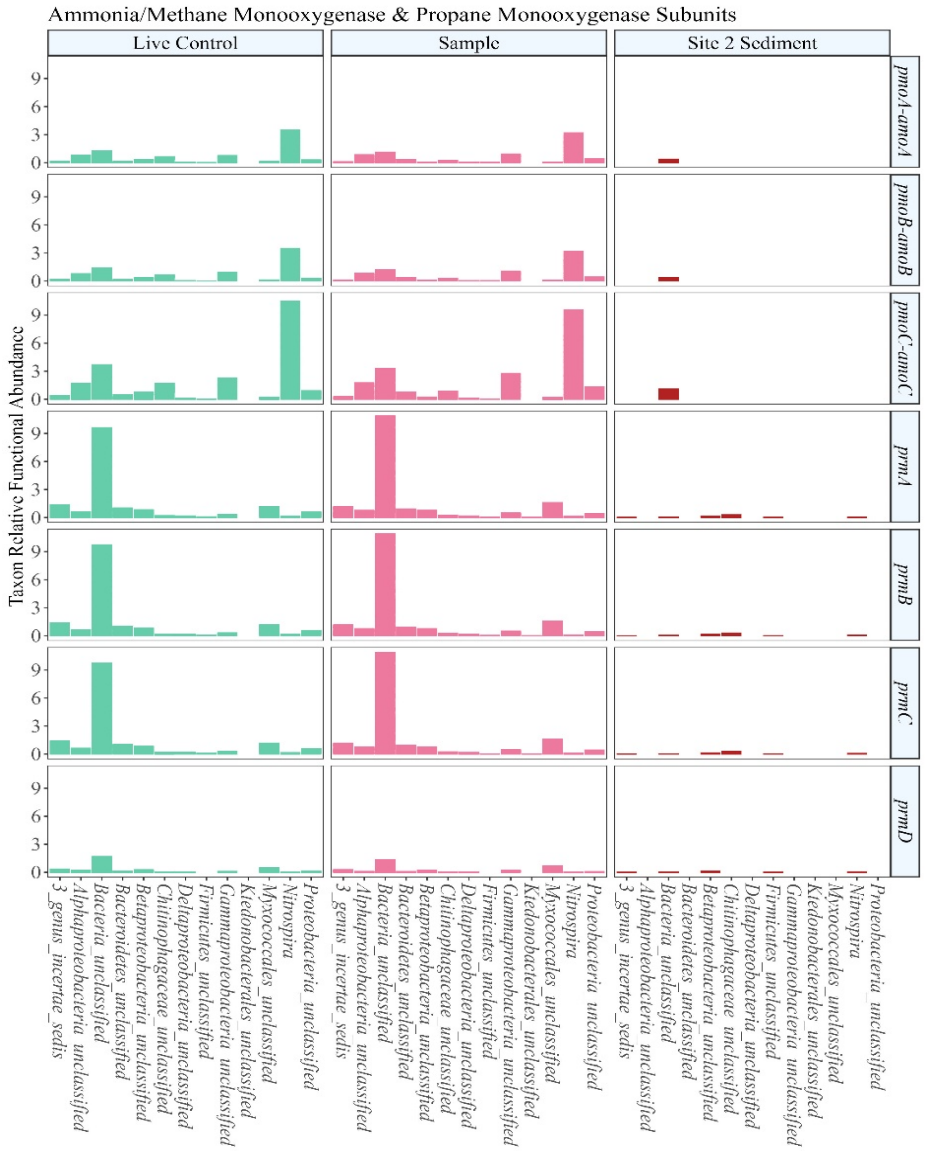

Figure A5.14 Relative abundance of enriched taxa (identified by DESeq analysis) associated with methane/ammonia monooxygenase subunits *pmoA-amoA* (K10944), *pmoB-amoB* (K10945) and *pmoC-amoC* (K10946) as well as taxa associated with all four subunits of propane monooxygenase *prmA* (K18223), *prmB* (K18225), *prmC* (K18224) and *prmD* (K18226) in the Site 2 sediment and agricultural soil microcosms combined.

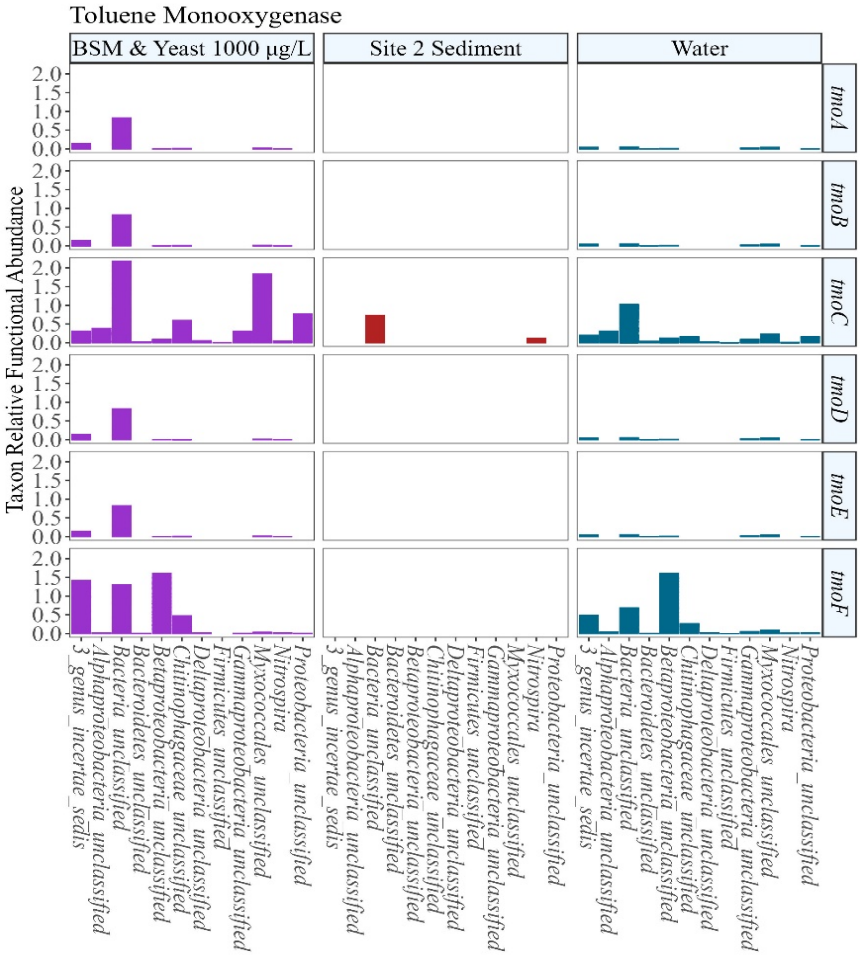

Figure A5.15. Relative abundance of enriched taxa (identified by DESeq analysis) associated with the six subunits of toluene monooxygenase, *tmoA/tbuA1/touA* (K15760), *tmoB/tbuU/touB* (K15761), *tmoC/tbuB/touC* (K15762), *tmoD/tbuV/touD* (K15763), *tmoE/tbuA2/touE* (K15764) and *tmoF/tbuC/touF* (K15765) in the Site 2 sediment and agricultural soil microcosms combined.

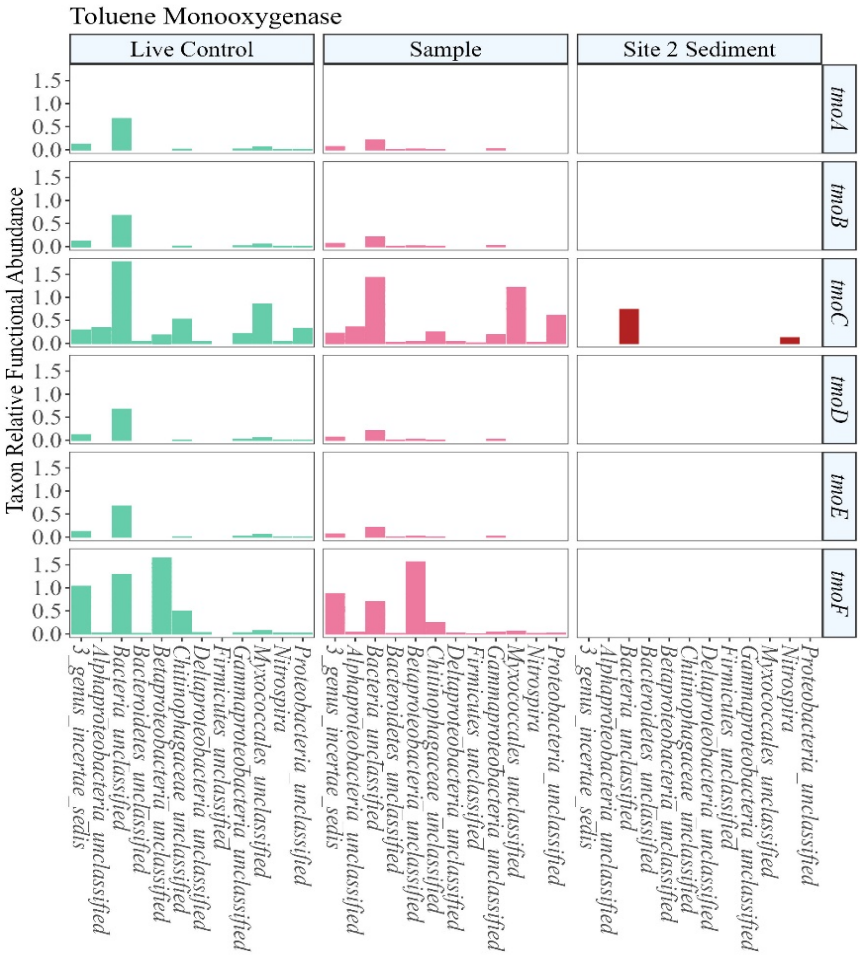

Figure A5.16 Relative abundance of enriched taxa (identified by DESeq analysis) associated with the six subunits of toluene monooxygenase, *tmoA/tbuA1/touA* (K15760), *tmoB/tbuU/touB* (K15761), *tmoC/tbuB/touC* (K15762), *tmoD/tbuV/touD* (K15763), *tmoE/tbuA2/touE* (K15764) and *tmoF/tbuC/touF* (K15765) in the Site 2 sediment and agricultural soil microcosms combined.

CHAPTER 6: CONCLUSIONS AND PERSPECTIVES

This dissertation advances the understanding of microbial processes including nitrogen and carbon cycling and the biodegradation of 1,4-dioxane in complex soil and sediment communities.

Chapter 2: This study investigated the taxonomic and functional profiles of the soil microbial communities associated with nitrogen metabolism, primarily denitrification, under different management practices by the analysis of shotgun sequences. This successfully links both taxonomic and functional data for the microbes associated with nitrogen cycling processes.

Chapter 3: This study identified the phylotypes related to the carbon uptake from added glucose using 16S rRNA gene sequencing coupled with SIP. The active phylotypes responsible for carbon uptake varied between treatments, soil pore sizes and incubation times. *Pseudomonas* (*Proteobacteria*) played an important role in carbon uptake from glucose in all short-term incubations and in the large pore long-term incubations. The enriched functional genes were also predicted. This is the first study to examine carbon assimilation from glucose as a function of pore architecture in these agricultural systems.

Chapter 4: This study demonstrated that the amendment of BSM and yeast extract significantly enhanced the 1,4-dioxane degradation at 2 mg/L for the impacted site sediments and agricultural soils. *Gemmatimonas*, *Solirubacteraceae*, *Solirubrobacter*, *RB4* and *oc3299* were identified as novel phylotypes linked to carbon uptake from 1,4-dioxane. Three genes (*Rhodococcus jostii* RHA1 *prmA* and *Rhodococcus* sp. RR1 *prmA*, *Pseudonocardia dioxanivorans* CB1190 plasmid pPSED02 Psed_6976) were detected in the mixed microbial communities. Overall, a variety of microbial communities were involved in the 1,4-dioxane

degradation. The amendment of BSM and yeast extract offers the potential to enhance 1,4-dioxane biodegradation.

Chapter 5: This study examines the impact of BSM and yeast extract on 1,4-dioxane degradation at low levels (< 500 μg/L). The amendment significantly accelerated the 1,4-dioxane degradation for one impacted site sediment but not for the other two site sediments. The rapid 1,4-dioxane degradation for the agricultural soils suggests higher levels of 1,4-dioxane degraders in these soils. The bioaugmentation with agricultural soils enhanced 1,4-dioxane degradation for the site sediments that previously showed no degradation. Overall, the amendment of BSM and yeast extract can enhance the 1,4-dioxane degradation in some cases. Agricultural soils provide options for bioaugmentation to enhance the 1,4-dioxane degradation at low levels.

Future research will apply quantitative SIP can be applied to quantify the variations in the growth of functional microbes and their isotope assimilation rates by coupling 13C-labeled carbon substrates with qPCR. This approach will provide deeper insights into microbial activity and their specific roles in biogeochemical processes. Additionally, geochemical properties of different soil types may be explored in the future research, as these properties may have crucial influence on the microbial communities. Correlating geochemical data with molecular data could help identify factors that influence functional genera, enabling the identification of soil characteristics that promote the growth of beneficial microbes. Instead of inoculating agricultural soils, future work could involve enriching 1,4-dioxane degrading consortia from uncontaminated sols for in situ 1,4-dioxane degradation. This could offer a sustainable and cost-effective approach for groundwater bioremediation.